

OF GELS, OFFGEL AND OFF WITH THE GEL: DEVELOPMENT OF ISOELECTRIC FOCUSING TOOLS FOR PROTEOMICS

THÈSE N° 3976 (2007)

PRÉSENTÉE LE 14 DÉCEMBRE 2007

À LA FACULTÉ DES SCIENCES DE BASE
LABORATOIRE D'ÉLECTROCHIMIE PHYSIQUE ET ANALYTIQUE
PROGRAMME DOCTORAL EN CHIMIE ET GÉNIE CHIMIQUE

ÉCOLE POLYTECHNIQUE FÉDÉRALE DE LAUSANNE

POUR L'OBTENTION DU GRADE DE DOCTEUR ÈS SCIENCES

PAR

Hoang-Trang LAM

Ingénieure chimiste diplômée de l'ECPM, Strasbourg, France
et de nationalité française

acceptée sur proposition du jury:

Prof. P. Vogel, président du jury
Prof. H. Girault, directeur de thèse
Prof. C. Comninellis, rapporteur
Prof. H. Jensen, rapporteur
Prof. M. Martin, rapporteur



ÉCOLE POLYTECHNIQUE
FÉDÉRALE DE LAUSANNE

Suisse
2008

A mes parents

ACKNOWLEDGEMENTS

I would like to sincerely thank Professor Hubert Girault for giving me the opportunity to do this research work in his laboratory. I will always remember him as the most brilliant and creative person I ever had the pleasure to meet, work with and talk to. If a PhD is a school for life, then I had the best teacher. I learnt a lot with him, whether at the scientific level, or the human one.

I wish to address special thanks to Professor Carlos Pereira, from whom I learnt a lot about electrochemistry. He changed my vision of the field and gave me a more practical approach. I am also thankful for the fruitful discussions and the “long-distance” support he gave me at the end of my thesis.

I also warmly thank Dr Jacques Josserand for giving me his time and sharing his experience and knowledge in numerical simulations, as well as in general matters of life. Dr Josserand is a kind person, and I enjoyed the interesting conversations, whether scientific or not. Next, I would like to thank Dr Niels Lion for his collaboration to my second paper and for the knowledge he shared. Dr Christophe Roussel is also thanked for reviewing my first paper.

This thesis would have been difficult without the help and support of my friends and colleagues, Dr Grégoire Lagger, the future doctors Mohamad Hojeij, Fernando Cortes and Michel Prudent, with whom I had many happy and precious moments. Thanks so much for your encouragements. To Greg, who always liked to challenge me, and who managed in doing so. To Mohamad, the “businessman” of the group. To Señor Cortes, the Latin spirit of the lab, my out of category friend, with whom I had many good laughing sessions and nice

times. To Michel Prudent, my truly helpful friend, who read my entire thesis and gave me his best advice and support at the end, and with whom I shared so many interesting talks. Their friendship made my life easier during the thesis and I wish them all the best for their future life.

Maria is also thanked for the great administrative work, André Fattet and Gérard Féryni for their technical help and availability.

I also thank my friends from France, Germany, and Switzerland, with whom I spent scarce but really nice moments. Thanks very much for the “long-distance” support. And my best thanks go to Vincent, who always believed in me during all these years, gave me strength, was there when I needed him, and gave me his best. I express all my gratefulness to him, from the bottom of my heart.

And finally, but most importantly, I would not be here today, with what I am and what I have done, without the help, advice and support of my parents, my brother and my sister. I owe them everything. This thesis is dedicated to them, with all my love.

RÉSUMÉ

Dans le contexte du développement de méthodes de pré-fractionation pour la protéomique, ce travail de thèse est basé sur la conception d'instruments électrophorétiques pour la focalisation isoélectrique de peptides et protéines, en vue de l'analyse de mélanges biologiques. A la lumière des techniques existantes dans le domaine de la focalisation isoélectrique, l'objectif est de développer des cellules multi-compartiments pour la focalisation isoélectrique de peptides et de protéines. Le premier choix de la focalisation OFFGEL comme technique de focalisation isoélectrique se justifie par sa facilité pour collecter les fractions de peptides en solution, de faibles volumes, et compatibles avec les analyses par chromatographie liquide (en tant que seconde dimension de la séparation) ou de spectrométrie de masse. La résolution est le facteur clé à considérer au cours de la fabrication des cellules de séparation.

Des simulations par éléments finis ont été effectuées, pour décrire la focalisation OFFGEL des peptides, et ont permis de réaliser le dimensionnement d'une cellule OFFGEL en format multi-puits pour une séparation à haute résolution de peptides. Ces simulations ont par ailleurs démontré l'importance de la mobilité proche du point isoélectrique (pI) au niveau de la cinétique de séparation ainsi que son influence sur la forme finale du pic focalisé. Le calcul de la distribution des mobilités proches du pI pour trois protéomes a permis de conclure sur la largeur optimale du puits de OFFGEL de manière à obtenir la meilleure résolution possible. Cette étude mathématique a illustré le fort pouvoir résolutif de la focalisation OFFGEL, pour son utilisation en protéomique.

Basée sur les résultats de la simulation, la fabrication d'une cellule OFFGEL multi-puits a ensuite pu être réalisée. La caractérisation de cette cellule a ensuite été effectuée. La reproductibilité du gradient de pH a été validée, la capacité de charge a été évaluée pour les protéines, et la haute résolution pour la séparation des peptides a été démontrée. Un mélange biologique a également été séparé. La focalisation OFFGEL a ensuite été intégrée dans une stratégie combinant le marquage chimique des résidus de cystéines dans les peptides. Cette approche a démontré le gain d'information sur la séquence des peptides, conduisant à une identification plus sûre et plus précise de la protéine.

Dans un contexte de protéomique « sans gel », une cellule différente a été fabriquée, permettant de réaliser la focalisation isoélectrique en l'absence d'un gel à gradient de pH immobilisé (IPG). La nouvelle cellule a été également caractérisée en termes de performances et a été utilisée pour la fractionation d'un échantillon d'*Escherichia coli*, permettant une séparation plus rapide des protéines que la focalisation OFFGEL, démontrant ainsi son potentiel pour une pré-fractionation rapide de protéomes.

Une cellule électrochimique a également été développée, pour le transfert d'espèces ionisables, par électrochimie à la micro-interface entre deux électrolytes immiscibles (μ -ITIES), supporté par un gel IPG pris en tant que phase aqueuse, et une gouttelette de phase organique. Cette étude a été initialement menée dans le but de réaliser une extraction en ligne des protéines et peptides au cours de la focalisation OFFGEL. L'utilisation du système développé a été démontrée pour des molécules modèles, et a ouvert les portes pour l'étude du transfert de protéines.

Mots-clés : protéines, peptides, focalisation isoélectrique, gradient de pH immobilisé, ampholytes porteurs, électrophorèse, OFFGEL, spectrométrie de masse, marquage chimique, électrochimie, ITIES.

ABSTRACT

In the context of prefractionation methods for proteomics, this work deals mainly with the development of electrophoretic tools for isoelectric focusing of peptides and proteins for the analysis of biological mixtures. In the light of existing devices for isoelectric focusing (IEF), the objective has been to develop multicompartment devices, designed for the IEF of peptides and proteins. The first choice of the OFFGEL for IEF among other techniques is justified by the easy recovery of liquid fractions of peptides, of small volumes, further amenable to liquid chromatography (as a second dimension separation) or mass spectrometry analyses. The resolution is a key point to consider in the design of separation units.

Finite element simulation of the isoelectric focusing of peptides by OFFGEL has allowed the design of a multicompartment OFFGEL device for high resolution separation of peptides. The numerical simulations have highlighted the importance of the mobility near pI for the IEF kinetics and the final peak shape. The calculation of the distribution of peptides mobility near pI for three proteomes has allowed concluding on the optimal width of the well to obtain best separation. This mathematical study has also illustrated the high focusing power of the OFFGEL technique as a separation tool for shotgun proteomics application.

The design of a multicompartment OFFGEL device was then done, based on the results of the simulations. The reproducibility of the pH gradient was validated, the loading capacity was evaluated for proteins, and a demonstration of the high resolution separation of peptides and proteins from a complex biological mixture was performed. The OFFGEL separation was then integrated in a workflow combining chemical tagging of the cysteine residues. This approach showed that the high resolution of peptide OFFGEL and the added

information on the sequence of the peptides permitted a more confident and accurate protein identification.

In the context of gel-free proteomics, another separation cell has been designed, that enables performing isoelectric focusing without the need of an immobilized pH gradient (IPG) gel. The novel device has been characterized in terms of performances and has been applied to a biological sample of *Escherichia coli*, showing a more rapid separation of proteins than OFFGEL IEF, thus demonstrating its potential for fast proteome prefractionation purposes.

An electrochemical cell has also been designed, for the transfer of ionizable species by electrochemistry at the micro-interface of two immiscible electrolytes (μ -ITIES), supported by an IPG gel as the aqueous phase and a small drop of organic phase. This study was initially motivated by the aim of performing online extraction of proteins/peptides during IEF separation. The use of this device for the transfer of model molecules was demonstrated, opening the door to further developments concerning the electrochemical transfer of proteins.

Key words: proteins, peptides, isoelectric focusing, immobilized pH gradient, carrier ampholytes, electrophoresis, OFFGEL, mass spectrometry, chemical labeling, electrochemistry, ITIES.

LIST OF SYMBOLS AND ABBREVIATIONS

Roman letters

a_i	Activity of species i	-
c_i	Concentration of species i	M = mol·L ⁻¹
D_i	Diffusion coefficient of species i	m ² ·s ⁻¹ or cm ² ·s ⁻¹
E	Electric field	V·m ⁻¹
F	Faraday constant	96485 C·mol ⁻¹
f	Frictional coefficient	-
h_{gel}	Height of the gel	mm or cm
h_{well}	Height of the well	mm or cm
J_i	Flux of species i	mol·m ⁻² ·s ⁻¹
k	Boltzmann constant	1.380504 · 10 ⁻²³ J·K ⁻¹
N_A	Avogadro's constant	6.02214 · 10 ²³ mol ⁻¹
P_i	Coefficient of partition of species i	-
P_i^0	Standard coefficient of partition of species i	-
R	Gas constant	8.314472 J·K ⁻¹ ·mol ⁻¹
T	Temperature	K
$u_{ep,i}$	Electrophoretic mobility of species i	m ² ·V ⁻¹ ·s ⁻¹
V_m	Migration velocity	m·s ⁻¹

Greek letters

α	Ionization coefficient	-
β	Buffer capacity	M = mol·L ⁻¹
γ_i	Coefficient of activity of species <i>i</i>	-
$\tilde{\mu}_i$	Electrochemical potential of species <i>i</i>	J·mol ⁻¹
$\tilde{\mu}_i^0$	Standard electrochemical potential of species <i>i</i>	J·mol ⁻¹
μ_i	Chemical potential of species <i>i</i>	J·mol ⁻¹
η	Viscosity	kg·m ⁻¹ ·s ⁻¹
ϕ	Electric potential	V
σ_i	Conductivity of species <i>i</i>	S·m ⁻¹
z_i	Charge of species <i>i</i>	-
$\Delta_{\beta}^{\alpha}\phi$	Transfer potential from phase α to phase β (Galvani potential)	V
$\Delta_{\beta}^{\alpha}\phi'$	Standard transfer potential from phase α to phase β	V
$\Delta G_{tr,i}^{0,\alpha\rightarrow\beta}$	Standard Gibbs energy of transfer from phase α to phase β	J·mol ⁻¹

Abbreviations

2D-GE	Two dimensional gel electrophoresis
2D-PAGE	Two dimensional polyacrylamide gel electrophoresis
BSA	Bovine serum albumin
CA	Carrier ampholytes
CE	Capillary electrophoresis

COFRADIC	Combined fractional diagonal chromatography
ECD	Electron capture dissociation
ESI	Electrospray ionization
FEM	Finite Element Model
FFE	Free flow electrophoresis
FFF	Field flow fractionation
FTICR	Fourier transform ion cyclotron resonance
ICAT	Isotope coded affinity tags
IEF	Isoelectric focusing
IPG	Immobilized pH gradient
IT	Ion trap
ITIES	Interface between two immiscible electrolytes
L/L	Liquid/liquid
LC	Liquid chromatography
MALDI	Matrix assisted laser desorption ionization
MCE	Multicompartment electrolyzers
MS	Mass spectrometry
MS/MS	Tandem mass spectrometry
OGE	OFFGEL electrophoresis (also Offgel)
OG-IEF	OFFGEL isoelectric focusing
PMF	Peptide mass fingerprint
PTM	Post-translational modification
RP	Reversed phase
SCX	Strong cation exchange
SDS	Sodium dodecyl sulfate

TOF Time of flight

TABLE OF CONTENTS

ACKNOWLEDGEMENTS	i
RÉSUMÉ	iii
ABSTRACT	v
LIST OF SYMBOLS AND ABBREVIATIONS.....	vii
TABLE OF CONTENTS	xi
CHAPTER I: Introduction	1
1. Why proteomics?	2
2. Technological tools of proteomics	4
3. Gel-based versus gel-free proteomics	7
4. Bottom up and top down approaches	9
5. Chemical labeling for the enrichment and isolation of proteins.....	10
6. Why prefractionation techniques in proteomics?	15
6.1. Fractional centrifugation	15
6.2. Chromatographic approaches	16
6.3. Electrophoretic approaches.....	20
6.4. Field-Flow Fractionation (FFF).....	27
7. On transfer of proteins.....	30
8. Objective of the work.....	32
9. References	36
CHAPTER II: Theoretical aspects of isoelectric focusing	45
1. Isoelectric focusing as a separation technique.....	46
2. Mathematical description of isoelectric focusing.....	47
2.1 General equation for the diffusion-migration of ions	47
2.2 IEF at the steady state.....	50

2.3 Resolving power.....	51
3. Gel electrophoresis.....	53
4. Generation of a pH gradient for isoelectric focusing.....	55
4.1 Carrier ampholytes (CA).....	55
4.2 Immobilized pH gradient (IPG) gels.....	66
5. OFFGEL isoelectric focusing (OG-IEF).....	76
6. References.....	79
CHAPTER III: Modeling the isoelectric focusing of peptides in an OFFGEL multicompartment cell.....	83
1. Introduction.....	84
2. Methods.....	87
2.1 Short introduction on the theory of finite element.....	87
2.2 Analytical Model.....	90
2.3 Finite Element Model.....	93
2.4 In silico proteome digestion and computation of physico-chemical parameters.....	96
3. Results and discussion.....	97
3.1 Model validation.....	97
3.2 Determination of the order of magnitude of dz/dpH at pI	98
3.3 Effect of the charge gradient dz/dx at the pI (1-D study).....	99
3.3.1 Effect on the peak width.....	99
3.3.2 Effect on the focusing time.....	101
3.4 Effect of the well height on the recovery and focusing time (2-D study).....	104
3.5 Effect of the well shape on the recovery and focusing time.....	107
3.6 IEF of peptides in a seven-well device.....	109
4. Concluding remarks.....	112
5. References.....	113
CHAPTER IV: Design and characterization of a homemade OFFGEL device.....	117
1. Introduction.....	118
2. Chemicals and instrumental.....	121
2.1 Chemicals and biologicals.....	121
2.2 OFFGEL (OG-) IEF in the homemade device.....	122

2.3 Capillary electrophoresis (CE)	123
2.4 Tryptic digestion.....	123
2.5 LC-MS.....	123
2.6 Protein extraction from E. coli	124
2.7 2-D PAGE	124
3. Results and discussion.....	125
3.1 Description of the OFFGEL homemade device	125
3.2 Voltage and current monitoring.....	127
3.3 pH characterization.....	130
3.4 Loading capacity for proteins	134
3.5 OG-IEF of peptides	138
3.6 OG-IEF of proteins under denaturing conditions	142
4. Concluding remarks	145
5. References	146
CHAPTER V: OFFGEL IEF combined with chemical tagging for improved protein identification	149
1. Introduction.....	150
2. Experimental	154
2.1 Chemicals	154
2.2 Tryptic digestion.....	154
2.3 OFFGEL IEF of peptides (OG-IEF).....	155
2.4 Chemical tagging reaction	155
2.5 MALDI-TOF	155
2.6 LC-ESI-MS	156
2.7 Database search parameters.....	156
3. Results and discussion.....	157
3.1 pI as validation information to eliminate false positive identifications	157
3.2 Counting cysteines for enhanced protein identification by PMF.....	162
4. Concluding remarks	172
5. References	173

CHAPTER VI: Gel-free isoelectric focusing in a membrane-sealed multicompartiment cell for proteome prefractionation.....	177
1. Introduction.....	178
2. Materials and methods	181
2.1 Chemicals and biologicals.....	181
2.2 Sample prefractionation by IEF in the static chamber.....	182
2.3 SDS–PAGE	182
2.4 2–D PAGE analysis.....	183
3. Results.....	183
3.1 Description of the instrument	183
3.2 Performance of the instrument	185
3.3 Biological results.....	186
4. Discussion	191
5. References.....	193
CHAPTER VII: Immobilized pH Gradient gel cell to study the pH dependence of drug lipophilicity.....	195
1. Introduction.....	196
2. Electrochemistry at the ITIES	199
2.1 Thermodynamics of ion transfer at ITIES	199
2.2 Electrochemistry to measure drug lipophilicity.....	201
2.3 Facilitated ion transfer	202
2.4 Differential Pulse Voltammetry.....	203
3. Experimental	204
3.1 Chemicals.....	204
3.2 Setup and electrochemical measurements	205
3.3 Methodology: use of an internal reference ion	207
4. Results and discussion.....	209
4.1 Experimental validation of the electrochemical cell based on transfer of simple permanent ions	209
4.2 Ionic partition diagram of ionizable compounds	211
5. Conclusions.....	217
6. References.....	219

CHAPTER VIII: Conclusions and Perspectives	223
Appendix I: Buffer capacity of ampholytes	229
Appendix II: Table of pKa	233
Appendix III: Numerical parameters	235
Curriculum Vitae.....	237

CHAPTER I: *Introduction*

1.	Why proteomics?.....	2
2.	Technological tools of proteomics.....	4
3.	Gel-based versus gel-free proteomics.....	7
4.	Bottom up and top down approaches.....	9
5.	Chemical labeling for the enrichment and isolation of proteins	10
6.	Why prefractionation techniques in proteomics?.....	15
6.1.	Fractional centrifugation	15
6.2.	Chromatographic approaches	16
6.3.	Electrophoretic approaches	20
6.4.	Field-Flow Fractionation (FFF)	27
7.	On transfer of proteins	30
8.	Objective of the work	32
9.	References	36

1. Why proteomics?

It is only recently that the Human Genome Project was completed (2003), 13 years after its launch by the US Department of Energy and the National Institute of Health. The goals of this huge project were mainly to identify all the approximately 30,000 genes in human DNA, determine the sequences of the 3 billion chemical base pairs that make up human DNA, store that information in database, and improve tools for data analysis.¹ The completion of the human genome led to results sometimes disappointing to many scientists, because counting genes was viewed as a way of quantifying the genetic complexity. With around 30,000 genes, the human gene count would be only one-third greater than that of the simple roundworm *C. elegans*, at about 20,000 genes. All the more as, knowing the sequence of letters (“the genetic code”) does not mean that we understand the subtleties of the language.

In parallel, proteomics, “the study of proteins expressed by a genome, and the systematic analysis of protein profiles in tissues” (1995),² was slowly but steadily making its way. The field of proteomics has known a tremendous growth after the rather costly genome projects, to become a necessary field, since it was widely concluded that the knowledge of the DNA sequences solely could not account for the complexity of living organisms.^{3, 4} For example, proteins, not genes, are responsible for the phenotype of the cells, thus the elucidation of the mechanisms of disease or aging cannot be done by studying the genome only. Such questions as the protein function, localization and compartmentalization, and protein-protein interactions, needed answers.

Proteomics however, was faced with multiple challenges. In 1997, during the third Sienna meeting, Anderson presented a multigene comparison plot of mRNA vs. protein abundance for cellular gene products, and showed a very low correlation of 0.43 between

them.⁵ Indeed, the processes occurring from the gene to the final protein are numerous (Figure 1).

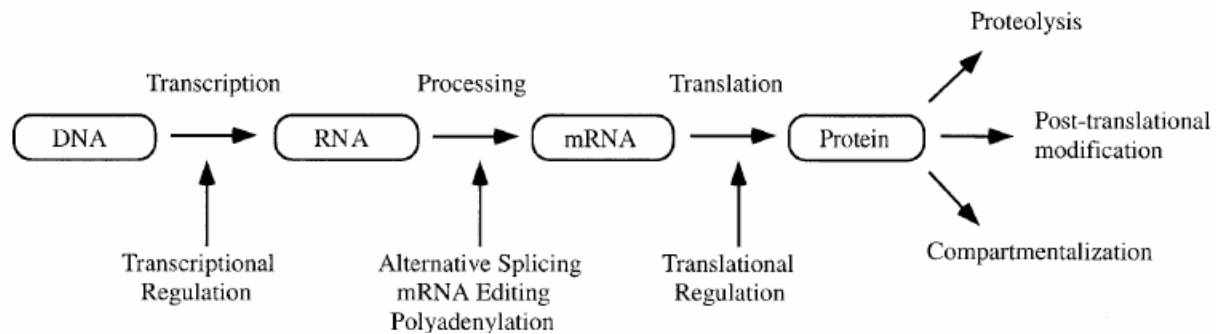


Figure 1: Mechanisms by which a single gene can give rise to multiple gene products. Multiple protein isoforms can be generated by RNA processing, when RNA is alternatively spliced or edited to form mature mRNA. mRNA, in turn, can be regulated by stability and efficiency of translation. Proteins can be regulated by additional mechanisms including post translational modifications, proteolysis or compartmentalization. Reprinted from⁴

The existence of post-translational modifications (phosphorylation, glycosylation...) as well as alternative splicing during the processing of proteins, leads to the painful conclusion that one initial gene can produce between five to fifteen final different gene products. If the human genome contains roughly 30,000 genes, the human body may contain more or less half a million different proteins having possibly very different functions.⁶ Thus, unlike the genome, the complexity of the proteome is far greater, especially if considering the proteome a dynamic ensemble, changing to reflect the environment of the cell. In addition, the complexity of the proteome lies in the wide range of physicochemical properties of proteins (charge, mass, hydrophobicity), as well as in the large dynamic range of concentrations, from 7-8 orders of magnitude up to 12 in serum or plasma.⁷ Unfortunately, there is, to date, no technology equivalent to Polymerase Chain Reaction (PCR) as for genes,⁸ thus proteomics analyses are generally limited by the substrate amount.

2. Technological tools of proteomics

Two main analytical tools have traditionally been used for protein identification: two dimensional gel electrophoresis (2D-GE, for reviews, see⁹⁻¹³), and mass spectrometry (MS, for reviews, see¹⁴⁻¹⁶), combined in a classical widely used approach (Figure 2).

2D gel electrophoresis has been the technique of choice for analysis of proteomes for the last 20 years,⁷ allowing a separation according to the charge in the first dimension and to the molecular weight in the second dimension. The advent of immobilized pH gradient (IPG) gels has drastically improved the reproducibility of the first dimension,¹¹⁻¹³ thus replacing the initial use of carrier ampholytes.^{9, 10} A typical 2D gel can resolve 2,000 spots with a usual loading of 5-10 mg of protein mixture, and up to 10,000 protein spots can be resolved on the best gels.¹⁷ The detection sensitivity depends on the staining method, for Coomassie brilliant blue staining, the limit of detection is 100 ng/spot while silver staining is more sensitive with down to 1 ng/spot.

Although 2D remains a standard tool for proteomic research, it is clear that this strategy has significant analytical limitations in addressing the many challenges presented by the systemic analysis of complex protein mixtures. The main limitations include: (i) limits in sample capacity and detection sensitivity, which restrains 2D-GE to identify only relatively abundant proteins, especially when analyzing un-fractionated protein mixtures from whole cell lysates, low abundant proteins usually remaining unseen,^{18, 19} (ii) the separation of insoluble membrane and hydrophobic proteins is still a major challenge, despite efforts in making 2D compatible to this class of proteins,¹³ (iii) co-migration of different proteins, and differently modified proteins migrating to multiple locations on the gel, complicating the quantitative analysis of visualized spots,¹⁸ (iv) proteins with extreme *pI* (below 3 and above 10-11) or extreme molecular weights are usually excluded from the separation.

The advent of mass spectrometry increased the sensitivity of detection, and catalyzed the field of proteomics.

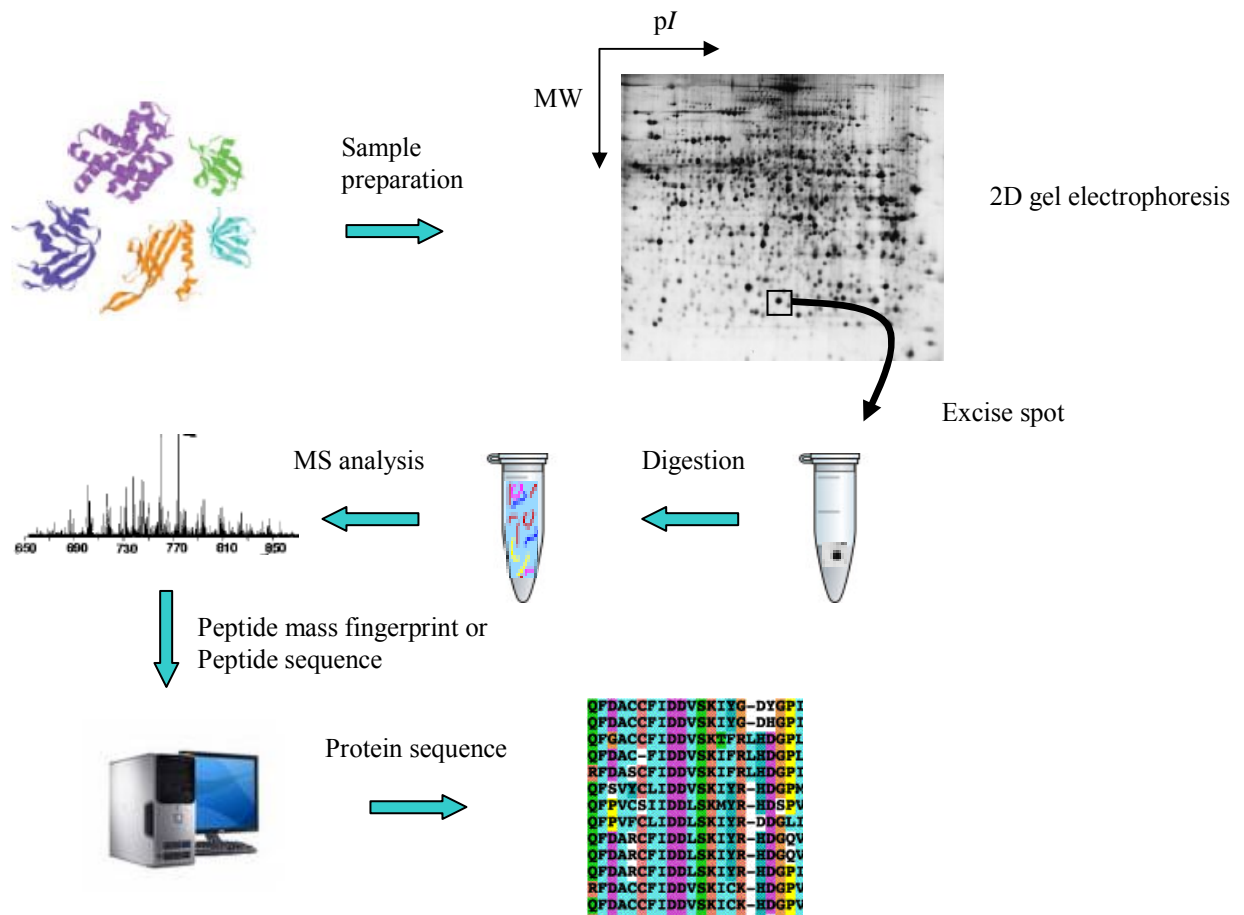


Figure 2: Scheme of a classical 2D gel electrophoresis combined to MS for protein identification.

Mass spectrometry has known a major breakthrough in late 1980's, with the introduction of two methods of soft ionization of molecules. In electrospray ionization mass spectrometry (ESI-MS),^{20, 21} the ions are formed from a solution at atmospheric pressure. In the most common configuration, ESI sources are used with quadrupole mass analyzers. In matrix-assisted laser-desorption ionization mass spectrometry (MALDI-MS),^{22, 23} ions are formed from the solid state. The analyte is deposited on a probe by co-crystallization with a matrix and then introduced to the ionization chamber, which is under vacuum. Ionization is

induced by short pulses of laser light focused on the sample probe. In the most common configuration, MALDI sources are coupled to time-of-flight (TOF) mass analyzers.

Concerning the practical aspects, MALDI-MS is compatible with buffers and additives commonly used for isolation of proteins or peptides,²⁴⁻²⁶ except sodium dodecyl sulfate (SDS).²⁷ Sensitivity of sub-picomoles can be achieved and low femtomoles in special cases. ESI-MS is less tolerant to solvent conditions than MALDI. High concentrations of salts lead to signal suppression¹⁴ and clustering effects. Sensitivity of low femtomole can be achieved through miniaturization of the ESI source: fused silica capillary sources,²⁸ glass capillaries,²⁹ glass microchips,³⁰ and polymer micro-spray emitters³¹ for ESI-MS were constructed to enhance sensitivity of analyses.

The introduction of tandem MS or MS/MS, pioneered by Cooks et al.,^{32, 33} and the instrumental developments (introduction of an ion collision cell in the instruments) has expanded the field of mass spectrometry. From a parent ion mass, it became possible to analyze the products of fragmentation, induced by high or low energy collision. The fragmentation pattern of peptides being predictable, this allowed obtaining the complete or partial sequence of the peptide, thus improving the database search and enhancing protein identification.

The developments in mass spectrometry are ongoing. Fourier Transform Ion Cyclotron Resonance mass spectrometers (FTICR-MS), with their extremely high mass accuracy and baseline isotopic resolution have shown very promising results³⁴ and start to be a necessary tool for the analysis of high mass biomolecules, needing high accuracy.³⁵

3. Gel-based versus gel-free proteomics

Over the past decades, the overall sensitivity, accuracy, and dynamic range of mass spectrometers have improved drastically.⁸ This and the limitations of the traditional method (2D gel electrophoresis) to address the many challenges for comprehensive proteomics, combined to the increasing public availability of completely sequenced genomes,³⁶ have motivated the development of gel-free MS-based strategies to obtain information not accessible until then: gel-free, non gel, shotgun and other peptide-centric strategies. In these strategies, instead of analyzing the protein directly, its peptides are analyzed. The latter are generally more soluble than their precursors, and are more readily subjected to MS.

Another driving force behind the emergence of proteomics methods not based on 2D-GE has also been the coupling of reverse phase liquid chromatography (RP-LC) with automated MS/MS³⁷ (strategy usually called “shotgun proteomics”). In gel-free proteomics, the starting point is an enzymatic digestion step. Clearly, when digesting an already complex mixture of proteins with an enzyme, that on average is expected to hydrolyze a peptide bond every ten amino acids, the generated peptide mixture will be even more complex. Even with an approach like LC-MS/MS, this would result in identifying only a very small part of the whole proteome.³⁸

One way to reduce this complexity and increase proteome coverage is to include a different (orthogonal) chromatographic separation step prior to RP-HPLC. The most common of multidimensional peptide separations couples strong cation exchange (SCX) with RP-LC. This method, termed MudPit (Multidimensional Protein Identification Technology), which principle is shown on Figure 3, was shown by Yates et al. to be effective in overcoming some limitations of 2DE, such as membrane protein analysis and low-abundance proteins.^{39, 40}

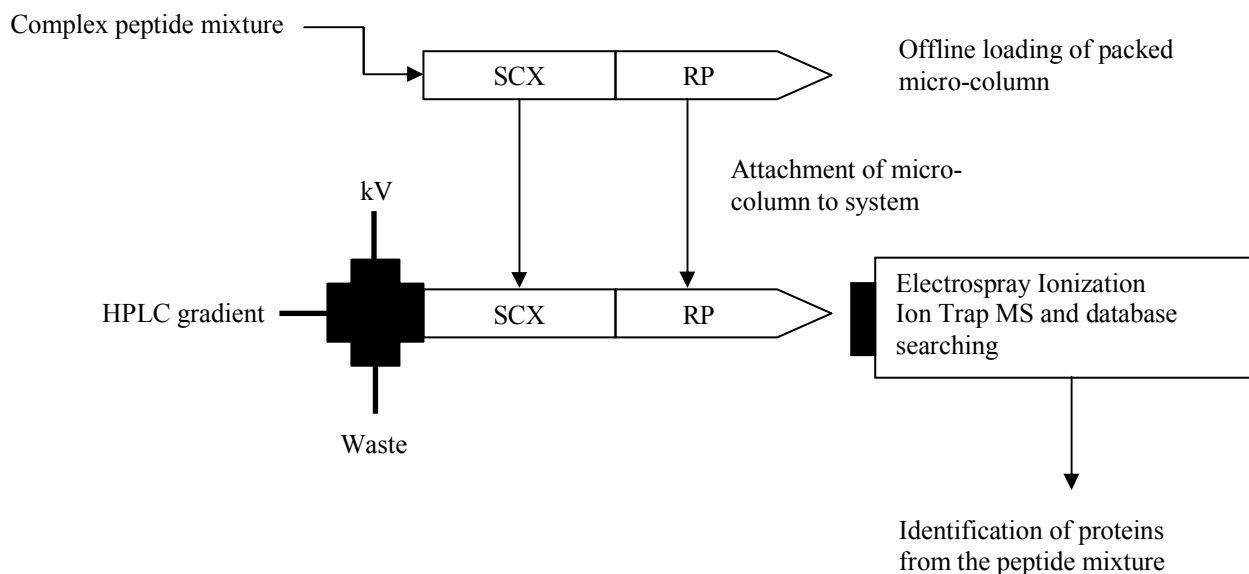


Figure 3: Principle of MudPit (Multidimensional Protein Identification Technology).

A variety of alternative non-gel based solution phase methodologies have also appeared recently as front end separations prior to automated MS/MS. The use of μ LC coupled to high resolution FTICR-MS has demonstrated high efficiency in resolving thousands of peptides with only one dimension of separation.⁴¹ Other multidimensional strategies have successfully combined electrophoretic and chromatographic fractionations, such as chromatofocusing with non-porous chromatography,⁴² or liquid phase IEF with RP-HPLC.⁴³ For a review on multidimensional fractionation methods, see Issaq et al.⁴⁴ In general, multidimensional peptide separation play an increasingly important role in the drive to identify and quantitate the proteome. By increasing the peak and load capacity, multidimensional approaches increase the number and dynamic range of peptides that can be analyzed in a complex biological organism. Separation methods using different physical properties of peptides have been combined with varying degrees of success.⁴⁵

4. Bottom up and top down approaches

The above described strategies, centered on peptide identification (peptide mass fingerprint or peptide sequence) to go up to the information on protein, belong to what is described as the “bottom up” approach. This approach is widely and successfully used today, numerous papers publish about the increase number of proteins identified compared to the classical 2D GE.⁴⁶⁻⁴⁹ “Shotgun” strategies also belong to this peptide-centered approach, this term designing strategies based on reverse phase LC separation of tryptic digests of whole cell lysate, coupled to MS or MS/MS.⁵⁰

However, while the “bottom up” strategy has turned out to be an excellent tool for the identification of a large number of proteins, complete sequence coverage of proteins is rarely achieved, thus limiting the ability to examine site-specific mutations and post-translational modifications of individual proteins, which are of utmost important in protein regulation. This justified the need for an alternative strategy, described by McLafferty et al.⁵¹ and called the “top down” approach, is based on the identification of native and intact proteins, using high accuracy mass measurement (FTICR), and performing MS/MS directly on the intact proteins,⁵² as described in Figure 4. Intact protein level analyses are generally less effective for protein identification than peptide level measurements, but offer insights unobtainable at the peptide level. Using electron capture dissociation (ECD), it was shown that post-translational modifications could be localized.⁵³

Both “bottom up” and “top down” approaches were successfully integrated in a comprehensive proteomics analysis, combining the capabilities of each approach.⁵⁴

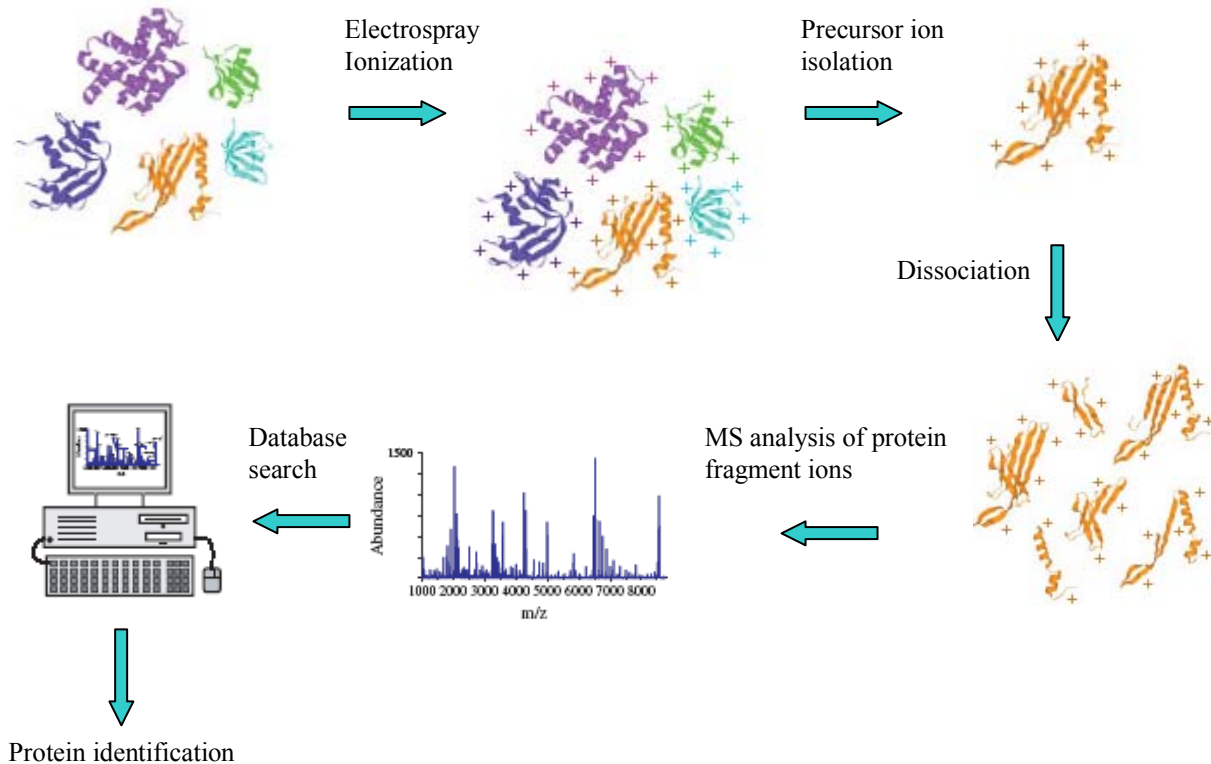


Figure 4: Schematic presentation of a top down experiment, adapted from⁵².

5. Chemical labeling for the enrichment and isolation of proteins

Despite the fact that mass spectrometers have become more powerful, easy-to-use and affordable in recent years, the successful outcome of proteomics projects relies also on the sample handling and pre-fractionation steps that reduce the enormous complexity of the protein mixtures obtained from biological systems.

In the context of an increasing use of gel-free “bottom up” approach based on liquid chromatography, a number of so-called tagging (or labeling) strategies have been developed that target specific amino acid residues or post-translational modifications, enabling the enrichment of subpopulations of peptides from the total digest (Figure 5), via affinity clean-up, resulting in the identification of an ever increasing number of proteins. For example, only those peptides that contain a certain amino acid will be targeted. Via chemical modification,

an affinity tag (*e.g.* containing a biotin moiety) is attached to the functional group of interest, allowing the sample to be purified by affinity chromatography (in this case, biotin-avidin chromatography). If a relatively rare amino acid like cysteine or tryptophan is chosen as a target, only a relatively small fraction of peptides will carry this residue, resulting in a significant reduction of sample complexity after the affinity separation. In most cases, it is still possible to deduce the parent protein from which the peptide was generated. With a similar strategy, it is also possible to isolate post-translationally modified peptides from a mixture.

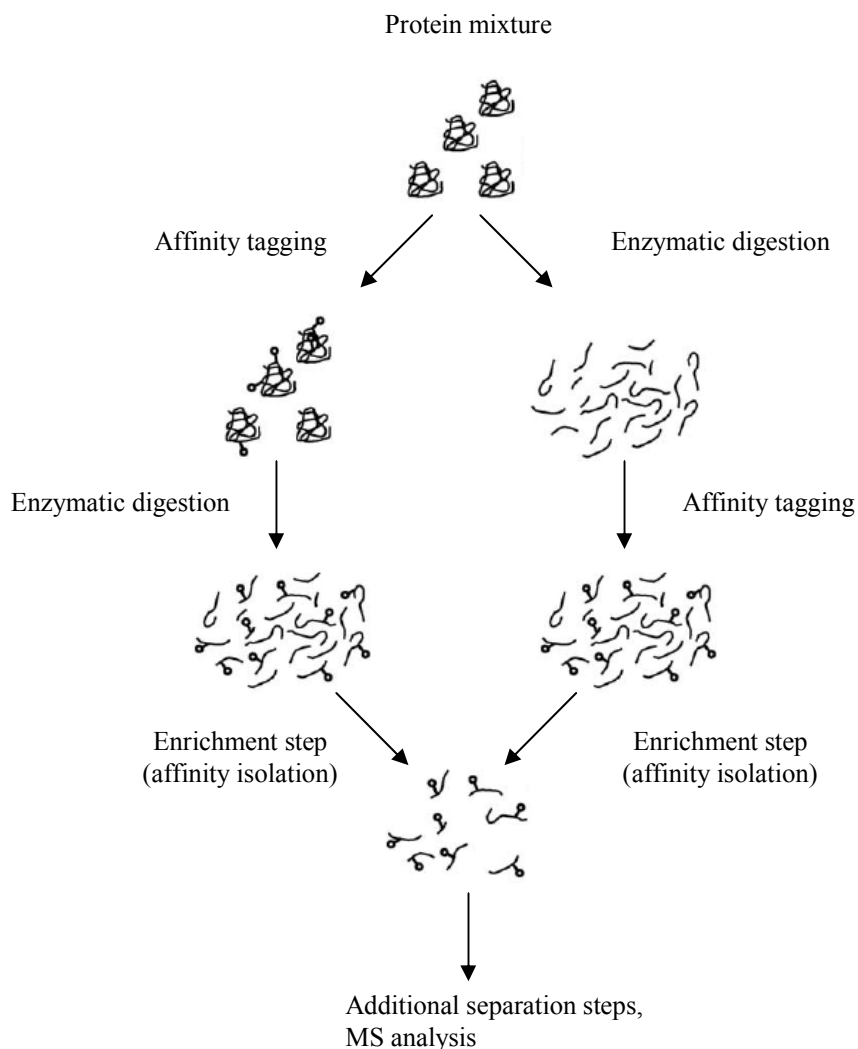


Figure 5: The use of chemical tagging strategies for sample fractionation. A protein mixture is either first labeled with an affinity tag and then digested (left) or first digested and then labeled (right). In both cases,

labeled peptides are subsequently enriched by an affinity chromatography step, so that ideally only the tagged peptides remain.

Frequently, affinity tagging is also combined with stable-isotope labeling to allow relative quantification of protein levels of two samples, *e.g.* representing two different cell states. This is for example very useful for comparing the expression of proteins in a variety of normal, developmental and disease states. Namely, one widely-used quantification method is the isotope-coded affinity tags (ICAT), developed by Aebersold et al.⁵⁵ Figure 6 illustrates the principle. One sample is labeled with an isotopically “light” tag (containing for example ^1H , ^{12}C , ^{14}N or ^{16}O), the other sample with the “heavy” tag containing ^2H (deuterium), ^{13}C , ^{15}N or ^{18}O . Samples are then combined and digested, and further isolated by affinity chromatography, prior to MS analyses. Thus, both forms of the peptides (light and heavy) are similarly affected by variations during the ionization process (*e.g.* suppression effects caused by co-eluting compounds in ESI, inhomogeneous crystallization in MALDI). The peaks corresponding to the light and heavy forms are shifted in mass spectrometry and this mass shift is constant and known from the structure of the tags reagents. Because light and heavy forms serve as mutual internal standards, the relative intensities of the two forms should accurately reflect the ratios of the peptides (and therefore the proteins) in the original samples.

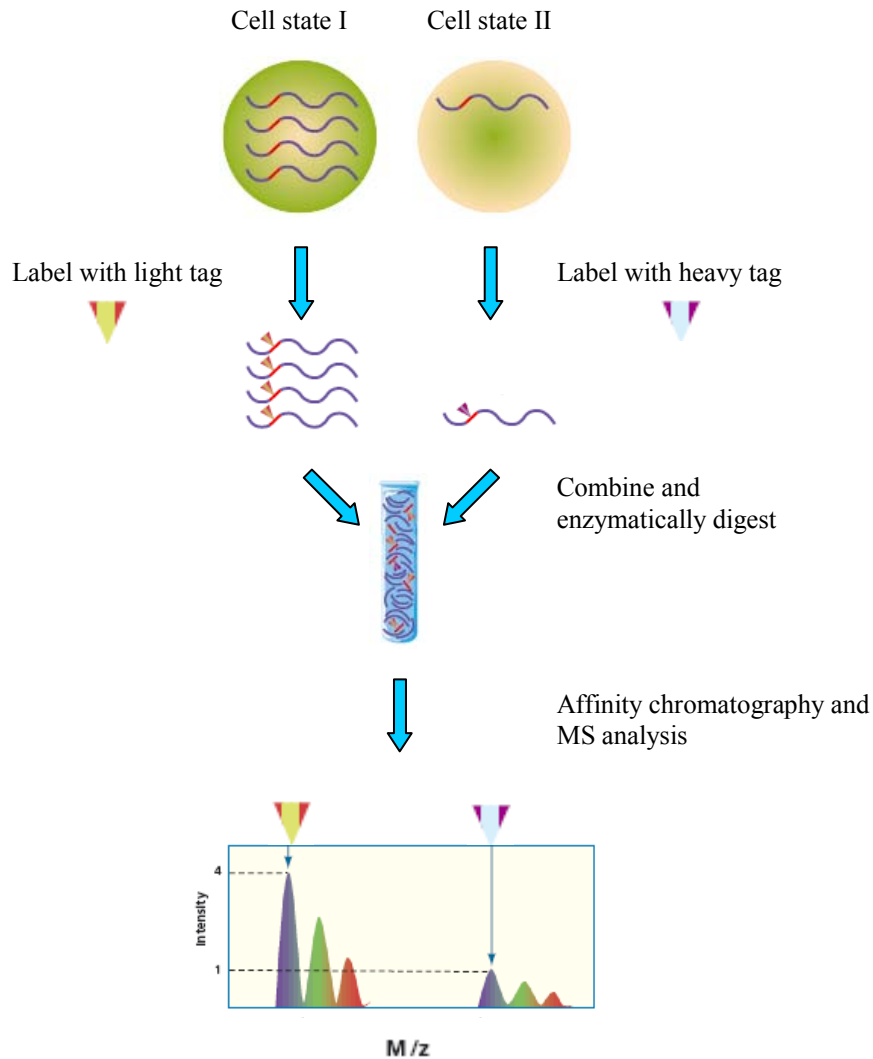


Figure 6: Principle of quantification by incorporation of stable isotope-coded affinity tags. Adapted from⁵⁶.

The labeling strategy can be implemented at different levels of the analysis (Figure 7), including *in vivo* incorporation of stable isotope containing amino acids to cell culture media (SILAC),⁵⁷ introduction of stable isotope chemical tags to isolated protein mixtures (ICAT),⁵⁵ labeling during protein proteolysis (^{16}O to ^{18}O exchange),⁵⁸ and labeling of peptides derived from enzymatic proteolysis (iTRAQ).⁵⁹

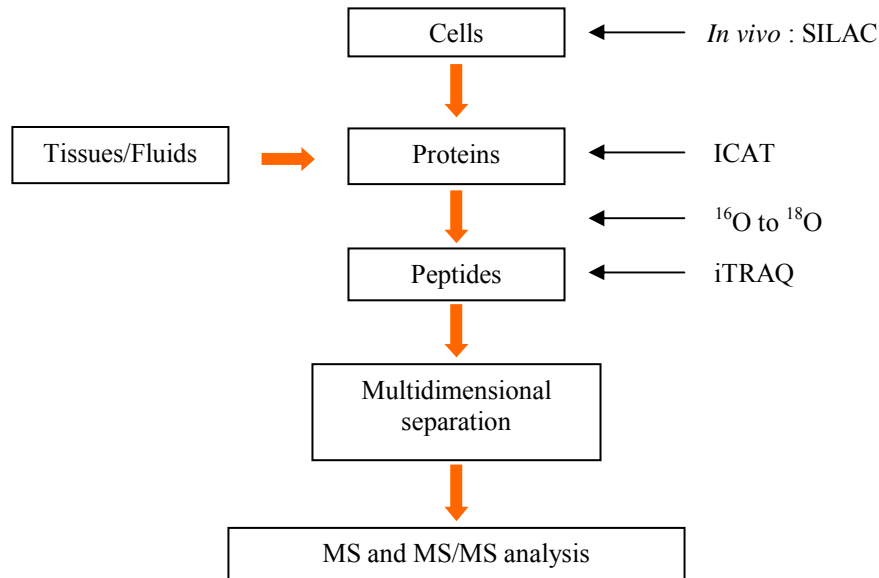


Figure 7: Summary of the commonly used stable isotope labeling strategies in comparative, quantitative proteomic experiments.

The particularity of SILAC, which is *in vivo* labeling, constitutes also one major limitation: its amenability to clinical protein samples such as those derived from tissues or fluids of patients. The enzymatic labeling of proteolyzed peptides with heavy oxygen (^{18}O) involves the proteolysis of proteins in the presence of light (H_2O^{16}) or heavy (H_2O^{18}) water. The hydrolytic activity of the protease (*e.g.* trypsin) results in the natural exchange of two oxygen atoms from the C-terminus of the peptides with two oxygen atoms from the surrounding water molecules. iTRAQ is based on amine reactive, isobaric, isotope tag reagents. This approach renders differentially labeled intact peptide masses indistinguishable, but produces diagnostic fragment peaks when selected for MS/MS analysis, that provide quantitative information on proteins.

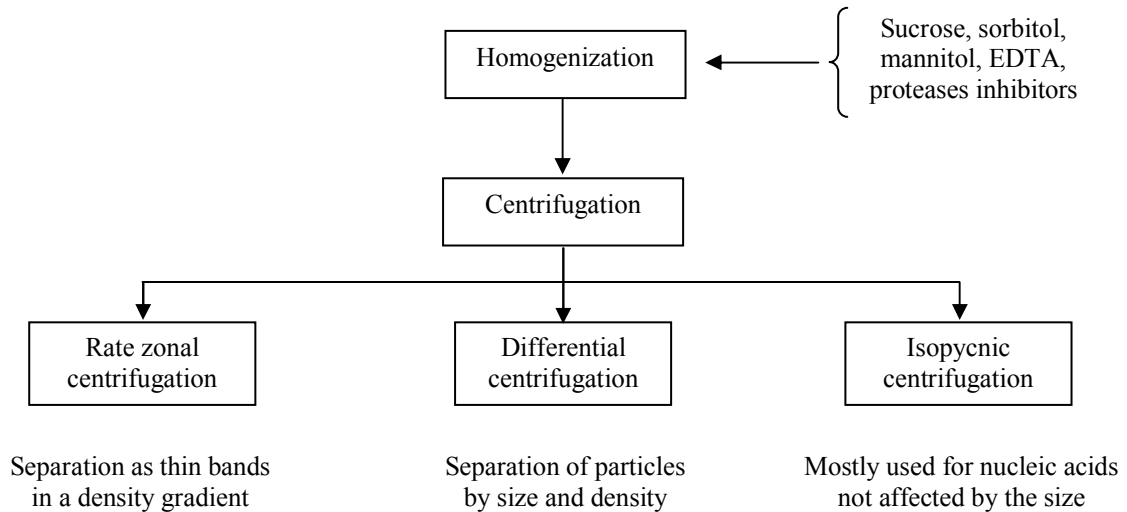
6. Why prefractionation techniques in proteomics?

Face to the challenging complexity of the mixtures to analyze, and more precisely, to the dynamic range in such mixtures, the development of effective fractionation and separation methods has become a critical component of any proteomic strategy. The dynamic range analyzed can reach 10-12 orders of magnitude when dealing with serum, plasma or cerebrospinal fluids (CSF).⁷ Prefractionation methods allow decreasing the dynamic range of the sample analyzed, and mining “below the tip of the iceberg”, for detecting the “unseen proteome”,¹⁹ meaning that the same set of proteins, *i.e.* the most abundant ones, is being re-discovered. Prefractionation techniques include fractional centrifugation, chromatographic and electrophoretic approach, as well as flow-field fractionation techniques, as reviewed below.

6.1. Fractional centrifugation

One of the oldest and still most effective methods to simplify a cell proteome is the separation of cell substructures by centrifugal fractionation. Via a series of run at different centrifugal forces (Figure 8), this technique allows isolating, in a reasonably pure form, subcellular organelles, such as nuclei, mitochondria, lysosomes, peroxisomes, etc. Clearly, it is the most direct method for enrichment of the desired protein fractions if one is studying the proteome of such organelles. Such a method has been recently re-discovered and widely applied in proteomics.⁶⁰⁻⁶⁴ In particular, centrifugal fractionation has been applied to the isolation of nuclei, and subsequently of nuclei matrix proteins. The fractionation allowed further successful analysis on a classical 2D gel.^{65, 66} Another main application is centrifugation by sucrose density gradient of mitochondria proteomes,^{67, 68} the method was shown to evidence

diseases that are related to mitochondrial dysfunctions, making it a powerful tool for diagnostics.



Size and density of some cell organelles

	Size (μm)	Density (g/cm^3)
Lysosomes	1-2	1.1
Ribosomes	0.02	1.6
Mitochondria	1-2	1.1
Nuclei	5-10	1.4

Figure 8: Schematic representation of cell substructure fractionation using centrifugation gradients.

6.2. Chromatographic approaches

Chromatographic methods are varied and allow the separation of analytes in complex mixtures in function of their distribution between two phases: a stationary phase and a mobile phase that percolates through the stationary phase. The analytes enter the column with the mobile phase, and migrate at different rates, depending on their affinity for each of the phase,

which provides separation. Many types of chromatography have been used, and only the principle of some will be shortly described. For extended review, see reference⁶⁹.

Ion-exchange chromatography uses stationary phases that bind proteins according to their charge. The elution is performed with increasing salt concentration buffers. The non-denaturing conditions limit the analysis to soluble proteins only. Fountoulakis et al.⁷⁰ successfully detected low-abundant proteins of the bacterium *H. Influenzae*. Strong cation exchange belongs to this category of chromatography and has been widely-used as a first dimension separation for proteomics,⁷¹⁻⁷³ or in MudPit as mentioned in section 3.

Reverse Phase liquid chromatography (RP-LC) separates proteins according to their hydrophobicity. Proteins are adsorbed on a stationary phase carrying hydrophobic groups, and are eluted with increasing concentration of acetonitrile. It is one of the most widely used type of chromatography in proteomics, namely in shotgun multidimensional strategies. Normal phase chromatography (polar stationary phase and mobile phase non-polar, in contrast to reversed-phase) is not so much used in proteomics, due to the poor compatibility of normal phase solvent and ESI-MS and low reproducibility compared to RP-HPLC. Recently however, it has become useful as chiral chromatography technique, to analyze enantiomeric bioactive lipids, using electron capture atmospheric chemical ionization/tandem mass spectrometry.⁷⁴

Affinity chromatography is based on the interaction between a particular compound constituting the stationary phase, and a subset of proteins. The nature of the compound used determines the range of proteins that bind to the column. For example, monoclonal antibody will bind a single protein, heparin and hydroxyapatite phase will bind thousands of proteins.

Heparin affinity chromatography uses gels containing heparin, a natural mixture of linear polymeric sulfated glycosaminoglycan, which has the highest negative charge density observed in biological molecule. This property also makes it a strong cation exchanger (SCX),

with affinity for a broad range of proteins, such as coagulation factors, nucleic acid-binding proteins (protein synthesis factors) or growth factors. An illustration of this technique is the work of Fountoulakis et al.,⁷⁵ who separated the soluble proteins of *H. Influenzae* and showed the enrichment of low-abundant proteins.

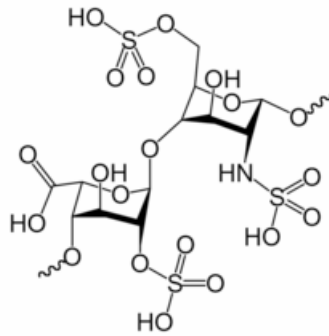


Figure 9: Heparin

Hydroxyapatite affinity chromatography uses a matrix carrying positively charged (calcium) and negatively charged (phosphate) sites. Proteins are retained in two ways, either by non-specific electrostatic interactions between their positive charges and the general negative charge of the hydroxyapatite when equilibrated in phosphate buffer, or by complexation of the proteins carboxyl sites with the calcium sites. Elution is performed by increasing salt concentration buffer. Fountoulakis et al. showed the fractionation of *E. coli* soluble proteins.⁷⁶

More interestingly, immunoaffinity columns are increasingly used for the depletion of high abundance proteins, to enhance sensitivity in proteome analysis, especially when dealing with plasma or serum samples (high complexity). This type of column was shown to be particularly useful for the detection of biomarkers in plasma.^{77, 78} Currently, there are three multi-parameter depletion resins commercially available: (a) the multiple affinity removal system (MARS) from Agilent Technologies, targeting 6 abundant plasma proteins (b) an IgY-based immunoaffinity resin against 12 individual proteins developed by Genway and now

commercialized by Beckman Coulter for the ProteomeLab IgY system, and (c) the ProteoPrep 20 immunodepletion kit from Sigma, to remove 20 different plasma proteins.

Size-exclusion chromatography separates proteins according to molecular mass, like the second dimension of 2D-GE. However, the main difference is the non-denaturing conditions of the chromatography, allowing studying protein complexes.⁷⁹ This technique is also called gel filtration and uses dextran derivatives-gels (Sephadex gels). A recent illustration of the technique is Hu.⁸⁰

A summary of these approaches and the physicochemical properties underlying the separation process is given in Table 1.

Table 1: Summary of fractionation methods and the physicochemical properties according to which the separation is performed.

Fractionation method	Physicochemical properties
Ultracentrifugation	Density
SCX, Ion-Exchange Chromatography	Charge
Reverse phase Chromatography (RP)	Hydrophobicity
Affinity Chromatography (heparin, hydroxyapatite)	Specific biomolecular interactions (Affinity + Charge)
Size Exclusion Chromatography	MW (Stokes radius)
Isoelectric focusing	pI
Gel electrophoresis	MW (Stokes radius)

One can also distinguish between analytical and preparative chromatography. Preparative elution chromatography is generally carried out under mass overload: the sample concentration is increased beyond the linear adsorption region, resulting in asymmetric band profiles, while analytical chromatography remains in the linear adsorption range. The main

difference lies in the working flow rates (a few up to 30 mL/min in preparative mode, and a few $\mu\text{L}/\text{min}$ in the analytical mode) and the collection of fractions (preparative) or not (analytical).

As a conclusion, chromatographic methods can be powerful tools for enrichment of low-abundance proteins prior to 2DE. However, the enrichment of abundant proteins is achieved simultaneously as for low-abundant ones. No clear correlation exists between the elution profile and a particular functional class of proteins. And the main drawback is the protein loss due to adsorption inherent to the technique. In addition, the sometimes large amount of salts (depending on which chromatography is used) and the large volumes of eluted fractions constitute significant challenges to the subsequent analysis of chromatographic fractions. Concentration and desalting steps are thus necessary, increasing the risk of protein loss.

In addition to prefractionation use, chromatographic methods have also been used in a two dimensional approach (MudPit, typically combination of strong cation exchange with RP). These powerful methods represent a way to overcome the limitations of 2DE, particularly for high MW and hydrophobic proteins. However, some limitations remain. Highly hydrophobic proteins are difficult to digest and necessitate additional cleavage steps. Low MW proteins are also a challenge due to the insufficient number of peptides available for MS analysis.

6.3. Electrophoretic approaches

The use of classical electrophoretic methods has been hindered by the limited loading capacity, but many improvements have been made, due to new instrumental developments. Most electrophoretic methods are based on isoelectric focusing (IEF) separation. Below is a non-exhaustive review of IEF-based methods only.

ROTOFOR

It is in 1998 that Bier, who had long been working on preparative electrophoretic separations in free zone, developed the concept of the Rotofor (rotationally stabilized focusing apparatus), based on recycling carrier ampholytes IEF.⁸¹ The device is today commercialized by BioRad. A typical instrumental setup is presented in Figure 10.

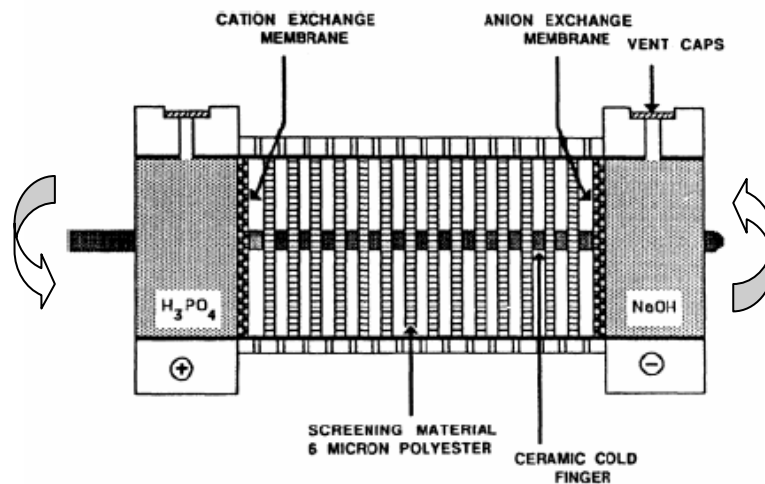


Figure 10: Schematic presentation of the Rotofor instrument. Rotation and the screen partitioning are essential for good separations. Reprinted from⁸¹

The apparatus is assembled from 20 sample chambers, separated by liquid-permeable nylon screens, except at the extremities, where cation- and anion-exchange membranes are placed against the anodic and cathodic compartments, respectively, to prevent diffusion within the sample chambers of undesired electrodic products. The whole setup is rotated along the axis perpendicular to the chambers, thus avoiding decantation. The initial purpose of the Rotofor was for preparative use, with a loading capability of up to 1 g of protein in a total volume of up to 55 mL. A mini-Rotofor, with a reduced volume of 18 mL is also available, and recently a micro-Rotofor sold by Bio-Rad as well.⁸²

The resulting pI fractions can then further be used for analysis on a conventional 2D gel electrophoresis.⁸³ But IEF with the Rotofor can also be integrated as a first dimension in a 2D methodology.⁴³ The fractions are further analyzed by RP-HPLC in a second dimension, each LC peak is then collected and tryptically digested, before being subjected to MALDI-MS analysis. This method was successfully applied to many challenging biological protein mixtures.^{43, 84, 85} The pI accuracy of this method was estimated to range from ± 0.65 to ± 1.73 pI units. More recently, Xiao et al. reported the application of the Rotofor for the fractionation of tryptic peptides from human serum in an ampholyte-free environment, and showed an “autofocusing” effect.⁸⁶

CONTINUOUS FREE FLOW ELECTROPHORESIS (FFE)

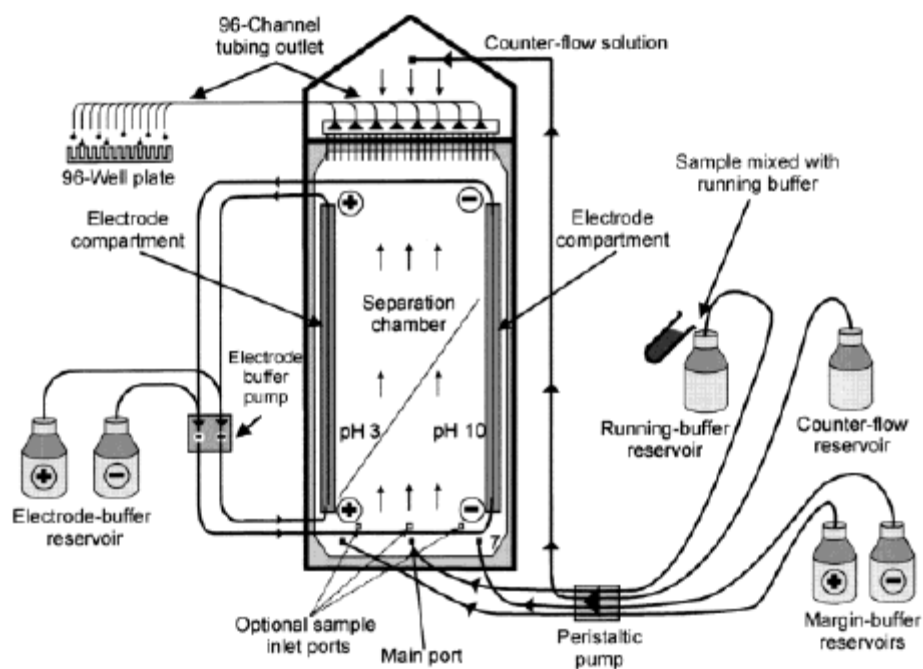


Figure 11: Schematic presentation of the Free Flow electrophoresis setup (commercial name Octopus). Separation chamber dimensions are $50 \times 10 \times 0.4$ cm (50 cm electrode length, 10 cm between electrodes and 0.4 cm chamber depth). Focused protein samples are collected into 96-well plates *via* an in-line multichannel outlet. The volume of each fraction is typically ~ 2 mL. Reprinted from⁸⁷

This liquid-based IEF technique was described in 1982 by Hannig⁸⁸ and more recently reviewed by Bocek et al.⁸⁹ A commercial version exists under the name of Octopus.⁹⁰ In FFE, the sample is injected continuously into a carrier ampholyte solution flowing as a thin film (0.4 cm thick) between two parallel plates and, by introducing an electric field perpendicular to the flow direction, proteins are separated by IEF according to their different *pI* values and finally collected into up to 96 fractions (Figure 11). Two main advantages of this method are the recovery of liquid fractions, and the sample loading capacity due to continuous sample feeding. FFE was used as prefractionation tool before 2D-GE,⁹¹ or integrated as a first dimension in a 2D strategy.^{92, 93} Conventional FFE was initially developed as a preparative-scale technique for isolation and purification purposes, but further developments have led to micro-fabricated devices (mFFE or μ FFE), reported by Kobayashi et al.,⁹⁴ and Manz and co-workers.⁹⁵⁻⁹⁷

MULTICOMPARTMENT ELECTROLYZERS WITH ISOELECTRIC MEMBRANES

Another apparatus that has also proved its efficiency is the multicompartiment electrolyzers (MCE) designed by Righetti et al.^{98, 99} The device is constituted of multiple compartments, separated by a polyacrylamide gel membrane with a specific pH produced by immobilines that are incorporated into the polyacrylamide membranes (Figure 12). Thus, the principle is to capture proteins in an isoelectric trap formed by two Immobiline membranes having *pI* values encompassing the *pI* of the protein under analysis.

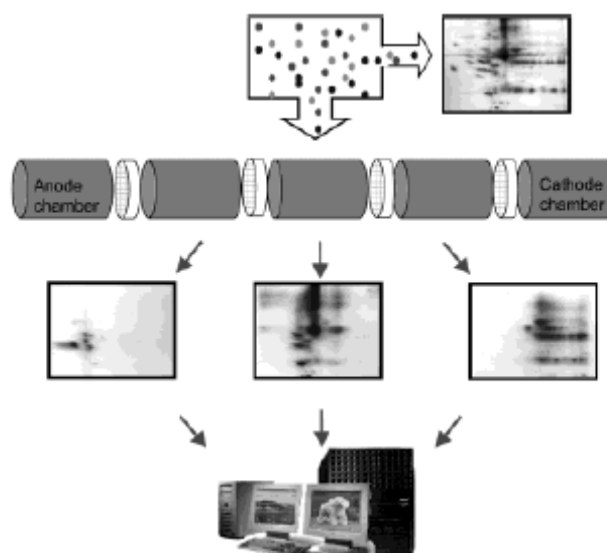


Figure 12: Schematic presentation of the multicompartiment electrolyzers. The upper right panel shows a 2D map of unfractionated sample *vs.* three different 2D maps (lower panel) of three isoelectric fractions, captured into traps having membranes with pI s 3-5, 5-6 and 6-10.5. Reprinted from¹⁰⁰.

A commercial apparatus, called IsoPrime, incorporating this principle has been marketed (Amersham Biosciences, Piscataway, NJ, USA). The commercial unit has been developed primarily for large scale purification (about 30 mL). The device was later miniaturized for proteomics purpose^{101, 102} and could detect low abundance proteins unseen until then. Good results have also been obtained by Zuo et al. with the same type of apparatus being used as prefractionation tool.^{103, 104}

While most of these devices can provide reasonable to high quality separations, the limitations encountered with either the Rotofor or the IsoPrime are the following: (1) they require a large sample volume; (2) they produce large volume, dilute fractions that need to be concentrated with attendant losses.

OFFGEL

Contrary to the previously mentioned devices, the OFFGEL was designed for analytical to semi-preparative purposes, the volumes required are much smaller compared to other techniques. However, just like the MCE, OFFGEL has been devised for IEF separation with direct recovery in solution, and without adding ampholytes to form the pH gradient.¹⁰⁵

The principle is to place a sample in a liquid chamber positioned on top of an IPG gel. The gel buffers a thin layer of the solution in the liquid chamber and the proteins are charged according to their pI values and to the pH imposed by the gel. Theoretical calculations have shown that the protonation of an ampholyte occurs in the thin layer of solvation close to the IPG gel/solution interface.¹⁰⁶ Upon application of a voltage gradient perpendicularly to the liquid chamber, the electric field penetrates into the channel and moves all charged species (those having pI above and below the pI of the IPG gel under the chamber) out of the chamber. After separation, only the globally neutral species ($pI = \text{pH}$ of the IPG gel) remain in solution. This technique offers high separation efficiency and allows easy recovery of the purified compounds directly in the liquid phase. In further developments, the OFFGEL electrophoresis format was adapted to a multicompartment device (Figure 13), composed of a series of chambers of small volumes (100-300 μL).¹⁰⁷

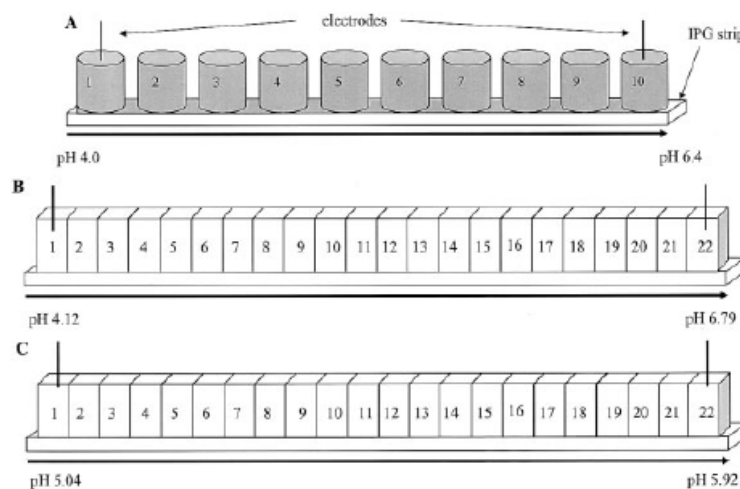


Figure 13: Schematic presentation of the multicompartment OFFGEL device. Reprinted from¹⁰⁷

The resolution thus depends on the pH gradient of the underlying IPG gel, and of the number of compartments for recovery. A resolution of 0.1 pH units could be obtained when operating in narrow ranges, for example the separation of β -lactoglobulin A and B. The capability of the multicompartiment device to fractionate complex biological mixture was also demonstrated, by the fractionation of an *E. coli* cell extract. Further developments were done and this device is now being commercialized by Agilent Technologies since last year.

The main concern about electrophoretic methods is to design instruments that effectively dissipate Joule heat or to limit that heating. In the Rotofor and multicompartiment electrolyzers for example, there is a cooling system that allows temperature control during electrophoresis. For the commercial OFFGEL, the electrophoresis is performed on a cooling plate, allowing that control. But another way to limit this Joule heating is to control the maximum current/power allowed. For example, this is done in the OFFGEL device, by limiting the current to few hundreds of micro-amperes.

A summary of electrophoretic methods is given in Table 2.

Table 2: Summary of electrophoretic methods and the volumes needed.

Electrophoretic methods	Usual volumes loaded	Use*
Rotofor: - preparative, mini	55 mL, 18 mL	P, SP
- micro	2.5 mL (ref. ⁸²)	A
Free Flow Electrophoresis (FFE)	Chamber: 50 (width) \times 10 (length) \times 0.4 (depth) cm	P
- continuous FFE	2 mL/fraction	
- micro devices mFFE and μ FFE	300 μL (ref. ⁹⁴) and 0.2 μL (ref. ⁹⁶) respectively	A
Multicompartiment Electrolyzers	30 mL up to 125 mL (IsoPrime device) (ref. ¹⁰³)	P
- miniaturized	500 μL/chamber \times 3 chambers = 1.5 mL (ref. ¹⁰³)	A
OFFGEL	100–300 μL/chamber \times 10–20 chambers = 1–6 mL	SP, A

* P = preparative, SP = semi-preparative, A = analytical use

6.4. Field-Flow Fractionation (FFF)

Recently, many papers have been published, describing the use of field-flow fractionation techniques for proteomics.¹⁰⁸⁻¹¹³

FFF is based on the simultaneous action of laminar flow of a carrier liquid inside a separation channel and an external physical field (acting perpendicularly to the flow direction). Clearly, FFF combines elements of elution methods and methods based on external force fields. The activity of an external field differentiates FFF from chromatography, but it cannot be classified as an electrophoretic method either, because the external field does not cause separation directly. It induces the motion of analytes to different positions across the channel, where the non-uniform flow velocity profile causes differential migration of analytes. Thus, their separation takes place in the longitudinal direction, perpendicularly to the field direction.

According to the nature of the external field, different FFF techniques can be described: sedimentation FFF, thermal FFF, electrical FFF and flow FFF (for theory, see¹¹⁴).

The last two techniques are of main interest for the separation of proteins.

In electrical FFF, an external electric field is applied perpendicularly to the separation channel, as shown in Figure 14.

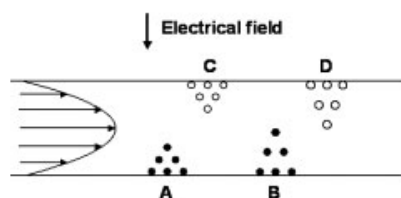


Figure 14: Separation of anionic (A, B) or cationic (C, D) species in various channels for electrical FFF, reprinted from¹¹⁵.

Interestingly, a variant of electrical FFF was described with the application of pH gradients, and called IEF FFF or hyperlayer electrical FFF. The separation of horse myoglobin components in a trapezoidal cross-section channel (Figure 15) was described,¹¹⁶ and later a model mixture of proteins was also fractionated.¹¹⁷ The performances of this technique were however not stable enough, due to the hydrodynamic flow. It was later supplanted by CIEF, which offers a more stable (electro-osmotic) flow and better resolution.

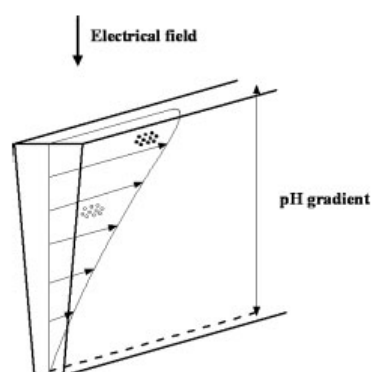


Figure 15: Separation of two amphoteric compounds in the trapezoidal channel for IEF FFF. Reprinted from¹¹⁵.

Recently, a rapid non-gel based 2D separation method was introduced for protein analysis, by Kang and Moon.¹¹³ It consists in the combination of pI -based separation by CIEF, followed by molecular mass-based separation in a hollow fiber by flow FFF.

Flow FFF is the most frequently and successfully used FFF technique for protein separation. It uses a fluid flow across the channel membrane to transport sample to the accumulation wall. This can be done either by using a second fluid flow across the channel, or by splitting the inlet flow into two flows, one eluting analytes towards the detector, and the other is a crossflow of the carrier liquid out of the channel, as described in Figure 16. All sample components are displaced with the same velocity towards the permeable wall. As a result, analytes are separated based on the differences in their diffusivity. The elution order is according to increasing protein molecular weight.

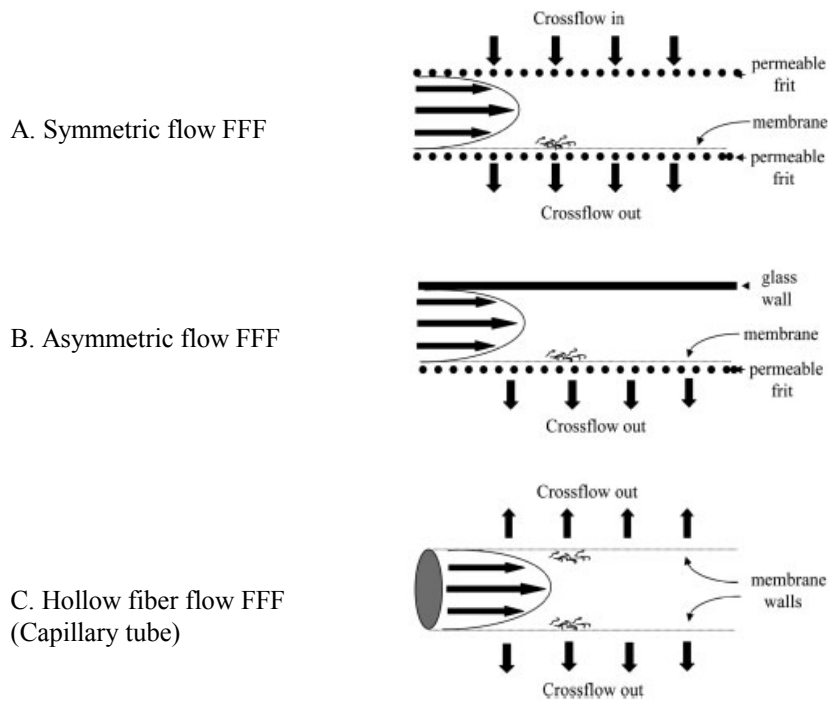


Figure 16: Examples of channels for flow FFF. Reprinted from¹¹⁵.

The advantages of flow FFF in comparison to chromatographic techniques are mainly the mild conditions of separation (lower pressure, smaller contact area of the analytes), which contribute to maintaining native protein conformations and allows the study of large protein complexes,¹⁰⁸ making this technique very attractive for “top-down” proteomics strategies, or for analysis of PTMs. Further instrumental developments should reveal the potential of these techniques for proteomics analyses.

Concluding remarks on prefractionation methods

With the advent of many gel-free fractionation techniques, efforts to develop devices to perform IEF in liquid phase, multi-dimensional chromatography strategies, one can wonder where the place of 2D-GE is today. Is it still predominant in proteomics? From our observations, highly sophisticated labs in Switzerland, either public or private, still use 2D GE

as the method of choice for routine analysis of proteomics. Why are the gel-free developed methods so difficult to implement in a proteomics routine?

The reason may be that most studies are comparative and thus, it is easier to compare results of 2D-GE between themselves. But one should add too, that despite its limitations, 2D-GE is still the method that allows giving most information at the same time, compared to others. And probably too, that until now, the rush into proteomics mainly consisted in looking for the most obvious data, the high abundant proteins, but scientists are no more satisfied with re-discovering the proteome, because it is believed that in the unseen proteome lie the keys to understanding mechanisms of regulation of proteins.

7. On transfer of proteins

One of the main challenges of separation techniques today is the loading capacity. Indeed, to detect the low abundance proteins (the “unseen proteome”¹⁹), it is very often necessary to increase the concentrations loaded on the separation device. This usually leads to problems such as decrease in resolution, or protein precipitation/aggregation.¹¹⁸ To overcome these limitations, as well as allow a continuous separation, the idea is to perform continuous online extraction of the proteins separated, to allow a continuous sample loading. In addition, this would allow continuous focusing, opening the possibility for enrichment of proteins.

In parallel, increasing interest has been devoted to the electrochemical transfer of biomolecules at the liquid-liquid interface (mostly water/organic solvent). Electrochemistry at the interface between two immiscible electrolytes (ITIES) has been extensively used for the study of transfer mechanisms for ions and ionizable drugs.¹¹⁹⁻¹²⁵

Concerning the transfer of amino acids across liquid-liquid interface, numerous papers can be cited, namely Shao et al. did a systematic study of the transfer, at micropipet electrode, of amino acids, facilitated by dibenzo-18-crown-6 (DB18C6).¹²⁶ Recently, Osakai et al. used

a voltammetric approach to study the transfer of amino acids, as well as di- and tripeptides, in the presence or absence of DB18C6 in nitrobenzene, to determine their hydrophobicity.^{127, 128} Other approaches with three-phase electrodes have also been used for peptide ions.^{129, 130}

Besides, numerous works also relate to the transfer of low molecular-weight polypeptides such as protamine and heparin across a liquid-liquid interface. The facilitated transfer of protamine in the presence of a negatively charged sulfonate ionophore was reported.^{131, 132} Since water-soluble proteins contain ionizable groups on their surface, and can even be considered as polyelectrolytes, there was much interest in extending this study to the transfer of proteins as well.

It was noted that to observe protein transfer across a liquid-liquid interface, it is necessary to decrease their re-solvation energy in the organic phase.¹³³ For that reason, an approach consisting in the formation of micelles was used. The usual four-electrode system was however not compatible with the micelle approach, due to breakdown of the interface at large surfactant concentration, and polarity of the solvent (micelles form only in non polar solvents). A solution described by Karyakin et al.,¹³³⁻¹³⁵ consisted of a special carbon electrode shielded with a layer of organic solvent containing a redox mediator. They managed to show the transfer of a few proteins (the highest molecular weight studied was 88 kDa). More recently, the transfer of proteins by reverse micelles was measured by voltammetry with a three-electrode setup (Figure 17).^{136, 137}

The observation of electroactivity of redox-inactive proteins at liquid-liquid interface is important and opens new horizons for electro-analytical chemistry, in particular in proteomics.

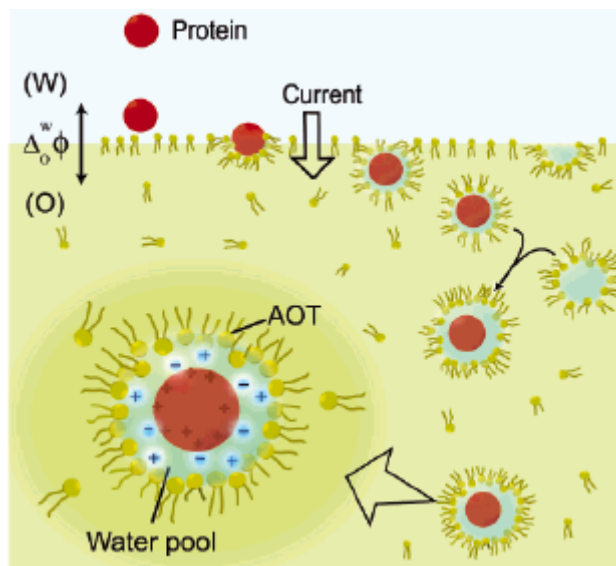


Figure 17: Possible mechanism for reverse-micelle electro-extraction of proteins, reprinted from¹³⁶.

8. Objective of the work

In the context of prefractionation methods for proteomics, this work deals mainly with the development of electrophoretic tools for isoelectric focusing of peptides and proteins for the analysis of biological complex mixtures.

In the light of existing devices for IEF, the objective is to develop a multicompartiment OFFGEL device, designed for the IEF of peptides in the perspective of shotgun proteomics (analysis of peptides derived from proteins). The choice of the OFFGEL for IEF among other techniques is justified as OFFGEL allows the recovery of liquid fractions of peptides, of small volumes, and that are further amenable to liquid chromatography (as a second dimension separation) or mass spectrometry analyses.

The resolution is a key point to consider in the design of such a unit, as well as the volumes required. If the device is designed for biological samples, the range of volume loaded will be the same order of magnitude as for analytical or semi-preparative purposes (hundreds

of μL to few mL). The resolution depends on the IPG gel used, as well as the dimensions of the compartments and the distance between them.

In such a device, the separation is performed mainly in the gel. Even though the collection of fractions is done in solution, the limiting step is still the migration in the gel. Thus, another objective is the design of a completely gel-free separation unit. However, the isoelectric focusing process requiring a pH gradient, the use of carrier ampholytes is then necessary, instead of a gel. This gel-free approach (justifying the title) should allow faster focusing of proteins, retaining the advantages of recovering liquid fractions at the end of the separation, and the small volumes, making it convenient for analytical purposes.

Finally, face to the usual problems encountered when loading a high quantity of sample on the separation unit (deterioration of resolution, precipitation of proteins at their pI), the final objective was to perform online extraction of proteins/peptides during IEF separation. This would allow continuous focusing, opening the possibility for enrichment of proteins. For that purpose, an electrochemical system was envisaged, allowing the transfer of species to another phase. The electrochemical cell was first tried on model molecules, to ensure the transfer of ionizable species at the liquid-liquid interface between two immiscible electrolytes (ITIES).

This thesis is thus articulated into the following sections:

Chapter II first describes the theory concerning isoelectric focusing, gives a mathematical description of the equations of IEF, the generation of the pH gradient, by carrier ampholytes (CA) and immobilized pH gradients (IPG), as well as an evaluation of the conductivity and buffer capacity of the species forming the pH gradient. It also discuss the use of IPG and CA nowadays.

Chapter III describes the numerical simulation of the IEF of peptides in an OFFGEL device. It illustrates how the mobility near pI is an important parameter for the IEF kinetics and the peak shape at steady state. With the help of an *in silico* digestion of three proteomes and the calculation of the distribution of the peptide mobility near pI , a width of the well could be deduced, to have best separation, with the recovery of peptides in at most two wells. The global study illustrated the high focusing power of the OFFGEL technique as a separation tool for shotgun proteomics application.

Chapter IV is the design and characterization of a multicompartiment OFFGEL device, based on the results of the simulations in chapter III. The reproducibility of the pH gradient (one important requirement for reproducible separations) was checked, the loading capacity evaluated for proteins, and a demonstration of the high resolution separation of peptides and proteins from a complex biological mixture was performed.

Chapter V illustrates the use of OFFGEL IEF and the inherent information obtained on the pI of peptides, as an efficient tool for the validation/filtering of peptides, thus allowing the elimination of false positives and more accurate protein identification in a shotgun approach. The isoelectric focusing was then combined to the chemical tagging of cysteinyl peptides, in order to enhance the level of confidence in the identification step. These two tools combined together (OFFGEL IEF and chemical tagging) were shown to be highly valuable for building a strategy for the improved identification of proteins by Peptide Mass Fingerprinting (PMF).

Chapter VI is the design of a completely gel-free device for IEF, to be used in the presence of carrier ampholytes. Like the OFFGEL, it has the advantage of small volumes fractions and

is easy-to-use, requiring no special equipment. The fractionation of biological samples of *E. coli* and human cancer cells showed a rapid separation of proteins, demonstrating that this IEF separation mode has high potential for fast prefractionation of proteomes.

Chapter VII is an excursion on the transfer of ionizable species by electrochemistry at the interface of two immiscible electrolytes (ITIES). This study was initially motivated by some recently interesting works on the electrochemical transfer of peptides and proteins at ITIES, cited in the previous pages. A setup was designed for the study of the transfer of ionizable species at a micro-ITIES, which is originally supported by an IPG gel as the aqueous phase and a small drop of organic phase. The use of this device for the transfer of model molecules was demonstrated.

The chapters have been written with the possibility to be read independently. Thus, to facilitate the independent reading, the experimental techniques used are sometimes described more than once.

9. References

1. http://www.ornl.gov/sci/techresources/Human_Genome/home.shtml.
2. Wasinger, V. C.; Cordwell, S. J.; Cerpapalj, A.; Yan, J. X.; Gooley, A. A.; Wilkins, M. R.; Duncan, M. W.; Harris, R.; Williams, K. L.; Humpherysmith, I., Progress with Gene-Product Mapping of the Mollicutes - Mycoplasma-Genitalium. *Electrophoresis* **1995**, 16, (7), 1090-1094.
3. Anderson, N. L.; Anderson, N. G., The human plasma proteome - History, character, and diagnostic prospects. *Molecular & Cellular Proteomics* **2002**, 1, (11), 845-867.
4. Graves, P. R.; Haystead, T. A. J., Molecular biologist's guide to proteomics. *Microbiology and Molecular Biology Reviews* **2002**, 66, (1), 39-+.
5. Anderson, L.; Seilhamer, J., A comparison of selected mRNA and protein abundances in human liver. *Electrophoresis* **1997**, 18, (3-4), 533-537.
6. Hochstrasser, D. F.; Sanchez, J. C.; Appel, R. D., Proteomics and its trends facing nature's complexity. *Proteomics* **2002**, 2, (7), 807-812.
7. Corthals, G. L.; Wasinger, V. C.; Hochstrasser, D. F.; Sanchez, J. C., The dynamic range of protein expression: A challenge for proteomic research. *Electrophoresis* **2000**, 21, (6), 1104-1115.
8. Patterson, S. D.; Aebersold, R. H., Proteomics: the first decade and beyond. *Nature Genetics* **2003**, 33, 311-323.
9. Ofarrell, P. H., High-Resolution 2-Dimensional Electrophoresis of Proteins. *Journal of Biological Chemistry* **1975**, 250, (10), 4007-4021.
10. Klose, J., Protein Mapping by Combined Isoelectric Focusing and Electrophoresis of Mouse Tissues - Novel Approach to Testing for Induced Point Mutations in Mammals. *Humangenetik* **1975**, 26, (3), 231-243.
11. Gorg, A.; Postel, W.; Gunther, S., The Current State of Two-Dimensional Electrophoresis with Immobilized Ph Gradients. *Electrophoresis* **1988**, 9, (9), 531-546.
12. Gorg, A.; Obermaier, C.; Boguth, G.; Harder, A.; Scheibe, B.; Wildgruber, R.; Weiss, W., The current state of two-dimensional electrophoresis with immobilized pH gradients. *Electrophoresis* **2000**, 21, (6), 1037-1053.
13. Gorg, A.; Weiss, W.; Dunn, M. J., Current two-dimensional electrophoresis technology for proteomics. *Proteomics* **2004**, 4, (12), 3665-3685.
14. Patterson, S. D.; Aebersold, R., Mass-Spectrometric Approaches for the Identification of Gel-Separated Proteins. *Electrophoresis* **1995**, 16, (10), 1791-1814.
15. Yates, J. R., Mass spectrometry and the age of the proteome. *Journal of Mass Spectrometry* **1998**, 33, (1), 1-19.
16. Gevaert, K.; Vandekerckhove, J., Protein identification methods in proteomics. *Electrophoresis* **2000**, 21, (6), 1145-1154.
17. Wittmann-Liebold, B.; Graack, H. R.; Pohl, T., Two-dimensional gel electrophoresis as tool for proteomics studies in combination with protein identification by mass spectrometry. *Proteomics* **2006**, 6, (17), 4688-4703.
18. Gygi, S. P.; Corthals, G. L.; Zhang, Y.; Rochon, Y.; Aebersold, R., Evaluation of two-dimensional gel electrophoresis-based proteome analysis technology. *Proceedings of the National Academy of Sciences of the United States of America* **2000**, 97, (17), 9390-9395.
19. Pedersen, S. K.; Harry, J. L.; Sebastian, L.; Baker, J.; Traini, M. D.; McCarthy, J. T.; Manoharan, A.; Wilkins, M. R.; Gooley, A. A.; Righetti, P. G.; Packer, N. H.; Williams, K. L.; Herbert, B. R., Unseen proteome: Mining below the tip of the iceberg to find low abundance and membrane proteins. *Journal of Proteome Research* **2003**, 2, (3), 303-311.

20. Covey, T. R.; Bruins, A. P.; Henion, J. D., Comparison of Thermospray and Ion Spray Mass-Spectrometry in an Atmospheric-Pressure Ion-Source. *Organic Mass Spectrometry* **1988**, 23, (3), 178-186.
21. Fenn, J. B.; Mann, M.; Meng, C. K.; Wong, S. F.; Whitehouse, C. M., Electrospray Ionization for Mass-Spectrometry of Large Biomolecules. *Science* **1989**, 246, (4926), 64-71.
22. Tanaka, K.; Waki, H.; Ido, Y.; Akita, S.; Yoshida, Y.; Yoshida, T.; Matsuo, T., Protein and polymer analyses up to m/z 100 000 by laser ionization time-of-flight mass spectrometry. *Rapid Communications in Mass Spectrometry* **1988**, 2(8), 151-153.
23. Karas, M.; Hillenkamp, F., Laser Desorption Ionization of Proteins with Molecular Masses Exceeding 10000 Daltons. *Analytical Chemistry* **1988**, 60, (20), 2299-2301.
24. Vorm, O.; Mann, M., Improved Mass Accuracy in Matrix-Assisted Laser Desorption/Ionization Time-of-Flight Mass-Spectrometry of Peptides. *Journal of the American Society for Mass Spectrometry* **1994**, 5, (11), 955-958.
25. Vorm, O.; Roepstorff, P.; Mann, M., Improved Resolution and Very High-Sensitivity in Maldi ToF of Matrix Surfaces Made by Fast Evaporation. *Analytical Chemistry* **1994**, 66, (19), 3281-3287.
26. Xiang, F.; Beavis, R. C., A Method to Increase Contaminant Tolerance in Protein Matrix-Assisted Laser-Desorption Ionization by the Fabrication of Thin Protein-Doped Polycrystalline Films. *Rapid Communications in Mass Spectrometry* **1994**, 8, (2), 199-204.
27. Beavis, R. C.; Chait, B. T., Rapid, Sensitive Analysis of Protein Mixtures by Mass-Spectrometry. *Proceedings of the National Academy of Sciences of the United States of America* **1990**, 87, (17), 6873-6877.
28. Emmett, M. R.; Caprioli, R. M., Micro-Electrospray Mass-Spectrometry - Ultra-High-Sensitivity Analysis of Peptides and Proteins. *Journal of the American Society for Mass Spectrometry* **1994**, 5, (7), 605-613.
29. Wilm, M.; Mann, M., Analytical properties of the nanoelectrospray ion source. *Analytical Chemistry* **1996**, 68, (1), 1-8.
30. Figeys, D.; Ning, Y. B.; Aebersold, R., A microfabricated device for rapid protein identification by microelectrospray ion trap mass spectrometry. *Analytical Chemistry* **1997**, 69, (16), 3153-3160.
31. Rohner, T. C.; Rossier, J. S.; Girault, H. H., Polymer microspray with an integrated thick-film microelectrode. *Analytical Chemistry* **2001**, 73, (22), 5353-5357.
32. Kruger, T. L.; Litton, J. F.; Kondrat, R. W.; Cooks, R. G., Mixture Analysis by Mass-Analyzed Ion Kinetic-Energy Spectrometry. *Analytical Chemistry* **1976**, 48, (14), 2113-2119.
33. McLafferty, F. W., Tandem mass spectrometric analysis of complex biological mixtures. *International Journal of Mass Spectrometry* **2001**, 212, (1-3), 81-87.
34. Smith, R. D.; Pasa-Tolic, L.; Lipton, M. S.; Jensen, P. K.; Anderson, G. A.; Shen, Y. F.; Conrads, T. P.; Udseth, H. R.; Harkewicz, R.; Belov, M. E.; Masselon, C.; Veenstra, T. D., Rapid quantitative measurements of proteomes by Fourier transform ion cyclotron resonance mass spectrometry. *Electrophoresis* **2001**, 22, (9), 1652-1668.
35. Williams, K.; Hawkrigde, A. M.; Muddiman, D. C., Sub parts-per-million mass measurement accuracy of intact proteins and product ions achieved using a dual electrospray ionization quadrupole Fourier transform ion cyclotron resonance mass spectrometer. *Journal of the American Society for Mass Spectrometry* **2007**, 18, (1), 1-7.
36. Wheeler, D. L.; Barrett, T.; Benson, D. A.; Bryant, S. H.; Canese, K.; Chetvernin, V.; Church, D. M.; DiCuccio, M.; Edgar, R.; Federhen, S.; Geer, L. Y.; Kapustin, Y.; Khovayko, O.; Landsman, D.; Lipman, D. J.; Madden, T. L.; Maglott, D. R.; Ostell, J.; Miller, V.; Pruitt, K. D.; Schuler, G. D.; Sequeira, E.; Sherry, S. T.; Sirotkin, K.; Souvorov, A.; Starchenko, G.; Tatusov, R. L.; Tatusova, T. A.; Wagner, L.; Yaschenko, E., Database resources of the National Center for Biotechnology Information. *Nucleic Acids Research* **2007**, 35, D5-D12.

37. Roe, M. R.; Griffin, T. J., Gel-free mass spectrometry-based high throughput proteomics: Tools for studying biological response of proteins and proteomes. *Proteomics* **2006**, *6*, (17), 4678-4687.
38. Gevaert, K.; Van Damme, P.; Ghesquière, B.; Impens, F.; Martens, L.; Helsens, K.; Vandekerckhove, J., A la carte Proteomics with an emphasis on gel-free techniques. *Proteomics* **2007**, *7*, 2698-2718.
39. Washburn, M. P.; Wolters, D.; Yates, J. R., Large-scale analysis of the yeast proteome by multidimensional protein identification technology. *Nature Biotechnology* **2001**, *19*, (3), 242-247.
40. Peng, J. M.; Elias, J. E.; Thoreen, C. C.; Licklider, L. J.; Gygi, S. P., Evaluation of multidimensional chromatography coupled with tandem mass spectrometry (LC/LC-MS/MS) for large-scale protein analysis: The yeast proteome. *Journal of Proteome Research* **2003**, *2*, (1), 43-50.
41. Shen, Y. F.; Zhao, R.; Belov, M. E.; Conrads, T. P.; Anderson, G. A.; Tang, K. Q.; Pasa-Tolic, L.; Veenstra, T. D.; Lipton, M. S.; Udseth, H. R.; Smith, R. D., Packed capillary reversed-phase liquid chromatography with high-performance electrospray ionization Fourier transform ion cyclotron resonance mass spectrometry for proteomics. *Analytical Chemistry* **2001**, *73*, (8), 1766-1775.
42. Chong, B. E.; Yan, F.; Lubman, D. M.; Miller, F. R., Chromatofocusing nonporous reversed-phase high-performance liquid chromatography/electrospray ionization time-of-flight mass spectrometry of proteins from human breast cancer whole cell lysates: a novel two-dimensional liquid chromatography/mass spectrometry method. *Rapid Communications in Mass Spectrometry* **2001**, *15*, (4), 291-296.
43. Wall, D. B.; Kachman, M. T.; Gong, S. Y.; Hinderer, R.; Parus, S.; Misek, D. E.; Hanash, S. M.; Lubman, D. M., Isoelectric focusing nonporous RP HPLC: A two-dimensional liquid-phase separation method for mapping of cellular proteins with identification using MALDI-TOF mass spectrometry. *Analytical Chemistry* **2000**, *72*, (6), 1099-1111.
44. Issaq, H. J.; Conrads, T. P.; Janini, G. M.; Veenstra, T. D., Methods for fractionation, separation and profiling of proteins and peptides. *Electrophoresis* **2002**, *23*, (17), 3048-3061.
45. Link, A. J., Multidimensional peptide separations in proteomics. *Trends in Biotechnology* **2002**, *20*, (12), S8-S13.
46. Boersema, P. J.; Divecha, N.; Heck, A. J. R.; Mohammed, S., Evaluation and optimization of ZIC-HILIC-RP as an alternative MudPIT strategy. *Journal of Proteome Research* **2007**, *6*, (3), 937-946.
47. Millea, K. M., Integration of multidimensional chromatographic protein separations with a combined "Top-Down" and "Bottom-Up" proteomic strategy. *Journal of Proteome Research* **2006**, *5*, (1), 135-146.
48. Lim, K. B., Phosphopeptides enrichment using on-line two-dimensional strong cation exchange followed by reversed-phase liquid chromatography/mass spectrometry. *Analytical Biochemistry* **2006**, *354*, (2), 213-219.
49. Brock, A.; Horn, D. M.; Peters, E. C.; Shaw, C. M.; Ericson, C.; Phung, Q. T.; Salomon, A. R., An automated matrix-assisted laser desorption/ionization quadrupole Fourier transform ion cyclotron resonance mass spectrometer for "bottom-up" proteomics. *Analytical Chemistry* **2003**, *75*, (14), 3419-3428.
50. Wolters, D. A.; Washburn, M. P.; Yates, J. R., An automated multidimensional protein identification technology for shotgun proteomics. *Analytical Chemistry* **2001**, *73*, (23), 5683-5690.
51. Kelleher, N. L.; Lin, H. Y.; Valaskovic, G. A.; Aaserud, D. J.; Fridriksson, E. K.; McLafferty, F. W., Top down versus bottom up protein characterization by tandem high-

- resolution mass spectrometry. *Journal of the American Chemical Society* **1999**, 121, (4), 806-812.
52. Reid, G. E.; McLuckey, S. A., 'Top down' protein characterization via tandem mass spectrometry. *Journal of Mass Spectrometry* **2002**, 37, (7), 663-675.
53. Kelleher, R. L.; Zubarev, R. A.; Bush, K.; Furie, B.; Furie, B. C.; McLafferty, F. W.; Walsh, C. T., Localization of labile posttranslational modifications by electron capture dissociation: The case of gamma-carboxyglutamic acid. *Analytical Chemistry* **1999**, 71, (19), 4250-4253.
54. VerBerkmoes, N. C.; Bundy, J. L.; Hauser, L.; Asano, K. G.; Razumovskaya, J.; Larimer, F.; Hettich, R. L.; Stephenson, J. L., Integrating "top-down" and "bottom-up" mass spectrometric approaches for proteomic analysis of *Shewanella oneidensis*. *Journal of Proteome Research* **2002**, 1, (3), 239-252.
55. Gygi, S. P.; Rist, B.; Gerber, S. A.; Turecek, F.; Gelb, M. H.; Aebersold, R., Quantitative analysis of complex protein mixtures using isotope-coded affinity tags. *Nature Biotechnology* **1999**, 17, (10), 994-999.
56. Mann, M., Quantitative proteomics? *Nature Biotechnology* **1999**, 17, (10), 954-955.
57. Ong, S. E., Stable isotope labeling by amino acids in cell culture, SILAC, as a simple and accurate approach to expression proteomics. *Molecular & Cellular Proteomics* **2002**, 1, (5), 376-386.
58. Yao, X. D.; Freas, A.; Ramirez, J.; Demirev, P. A.; Fenselau, C., Proteolytic O-18 labeling for comparative proteomics: Model studies with two serotypes of adenovirus. *Analytical Chemistry* **2001**, 73, (13), 2836-2842.
59. Ross, P. L., Multiplexed protein quantitation in *Saccharomyces cerevisiae* using amine-reactive isobaric tagging reagents. *Molecular & Cellular Proteomics* **2004**, 3, (12), 1154-1169.
60. Huber, L. A.; Pfaller, K.; Vietor, I., Organelle proteomics - Implications for subcellular fractionation in proteomics. *Circulation Research* **2003**, 92, (9), 962-968.
61. Dreger, M., Proteome analysis at the level of subcellular structures. *European Journal of Biochemistry* **2003**, 270, (4), 589-599.
62. Dreger, M., Subcellular proteomics. *Mass Spectrometry Reviews* **2003**, 22, (1), 27-56.
63. Jung, E.; Heller, M.; Sanchez, J. C.; Hochstrasser, D. F., Proteomics meets cell biology: The establishment of subcellular proteomes. *Electrophoresis* **2000**, 21, (16), 3369-3377.
64. Cordwell, S. J.; Nouwens, A. S.; Verrills, N. M.; Basseal, D. J.; Walsh, B. J., Subproteomics based upon protein cellular location and relative solubilities in conjunction with composite two-dimensional electrophoresis gels. *Electrophoresis* **2000**, 21, (6), 1094-1103.
65. Turck, N.; Richert, S.; Gendry, P.; Stutzmann, J.; Kedinger, M.; Leize, E.; Simon-Assmann, P.; Van Dorsselaer, A.; Launay, J. F., Proteomic analysis of nuclear proteins from proliferative and differentiated human colonic intestinal epithelial cells. *Proteomics* **2004**, 4, (1), 93-105.
66. Willsie, J. K.; Clegg, J. S., Small heat shock protein p26 associates with nuclear lamins and HSP70 in nuclei and nuclear matrix fractions from stressed cells. *Journal of Cellular Biochemistry* **2002**, 84, (3), 601-614.
67. Rabilloud, T.; Kieffer, S.; Procaccio, V.; Louwagie, M.; Courchesne, P. L.; Patterson, S. D.; Martinez, P.; Garin, J.; Lunardi, J., Two-dimensional electrophoresis of human placental mitochondria and protein identification by mass spectrometry: Toward a human mitochondrial proteome. *Electrophoresis* **1998**, 19, (6), 1006-1014.

68. Hanson, B. J.; Schulenberg, B.; Patton, W. F.; Capaldi, R. A., A novel subfractionation approach for mitochondrial proteins: A three-dimensional mitochondrial proteome map. *Electrophoresis* **2001**, *22*, (5), 950-959.
69. Lescuyer, P.; Hochstrasser, D. F.; Sanchez, J. C., Comprehensive proteome analysis by chromatographic protein prefractionation. *Electrophoresis* **2004**, *25*, (7-8), 1125-1135.
70. Fountoulakis, M.; Langen, H.; Gray, C.; Takacs, B., Enrichment and purification of proteins of Haemophilus influenzae by chromatofocusing. *Journal of Chromatography A* **1998**, *806*, (2), 279-291.
71. Motoyama, A., Anion and cation mixed-bed ion exchange for enhanced multidimensional separations of peptides and phosphopeptides. *Analytical Chemistry* **2007**, *79*, 3623-3634.
72. Liu, X. Y., Mapping the human plasma proteome by SCX-LC-IMS-MS. *Journal of the American Society for Mass Spectrometry* **2007**, *18*, 1249-1264.
73. Saito, H., Multiplexed two-dimensional liquid chromatography for MALDI and nanoelectrospray ionization mass spectrometry in proteomics. *Journal of Proteome Research* **2006**, *5*, (7), 1803-1807.
74. Lee, S. H.; Williams, M. V.; Blair, I. A., Targeted chiral lipidomics analysis. *Prostaglandins & Other Lipid Mediators* **2005**, *77*, (1-4), 141-157.
75. Fountoulakis, M.; Langen, H.; Evers, S.; Gray, C.; Takacs, B., Two-dimensional map of Haemophilus influenzae following protein enrichment by heparin chromatography. *Electrophoresis* **1997**, *18*, (7), 1193-1202.
76. Fountoulakis, M., Enrichment of low abundance proteins of Escherichia coli by hydroxyapatite chromatography. *Electrophoresis* **1999**, *20*, (11), 2181-2195.
77. Brand, J.; Haslberger, T.; Zolg, W.; Pestlin, G.; Palme, S., Depletion efficiency and recovery of trace markers from a multiparameter immunodepletion column. *Proteomics* **2006**, *6*, (11), 3236-3242.
78. Steel, L. F.; Trotter, M. G.; Nakajima, P. B.; Mattu, T. S.; Gonye, G.; Block, T., Efficient and specific removal of albumin from human serum samples. *Molecular & Cellular Proteomics* **2003**, *2*, (4), 262-270.
79. Xie, R. M., A study of the interactions between carboplatin and blood plasma proteins using size exclusion chromatography coupled to inductively coupled plasma mass spectrometry. *Analytical and Bioanalytical Chemistry* **2007**, *387*, (8), 2815-2822.
80. Hu, L. H., Comprehensive peptidome analysis of mouse livers by size exclusion chromatography prefractionation and NanoLC-MS/MS identification. *Journal of Proteome Research* **2007**, *6*, (2), 801-808.
81. Bier, M., Recycling isoelectric focusing and isotachopheresis. *Electrophoresis* **1998**, *19*, (7), 1057-1063.
82. Thorsell, A.; Portelius, E.; Blennow, K.; Westman-Brinkmalm, A., Evaluation of sample fractionation using micro-scale liquid-phase isoelectric focusing on mass spectrometric identification and quantitation of proteins in a SILAC experiment. *Rapid Communications in Mass Spectrometry* **2007**, *21*, (5), 771-778.
83. Hochstrasser, A. C.; James, R. W.; Pometta, D.; Hochstrasser, D. F., Preparative isoelectrofocusing and high resolution 2-dimensional gel electrophoresis for concentration and purification of proteins. *Applied and Theoretical Electrophoresis* **1991**, *1*(6), 333-337.
84. Davidsson, P.; Paulson, L.; Hesse, C.; Blennow, K.; Nilsson, C. L., Proteome studies of human cerebrospinal fluid and brain tissue using a preparative two-dimensional electrophoresis approach prior to mass spectrometry. *Proteomics* **2001**, *1*, (3), 444-452.
85. Wang, H. X.; Kachman, M. T.; Schwartz, D. R.; Cho, K. R.; Lubman, D. M., A protein molecular weight map of ES2 clear cell ovarian carcinoma cells using a two-

- dimensional liquid separations/mass mapping technique. *Electrophoresis* **2002**, 23, (18), 3168-3181.
86. Xiao, Z.; Conrads, T. P.; Lucas, D. A.; Janini, G. M.; Schaefer, C. F.; Buetow, K. H.; Issaq, H. J.; Veenstra, T. D., Direct ampholyte-free liquid-phase isoelectric peptide focusing: Application to the human serum proteome. *Electrophoresis* **2004**, 25, (1), 128-133.
87. Moritz, R. L.; Simpson, R. J., Liquid-based free-flow electrophoresis-reversed-phase HPLC: a proteomic tool. *Nature Methods* **2005**, 2, (11), 863-873.
88. Hannig, K., New Aspects in Preparative and Analytical Continuous Free-Flow Cell Electrophoresis. *Electrophoresis* **1982**, 3, (5), 235-243.
89. Krivankova, L.; Bocek, P., Continuous free-flow electrophoresis. *Electrophoresis* **1998**, 19, (7), 1064-1074.
90. Kuhn, R.; Wagner, H., Application of Free-Flow Electrophoresis to the Preparative Purification of Basic-Proteins from an Escherichia-Coli Cell Extract. *Journal of Chromatography* **1989**, 481, 343-351.
91. Burggraf, D.; Weber, G.; Lottspeich, F., Free-Flow Isoelectric-Focusing of Human Cellular Lysates as Sample Preparation for Protein-Analysis. *Electrophoresis* **1995**, 16, (6), 1010-1015.
92. Hoffmann, P.; Ji, H.; Moritz, R. L.; Connolly, L. M.; Frecklington, D. F.; Layton, M. J.; Eddes, J. S.; Simpson, R. J., Continuous free-flow electrophoresis separation of cytosolic proteins from the human colon carcinoma cell line LIM 1215: A non two-dimensional gel electrophoresis-based proteome analysis strategy. *Proteomics* **2001**, 1, (7), 807-818.
93. Moritz, R. L.; Clippingdale, A. B.; Kapp, E. A.; Eddes, J. S.; Ji, H.; Gilbert, S.; Connolly, L. M.; Simpson, R. J., Application of 2-D free-flow electrophoresis/RP-HPLC for proteomic analysis of human plasma depleted of multi high-abundance proteins. *Proteomics* **2005**, 5, (13), 3402-3413.
94. Kobayashi, H.; Shimamura, K.; Akaida, T.; Sakano, K.; Tajima, N.; Funazaki, J.; Suzuki, H.; Shinohara, E., Free-flow electrophoresis in a microfabricated chamber with a micromodule fraction separator - Continuous separation of proteins. *Journal of Chromatography A* **2003**, 990, (1-2), 169-178.
95. Raymond, D. E., Continuous separation of high molecular weight compounds using a microliter volume free-flow electrophoresis microstructure. *Analytical Chemistry* **1996**, 68, (15), 2515-2522.
96. Xu, Y.; Zhang, C. X.; Janasek, D.; Manz, A., Sub-second isoelectric focusing in free flow using a microfluidic device. *Lab on a Chip* **2003**, 3, (4), 224-227.
97. Zhang, C. X., High-speed free-flow electrophoresis on chip. *Analytical Chemistry* **2003**, 75, (21), 5759-5766.
98. Righetti, P. G.; Wenisch, E.; Faupel, M., Preparative Protein-Purification in a Multi-Compartment Electrolyzer with Immobiline Membranes. *Journal of Chromatography* **1989**, 475, 293-309.
99. Righetti, P. G.; Wenisch, E.; Jungbauer, A.; Katinger, H.; Faupel, M., Preparative Purification of Human Monoclonal-Antibody Isoforms in a Multicompartment Electrolyzer with Immobiline Membranes. *Journal of Chromatography* **1990**, 500, 681-696.
100. Righetti, P. G.; Castagna, A.; Herbert, B.; Reymond, F.; Rossier, J. S., Prefractionation techniques in proteome analysis. *Proteomics* **2003**, 3, (8), 1397-1407.
101. Herbert, B.; Righetti, P. G., A turning point in proteome analysis: Sample prefractionation via multicompartment electrolyzers with isoelectric membranes. *Electrophoresis* **2000**, 21, (17), 3639-3648.
102. Righetti, P. G.; Castagna, A.; Herbert, B., Prefractionation techniques in proteome analysis. *Analytical Chemistry* **2001**, 73, (11), 320A-326A.

103. Zuo, X.; Speicher, D. W., A method for global analysis of complex proteomes using sample prefractionation by solution isoelectrofocusing prior to two-dimensional electrophoresis. *Analytical Biochemistry* **2000**, 284, (2), 266-278.
104. Zuo, X.; Speicher, D. W., Comprehensive analysis of complex proteomes using microscale solution isoelectrofocusing prior to narrow pH range two-dimensional electrophoresis. *Proteomics* **2002**, 2, (1), 58-68.
105. Ros, A.; Faupel, M.; Mees, H.; van Oostrum, J.; Ferrigno, R.; Reymond, F.; Michel, P.; Rossier, J. S.; Girault, H. H., Protein purification by Off-Gel electrophoresis. *Proteomics* **2002**, 2, (2), 151-156.
106. Arnaud, I. L.; Josserand, J.; Rossier, J. S.; Girault, H. H., Finite element simulation of Off-Gel (TM) buffering. *Electrophoresis* **2002**, 23, (19), 3253-3261.
107. Michel, P. E.; Reymond, F.; Arnaud, I. L.; Josserand, J.; Girault, H. H.; Rossier, J. S., Protein fractionation in a multicompartiment device using Off-Gel (TM) isoelectric focusing. *Electrophoresis* **2003**, 24, (1-2), 3-11.
108. Reschiglian, P.; Zattoni, A.; Roda, B.; Cinque, L.; Parisi, D.; Roda, A.; Dal Piaz, F.; Moon, M. H.; Min, B. R., On-line hollow-fiber flow field-flow fractionation-electrospray ionization/time-of-flight mass spectrometry of intact proteins. *Analytical Chemistry* **2005**, 77, (1), 47-56.
109. Reschiglian, P.; Zattoni, A.; Roda, B.; Michelini, E.; Roda, A., Field-flow fractionation and biotechnology. *Trends in Biotechnology* **2005**, 23, (9), 475-483.
110. Kang, D.; Moon, M. H., Hollow fiber flow field-flow fractionation of proteins using a microbore channel. *Analytical Chemistry* **2005**, 77, (13), 4207-4212.
111. Park, Y.; Paeng, K. J.; Kang, D.; Moon, M. H., Performance of hollow-fiber flow field-flow fractionation in protein separation. *Journal of Separation Science* **2005**, 28, (16), 2043-2049.
112. Roda, A.; Parisi, D.; Guardigli, M.; Zattoni, A.; Reschiglian, P., Combined approach to the analysis of recombinant protein drugs using hollow-fiber flow field-flow fractionation, mass spectrometry, and chemiluminescence detection. *Analytical Chemistry* **2006**, 78, (4), 1085-1092.
113. Kang, D. J.; Moon, M. H., Development of non-gel-based two-dimensional separation of intact proteins by an on-line hyphenation of capillary Isoelectric focusing and hollow fiber flow field-flow fractionation. *Analytical Chemistry* **2006**, 78, (16), 5789-5798.
114. Martin, M., Theory of field flow fractionation. *Advances in Chromatography, Vol 39* **1998**, 39, 1-138.
115. Chmelik, J., Applications of field-flow fractionation in proteomics: present and future. *Proteomics* **2007**, 7, 2719-2728.
116. Chmelik, J.; Deml, M.; Janca, J., Separation of 2 Components of Horse Myoglobin by Isoelectric-Focusing Field-Flow Fractionation. *Analytical Chemistry* **1989**, 61, (8), 912-914.
117. Chmelik, J.; Thormann, W., Isoelectric-Focusing Field-Flow Fractionation 4. Investigations on Protein Separations in the Trapezoidal Cross-Section Channel. *Journal of Chromatography* **1992**, 600, (2), 305-311.
118. Sabounchi-Schutt, F.; Astrom, J.; Olsson, I.; Eklund, A.; Grunewald, J.; Bjellqvist, B., An Immobiline DryStrip application method enabling high-capacity two-dimensional gel electrophoresis. *Electrophoresis* **2000**, 21, (17), 3649-3656.
119. Wang, E.; Yu, Z.; Li, N., Anesthetic Lidocaine and Dicine Transfer across Liquid Liquid Interfaces. *Electroanalysis* **1992**, 4, (9), 905-909.
120. Arai, K.; Ohsawa, M.; Kusu, F.; Takamura, K., Drug Ion Transfer across on Oil-Water Interface and Pharmacological Activity. *Bioelectrochemistry and Bioenergetics* **1993**, 31, (1), 65-76.

121. Reymond, F.; Steyaert, G.; Pagliara, A.; Carrupt, P. A.; Testa, B.; Girault, H., Transfer mechanism of ionic drugs: Piroxicam as an agent facilitating proton transfer. *Helvetica Chimica Acta* **1996**, 79, (6), 1651-1669.
122. Reymond, F.; Steyaert, G.; Carrupt, P. A.; Testa, B.; Girault, H. H., Mechanism of transfer of a basic drug across the water 1,2-dichloroethane interface: The case of quinidine. *Helvetica Chimica Acta* **1996**, 79, (1), 101-117.
123. Ulmeanu, S. M.; Jensen, H.; Samec, Z.; Bouchard, G.; Carrupt, P. A.; Girault, H. H., Cyclic voltammetry of highly hydrophilic ions at a supported liquid membrane. *Journal of Electroanalytical Chemistry* **2002**, 530, (1-2), 10-15.
124. Bouchard, G.; Carrupt, P. A.; Testa, B.; Gobry, V.; Girault, H. H., Lipophilicity and solvation of anionic drugs. *Chemistry-a European Journal* **2002**, 8, (15), 3478-3484.
125. Kubota, K.; Katano, H.; Senda, M., Ion-transfer voltammetry of local anesthetics at an organic solvent/water interface and pharmacological activity vs. ion partition coefficient relationship. *Analytical Sciences* **2001**, 17, (1), 65-70.
126. Chen, Y.; Yuan, Y.; Zhang, M. Q.; Li, F.; Sun, P.; Gao, Z.; Shao, Y. H., Systematic study of the transfer of amino acids across the water/1,2-dichloroethane interface facilitated by dibenzo-18-crown-6. *Science in China Series B-Chemistry* **2004**, 47, (1), 24-33.
127. Osakai, T.; Hirai, T.; Wakamiya, T.; Sawada, S., Quantitative analysis of the structure-hydrophobicity relationship for di- and tripeptides based on voltammetric measurements with an oil/water interface. *Physical Chemistry Chemical Physics* **2006**, 8, (8), 985-993.
128. Sawada, S.; Osakai, T., Hydrophobicity of oligopeptides: a voltammetric study of the transfer of dipeptides facilitated by dibenzo-18-crown-6 at the nitrobenzene/water interface. *Physical Chemistry Chemical Physics* **1999**, 1, (20), 4819-4825.
129. Gulaboski, R.; Mirceski, V.; Scholz, F., Determination of the standard Gibbs energies of transfer of cations and anions of amino acids and small peptides across the water nitrobenzene interface. *Amino Acids* **2003**, 24, (1-2), 149-154.
130. Gulaboski, R.; Scholz, F., Lipophilicity of peptide anions: An experimental data set for lipophilicity calculations. *Journal of Physical Chemistry B* **2003**, 107, (23), 5650-5657.
131. Amemiya, S.; Yang, X. T.; Wazenegger, T. L., Voltammetry of the phase transfer of polypeptide protamines across polarized liquid/liquid interfaces. *Journal of the American Chemical Society* **2003**, 125, (39), 11832-11833.
132. Yuan, Y.; Amemiya, S., Facilitated protamine transfer at polarized water/1,2-dichloroethane interfaces studied by cyclic voltammetry and chronoamperometry at micropipet electrodes. *Analytical Chemistry* **2004**, 76, (23), 6877-6886.
133. Vagin, M. Y.; Trashin, S. A.; Ozkan, S. Z.; Karpachova, G. P.; Karyakin, A. A., Electroactivity of redox-inactive proteins at liquid/liquid interface. *Journal of Electroanalytical Chemistry* **2005**, 584, (2), 110-116.
134. Vagin, M. Y.; Malyh, E. V.; Larionova, N. I.; Karyakin, A. A., Spontaneous and facilitated micelles formation at liquid vertical bar liquid interface: towards amperometric detection of redox inactive proteins. *Electrochemistry Communications* **2003**, 5, (4), 329-333.
135. Karyakin, A. A.; Vagin, M. Y.; Ozkan, S. Z.; Karpachova, G. P., Thermodynamics of ion transfer across the liquid|liquid interface at a solid electrode shielded with a thin layer of organic solvent. *Journal of Physical Chemistry B* **2004**, 108, (31), 11591-11595.
136. Shinshi, M.; Sugihara, T.; Osakai, T.; Goto, M., Electrochemical extraction of proteins by reverse micelle formation. *Langmuir* **2006**, 22, (13), 5937-5944.
137. Shinshi, M.; Sugihara, T.; Osakai, T.; Goto, M., Electrochemical extraction of proteins by reverse micelle formation (vol 22, pg 5937, 2006). *Langmuir* **2006**, 22, (20), 8614-8614.

CHAPTER II: *Theoretical aspects of isoelectric focusing (IEF)*

1. Isoelectric focusing as a separation technique.....	46
2. Mathematical description of isoelectric focusing.....	47
2.1 General equation for the diffusion-migration of ions	47
2.2 IEF at the steady state.....	50
2.3 Resolving power.....	51
3. Gel electrophoresis.....	53
4. Generation of a pH gradient for isoelectric focusing.....	55
4.1 Carrier ampholytes (CA)	55
4.2 Immobilized pH gradient (IPG) gels	66
5. OFFGEL isoelectric focusing (OG-IEF).....	76
6. References.....	79

1. Isoelectric focusing as a separation technique

Isoelectric focusing (IEF) is a method dedicated to the separation of amphoteric species, that are molecules that can act both as acids and as bases. Peptides and proteins are mainly the samples fractionated by IEF, their amphoteric nature stemming from the presence of both carboxylic and amino groups. This type of ampholyte, to be distinguished from a species such as H_2PO_4^- , can exhibit both a net positive charge and a net negative charge, in response to the pH of its environment. Therefore, there is a pH called the isoelectric point, and noted pI , where the molecule displays a zero net charge. A peptide or protein is usually represented by its titration curve, expressed as the net charge versus the pH (Figure 1).

The separation principle of IEF is based on differences in pI , and a pH gradient is required to achieve the focusing of samples.

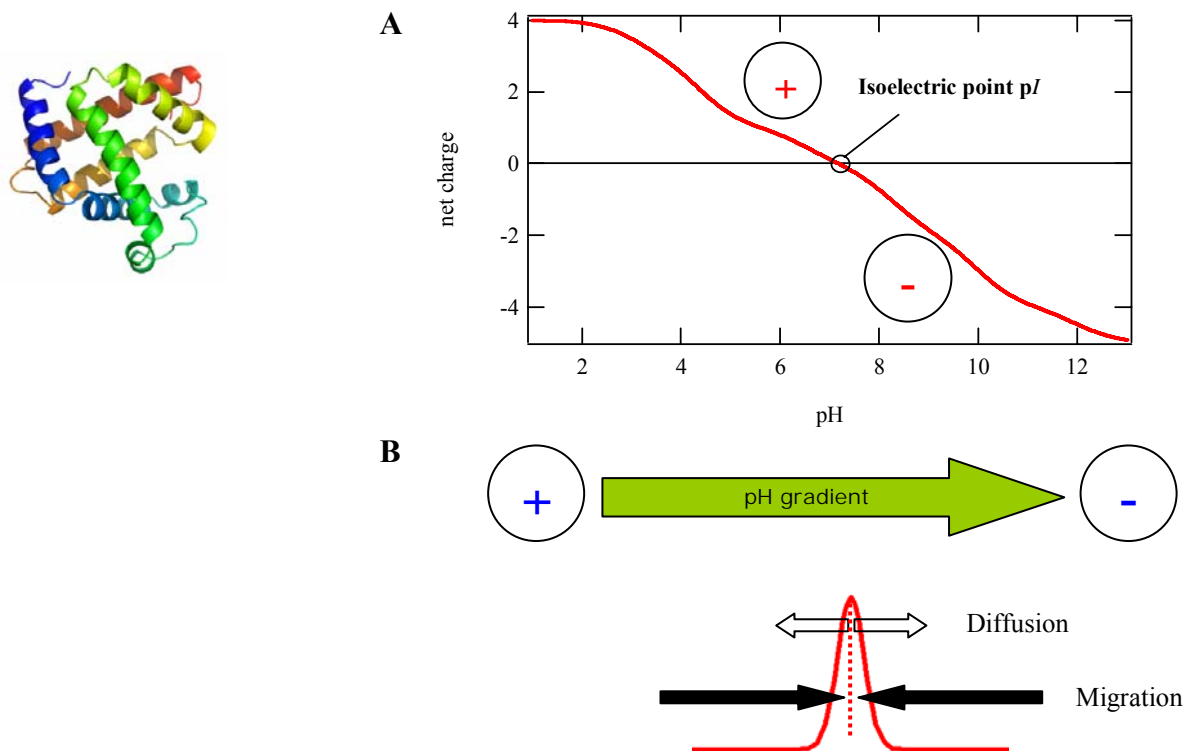


Figure 1: A shows the titration curve associated to the protein, B is the representation of the pH gradient and electric field, and the focusing peak around the pI .

A protein which is at a point in a pH gradient below its pI has a net positive charge, and a net negative charge above its pI . The presence of the electric field of the appropriate polarity will therefore move the molecule toward the isoelectric pH, at which point it ceases to respond to the electric field, because of the lack of a net charge. Any movement of diffusion away from this point in the pH gradient will cause the molecule to acquire a net charge and migrate back to its pI . IEF is therefore a constant dynamic equilibrium. So the two main parameters for IEF are the pH gradient and the electric field. The generation of the pH gradient will be discussed here, and the influence of the electric field will be shown in this chapter and in chapter III as well.

2. Mathematical description of isoelectric focusing¹⁻³

2.1 General equation for the diffusion-migration of ions

The transport of ions in solution can be attributed to convection (thermal or mechanical agitation), or to the influence of a gradient of Gibbs energy. The flux through a defined surface area is given by:

$$J_i = c_i v \quad (2.1)$$

where J_i and c_i are the flux and concentration of the species i , and v is the velocity.

In solution, basically two forces act on the ion in motion.

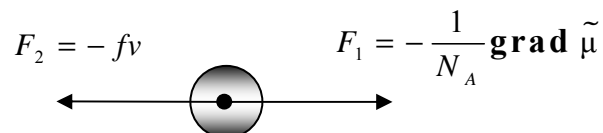


Figure 2: Forces acting on an ion in solution.

The force F_1 is the force due to the electrochemical potential $\tilde{\mu}$ gradient:

$$F_1 = -\frac{1}{N_A} \mathbf{grad} \tilde{\mu} \quad (2.2)$$

The second force F_2 , in the opposite direction, is the frictional force, proportional to the velocity and the frictional coefficient of viscosity f :

$$F_2 = -fv \quad (2.3)$$

In the steady-state, the sum of the forces equals zero and the velocity can be expressed as:

$$v = -\frac{1}{N_A f} \mathbf{grad} \tilde{\mu} \quad (2.4)$$

According to Equation (2.1), the flux is proportional to the velocity and the concentration of the ion, resulting in:

$$J_i = -\frac{c_i}{N_A f} \mathbf{grad} \tilde{\mu}_i = -c_i \tilde{u}_i \mathbf{grad} \tilde{\mu}_i \quad (2.5)$$

where \tilde{u}_i is defined as the electrochemical mobility of the ion.

The electrochemical potential is defined as:

$$\tilde{\mu}_i = \mu_i^0 + RT \ln a_i + z_i F \phi \quad (2.6)$$

where μ_i^0 is the standard chemical potential, a_i the activity of species i , z_i the charge of the species, ϕ the electric potential, F the Faraday constant, R the gas constant and T the temperature. In an ideally diluted solution, it results in:

$$\tilde{\mu}_i = \mu_i^0 + RT \ln c_i + z_i F \phi \quad (2.7)$$

The flux under an electrochemical potential can thus be expressed as follows:

$$J_i = -c_i \tilde{u}_i \mathbf{grad} \mu_i - z_i F c_i \tilde{u}_i \mathbf{grad} \phi \quad (2.8)$$

where μ_i is the chemical potential, defined by:

$$\mu_i = \mu_i^0 + RT \ln c_i \quad (2.9)$$

Diffusion term (first term of the flux equation)

The flux of diffusion is proportional to the gradient of concentration, as defined by Fick's first law:

$$J_i = -D_i \left(\frac{\partial c_i}{\partial x} \right)_\phi \quad (2.10)$$

where D_i is the diffusion coefficient of species i .

If comparing with the diffusion term in Equation (2.8), the diffusion coefficient can be written as:

$$D_i = RT \tilde{u}_i \quad (2.11)$$

According to the Stokes-Einstein equation, which describes the way that diffusion increases with temperature and inversely proportional to the frictional force:

$$D_i = \frac{kT}{f} \quad (2.12)$$

where k is the Boltzmann constant. The frictional force depends on the size and shape of the molecule. The larger the molecule is, the larger the frictional coefficient (*i.e.* more resistance to the motion of the molecule). For a spherical particle of radius r , Stokes' relation gives:

$$f = 6\pi\eta r \quad (2.13)$$

where η is the viscosity.

The coefficient of diffusion can thus be expressed as:

$$D_i = \frac{kT}{6\pi\eta r} \quad (2.14)$$

Migration term (second term of the flux equation)

In ionic conductors (ionic solutions), proportionality exists between the current and the applied electric field, as expressed by Ohm's law. The current density, which is a flux due to the migration of charges (ions), is thus written as:

$$j_i = z_i F J_i = -\sigma_i \mathbf{grad} \phi \quad (2.15)$$

The proportionality factor σ_i is named ionic conductivity and by comparing with the migration term in the flux Equation (2.8), σ_i writes as:

$$\sigma_i = z_i^2 F^2 c_i \tilde{u}_i = z_i F c_i u_{ep,i} \quad (2.16)$$

where $u_{ep,i}$ is the electrophoretic mobility, defined as:

$$u_{ep,i} = z_i F \tilde{u}_i \quad (2.17)$$

For a cation, it is always positive, for an anion, it is always negative. The electrophoretic mobility is the proportionality factor between the velocity and the electric field:

$$v_i = -z_i F \tilde{u}_i \mathbf{grad} \phi = z_i F \tilde{u}_i E = u_{ep,i} E \quad (2.18)$$

If coming back to the expression of the velocity given by Equation (2.4), and considering the Stokes' relation for the frictional coefficient f , we have:

$$v_i = -\frac{1}{N_A f} \mathbf{grad} \tilde{\mu}_i = \frac{z_i F E}{N_A 6\pi\eta r} \quad (2.19)$$

And thus the electrophoretic mobility:

$$u_{ep,i} = \frac{z_i F}{N_A 6\pi\eta r} \quad (2.20)$$

Therefore, the electrophoretic mobility is proportional to the charge density (charge/size ratio) of the particle.

2.2 IEF at the steady state

For a stationary regime of isoelectric focusing without chemical reactions, the equation of conservation of flux is given by:

$$\frac{\partial c_i}{\partial t} = -\text{div} J_i = 0 \quad (2.21)$$

Considering only the diffusion-migration transport in one direction, and substituting with Equation (2.8), this equation reduces to the following 1-D steady-state equation:

$$\frac{\partial}{\partial x} \left(-\frac{c_i \tilde{u}_i RT}{c_i} \frac{\partial c_i}{\partial x} - c_i \tilde{u}_i z_i F \frac{\partial \phi}{\partial x} \right) = 0 \quad (2.22)$$

It results from Equation (2.22) that the flux of species i (term in brackets) is uniform over x . Since at the isoelectric point, the concentration is maximal and the charge zero, the global flux at the steady-state is zero.

$$-\tilde{u}_i RT \frac{\partial c_i}{\partial x} - c_i \tilde{u}_i z_i F \frac{\partial \phi}{\partial x} = 0 \quad (2.23)$$

By rearranging and taking the electrophoretic mobility, $u_{ep,i} = z_i \tilde{u}_i F$, this equation becomes:

$$\tilde{u}_i RT \frac{\partial c_i}{\partial x} = c_i u_{ep,i} E \quad (2.24)$$

And if combining with the definition of the diffusion coefficient (Equation (2.11)):

$$D_i \frac{\partial c_i}{\partial x} = c_i u_{ep,i} E \quad (2.25)$$

The concentration distribution of an electrolyte at the isoelectric point is the “equilibrium” between mass transport and diffusional flow.

2.3 Resolving power

The mobility $u_{ep,i}$ can be regarded as a linear function of x , because of the narrowness of the focused zone near pI. With the proportionality factor p , it can thus be written:

$$u_{ep,i} = -p_i x \quad (2.26)$$

We can note that if the x -axis is pointing in the direction of a positive pH gradient, the mobility slope is then negative (cf. titration curve), thus the negative factor.

(Equation (2.25)) can then be written:

$$\partial c_i / c_i = (-p_i E / D_i) x dx \quad (2.27)$$

The integration of this equation gives:

$$c_i(x) = c_{i,\max} e^{\left(\frac{-p_i E x^2}{2 D_i} \right)} \quad (2.28)$$

where $c_{i,\max}$ is the maximum local concentration of the species i in the focusing region. The concentration thus expresses a Gaussian concentration distribution with a standard deviation σ :

$$\sigma = \sqrt{D_i / (p_i E)} \quad (2.29)$$

If we consider a narrow focused zone, the pH gradient dpH/dx and the electrophoretic mobility slope $du_{ep,i}/dpH$ can be regarded as linear functions of x . The proportionality factor (mobility slope around the pI) can be written as:

$$p_i = - \left(\frac{du_{ep,i}}{dx} \right) \approx - \left(\frac{du_{ep,i}}{dpH} \right) \left(\frac{dpH}{dx} \right) \quad (2.30)$$

By substituting Equation (2.30) into Equation (2.29), one obtains:

$$\sigma = \sqrt{\frac{D_i}{E} \left(- \frac{dpH}{du_{ep,i}} \right) \left(\frac{dx}{dpH} \right)} \quad (2.31)$$

According to calculations of Vesterberg and Svensson,⁴ two adjacent zones are considered to be resolved when their peak to peak separation is three times larger than the distance from the peak to the inflection point:

$$\Delta pH = \Delta x \frac{dpH}{dx} = 3\sigma \frac{dpH}{dx} \quad (2.32)$$

Substitution of Equation (2.31) into Equation (2.32) gives at the pI :

$$\Delta pI = 3 \sqrt{\frac{D_i \left(\frac{dpH}{dx} \right)}{E \left(- \frac{du_{ep,i}}{dpH} \right)}} \quad (2.33)$$

where ΔpI is the difference in isoelectric points between two proteins to be separated by IEF. A similar equation was later demonstrated by Giddings et al.,⁵ in an approach similar to the chromatographic one. They pointed out the relevance of the peak capacity as a general criterion of over-all resolving power.

Equation (2.33) shows how the resolution can be increased. When the diffusion coefficient is high, a gel with small pores should be chosen, to limit diffusion. The flatter the pH gradient is, the better the resolution. But it also shows the limits of IEF: a high electric field increases the resolution, but the field strength cannot be increased indefinitely. And $-du_{ep,i}/dpH$, the mobility slope at the pI is a property inherent to the protein.

3. Gel electrophoresis

Electrophoretic separation in solution is due to differences in the mass/charge ratio. However, the resolution is poor, because of Joule heating effects, which can create temperature gradient, thus density gradients, leading to natural convection and disturbance in the focused zone. Diffusion in solution also has a negative effect on the sharpness of the focusing. To minimize these effects, electrophoretic separations are mainly carried out in supporting media, such as aqueous gels. Depending on the pore size, the gel modifies the diffusion coefficient of proteins, as well as the apparent radius, thus the mobility.

The gel material that best fulfills the requirements for protein separation and pore size optimization is polyacrylamide gel. This kind of gel was first used by Raymond and Weintraub in 1959,⁶ for zone electrophoresis. It is formed by co-polymerization of acrylamide monomers with a cross-linking reagent (usually N,N'-methylenebisacrylamide), resulting into a chemically inert and transparent gel, stable over a wide temperature, pH and ionic strength range. The polymerization reaction scheme is shown on Figure 3. To initiate the reaction,

several polymerization catalysts are used, most commonly ammonium persulfate (APS) and N,N,N',N'-tetramethylethylenediamine (TEMED). The pore size can be reproducibly controlled by the total acrylamide concentration $T\%$ and the degree of cross-linking $C\%$.⁷

$$T\% = \frac{a+b}{V} \times 100 \quad \text{and} \quad C\% = \frac{b}{a+b} \times 100 \quad (2.34)$$

a is the mass of acrylamide in g, b is the mass of methylenebisacrylamide in g and V is the volume in mL.

When $C\%$ remains constant and $T\%$ increases, the pore size decreases. When $T\%$ remains constant and $C\%$ increases, the pore size follows a parabolic function: at high and low values of $C\%$, the pores are large, the minimum being at $C\% = 5\%$. For example, for $T\% = 5\%$ and $C\% = 5\%$, a pore size of approx. 20 nm can be obtained.³ For higher $C\%$ (25 to 60%), Righetti et al. report on pore size increasing from 200 to 600 nm.⁸ Some further studies were done on the kinetics of the polymerization, namely on the effect of different cross-linkers and the effect of the temperature.^{9, 10} From information given by Amersham,¹¹ a gel with $T\% = 5\%$ and $C\% = 3\%$ has a pore diameter of 5.3 nm. Commercialized IPG gels ($T\% = 4\%$, $C\% = 3\%$) should have a pore size of a few nm.

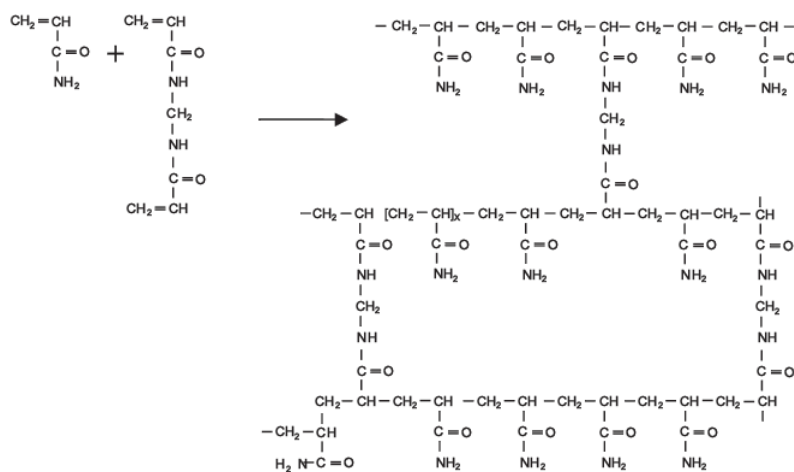


Figure 3: Polymerization reaction of acrylamide and methylenebisacrylamide from¹²

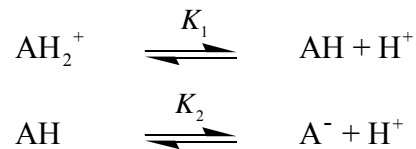
4. Generation of a pH gradient for isoelectric focusing

The prerequisite for highly resolved and reproducible separations is a stable and continuous pH gradient with constant conductivity and buffering capacity. Two concepts meet these demands: pH gradients which are formed in the electric field by amphoteric buffers, the carrier ampholytes, or immobilized pH gradients, in which the buffering groups are part of the gel.

4.1 Carrier ampholytes (CA)

That important concept was introduced by Svensson in 1961,¹³ to synthesize the minimum basic requirements for stable pH gradients in an electric field. The buffers used to form a pH gradient had to have two fundamental properties: 1) to be amphoteric so that they could also reach a steady state position during the separation and 2) to be “carrier”. The concept of carrier is more subtle, but just as fundamental. The carrier species has to be capable of “carrying” the current (a good conducting species) and capable of carrying the pH (a good buffering species).¹⁴ In the following section, these two properties will be defined following Rilbe-Svensson’s description¹⁵ and illustrated by some examples.

If we consider a biprotic ampholyte:



The two dissociation constants associated to these reactions can be written as follows:

$$K_1 = \frac{c_{\text{AH}} c_{\text{H}^+}}{c_{\text{AH}_2^+}} \quad (2.35)$$

$$K_2 = \frac{c_{\text{A}^-} c_{\text{H}^+}}{c_{\text{AH}}} \quad (2.36)$$

From the dissociation constants, we can derive:

$$c_{AH_2^+} = c_{H^+} c_{AH} / K_1 \quad (2.37)$$

$$c_{A^-} = K_2 c_{AH} / c_{H^+} \quad (2.38)$$

The total concentration c_{tot} of the ampholyte is noted:

$$c_{tot} = c_{AH_2^+} + c_{AH} + c_{A^-} \quad (2.39)$$

By adding the two equations together with c_{AH} to obtain the total concentration, the concentration of the three species can be deduced:

$$c_{AH_2^+} = c_{H^+}^2 c_{tot} / (c_{H^+}^2 + c_{H^+} K_1 + K_1 K_2) \quad (2.40)$$

$$c_{AH} = c_{H^+} K_1 c_{tot} / (c_{H^+}^2 + c_{H^+} K_1 + K_1 K_2) \quad (2.41)$$

$$c_{A^-} = K_1 K_2 c_{tot} / (c_{H^+}^2 + c_{H^+} K_1 + K_1 K_2) \quad (2.42)$$

The charge is defined as:

$$z = \frac{c_{AH_2^+} - c_{A^-}}{c_{tot}} = \frac{c_{H^+}^2 - K_1 K_2}{(c_{H^+}^2 + c_{H^+} K_1 + K_1 K_2)} \quad (2.43)$$

At the isoelectric point, the charge equals zero, thus:

$$c_{H^+}^2 = K_1 K_2 \quad (2.44)$$

And the isoelectric point is defined by:

$$pI = (pK_1 + pK_2) / 2 \quad (2.45)$$

Note on the influence of the ionic strength on the pI

These calculations are made assuming ideally diluted solutions. If this hypothesis is not valid (high ionic strength), the activity coefficients have to be taken into account. The equations (2.35) and (2.36) can then be rewritten as K_{11} and K_{22} respectively:

$$K_{11} = \frac{a_{AH} a_{H^+}}{a_{AH_2^+}} = \frac{\gamma_{AH} \gamma_{H^+}}{\gamma_{AH_2^+}} \cdot \frac{c_{AH} c_{H^+}}{c_{AH_2^+}} \quad (2.46)$$

$$K_{22} = \frac{a_{A^-} a_{H^+}}{a_{AH}} = \frac{\gamma_{A^-} \gamma_{H^+}}{\gamma_{AH}} \cdot \frac{c_{A^-} c_{H^+}}{c_{AH}} \quad (2.47)$$

If assuming that the activity coefficient for the uncharged species is unitary, this leads to:

$$K_{11} > K_1 \text{ and } K_{22} < K_2 \quad (2.48)$$

These changes in the dissociation constants do not change the value of the pI (compensated in the half sum of the pK_a according to equation (2.45)), but should influence the slope of the titration curve near the pI .

Buffer capacity of ampholytes

The buffer capacity of carrier ampholytes near their isoelectric point is important, because they should exhibit a buffer action stronger than that of the proteins and therefore control the pH gradient. The buffer capacity β is defined as the amount of acid or base necessary to change the pH by one unit. If a concentration of base c_B is added, β is written as:

$$\beta = \frac{dc_B}{d(\text{pH})} \quad (2.49)$$

The higher the buffer capacity of an ampholyte is, the better its buffering power (meaning the change in pH is not so much affected by the addition of acid or base).

The charge balance for the ampholyte solution to which a certain amount of base c_B is added, can be written as (if neglecting water dissociation):

$$c_B + c_{AH_2^+} = c_{A^-} \quad (2.50)$$

Combining Equations (2.40) and (2.42), the base concentration can be expressed as:

$$c_B = \frac{c_{tot} (K_1 K_2 - c_{H^+}^2)}{c_{H^+}^2 + c_{H^+} K_1 + K_1 K_2} \quad (2.51)$$

The expression of the buffering capacity is thus:¹⁶

$$\beta = \frac{dc_B}{d(\text{pH})} = \frac{\ln 10 c_{tot} K_1 c_{H^+} (K_1 K_2 + 4c_{H^+} K_2 + c_{H^+}^2)}{(c_{H^+}^2 + c_{H^+} K_1 + K_1 K_2)^2} \quad (2.52)$$

At the isoelectric point, the relative molar buffering capacity can thus be written as (see Appendix 1):

$$B_{i,rel} = \frac{4}{1 + \sqrt{K_1/4K_2}} = \frac{4}{1 + \sqrt{(1/4) \cdot 10^{\Delta pK}}} \quad (2.53)$$

Conductivity of ampholytes

Another important factor for a good ampholyte is the conductivity at and near the isoelectric point. Regions of low conductivity cause local overheating because of the resulting high local electric field. The conductivity is directly proportional to the concentration of ions in solution, which is dependent on the degree of dissociation α of the ampholytes. For a bivalent ampholyte, the degree of dissociation can be written as:

$$\alpha = \frac{c_{AH_2^+} + c_{A^-}}{c_{tot}} \quad (2.54)$$

By using Equation (2.40) and Equation (2.42), the degree of dissociation can also be written as:

$$\alpha = \frac{c_{H^+}^2 + K_1K_2}{c_{H^+}^2 + c_{H^+}K_1 + K_1K_2} \quad (2.55)$$

At the isoelectric point, the degree of ionization can thus be written as:

$$\alpha_i = \frac{1}{1 + \sqrt{K_1/4K_2}} = \frac{1}{1 + \sqrt{(1/4) \cdot 10^{\Delta pK}}} \quad (2.56)$$

If comparing Equations (2.53) and (2.56), at the isoelectric point, there is a direct proportionality between the conductivity and the buffering capacity.

$$\beta_i = 4\alpha_i \quad (2.57)$$

Thus, at the isoelectric point, a high degree of ionization (good conductivity) is accompanied by a good buffer capacity, and vice versa.

The dependence of both the buffering capacity and the conductivity on the ΔpK is summarized on Figure 4. Panel A shows the relative buffer capacity for a biprotic ampholyte, with $pI = 7$ and different values of ΔpK . This confirms that ampholytes that have a ΔpK greater than 4 possess little buffering capacity in the isoelectric state and therefore are of little use as carrier ampholytes.¹⁷ The conductivity profile in panel B shows the same behavior. Ampholytes that have a ΔpK greater than 4 show little conductivity in the isoelectric region, they are thus not useful ampholytes.

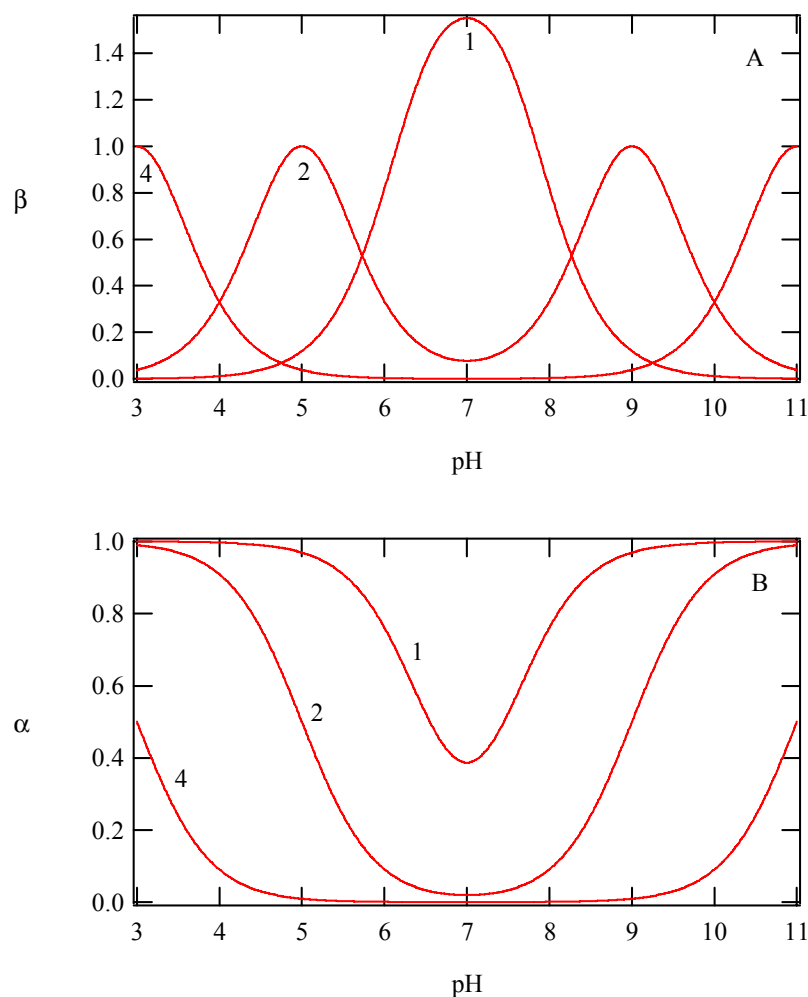


Figure 4: The relative molar buffer capacity of biprotic ampholytes (panel A) and their degree of ionization (panel B) as a function of $\Delta pK = 1, 2, 4$.

Svensson¹⁸ reviewed and listed possible CAs based on their ΔpK values. Amino acids can be found in that list. However, if tracing the buffering capacity of some amino acids (Figure 5), it can be seen that not only the ΔpK value is important, but also the pI value. For histidine, $\Delta pK = 3$ and the pI is located half a way between the two basic groups. The buffer capacity is acceptable, but it is not one of the best CAs. For example, lysine is a much better one: the pI is located between two closely spaced pK values, and the buffer capacity is quite high, close to the maximum value. For the same reasons, cysteine and tyrosine are bad potential CAs, even though their ΔpK values meet the requirements. In the same review, however, it is noted that there is a crucial gap of missing CAs in the pH region between 4 and 7, this being one difficult challenge of CAs.

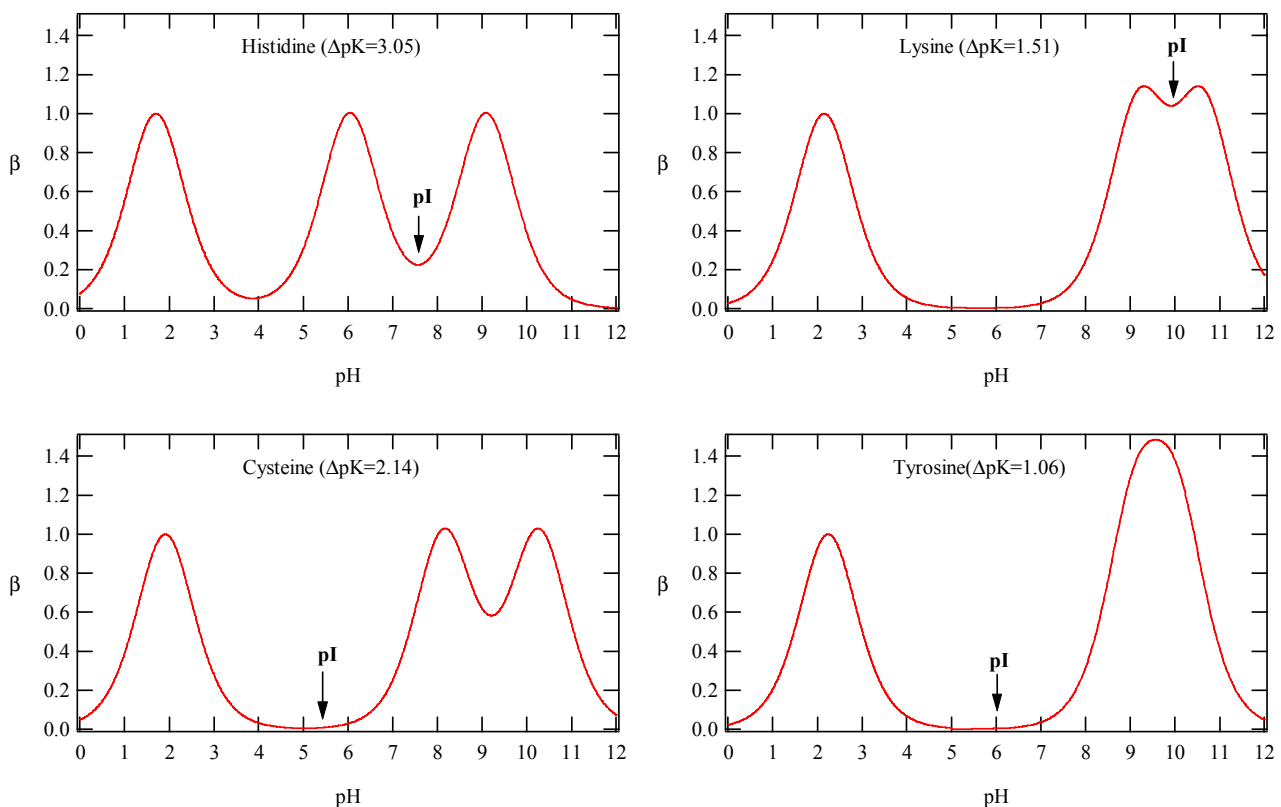


Figure 5: Importance of the relative buffer capacity at the pI value for some amino acids.

Formation of the pH gradient with ampholytes

Once the ampholytes properties discussed, it is important to describe and understand how these compounds align themselves in order to form a stable and linear pH gradient.

If an ampholyte is placed in an electric field, it will migrate away from the electrodes, to position itself at its pI position. Thus the most acidic ampholyte (lowest pI) will migrate closer to the anode where it condenses in its isoelectric state, and a basic ampholyte (highest pI) will migrate closer to the cathode. If a mixture of carrier ampholytes is used with intermediate pI values, they will focus along the electric field, so that a pH gradient is formed, defined by the pH of ampholytes at their point of focusing. The nature and linearity of the pH gradient will depend on the range of isoelectric points, the number of CAs in the system, and their relative concentration and buffer capacity.¹⁶

To describe the behavior of CAs in an electric field and the subsequent establishment of the pH gradient, numerous simulations were performed and confronted with experiments. One of the early works are from Thormann et al., who simulated the focusing dynamics of a mixture of three ampholyte amino acids (Glu, His, Arg) and described the concentration and pH profiles obtained.¹⁹ They concluded on a two-phase process, a relatively rapid separation step, and a slower stabilization step.

However, a three-ampholytes mixture was quite simplistic and commercial systems are more complicated, with hundreds of different species. Thus, a mixture of 15 components was later simulated, showing the increasing complexity of the process.²⁰ And recently, even more sophisticated simulation programs allowed describing up to 150 carrier ampholytes,^{21, 22} as shown in Figure 6.

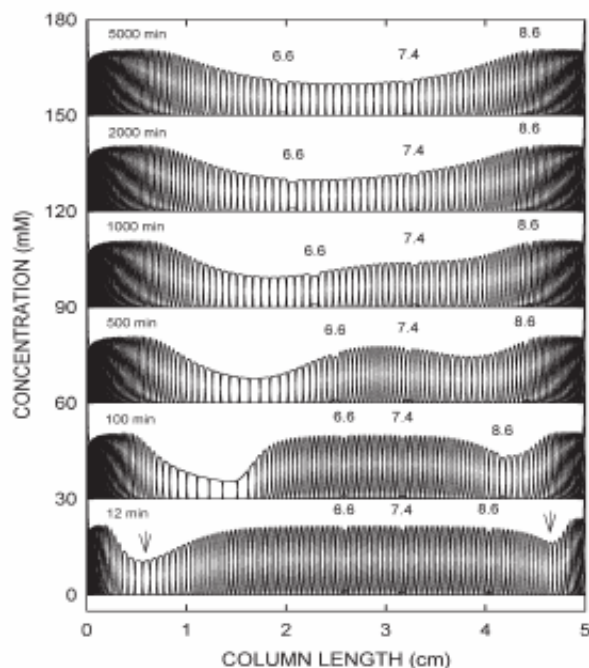


Figure 6: Computer-simulated distributions of 140 carrier components and three dyes after 12, 100, 500, 1000 and 5,000 min of current flow under IEF conditions. The numbers 6.6, 7.4 and 8.6 refer to the pI values of three colored marker dyes and the arrowheads point to their locations. The arrows of the bottom graph mark the two transient concentration valleys that are characteristic for the stabilizing phase. Cathode is at the right. Reprinted with permission from²².

Carrier ampholytes nowadays

Today, on the market, there are four brands of carrier ampholytes commercialized: Ampholine, Servalyt, Pharmalyt and Bio-Lyte.

The synthesis of the first CAs was done by Vesterberg in 1969, a student of Svensson, through a “remarkable chaotic” process. Initially, it consisted in mixing aliphatic oligoamines (from two to nine amino groups) to oligocarboxylic acids.^{23, 24} Some 360 isomers were estimated to be obtained on the pH 3–10 range. This number of isomers could be increased when adding some methyl or ethyl residues on the amino groups.²⁴ The pH interval could also be extended to more basic (pH 9–11) or more acidic (pH 2.5–4) intervals, as suggested by Vesterberg,²⁵ by using aliphatic oligoamines having amino groups more than three methylene

groups apart (1,6-diaminohexane) or dicarboxylic acids (malonic acid). Vesterberg's synthesis process was patented and those CAs are today commercialized under the name of **Ampholine**.

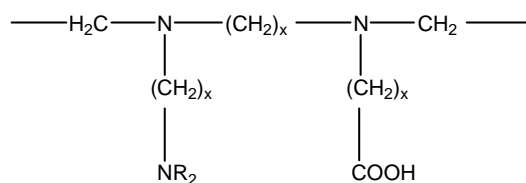


Figure 7: General chemical formula of Ampholines.

Despite a slow growth since its first introduction in vertical columns stabilized by density gradients, IEF saw its popularity increased in the 1970s thanks to the use of thin polyacrylamide gels for IEF.²⁶ This motivated other companies to enter the competition and synthesize carrier ampholytes via alternative routes. The first attempts were initiated by Pogacar and Jarecki²⁷ and by Grubhofer and Borja.²⁸ Their oligoamino mixture was obtained from the condensation of ethylene imine with propylene diamine. To introduce the acidic groups, propansulfone, Na-vinylsulfonate and Na-chloromethyl phosphate were used, thus yielding CAs containing sulphate and phosphate groups instead of carboxylic groups, as counter-ions to the basic groups. Although this was the only way to avoid patent infringement, these species had a big gap in the pH 3.5-5.8 interval, thus they had to introduce also carboxylic acids, which provide enough buffering power in that zone. These compounds were marketed by Grubhofer under the name of **Servalyt**.

The next attempt was from Williams and Söderberg,²⁹ scientists from Pharmacia Biosciences. Their synthesis process consisted in the co-polymerization of amines, amino acids and dipeptides with epichlorohydrin.

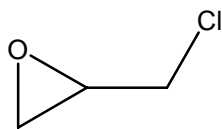


Figure 8: Epichlorohydrin or chloromethyloxirane.

By an appropriate choice of amines and amino acids, five narrow intervals could be generated, which is a major difference to the other syntheses, where a wide range would be generated and narrow cuts would be obtained by focusing in a multicompartiment electrolyzer.³⁰ Until now, it turns out that **Pharmalyte** (trade name of the marketed CAs) are the best CAs, offering the smoothest conductivity and buffering capacity over the pH 3-10 range (Figure 9).³¹ **Bio-Lyte** carrier ampholytes are assumed to be derivatives of Servalyt and are commercialized by Bio-Rad.

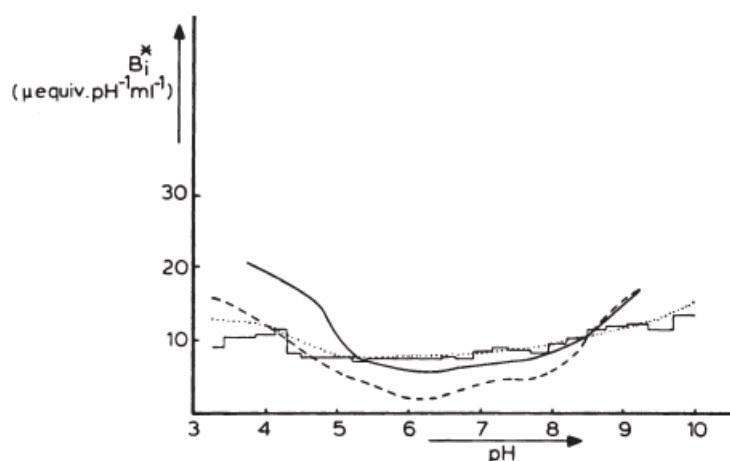


Figure 9: Buffering capacity versus pH of focused Ampholines (solid line), Servalytes (broken line) and Pharmalytes (dotted line). Reprinted from¹⁴ with permission.

For many years since the introduction of the concept by Svensson in 1961, CAs have been used and commercialized under four different brand names indicating different synthesis processes but for all of them, the exact composition of the CAs was never known, as well as CAs structure and effective properties. Until recently, it was assumed that they were complex mixtures, ranging from > 360 for Ampholine, up to 2,000 to 3,000 species for Pharmalyte.

However, recent studies have shown surprising results concerning the mass distribution and focusing properties of CAs for IEF,³¹ which reportedly led to much debate, by “crumbling the Berlin wall” in the knowledge of CA-based IEF.

Indeed, according to Svensson’s definition, CAs would be good as ampholytes and carriers and should be focusing into sharp zones. In this study,³¹ the four brands of CAs were studied in terms of mass composition and isoforms composition, and unexpected new results were shown. First, the CAs narrow cuts turn out to be still polydisperse considering their narrow pH range (0.1 pH unit), exhibiting from 85 to 306 isomers in 2 pH units of the alkaline region, most of them being isoforms (same molecular weight, but different pI and mobilities). A second important pattern also appeared: contrary to theory, for all of them, a very large proportion of CAs (75%) are “poor carrier ampholytes”, in that they are unable to focus and are evenly distributed along the generated pH gradient in the electric field (Figure 10). The pH is created and sustained by the minority of species, which appear to focus at their pI into sharp zones.

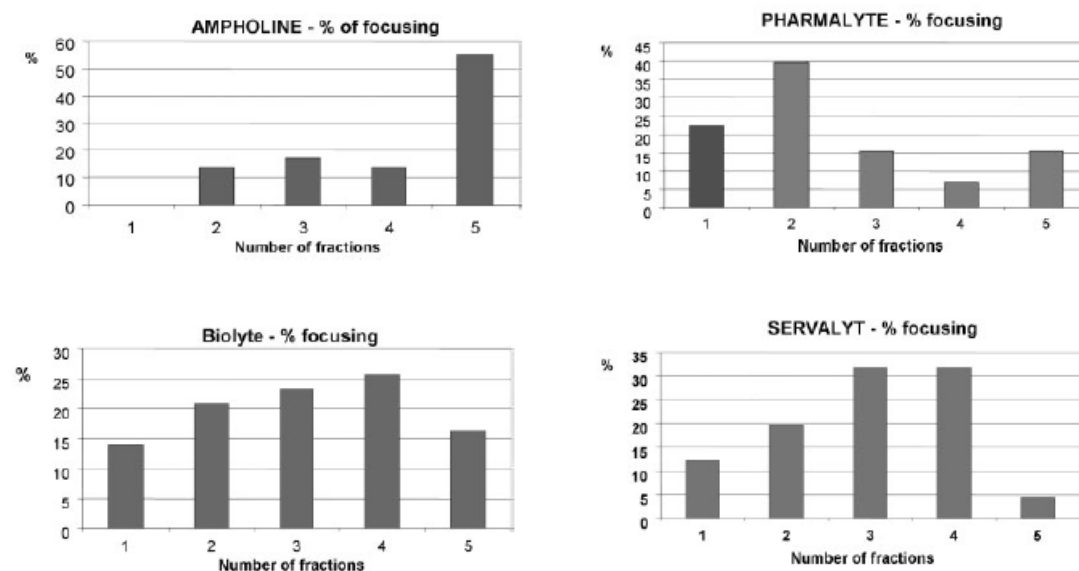


Figure 10: Percentage of species focusing in either a single fraction or over the entire pH gradient (5 fractions).

Reprinted from ³¹ with permission.

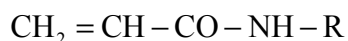
This study shows the still existing challenges of CA-based IEF, faced to IPG-based IEF (where a total of only ten chemicals generate the smoothest possible pH gradients, of any shape and interval). The short term remedy suggested is to mix the three best brands of CAs (according to this study, Bio-Lyte, Pharmalyte and Servalyt contain the larger number of species), to obtain a better resolution and shape of pH gradient. But in the long term, if the CAs are to be used as narrow cuts, the synthesis routes could be improved.

4.2 Immobilized pH gradient (IPG) gels

It is in the 1980s, almost twenty years after the works of Svensson on the carrier ampholytes, that works with immobilized pH gradients were first published, by Bjellqvist et al.³² Despite the enormous success of carrier ampholyte based IEF since its introduction, the technique still had certain inherent limitations and problems, which justified the need for another way towards a pH gradient. The main drawbacks mentioned of the CA-based IEF were: the “cathodic drift” or “plateau phenomenon”^{33, 34} (slow change of what was expected to be a stable pH gradient with time), conductivity and buffer capacity gaps (due to the cathodic drift leading to the depletion of carrier ampholytes in some parts of the pH gradient), too low and uncontrolled ionic strength. The main weakness of CAs was that the pH gradient was generated thanks to a large number of amphoteric compounds, and that the distribution of these compounds was not even (and unknown), as well as their conductivity and buffer capacity.³⁵

To overcome these limitations, alternative ways for creating stable pH gradients without CAs had thus been explored, namely thermal pH gradient,³⁶ dielectric pH gradient,³⁷ rheoelectrolytic generation of pH gradient,³⁸ or isoelectric membranes IEF.³⁹ More interestingly, a patent by Gasparic et al.⁴⁰ was published by the end of the 1980s, on the

original concept of binding the buffering groups generating the pH gradients to the matrix used for convectional stabilization. For the generation of this type of pH gradient in polyacrylamide gels, a set of buffering monomers, called Immobilines (in analogy with Ampholine), is used. The Immobilines™ are acrylamide derivatives with the general chemical formula:



where R contains either a carboxylic acid or an amino group.

An Immobiline is thus a weak acid or base defined by its $\text{p}K_a$ values. These monomers are incorporated in the polyacrylamide gel during polymerization (Figure 11). The gel will thus have a pH defined by the concentrations and dissociation constants of the Immobilines. The conductivity of the gel will also be related, not only to H^+ and OH^- , but also to the amount of incorporated Immobilines and their buffer capacity.

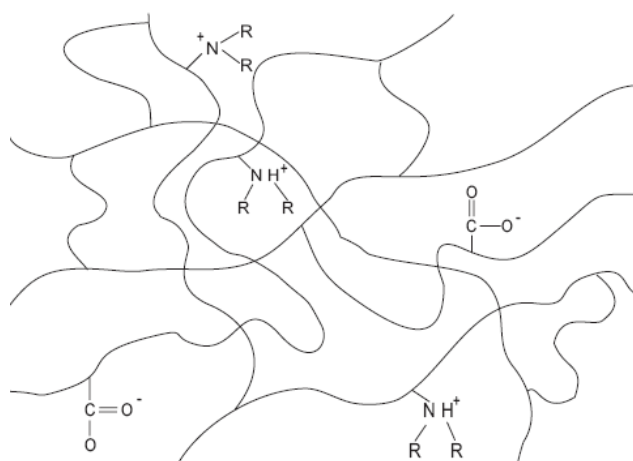


Figure 11: Polyacrylamide matrix with bound Immobilines

The available Immobilines allow the generation of any narrow pH gradient between pH 3 and 10. Table 1 lists the available Immobilines and their $\text{p}K$ values determined experimentally and in different medium by Bjellqvist et al.:³² three acidic and four basic, with

p*K* values spanning the pH range 3.6–9.3. These values have been determined in gels (dimensions 240×110×1 mm) by titration of an Immobiline with another, fully dissociated Immobiline. The results show that the differences observed between the monomer and the buffering groups incorporated in the gel are mainly due to medium effects and temperature variations.³²

Table 1: Apparent p*K* values for Immobilines from reference.³² T is the total acrylamide concentration and C is the degree of cross-linking.

	H ₂ O		Polyacrylamide gel T% = 5%, C% = 3%		Polyacrylamide gel T% = 5%, C% = 3% glycerol 25% (w/v)	
	10°C	25°C	10°C	25°C	10°C	25°C
Acid						
Immobiline p <i>K</i> 3.6	3.57	3.58	-	-	3.68 ± 0.02	3.75 ± 0.02
Immobiline p <i>K</i> 4.4	4.39	4.39	4.30 ± 0.02	4.36 ± 0.02	4.40 ± 0.03	4.47 ± 0.03
Immobiline p <i>K</i> 4.6	4.60	4.61	4.51 ± 0.02	4.61 ± 0.02	4.61 ± 0.02	4.71 ± 0.03
Base						
Immobiline p <i>K</i> 6.2	6.41	6.23	6.21 ± 0.05	6.15 ± 0.03	6.32 ± 0.08	6.24 ± 0.07
Immobiline p <i>K</i> 7.0	7.12	6.97	7.06 ± 0.07	6.96 ± 0.05	7.08 ± 0.07	6.95 ± 0.06
Immobiline p <i>K</i> 8.5	8.96	8.53	8.50 ± 0.06	8.38 ± 0.06	8.66 ± 0.09	8.45 ± 0.07
Immobiline p <i>K</i> 9.3	9.64	9.28	9.59 ± 0.08	9.31 ± 0.07	9.57 ± 0.06	9.30 ± 0.05

After the original article of 1982, further developments were made concerning the immobilized gradients, computer modeling for calculation of extended IPG,⁴¹⁻⁴⁴ as well as development of the chemistry of the buffering compounds.^{45, 46} Further work was thus performed to better understand the properties of Immobiline chemicals,⁴⁷ namely on the basic compounds and their hydrophobicity. Those works led to the development of new basic Immobiline chemicals, which have better properties in terms of hydrophobicity and stability. Table 2 gives the chemical structure of some Immobilines.⁴⁷

Table 2: Immobilines chemical formula from reference.⁴⁷

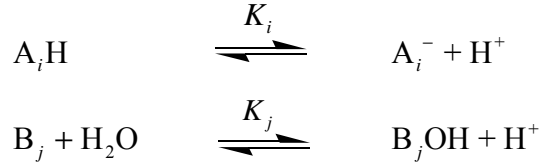
pK	Formula	Name	MW (g·mol ⁻¹)
Acid			
1.0	$\text{CH}_2=\text{CH}-\text{CO}-\text{NH}-\begin{array}{c} \text{CH}_3 \\ \\ \text{C}-\text{CH}_3 \\ \\ \text{CH}_2\text{SO}_3\text{H} \end{array}$	2-Acrylamido-2methylpropane sulfonic acid	207
3.1	$\text{CH}_2=\text{CH}-\text{CO}-\text{NH}-\begin{array}{c} \text{CH}-\text{COOH} \\ \\ \text{OH} \end{array}$	2-Acrylamidoglycolic acid	145
3.6	$\text{CH}_2=\text{CH}-\text{CO}-\text{NH}-\text{CH}_2-\text{COOH}$	N-Acryloylglycine	129
4.4	$\text{CH}_2=\text{CH}-\text{CO}-\text{NH}-(\text{CH}_2)_2-\text{COOH}$	3-Acrylamidopropanoic acid	143
4.6	$\text{CH}_2=\text{CH}-\text{CO}-\text{NH}-(\text{CH}_2)_3-\text{COOH}$	4-Acrylamidobutyric acid	157
Base			
6.2	$\text{CH}_2=\text{CH}-\text{CO}-\text{NH}-(\text{CH}_2)_2-\text{N} \begin{array}{c} \diagup \text{O} \diagdown \\ \diagdown \text{O} \diagup \end{array}$	2-Morpholinoethylacrylamide	184
7.0	$\text{CH}_2=\text{CH}-\text{CO}-\text{NH}-(\text{CH}_2)_3-\text{N} \begin{array}{c} \diagup \text{O} \diagdown \\ \diagdown \text{O} \diagup \end{array}$	3-Morpholinopropylacrylamide	198
8.5	$\text{CH}_2=\text{CH}-\text{CO}-\text{NH}-(\text{CH}_2)_2-\text{N}(\text{CH}_3)_2$	N,N-Dimethylaminoethylacrylamide	142
9.3	$\text{CH}_2=\text{CH}-\text{CO}-\text{NH}-(\text{CH}_2)_3-\text{N}(\text{CH}_3)_2$	N,N-Dimethylaminopropylacrylamide	156
10.3	$\text{CH}_2=\text{CH}-\text{CO}-\text{NH}-(\text{CH}_2)_2-\text{N}(\text{C}_2\text{H}_5)_2$	N,N-Diethylaminopropylacrylamide	184

Altland^{48, 49} and Giaffreda⁵⁰ have published software, which allow the calculation of the desired pH gradients with optimization of the distribution of buffer concentration and ionic strength. Developments have also been performed to expand the existing pH range in both directions by using additional types of Immobilines and also to prepare very acidic and basic narrow pH gradients.^{45, 46, 51, 52} The use of immobilized pH gradients is at present restricted to polyacrylamide gels only, but some developments had been done concerning the matrix as well.⁵³

Buffer capacity of IPG gels

Following the introduction of the concept of immobilized pH gradients, some work was done on the simulation of pH gradient and buffer systems⁵⁴, to optimize and determine the concentrations needed for the formation of wide range pH gradient. This work further allowed the calculation of the effective pH gradient, the buffer capacity as well as the ionic strength of

a given mixture of Immobilines. This calculation is based on the consideration of the buffer capacity of monoprotic weak acids A_iH and bases B_j :



The total concentration of A_iH and B_jOH are:

$$c_A = c_{A_i^-} + c_{A_iH} \quad (2.58)$$

$$c_B = c_{B_j^+} + c_{B_jOH} \quad (2.59)$$

By substituting c_{A_iH} and c_{B_jOH} by the appropriate expressions in the dissociation constants K_i and K_j , it can be written:

$$c_{A_i^-} / c_A = K_i / (K_i + c_{H^+}) \quad (2.60)$$

$$c_{B_j^+} / c_B = c_{H^+} / (K_j + c_{H^+}) \quad (2.61)$$

The partial buffer capacity for each acid and basic species in the mixture is:

$$dc_{A_i^-} / dpH = -\ln 10 K_i c_{H^+} c_A / (K_i + c_{H^+})^2 \quad (2.62)$$

$$dc_{B_j^+} / dpH = -\ln 10 K_j c_{H^+} c_B / (K_j + c_{H^+})^2 \quad (2.63)$$

The electroneutrality condition imposes:

$$\sum_{i=1}^m c_{A_i^-} = \sum_{j=1}^l c_{B_j^+} \quad (2.64)$$

where m is the number of acidic Immobilines and l the number of basic Immobilines. If neglecting the H^+ and OH^- concentrations compared to the concentration of other ions, and summing for all the $m+l$ species present in the Immobiline mixture, the total buffer capacity can be written as:

$$\beta = \ln 10 \sum_{i=1}^{m+l} C_i K_i c_{H^+} / (K_i + c_{H^+})^2 \quad (2.65)$$

with C_i the total acid and base concentrations.

Conductivity of the Immobiline gels

The immobilized gradients theoretically exhibit a very low conductivity because the buffers are not freely mobile. Bjellqvist et al. had showed that the conductivity of the Immobilines could be 100 times lower than the one of carrier ampholytes.³² Computer simulations for pH gradient engineering allowed the control of important parameters such as buffer capacity, conductivity and ionic strength (see Figure 12), while generating a pH gradient as linear as possible.⁴¹

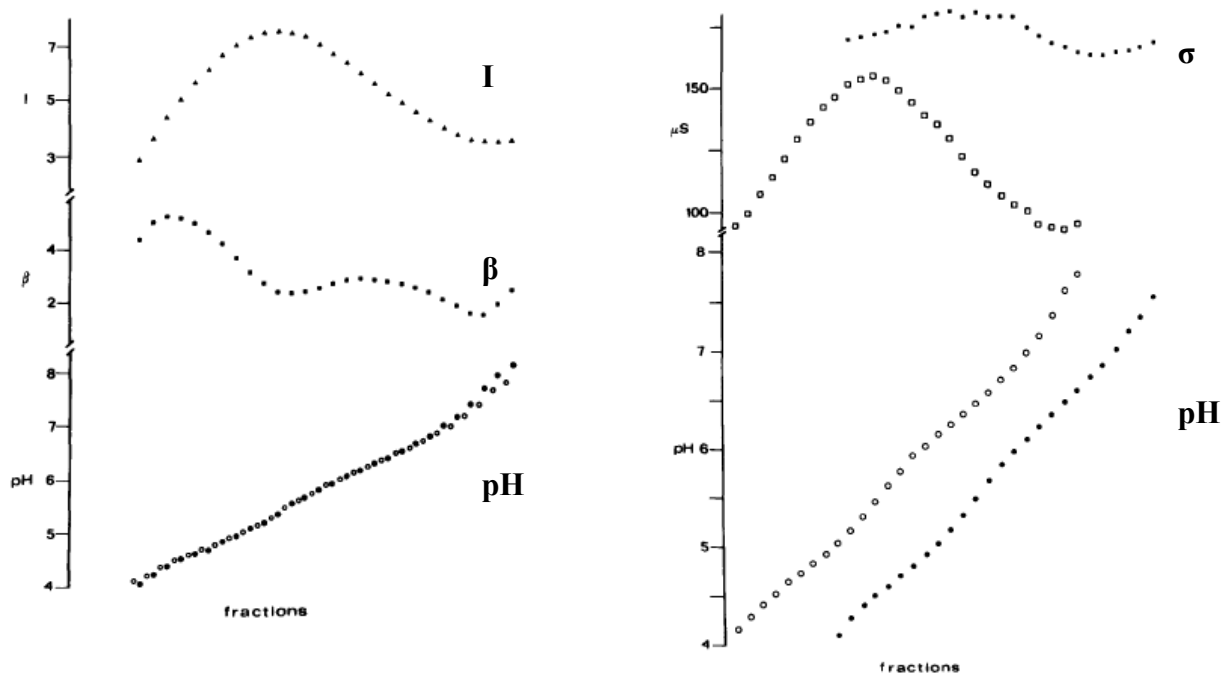


Figure 12: Panel A is the computer simulation of the pH, buffer capacity and ionic strength, and Panel B is the optimization (flattening) of the conductivity. Reprinted from⁴¹ with permission.

Generation of the immobilized pH gradients

In practice, immobilized gradients were obtained by copolymerizing in the polyacrylamide gel matrix reactive compounds (buffering Immobilines) titrated with reactive counterions (non-buffering Immobilines). For narrow range of pH gradient, a simple variation of the Immobiline / titrant ratio is done. If the buffering Immobiline is an acid and c_A and c_B the

concentrations of acidic and basic Immobilines, respectively, the pH is given by the Henderson-Hasselbach equation:

$$\text{pH} = \text{p}K_A + \log\left(\frac{c_A}{c_A - c_B}\right) \quad (2.66)$$

In the case of a basic Immobiline:

$$\text{pH} = \text{p}K_B + \log\left(\frac{c_B}{c_B - c_A}\right) \quad (2.67)$$

If the buffering Immobiline concentration is kept constant, the pH gradient resulting from linear mixing of two solutions will correspond to an ordinary titration curve. The best pH gradients, in terms of linearity and buffer capacity, will in this case be those centered at the $\text{p}K$ of the buffering group. When using only one buffering species, gradients of 1.2 pH unit could be generated.³²

For the generation of extended pH gradients, the use of more than two Immobilines is necessary to create gradients spanning linear pH ranges wider than one unit. The first approach from Righetti was to use multiple chamber mixers and adequate computer programs to calculate the Immobiline concentrations for the different chambers.⁵⁵ Multiple chambers were soon replaced by the easier to use two-chamber mixers. In this method, two solutions containing Immobilines are required, one for the acidic and one for the basic end of the gradient. These two solutions are then cast using a two-vessel gradient mixer to establish the desired pH gradient. The concentration c_i of species in the output flow of a gradient mixer can be calculated. Peterson and Sober⁵⁶ give the basic equation of the output concentration in a mixer with hydrodynamic equilibrium:

$$c_i = L_i \frac{(N-1)!}{(N-n)!(n-1)!} \left(1 - \frac{v}{V}\right)^{N-n} \left(\frac{v}{V}\right)^{n-1} \quad (2.68)$$

with L_i is the concentration of species i in the vessel, N the number of vessels, v the output volume at a certain point, V the total volume in the mixer and n the number of the chamber, in which the species of concentration L_i is placed. The compound i is only placed in one chamber of the mixer. Placing the compound of interest in two or more vessels, the output concentration c_i is obtained from the summation of the *Peterson Sober* equation as follows:

$$c_i = \sum_{n=1}^N L_{in} \frac{(N-1)!}{(N-n)!(n-1)!} \left(1 - \frac{v}{V}\right)^{N-n} \left(\frac{v}{V}\right)^{n-1} \quad (2.69)$$

with L_{in} the concentration of the Immobiline species i in the n^{th} chamber, N the total number of chambers, V the total volume of the system and v the dispensed volume.

Use of IPG gels nowadays

The use of IPG gels has by far exceeded the expectations. The pioneers of this technology thought that IPG gels would be used only when their advantages would be needed, such as the generation of ultra-narrow pH ranges when high resolution is needed.⁴¹ Today, IPG gels are used routinely in 2-D gel electrophoresis, OFFGEL IEF, shotgun proteomics, because of the reproducibility of the pH gradient and the ready-made format. Immobilines are commercialized by GE Healthcare (former Amersham Biosciences), as well as ready-made dried gels (brand name Immobiline DryStrip gels). Bio-Rad commercializes the ReadyStrip gels, containing already the Immobilines. Both type of gels just need to be rehydrated in the appropriate sample solution before use. Their development contributed to the fast development of 2-D gel electrophoresis as well, because they are used in the first dimension of that methodology.

Example of the focusing of an amino acid in an IPG

Once the pH gradient established, the focusing of ampholyte species in an IPG can be described, for example of an amino acid without side chains. The amino acid has one C-terminus acid group (dissociation constant K_{a1}) and one N-terminus basic group (dissociation constant K_{a2}). For the acidic group:

$$c_{A^-} + c_{AH} = c_{tot} \quad \text{and} \quad K_1 = \frac{c_{A^-} \cdot c_{H^+}}{c_{AH}} \quad (2.70)$$

This gives:

$$c_{A^-} = c_{tot} \frac{K_1 \cdot 10^{\text{pH}}}{1 + K_1 \cdot 10^{\text{pH}}} \quad (2.71)$$

$$c_{AH} = c_{tot} \frac{1}{1 + K_1 \cdot 10^{\text{pH}}} \quad (2.72)$$

For the basic group, the same reasoning gives:

$$c_{BH^+} = c_{tot} \frac{1}{1 + K_2 \cdot 10^{\text{pH}}} \quad (2.73)$$

$$c_B = c_{tot} \frac{K_2 \cdot 10^{\text{pH}}}{1 + K_2 \cdot 10^{\text{pH}}} \quad (2.74)$$

The amino acid is thus present under four forms: in the cationic form ($AH-BH^+$), neutral ($AH-B$), zwitterionic (A^-BH^+) or anionic form (A^-B). The following concentrations are thus obtained, assuming that the two groups do not interact:

$$c_{AH-BH^+} = c_{AH} c_{BH^+} = c_{tot}^2 \left(\frac{1}{1 + K_1 \cdot 10^{\text{pH}}} \right) \cdot \left(\frac{1}{1 + K_2 \cdot 10^{\text{pH}}} \right) \quad (2.75)$$

$$c_{AH-B} = c_{AH} c_B = c_{tot}^2 \left(\frac{1}{1 + K_1 \cdot 10^{\text{pH}}} \right) \cdot \left(\frac{K_2 \cdot 10^{\text{pH}}}{1 + K_2 \cdot 10^{\text{pH}}} \right) \quad (2.76)$$

$$c_{A^-BH^+} = c_{A^-} c_{BH^+} = c_{tot}^2 \left(\frac{K_1 \cdot 10^{\text{pH}}}{1 + K_1 \cdot 10^{\text{pH}}} \right) \cdot \left(\frac{1}{1 + K_2 \cdot 10^{\text{pH}}} \right) \quad (2.77)$$

$$c_{A^-B} = c_{A^-} c_B = c_{tot}^2 \left(\frac{K_1 \cdot 10^{\text{pH}}}{1 + K_1 \cdot 10^{\text{pH}}} \right) \cdot \left(\frac{K_2 \cdot 10^{\text{pH}}}{1 + K_2 \cdot 10^{\text{pH}}} \right) \quad (2.78)$$

The distribution of the species is represented on Figure 13, panel A is the distribution before focusing, panel B is after focusing and panel C is after focusing with a stronger electric field.

By increasing the electric field, the charged species disappear completely, to focus into a total concentration. The peak corresponding to the zwitterionic species is superposed to the total concentration peak (panel C).

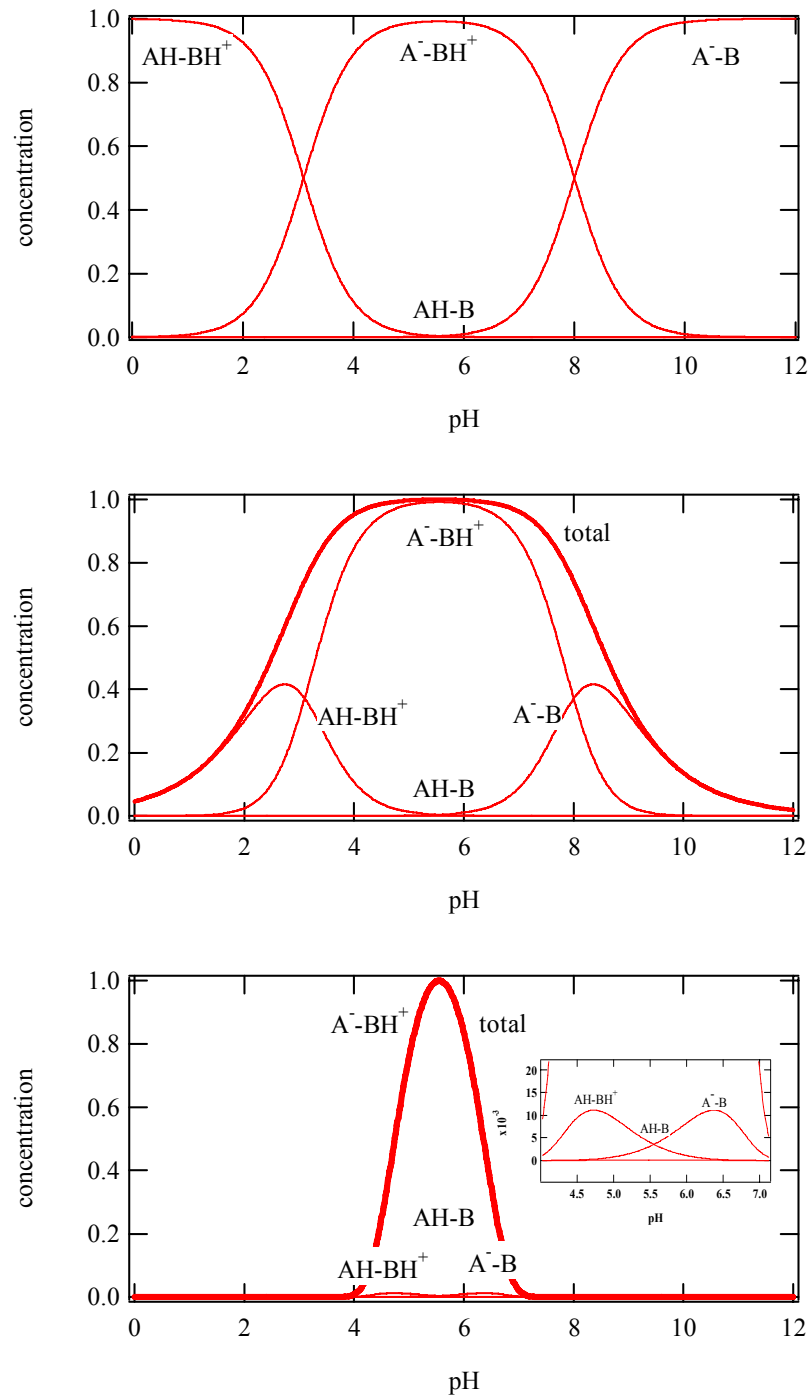


Figure 13: Panel A is the distribution of the different forms of the amino acid, panel B is the distribution obtained after focusing with an electric field of 1 and panel C with an electric field of 10.

For the focalization of peptides in an IPG, the peptide is then represented by its titration curve. But this point will be further discussed in the chapter III, where the transient IEF equation is solved for peptides.

5. OFFGEL isoelectric focusing (OG-IEF)

OFFGEL IEF is a concept recently developed in the lab.⁵⁷ It is a method for IEF, using an immobilized pH gradient, and which consists in using the pH gradient in the gel and the buffering capacity near the gel surface, to separate proteins and recover them in liquid fractions. The gel buffers the solution in the chamber and the proteins are charged according to their pI and to the pH imposed by the gel (Figure 14).

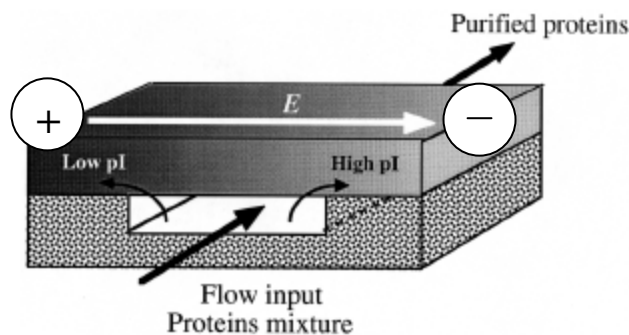


Figure 14: Principle of the OFFGEL IEF separation. Cations migrate to the cathode, placed on the alkaline extremity of the gel, and anions migrate to the anode, placed on the acidic extremity of the gel. Neutral species go through the chamber. Reprinted from⁵⁷.

Upon application of an electric field perpendicularly to the liquid chamber, the current lines penetrate into the chamber and extracts charged species from the solution into the gel (Figure 15). After separation, only the globally neutral species ($pI = pH$ of the IPG gel) remain in solution.

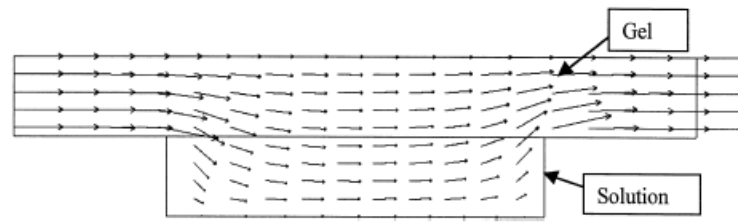


Figure 15: Current line distribution in a cross section of the OFFGEL chamber, the length of the arrow is proportional to the current intensity. Reprinted from⁵⁷.

The necessary condition for OFFGEL is the buffering of the solution by the gel. Thus the buffering of the solution by the Immobilines present in the gel was studied, and described the pH profile in the thin layer of solution close to the gel. The OFFGEL focusing of two ampholytes was also studied and showed the progressive buffering of the chamber (Figure 16).

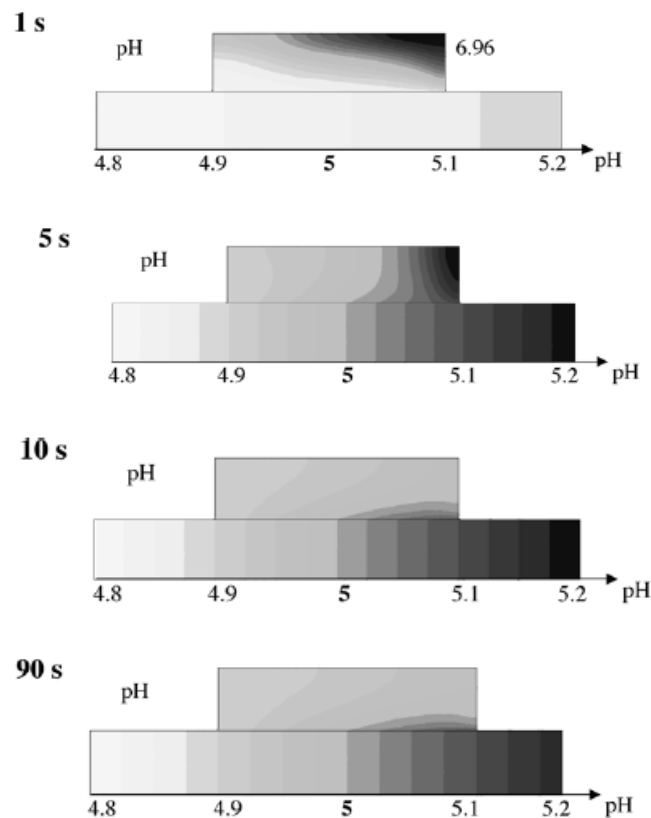


Figure 16: pH isovalues as a function of time, during the focusing of two ampholytes by OFFGEL. Reprinted from².

The OFFGEL technique, as described above, was initially developed for protein purification purposes. It was later adapted to a multicompartiment format, in order to recover the protein fractions and further analyze them (semi-preparative use).⁵⁸ The system was able to resolve the two forms of β -lactoglobulin A (pI 5.1) and B (pI 5.2). The technique was later used for the separation of peptides generated from tryptic digestion of proteins, in a two dimensional approach.⁵⁹ Numerical simulations of the OGE of peptides will be described in details in the next chapter, and experimental results will be discussed in chapter IV and V.

6. References

1. Girault, H. H., *Electrochimie physique et analytique* Presses Polytechniques et Universitaires Romandes: Lausanne, 2007.
2. Di Maio, I., Off-Gel (TM) electrophoresis: characterisation of a novel isoelectric focusing fractionation method. *Thesis N° 3064 2004*, EPFL.
3. Ros, A., New protein separation and analysis techniques. *PhD thesis, New protein separation and analysis techniques 2000*.
4. Vesterbe.O; Svensson, H., Isoelectric Fractionation Analysis and Characterization of Ampholytes in Natural Ph Gradients .4. Further Studies on Resolving Power in Connection with Separation of Myoglobins. *Acta Chemica Scandinavica 1966*, 20, (3), 820-&.
5. Giddings, J. C.; Dahlgren, K., Resolution and Peak Capacity in Equilibrium-Gradient Methods of Separation. *Separation Science 1971*, 6, (3), 345-356.
6. Raymond, S.; Weintraub, L., Acrylamide Gel as a Supporting Medium for Zone Electrophoresis. *Science 1959*, 130, (3377), 711-711.
7. Hjerten, S., Chromatographic Separation According to Size of Macromolecules and Cell Particles on Columns of Agarose Suspensions. *Archives of Biochemistry and Biophysics 1962*, 99, (3), 466-&.
8. Righetti, P. G.; Brost, B. C. W.; Snyder, R. S., On the Limiting Pore-Size of Hydrophilic Gels for Electrophoresis and Isoelectric-Focusing. *Journal of Biochemical and Biophysical Methods 1981*, 4, (5-6), 347-363.
9. Gelfi, C.; Righetti, P. G., Polymerization Kinetics of Polyacrylamide Gels .1. Effect of Different Cross-Linkers. *Electrophoresis 1981*, 2, (4), 213-219.
10. Gelfi, C.; Righetti, P. G., Polymerization Kinetics of Polyacrylamide Gels .2. Effect of Temperature. *Electrophoresis 1981*, 2, (4), 220-228.
11. Guide to Isoelectric Focusing. *Amersham Biosciences*.
12. Westermeier, R., Electrophoresis in practice. *Electrophoresis in practice 4th Edition, Wiley-VCH, Weinheim 2001*.
13. Svensson, H., Isoelectric Fractionation, Analysis, and Characterization of Ampholytes in Natural Ph Gradients .1. Differential Equation of Solute Concentrations at a Steady State and Its Solution for Simple Cases. *Acta Chemica Scandinavica 1961*, 15, (2), 325-&.
14. Righetti, P. G., The Alpher, Bethe, Gamow of isoelectric focusing, the alpha-Centaury of electrokinetic methodologies. Part I. *Electrophoresis 2006*, 27, (5-6), 923-938.
15. Rilbe, H., Rapid Isoelectric Focusing in Density Gradient Columns. *Annals of the New York Academy of Sciences 1973*, 209, (Jun15), 80-93.
16. Catsimpoolas, N., Isoelectric Focusing - Fundamental Aspects. *Separation Science 1975*, 10, (1), 55-76.
17. Rilbe, H., *pH and Buffer Theory*. Chichester, 1996; p 87-92.
18. Svensson, H., Isoelectric Fractionation, Analysis and Characterization of Ampholytes in Natural Ph Gradients .2. Buffering Capacity and Conductance of Isoionic Ampholytes. *Acta Chemica Scandinavica 1962*, 16, (2), 456-&.
19. Thormann, W.; Mosher, R. A.; Bier, M., Experimental and Theoretical Dynamics of Isoelectric-Focusing - Elucidation of a General Separation Mechanism. *Journal of Chromatography 1986*, 351, (1), 17-29.
20. Thormann, W.; Mosher, R. A., Advances in Electrophoresis. *Advances in Electrophoresis, Vol. 2, VCH Publishers, New York 1988*.
21. Mao, Q. L.; Pawliszyn, J.; Thormann, W., Dynamics of capillary isoelectric focusing in the absence of fluid flow: High resolution computer simulation and experimental validation with whole column optical imaging. *Analytical Chemistry 2000*, 72, (21), 5493-5502.

22. Mosher, R. A.; Thormann, W., High-resolution computer simulation of the dynamics of isoelectric focusing using carrier ampholytes: The post-separation stabilizing phase revisited. *Electrophoresis* **2002**, *23*, (12), 1803-1814.
23. Vesterbe.O, Synthesis and Isoelectric Fractionation of Carrier Ampholytes. *Acta Chemica Scandinavica* **1969**, *23*, (8), 2653-&.
24. Vesterbe.O, Physicochemical Properties of Carrier Ampholytes and Some Biochemical Applications. *Annals of the New York Academy of Sciences* **1973**, *209*, (Jun15), 23-33.
25. Vesterberg, O., Isoelectric focusing, New York. in *Catsimpoalas, N. (Ed): Isoelectric focusing, Academic Press, New York 1976*.
26. Righetti, P.; Drysdale, J. W., Isoelectric Focusing in Polyacrylamide Gels. *Biochimica Et Biophysica Acta* **1971**, *236*, (1), 17-24.
27. Pogacar, P.; Jarecki, R.; in Allen, R. C.; Maurer, H.; (Eds), Electrophoresis and Isoelectric focusing in polyacrylamide gels. *Electrophoresis and Isoelectric focusing in polyacrylamide gels* **1974**, de Gruyter, Berlin, 153-158.
28. Grubhofer, N.; Borja, C.; in Radola, B. J.; Graesslin, D.; (Eds), Electrofocusing and Isotachopheresis. *Electrofocusing and Isotachopheresis* **1977**, de Gruyter, Berlin, 111-120.
29. Williams, K. W.; Soderberg, L., Carrier Ampholyte for Isoelectric-Focusing. *International Laboratory* **1979**, (Jan-), 45-&.
30. Gianazza, E.; Pagani, M.; Luzzana, M.; Righetti, P. G., Fractionation of Carrier Ampholytes for Isoelectric Focusing. *Journal of Chromatography* **1975**, *109*, (2), 357-364.
31. Sebastiano, R.; Simo, C.; Mendieta, M. E.; Antonioli, P.; Citterio, A.; Cifuentes, A.; Peltre, G.; Righetti, P. G., Mass distribution and focusing properties of carrier ampholytes for isoelectric focusing: I. Novel and unexpected results. *Electrophoresis* **2006**, *27*, (20), 3919-3934.
32. Bjellqvist, B.; Ek, K.; Righetti, P. G.; Gianazza, E.; Gorg, A.; Westermeier, R.; Postel, W., Isoelectric-Focusing in Immobilized Ph Gradients - Principle, Methodology and Some Applications. *Journal of Biochemical and Biophysical Methods* **1982**, *6*, (4), 317-339.
33. Righetti, P. G.; Drysdale, J. W., Small-Scale Fractionation of Proteins and Nucleic-Acids by Isoelectric Focusing in Polyacrylamide Gels. *Annals of the New York Academy of Sciences* **1973**, *209*, (Jun15), 163-186.
34. Chrambac.A; Doerr, P.; Finlayso.Gr; Miles, L. E. M.; Sherins, R.; Rodbard, D., Instability of Ph Gradients Formed by Isoelectric Focusing in Polyacrylamide-Gel. *Annals of the New York Academy of Sciences* **1973**, *209*, (Jun15), 44-64.
35. Righetti, P. G., Distribution of Carrier Ampholytes in Isoelectric-Focusing. *Journal of Chromatography* **1977**, *138*, (1), 213-215.
36. Luner, S. J.; Kolin, A., A New Approach to Isoelectric Focusing and Fractionation of Proteins in a Ph Gradient. *Proceedings of the National Academy of Sciences of the United States of America* **1970**, *66*, (3), 898-&.
37. Troitsky, G. V.; Zavyalov, V. P.; Kirjukhin, I. F.; Abramov, V. M.; Agitsky, G. J., Isoelectric Focusing of Proteins Using a Ph Gradient Created by a Concentration Gradient of Nonelectrolytes in Solution. *Biochimica Et Biophysica Acta* **1975**, *400*, (1), 24-31.
38. Rilbe, H., Steady-State Rheoelectrolysis. *Journal of Chromatography* **1978**, *159*, (1), 193-205.
39. Martin, A. J. P.; Hampson, F., New Apparatus for Isoelectric-Focusing. *Journal of Chromatography* **1978**, *159*, (1), 101-110.
40. Gasparic, V.; Bjellqvist, B.; Rosengren, A., 1975 Swedish patent, 1978 US patent, 1981 German patent.

41. Dossi, G.; Celentano, F.; Gianazza, E.; Righetti, P. G., Isoelectric-Focusing in Immobilized Ph Gradients - Generation of Extended Ph Intervals. *Journal of Biochemical and Biophysical Methods* **1983**, 7, (2), 123-142.
42. Gianazza, E.; Dossi, G.; Celentano, F.; Righetti, P. G., Isoelectric-Focusing in Immobilized Ph Gradients - Generation and Optimization of Wide Ph Intervals with 2-Chamber Mixers. *Journal of Biochemical and Biophysical Methods* **1983**, 8, (2), 109-133.
43. Gianazza, E.; Celentano, F.; Dossi, G.; Bjellqvist, B.; Righetti, P. G., Preparation of Immobilized Ph Gradients Spanning 2-6 Ph Units with 2-Chamber Mixers - Evaluation of 2 Experimental Approaches. *Electrophoresis* **1984**, 5, (2), 88-97.
44. Gianazza, E.; Celentano, F.; Magenes, S.; Etori, C.; Righetti, P. G., Formulations for Immobilized Ph Gradients Including Ph Extremes. *Electrophoresis* **1989**, 10, (11), 806-808.
45. Chiari, M.; Casale, E.; Santaniello, E.; Righetti, P. G., Synthesis of buffers for generating immobilized pH gradients. I: Acidic acrylamido buffers. *Applied and theoretical electrophoresis* **1989**, 1, ((2)), 99-102.
46. Chiari, M.; Casale, E.; Santaniello, E.; Righetti, P. G., Synthesis of buffers for generating immobilized pH gradients. II: Basic acrylamido buffers. *Applied and theoretical electrophoresis* **1989**, 1, (2), 103-7.
47. Chiari, M.; Righetti, P. G., The Immobiline Family - from Vacuum to Plenum Chemistry. *Electrophoresis* **1992**, 13, (4), 187-191.
48. Altland, K., Ipgmaker - a Program for Ibm-Compatible Personal Computers to Create and Test Recipes for Immobilized Ph Gradients. *Electrophoresis* **1990**, 11, (2), 140-147.
49. Altland, K.; Altland, A., Pouring Wide-Range Immobilized Ph Gradient Gels with a Window of Extremely Flattened Slope. *Electrophoresis* **1990**, 11, (4), 337-342.
50. Giaffreda, E.; Tonani, C.; Righetti, P. G., Ph Gradient Simulator for Electrophoretic Techniques in a Windows Environment. *Journal of Chromatography* **1993**, 630, (1-2), 313-327.
51. Chiari, M.; Pagani, L.; Righetti, P. G.; Jain, T.; Shorr, R.; Rabilloud, T., Synthesis of an Hydrophilic, Pk 8.05 Buffer for Isoelectric-Focusing in Immobilized Ph Gradients. *Journal of Biochemical and Biophysical Methods* **1990**, 21, (2), 165-172.
52. Chiari, M.; Righetti, P. G.; Ferraboschi, P.; Jain, T.; Shorr, R., Synthesis of Thiomorpholino Buffers for Isoelectric-Focusing in Immobilized Ph Gradients. *Electrophoresis* **1990**, 11, (8), 617-620.
53. Chiari, M.; Micheletti, C.; Nesi, M.; Fazio, M.; Righetti, P. G., Towards New Formulations for Polyacrylamide Matrices - N-Acryloylaminoethoxyethanol, a Novel Monomer Combining High Hydrophilicity with Extreme Hydrolytic Stability. *Electrophoresis* **1994**, 15, (2), 177-186.
54. Celentano, F.; Gianazza, E.; Dossi, G.; Righetti, P. G., Buffer Systems and Ph Gradient Simulation. *Chemometrics and Intelligent Laboratory Systems* **1987**, 1, (4), 349-358.
55. Righetti, P. G., *Immobilized pH Gradients: Theory and Methodology*. Elsevier: Amsterdam, 1990.
56. Peterson, E. A.; Sober, H. A., Variable Gradient Device for Chromatography. *Analytical Chemistry* **1959**, 31, (5), 857-862.
57. Ros, A.; Faupel, M.; Mees, H.; van Oostrum, J.; Ferrigno, R.; Reymond, F.; Michel, P.; Rossier, J. S.; Girault, H. H., Protein purification by Off-Gel electrophoresis. *Proteomics* **2002**, 2, (2), 151-156.
58. Michel, P. E.; Reymond, F.; Arnaud, I. L.; Josserand, J.; Girault, H. H.; Rossier, J. S., Protein fractionation in a multicompartiment device using Off-Gel (TM) isoelectric focusing. *Electrophoresis* **2003**, 24, (1-2), 3-11.
59. Heller, M.; Michel, P. E.; Morier, P.; Crettaz, D.; Wenz, C.; Tissot, J. D.; Reymond, F.; Rossier, J. S., Two-stage Off-Gel (TM) isoelectric focusing: Protein followed by peptide

fractionation and application to proteome analysis of human plasma. *Electrophoresis* **2005**, 26, (6), 1174-1188.

CHAPTER III: Modeling the Isoelectric Focusing of Peptides in an OFFGEL Multicompartment Cell*

1. Introduction.....	84
2. Methods.....	87
2.1 Short introduction on the theory of finite element.....	87
2.2 Analytical Model.....	90
2.3 Finite Element Model.....	93
2.4 In silico proteome digestion and computation of physico-chemical parameters.....	96
3. Results and discussion.....	97
3.1 Model validation.....	97
3.2 Determination of the order of magnitude of dz/dpH at pI	98
3.3 Effect of the charge gradient dz/dx at the pI (1-D study).....	100
3.3.1 Effect on the peak width.....	100
3.3.2 Effect on the focusing time.....	102
3.4 Effect of the well height on the recovery and focusing time (2-D study).....	105
3.5 Effect of the well shape on the recovery and focusing time.....	108
3.6 IEF of peptides in a seven-well device.....	110
4. Concluding Remarks.....	112
5. References.....	113

* based on H.-T. Lam, J. Josserand, N. Lion and H. H. Girault, Journal of Proteome Research 2007, 6, 1666-1766

1. Introduction

Isoelectric focusing (IEF) is a high-resolution electrophoretic technique used to separate and concentrate amphoteric biomolecules at their isoelectric point (pI) in a pH gradient and under the application of an electric field. IEF is classically used in buffered free solution (in the presence of so-called carrier ampholytes), or in Immobilized pH Gradient (IPG) gels. In the past decades, isoelectric focusing has gained great significance due to its wide applicability in different fields.

In the field of proteomics, in-gel IEF of proteins is used routinely as the first dimension of two-dimensional gel electrophoresis,^{1, 2} which remains the workhorse for proteome analysis.³ But because further protein analysis and characterization by mass spectrometry⁴ require tedious sample preparation, new IEF schemes and devices have been designed for prefractionation of proteins by IEF.^{5, 6} Several teams have explored the use of free-flow electrophoresis for the fractionation of proteomic samples.⁷⁻¹² Righetti et al. have introduced multicompartiment electrolyzers, in which proteins are separated into different compartments separated by Immobiline membranes.¹³⁻¹⁵ Wall et al. have also validated the use of Rotofor for fractionation of proteins prior to RP-HPLC and MALDI-TOF analysis of intact proteins.¹⁶ We have introduced a new concept named OFFGEL IEF with the first aim to purify proteins.¹⁷ The technique was later successfully used for the isoelectric fractionation of *Escherichia coli* proteins, proving to be a promising tool for proteomic applications.¹⁸

Besides these general efforts to develop IEF for protein fractionation, IEF has also been used for peptide separation in a shotgun approach, where proteins are first proteolyzed, and the resulting peptides mixture separated and analyzed by tandem mass spectrometry. Several groups have used in-gel IEF as a first separation dimension in shotgun proteomics¹⁹⁻²³ as well as free-flow electrophoresis²⁴⁻²⁶ and homemade devices based on Immobiline

membranes.²⁷⁻²⁹ OFFGEL IEF was demonstrated to be of great interest in shotgun proteomics.³⁰⁻³⁴ a commercial device is now marketed by Agilent Technologies. But not only does IEF provide a separation means for peptides, but it also provides an additional physico-chemical information about each peptide, its isoelectric point, which can then be used to validate MS/MS peptide sequence identification, and ultimately filter out false peptide identifications.^{20-23, 30-32} IEF separation of peptides can thus play a crucial role, not only as an efficient separation dimension, but also as a validation / filtering tool when combined with tandem mass spectrometry. As such, it is thus relevant to optimize devices used to separate peptides by IEF, such as OFFGEL.

The multiwell format of OFFGEL electrophoresis initially consists in placing the sample in wells, which are opened at top and bottom extremities and are placed on an IPG gel. The gel buffers a thin layer of the solution in the liquid chambers and the proteins are charged according to their pI and to the pH imposed by the underlying gel. Two electrodes are respectively placed in the extreme compartments of the setup (lowest and highest pH). Upon application of an electric field, the charged species migrate through the gel from well to well until they reach the well where they are neutral ($pI = pH$ gel) and from where they are directly recovered in solution. For the solution to be buffered by the Immobilines present in the gel, the ampholyte concentration in the solution must not be too high and the buffering capacity of the gel must be efficient. Numerical simulations were used to study the influence of the ampholyte concentration in solution and the buffering capacity in OFFGEL IEF.³⁵

Dynamic computer simulation of electrophoresis has already demonstrated considerable value as a research tool. Since the 1980s, numerical simulations have been performed to better understand and describe IEF³⁶⁻⁴⁰ and have shown a qualitative agreement between predictions and experimental results. Recent advances in computer simulation have led to the development of a simulator that can handle up to 150 components and voltages

typically used in experiments. This recently allowed Thormann et al. to perform the simulation of the dynamics of protein IEF in the presence of a large number of carrier ampholytes.^{41, 42} Computer simulation of immobilized pH gradient gels were also done, at acidic and alkaline conditions, showing the focusing dynamics, as well as the conductivity and buffering capacity in these regions.⁴³ Previous works had already led to the creation of a pH gradient simulator for the engineering of IPG gels and isoelectric membranes.^{44, 45} Regarding OFFGEL electrophoresis, the buffering capacity has been studied numerically, and a model has also been developed to describe the isoelectric separation of two simple ampholytes in a 2-D chamber.⁴⁶

In this chapter, we have addressed the questions how sharp the separation of peptides by OFFGEL IEF is and how the fractionation cell can be optimized to obtain the best resolution in the shortest time. We have taken as model biomolecules the peptides generated by *in silico* digestion of the proteomes of *Deinococcus radiodurans*, *Saccharomyces cerevisiae*, and *Homo sapiens* and simulated the OFFGEL isoelectric focusing in a multicompartiment device. The peptide charge slope at *pI* was demonstrated to be a key parameter in the focusing dynamics, and its influence on the peak width and focusing time was studied in order to determine the proportion of correctly focused peptides (peptides recovered in one or two wells at most). This allowed the determination of the optimal well width to obtain the best focusing. The effects of the well height and shape were further studied, to determine the well configuration allowing the highest peptide recovery in the shortest time. In this analysis, we show that the high-resolving power of OFFGEL makes it a highly valuable tool to fractionate peptides in shotgun proteomics, and that it is relevant to optimize the fractionation unit to obtain the best recovery.

2. Methods

2.1 Short introduction on the theory of finite element

In the history of isoelectric focusing, and for other electrophoretic techniques as well, computer simulations have always been of great help in understanding the separation process. Here, the method mainly used for modeling IEF is the finite element method (abbreviated FEM)

The FEM is a numerical method allowing the resolution of partial differential equations, for either stationary or transient problems, linear or non linear, for one to three independent space variables. The domain of study, noted W , is divided into sub-domains, called the finite elements, defined by the nodes, where the unknowns are discretized. Overall, the method consists in transforming partial derivatives into algebraic expressions, allowing further simplification of the equation.

The equation of diffusion – migration is here taken as example to describe the principle of the method. Its local form is:

$$\frac{\partial c}{\partial t} + \nabla \cdot (-D \nabla c - V_m c) = 0 \quad (3.1)$$

with $V_m = \frac{zF}{RT} D \nabla \phi$ the migration velocity (3.2)

The unknown concentration is a function of space and temporal variables. The determination of the concentration profile by the F.E.M. consists in solving the previous equation on the nodes of the finite elements. The continuous unknown, c , is approximated by \tilde{c} , using the interpolation functions β_j and the values of the unknown at the nodes, c_j (see Figure 1):

$$\tilde{c} = \sum_{j=1}^N c_j \beta_j \quad (3.3)$$

N is the total number of nodes.

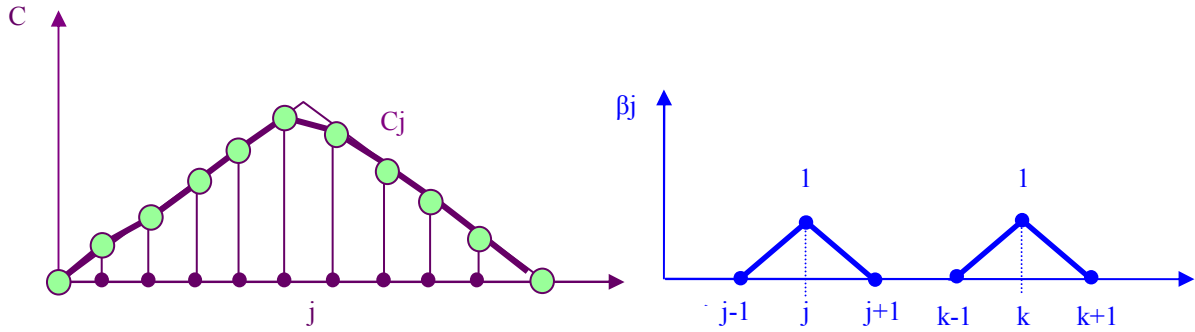


Figure 1: Discretization and interpolation of the unknown concentration. The interpolation function β_j is of the first order.

The interpolation function is, in this case, of the first order, and is described as (see Figure 1):

$$\begin{aligned}\beta_{j,j=i} &= 1 \\ \beta_{j,j \neq i} &= 0\end{aligned}\quad (3.4)$$

If the concentration is replaced by the approximated concentration in Equation (3.1), a residue function appears:

$$\frac{\partial \tilde{c}}{\partial t} + \nabla \cdot \left(-D \nabla \tilde{c} - \frac{zF}{RT} D \tilde{c} \nabla \phi \right) = R \quad (3.5)$$

So the resolution of the primary Equation (3.1) consists in determining the concentration profile by minimizing R . To do so, the expression of R is multiplied by a projection function, α , and integrated over the domain of study W . This is called the **Galerkin formulation**:

$$\iint_W \alpha \left[\frac{\partial \tilde{c}}{\partial t} + \nabla \cdot \left(-D \nabla \tilde{c} - \frac{zF}{RT} D \tilde{c} \nabla \phi \right) \right] dW = 0 \quad (3.6)$$

The projection function (Galerkin) allows lowering the order of derivativization of the unknowns (passing from the **strong formulation** to the **weak formulation**). This is realized

by using the properties of the derivative. By decomposing the product between α and the divergence in Equation (3.6), the second order derivative becomes:

$$\alpha \nabla \cdot (-D \nabla \tilde{c}) = \nabla \cdot (-\alpha D \nabla \tilde{c}) + D \nabla \alpha \cdot \nabla \tilde{c} \quad (3.7)$$

and

$$\alpha \nabla \cdot (V_m \tilde{c}) = \nabla \cdot (\alpha V_m \tilde{c}) + V_m \tilde{c} \cdot \nabla \alpha \quad (3.8)$$

Injecting (3.7) and (3.8) into (3.6), and using the following Green-Ostrogradski theorem:

$$\iint_W \nabla \cdot [\alpha (-D \nabla \tilde{c})] dW = \int_{\ell} \alpha (-D \nabla \tilde{c}) \cdot d\mathbf{l} = \int_{\ell} \alpha (J_{diff}) \cdot d\mathbf{l} \quad (3.9)$$

and

$$\iint_W \nabla \cdot [\alpha (V_m \tilde{c})] dW = \int_{\ell} \alpha (V_m \tilde{c}) \cdot d\mathbf{l} = \int_{\ell} \alpha (J_m) \cdot d\mathbf{l} \quad (3.10)$$

where J_{diff} and J_m are the diffusion and migration flux, respectively. Thus, the divergence term (second term of (3.6)) is rejected at the boundary, where it expresses the diffusion and migration flux conditions of the species. In the present case of study, these boundary conditions are equal to zero (no flux across the boundaries of the domain, because the length of the gel is finite) and only the products of the gradients are conserved in (3.7) and (3.8).

Equation (3.6) becomes:

$$\iint_W \left[\alpha \frac{\partial \tilde{c}}{\partial t} + D \nabla \alpha \cdot \nabla \tilde{c} + V_m \tilde{c} \cdot \nabla \alpha \right] dW = 0 \quad (3.11)$$

So the projection function allowed passing from the second order $\nabla \cdot (-D \nabla \tilde{c})$ in equation (3.6) to the first order $D \nabla \alpha \cdot \nabla \tilde{c}$ in equation (3.11).

Using the interpolation function of the concentration (Equation(3.4)), we obtain:

$$\sum_{j=1}^N \iint_W \left[\alpha \frac{\partial \beta_j}{\partial t} + (D \nabla \alpha \cdot \nabla \beta_j + V_m \cdot \nabla \alpha \beta_j) c_j \right] dW = 0 \quad (3.12)$$

Like the concentration c , α can also be discretized using an interpolation function φ_j :

$$\alpha = \sum_{j=1}^N \alpha_j \varphi_j \quad (3.13)$$

φ_j is of the same type as the function β_j (Galerkin formulation):

$$\begin{aligned} \varphi_{j,j=i} &= 1 \\ \varphi_{j,j \neq i} &= 0 \end{aligned} \quad (3.14)$$

Thus the final **discretized form** of the equation:

$$\sum_{j=1}^N \iint_W \left[\alpha_i \frac{\partial \beta_j}{\partial t} + (D \nabla \alpha_i \cdot \nabla \beta_j + V_m \cdot \nabla \alpha_i \beta_j) \right] dW [c_j] = 0 \quad (3.15)$$

for $i = 1..N$

This equation leads to a square matrix with a linear system of N equations for the N unknowns c_j :

$$[m_{ij}] [c_j] = 0$$

The matrixes m_{ij} and c_j are then described in the generator of equations of the software FLUX-EXPERT™. Thus, solving the problem consists in an inversion of the matrix m_{ij} , to find the solutions which are the coefficients of interpolation, c_j (i.e. the values at the nodes j).

2.2 Analytical Model

The isoelectric point (pI) of a peptide is the pH at which the sum of all the electrical charges is equal to zero. In a peptide, the global charge can be calculated by taking into account the charge of the N-terminus (N-ter) and the C-terminus (C-ter), as well as the charge of ionizable side chains. In addition to the N-terminus, the positive charges can be provided by three amino acids which are lysine (K), arginine (R) and histidine (H). The negative charges originate from the C-terminus and four amino acids, tyrosine (Y), cysteine (C), aspartate (D)

and glutamate (E). The charges of the ionizable groups depend on their pK_a values and on the local value of the pH. For a given ionizable amino acid i , the positive charge $z_i^+(\text{pH})$ or the negative charge $z_i^-(\text{pH})$ is estimated from Henderson–Hasselbach’s equation:

$$z_i^+(\text{pH}) = \frac{1}{1 + \frac{K_i}{10^{-\text{pH}}}} \quad (3.16)$$

$$z_i^-(\text{pH}) = -\frac{1}{1 + \frac{10^{-\text{pH}}}{K_i}} \quad (3.17)$$

where K_i is the acidic dissociation constant of the amino acid i .

Under these assumptions, the global charge of a peptide can be expressed as follows:

$$z(\text{pH}) = - \sum_{i \in A^-} \frac{1}{1 + \frac{10^{-\text{pH}}}{K_i}} + \sum_{i \in A^+} \frac{1}{1 + \frac{K_i}{10^{-\text{pH}}}} \quad (3.18)$$

where $A^- = \{\text{Y, C, D, E, C-ter}\}$ and $A^+ = \{\text{K, R, H, N-ter}\}$.

This approach assumes that the pK_a value of an ionizable group is independent of its position in the molecule, and that all the individual acid–base equilibria can be considered as independent. It should be noted that the calculated pI depends considerably on the set of pK values assumed for the ionizable groups. It was shown that when different sets of published pK values were used, the predicted pI of some proteins or peptides differed by up to 1 pH unit.⁴⁷ However, the aim of the present paper is to describe the focusing phenomenon in an OFFGEL device, rather than to give exact values of pI . All the data presented in this study use the pK values of amino acids from⁴⁸. Other values from Expasy⁴⁹ and Promost⁵⁰ have been used and qualitatively showed the same distributions for peptide pI and charge derivative (results not shown).

For a stationary regime of isoelectric focusing without chemical reactions, the equation of conservation of flux is given by:

$$\frac{\partial c_i}{\partial t} = -\text{div}J_i = 0 \quad (3.19)$$

where c_i and J_i are the concentration and the flux density of species i . Considering only the diffusion-migration transport in one direction, this equation reduces to the following 1-D steady-state equation:

$$\frac{\partial}{\partial x} \left(-D_i \frac{\partial c_i}{\partial x} - \frac{z_i F}{RT} D_i c_i \frac{\partial \phi}{\partial x} \right) = 0 \quad (3.20)$$

where D_i , and z_i are the diffusion coefficient of species i and its charge as calculated in equation (3.18). F is the Faraday constant, R is the molar gas constant, T is the temperature and ϕ is the local electric potential.

It results from equation (3.20) that the flux of species i (term in brackets) is uniform over x . Since at the isoelectric point, the concentration is maximal and the charge zero, the global flux at the steady-state is zero. The flux of species due to diffusion is thus compensated by the flux due to electromigration, leading to:

$$\frac{\partial c_i}{\partial x} = \frac{FE}{RT} z_i(x) c_i(x) \quad (\text{where } E = -\nabla\phi) \quad (3.21)$$

This differential equation describes the isoelectric focusing in a steady-state regime, the charge of the peptide being a function of the pH or of the distance (in the cases studied, the pH gradient is linear). Assuming a uniform electric field, equation (3.21) was solved analytically with Igor software (Wavemetrics, Portland) and allowed to display the steady-state concentration profile of the focused peptide for different values of electric field (no geometry effect taken into account here). This model will be taken as reference to validate the following Finite Element Model.

2.3 Finite Element Model

Numerous studies have been presented in the literature on the diffusion–migration phenomena to describe capillary electrophoresis or IEF processes.³⁶⁻⁴² Regarding OFFGEL, various finite element models based on diffusion, ampholyte reactions, and/or migration have been developed.^{35, 46, 51} In the previous case of diffusion–migration–reaction of two model ampholytes,⁴⁶ one protonation site per ampholyte molecule was considered to facilitate the study. The main difference here is the consideration of not only one protonation site, but the global charge of the peptide, taking into account the many possible ionization sites existing on such a molecule, resulting in a pH-dependent global charge (as the pH is a function of the distance on the gel, the charge thus depends on the location of the peptide on the gel).

The numerical model was developed for 1-D and 2-D geometries and computes the peptides concentration profiles at different time steps of the focusing. The electric field was first calculated by solving the Laplace equation:

$$\text{div}(j) = \nabla \cdot (-\sigma \nabla \phi) = 0 \quad (3.22)$$

where j is the electrical current density and σ is the electrical conductivity. Next, the electric field $\nabla \phi$ was injected into equation 8, describing the transient transport of a species i by diffusion-migration:

$$\frac{\partial c_i}{\partial t} + \nabla \cdot \left(-D_i \nabla c_i - \frac{z_i(\text{pH}(x))F}{RT} D_i c_i \nabla \phi \right) = 0 \quad (3.23)$$

Assumptions for the numerical model

- No standard transfer potential is considered at the gel/solution interface, as the solution and the gel are considered aqueous media. This assumption was proved elsewhere.⁵²

- Gel and solution are assumed to be convection-free and isothermal.
- A uniform diffusion coefficient of $10^{-9} \text{ m}^2 \cdot \text{s}^{-1}$ is taken for peptides.
- To decouple the electric field calculation (equation (3.22) from the transport equation (3.23), a uniform conductivity is assumed both in the gel and in the solution. This assumption is valid at neutral pH but becomes less accurate at extreme values of pH, as under real conditions, the conductivity is lower at neutral pH and higher in acidic and basic compartments. The conductivity in the gel is taken to be equal to the one in solution, as they have been measured⁴⁶ and show the same order of magnitude.
- The pH gradient is linear along the gel and the sample solution in the well is assumed to be totally buffered⁴⁶. The establishment of the pH gradient in the solution is assumed to be much faster than the focusing of peptides.

Geometries of interest

1-D geometry consists of a vertical cross-section of an IPG gel (Figure 2a) to study the influence of peptide charge gradient on the focusing time and focused peak width. 2-D geometry consists of a vertical cross-section of the multicompartiment OFFGEL device (Figure 2b). The 2-D geometry (dimensions consistent with the experimental setup described by Michel et al.¹⁸) is used to study the influence of the well height and shape on the focusing, as well as to describe the IEF of three peptides under conditions close to experimental ones. The potential gradient applied across the gel as boundary conditions is $100 \text{ V} \cdot \text{cm}^{-1}$ for both 1-D and 2-D studies. The initial peptide concentration was fixed at 1 mM for all the calculations (uniform distribution along the gel and in the solution). The model was implemented on the finite element commercial software Flux-ExpertTM (Astek Rhône-Alpes, Grenoble, France).

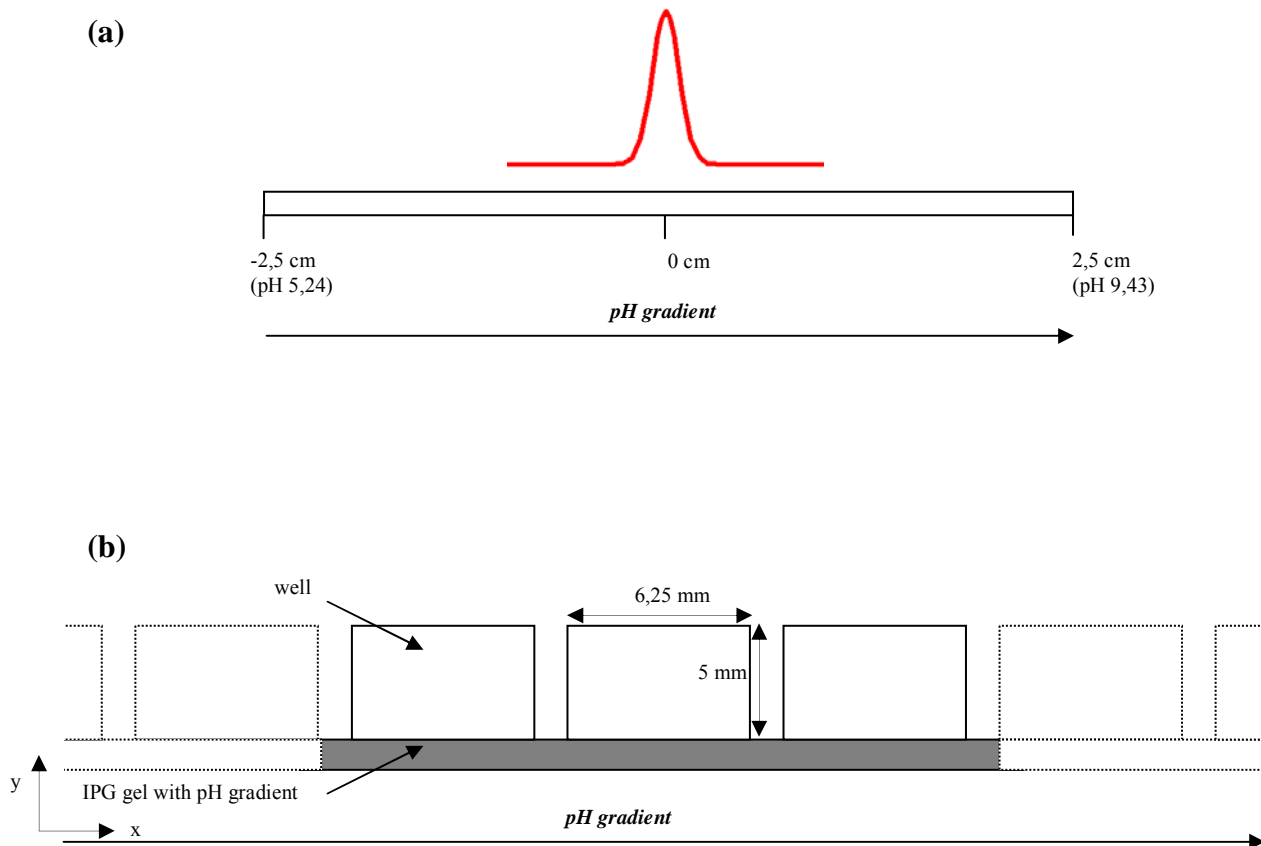


Figure 2: Geometries used in the simulation: (a) the 1-D geometry (calibration) is constituted of an IPG gel of 5 cm length; (b) the 2-D geometry is constituted of three or seven wells of 6.25 mm width, 5 mm height and distant of 0.75 mm with an underlying IPG gel.

Boundary conditions

For the gel strip, the concentration of the species of interest was set to zero at the anode and cathode (Dirichlet conditions in FEM, corresponding to a gel of finite length). For the wells, the condition of zero flux is set at the borders of the wells (Neumann conditions in FEM).

2.4 In silico proteome digestion and computation of physico-chemical parameters

A program simulating tryptic digestion was written with Igor. Proteomes of *D. radiodurans*, *S. cerevisiae*, and *H. sapiens* were downloaded from the Swiss-Prot database through the Sequence Retrieval System (<http://www.expasy.ch/ftp/>) (July 2006). The homemade program was used to:

1. Perform the tryptic digestion of proteins with two miscleavages.
2. Calculate the MW and *pI* of peptides resulting from their sequence, using the amino acids *pK* values from reference⁴⁸ (see Appendix 2)
3. Trace the titration curve for each peptide (net charge vs pH), and calculate the charge derivative at *pI*.

Values of *pI*s were estimated by a secant algorithm from the titration curve, with a precision of 0.02 pH unit. The titration curve was obtained from the sequence of amino acids and based on Eq.3. The charge slope dz/dpH at *pI* was obtained from the derivation in pH of Eq.3. Peptide/protein masses and *pI* calculation were validated through manual comparison with **pI/MW compute** available on Expasy (<http://www.expasy.ch>). Values of *pI* are slightly different from those obtained with **pI/MW compute** due to the different values of *pK* used. The *pI* distribution of proteins was calculated for a few species and produced the well-known bimodal *pI* distribution⁴⁷ (data not shown), which adds to the validation of our calculations. The tryptic digestion was also validated by comparison to the tool MS-digest from <http://prospector.ucsf.edu/>.

3. Results and discussion

3.1 Model validation

The numerical model is validated by comparing the focused peaks obtained at steady state with the peaks calculated with the analytical model. The comparison shows a good agreement (Figure 3). The focusing peaks from numerical simulations can be exactly superposed to the peaks from analytical calculations. The shape and peak width are the same for both methods of calculation, and this for all values of electric field.

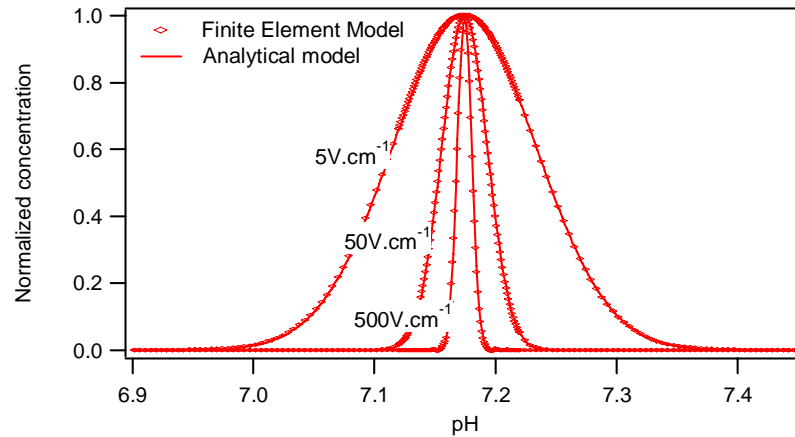


Figure 3: IEF on a linear pH gradient gel ($0,5 \text{ pH}\cdot\text{cm}^{-1}$) simulated for a peptide ($n_{asp} = n_{glu} = n_{his} = n_{cys} = n_{tyr} = n_{lys} = n_{arg} = 1$). The normalized concentrations were obtained from numerical (dots) and analytical models (lines) for different values of electric field ($5, 50$ and $500 \text{ V}\cdot\text{cm}^{-1}$).

However, numerical simulations allow observing transient states of the focusing, whereas the analytical calculation gives results at the steady state of focusing only. Another drawback of the analytical model is the 1-D limitation. Following this validation, numerical simulations with Flux-Expert™ were used for further investigation.

3.2 Determination of the order of magnitude of dz/dpH at pI

The *in silico* tryptic digestion of the different proteomes was performed and the resulting peptides were analyzed. Figure 4 shows the distribution of the charge derivative dz/dpH calculated at pI for peptides generated from the proteome digestion of *D. radiodurans*, *S. cerevisiae*, and *H. sapiens*. As shown, charge slopes are mostly comprised between 0 and -3 . The highest bar corresponds to the “flattest” peptides, illustrated by the titration curve of the peptide NSSVY (see Figure 4, bottom). It is in that case more relevant to define a “ pI zone” rather than a pI value, as the charge of the peptide does not vary much around its pI . The peptides having a charge derivative at pI comprised between -0.1 and -3 (illustrated by the titration curve peptide DLTFLLLEESRDKVNQLEEK, Figure 4, bottom) represent 76.8% (*D. radiodurans*), 77.4% (*S. cerevisiae*) and 79.0% (*H. sapiens*). For these peptides, the charge gradient is steeper around the pI .

Simply for comparison, as this study can be applied to proteins as well, the charge derivatives for proteins were calculated (results not shown) and unsurprisingly showed larger a range than that for peptides, as proteins charge is higher than peptides charge. For peptides, interestingly, the distribution of charge derivative is quite similar for the three organisms. It gives an overview of the diversity of peptides’ charge properties near pI and allows estimating the range of charge slope at pI .

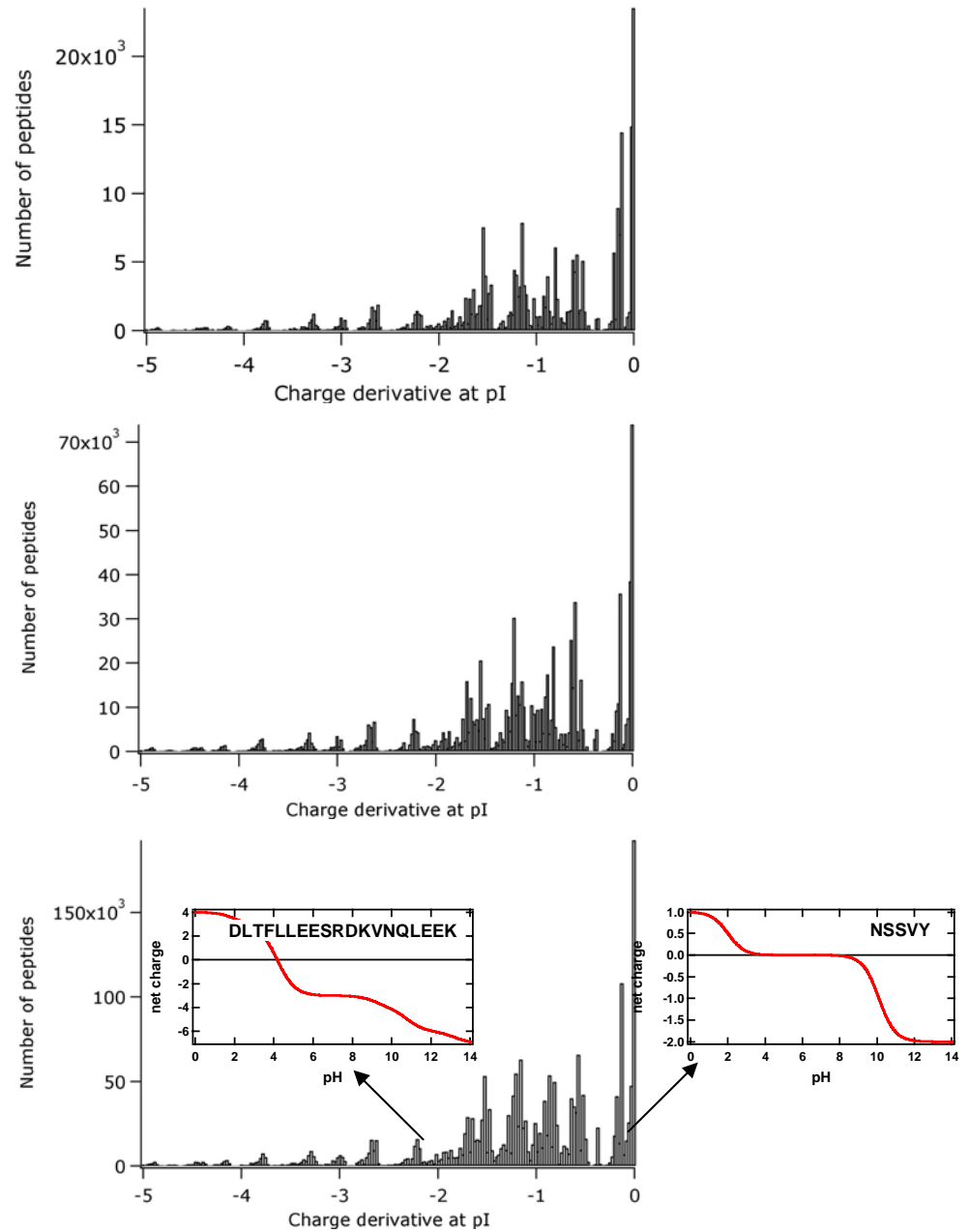


Figure 4: Distribution of charge derivative dz/dpH at pI for the peptides generated by the simulated digestion of *D. radiodurans* (top), *S. cerevisiae* (middle) and *H. sapiens* (bottom).

3.3 Effect of the charge gradient dz/dx at the pI (1-D study)

As seen in the previous distribution, the range of dz/dpH for most peptides from the digestion of different proteomes varies between -0.1 and -3 . The charge gradient can be written as follows: $(dz/dx)=(dz/dpH)(dpH/dx)$

As the pH gradient dpH/dx is linear, if in a small region near the pI the slope of the titration curve dz/dpH is assumed to be linear, the charge gradient dz/dx will also be linear. In the following study, a value of $1 \text{ pH}\cdot\text{cm}^{-1}$ is taken for the pH gradient. The influence of a linear charge gradient value on the focusing will be studied numerically. The comparison with the case of peptides will be done to show that the peptide charge slope at pI is the key parameter for the focusing. The following study is done considering the 1D geometry consisting of an IPG gel.

3.3.1 Effect on the peak width

Figure 5a shows the shape of the focused peak for different linear charge gradients from 0.05 to 2 (absolute values). As expected, the higher the charge gradient, the higher the final concentration and the narrower the focused peak width at steady state, because with a greater charge gradient, the mobility gradient is higher. The peak is thus more “focused” and concentrated. The effect of the charge slope at pI on the peak width was then studied for peptides, by giving as input to the simulation the expression of the charge as a function of pH. For this, three peptides were chosen according to their charge curve and slope at pI : leucine enkephalin (YGGFL), angiotensin II (DRVYIHPF) and a peptide from the human proteome digestion (DLTFLLEESRDKVNQLEEK) were used. Simulations of IEF were performed on these peptides, and the focused peak width at steady state was reported for each one on Figure 5a. The peptides fit to the curve deduced from linear charge gradients, which validates the

idea that the slope near pI is the most important factor, and the shape of the titration curve far from pI has no influence on the width of the focused peak.

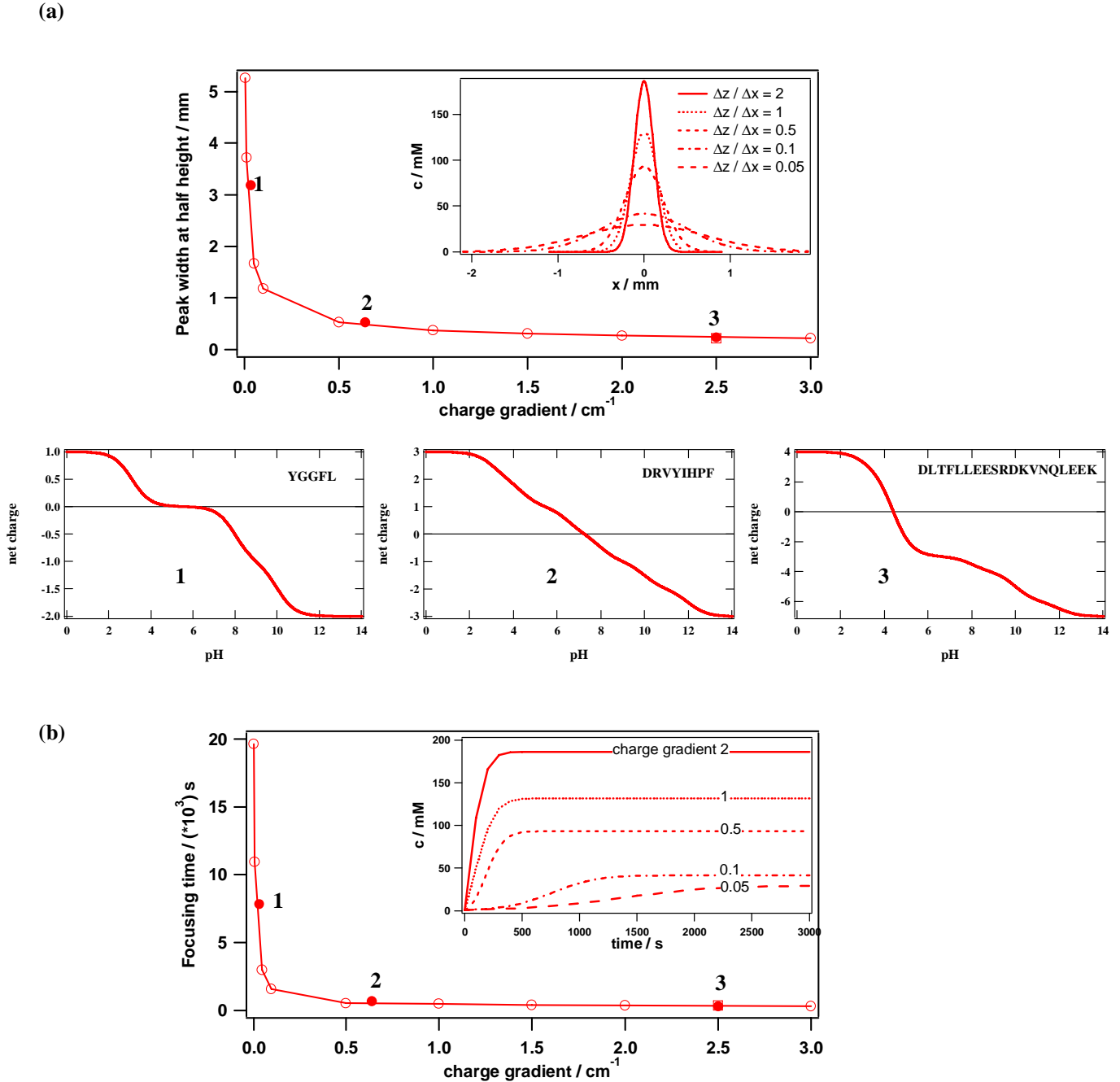


Figure 5: (a) Evolution of the focused peak width at half height versus absolute values of charge gradient, (insert: focused peak for different linear charge gradients from 0.05 to 2 $\text{pH}\cdot\text{cm}^{-1}$) and validation with three peptides: (1) leucine enkephalin (flat slope at pI), (2) angiotensin II (intermediate slope at pI) and (3) a peptide from the human proteome digestion (steep slope at pI), (b) evolution of the focusing time versus charge gradient (insert: transient concentrations for different linear charge gradients from 0.05 to 2 $\text{pH}\cdot\text{cm}^{-1}$).

From the top panel of Figure 5, the theoretical peak width of any peptide can be calculated from its charge derivative at pI . Figure 6 thus shows the theoretical peak width distributions of *in silico* digested proteomes; bars represent the percentage of peptides focusing with a given peak width at baseline, whereas the continuous line shows the percentage of peptides focusing with a peak width at baseline below a given value. Interestingly, the three species exhibit a very similar peak width distribution, which demonstrates the versatility of OFFGEL electrophoresis in the context of shotgun proteomics. Additionally, for the three species considered, around 90% of peptides focus within less than 6 mm (the well width used in practice), which means that in theory, 90% of peptides should be recovered in no more than two wells. This result is well in line with the experimental findings of Hörth et al. who found that 74% of tryptic peptides of *E. coli* focus in one well, and 90% focus in two wells at most.³²

3.3.2 Effect on the focusing time

Figure 5b illustrates the evolution of the focusing time for different values of linear charge gradient from 0.05 to 2 (absolute values). The steeper the charge gradient at pI , the higher the final concentration and the faster the steady state is reached. As previously stated, to validate our approach (linearization of the charge slope at pI), the effect of peptide charge slope at pI on the focusing time was studied. For this, the same peptides as before were used. For each of them, the focusing time (defined as the time needed to reach 99% of the steady-state concentration) was reported on Figure 5b. For the three peptides, focusing times fit to the linear gradient curve, showing that the slope at pI is the key parameter for the focusing time as well. As a consequence, the shape of the titration curve far from pI has no influence on the focusing time. One can easily understand this tendency by seeing that the migration velocity

far from pI is so high that only the migration near pI determines the kinetics of focusing, as the limiting factor.

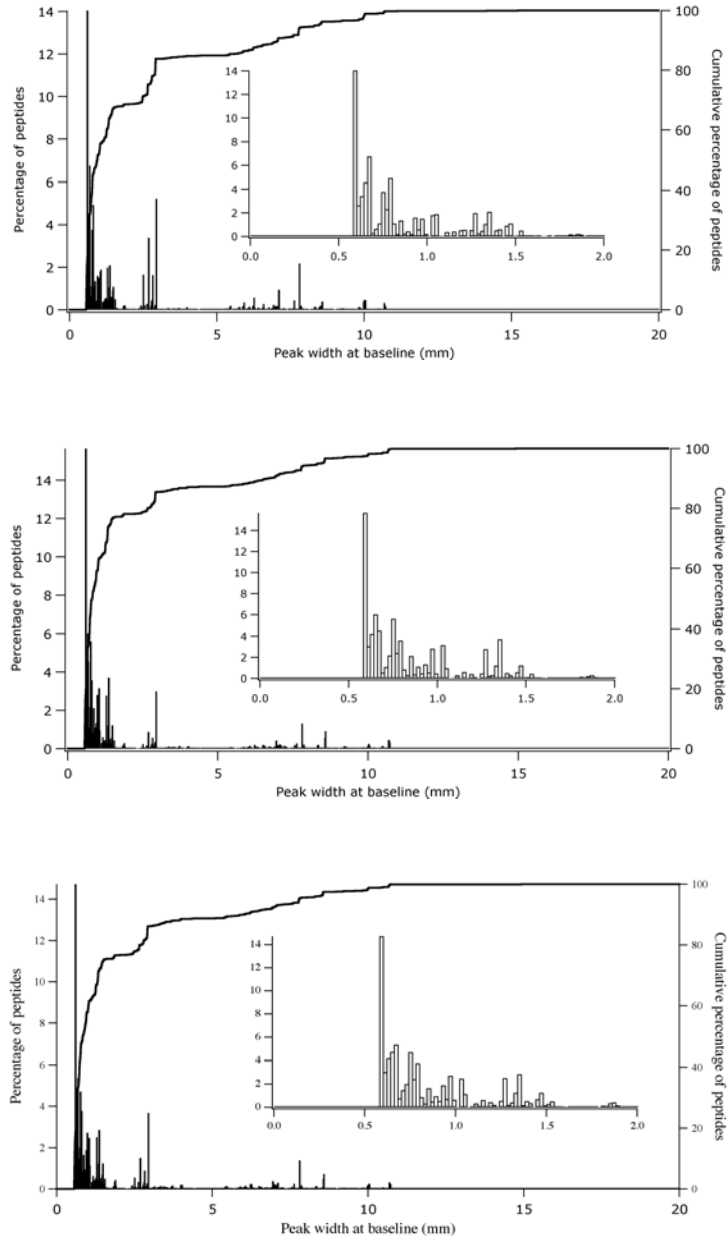


Figure 6: Histogram of peak widths at baseline, as fitted from the numerical simulations for *D. radiodurans* (top), *S. cerevisiae* (middle), and *H. sapiens* (bottom). In each graph, the inset shows a magnification of the bar histogram, and the continuous line shows the cumulative percentage of peptides focusing with a given peak width.

In this section, it was shown that, given the distribution of dz/dpH for the *in silico* digested proteomes (charge gradient between -0.1 and -3), and if taking a particular pH gradient (e.g., pH 3–10 on a 13 cm long strip), an optimal dimension of the well can be given, for a chosen percentage of correctly focused peptides. It is estimated that the optimal well width in an OFFGEL device (given by the largest peak width obtained with a flat titration curve) is 6–7 mm, which allows recovering 90% of peptides in at most two wells.

From the main results on the peak width and focusing time, some practical conclusions can be drawn for the IEF of peptides in an OFFGEL device. Assuming the initial peptide sample solution is loaded in all the wells, the starting voltage should be low in the first step. As we see, the focusing process is quite fast at the start, as most of the species are highly charged (far from pI). In practice, the presence of salts accompanying the sample at the start should be taken into account as well. Thus a low starting voltage should allow performing efficient focusing meanwhile avoiding too much heating. Then the voltage should be increased gradually or stepwise to reach the steady state of focusing, as the charge decreases, and the closer the species gets to its pI , the slower it is migrating. Thus, to allow a sharp focusing at the end, it is recommended to apply a high final voltage. The current, if monitored, is also a good indicator of the advancement of the focusing process. The current at the beginning is at the maximum (highly charged species migrating) and should decrease to finally reach a steady-state residual value (dynamic equilibrium between migration and diffusion). To give an idea of the focusing time, some authors have recently published interesting results concerning the IEF of peptides in gel,²³ and papers concerning the OFFGEL IEF of peptides can be taken as reference.^{30, 32, 33}

Concerning the use of peptides pI as a filtering/validating tool in the identification of peptides and proteins, not only the pI value is important, but also the slope of the titration curve at pI . Thus, in setting the limits of exclusion based on the pI of peptides, this slope

should also be taken into account, to avoid eliminating true peptides, which did focus but in several wells, due to their characteristic titration curve.

3.4 Effect of the well height on the recovery and focusing time (2-D study)

To study the influence of the well height on the focusing, numerical simulation of OFFGEL IEF was performed for a given peptide (Angiotensin II) in a three-compartment device (2D geometry). Different height ratios were studied: $h_{\text{well}}/h_{\text{gel}} = 1, 2, 4$ and 10. Figure 7 displays the peptide concentration at different time steps, for the ratios $h_{\text{well}}/h_{\text{gel}} = 10$ (high wells) and $h_{\text{well}}/h_{\text{gel}} = 2$ (low wells). The initial concentration of peptides was fixed at 1 mM for all the calculations.

The focusing can be described in two phases. These two phases can be best seen for $h_{\text{well}}/h_{\text{gel}} = 10$ on Figure 7a. In a first phase (for times < 800 s), the peptide migrates essentially in the gel underneath the wells toward its pI (***horizontal focusing***). In a second phase (for times > 800 s), the species diffuses to the solution in the well (***vertical focusing*** due to 2-D geometry). For the low wells, $h_{\text{well}}/h_{\text{gel}} = 2$, the process consists mostly of the first phase, because the vertical focusing is strongly limited by the height of the well.

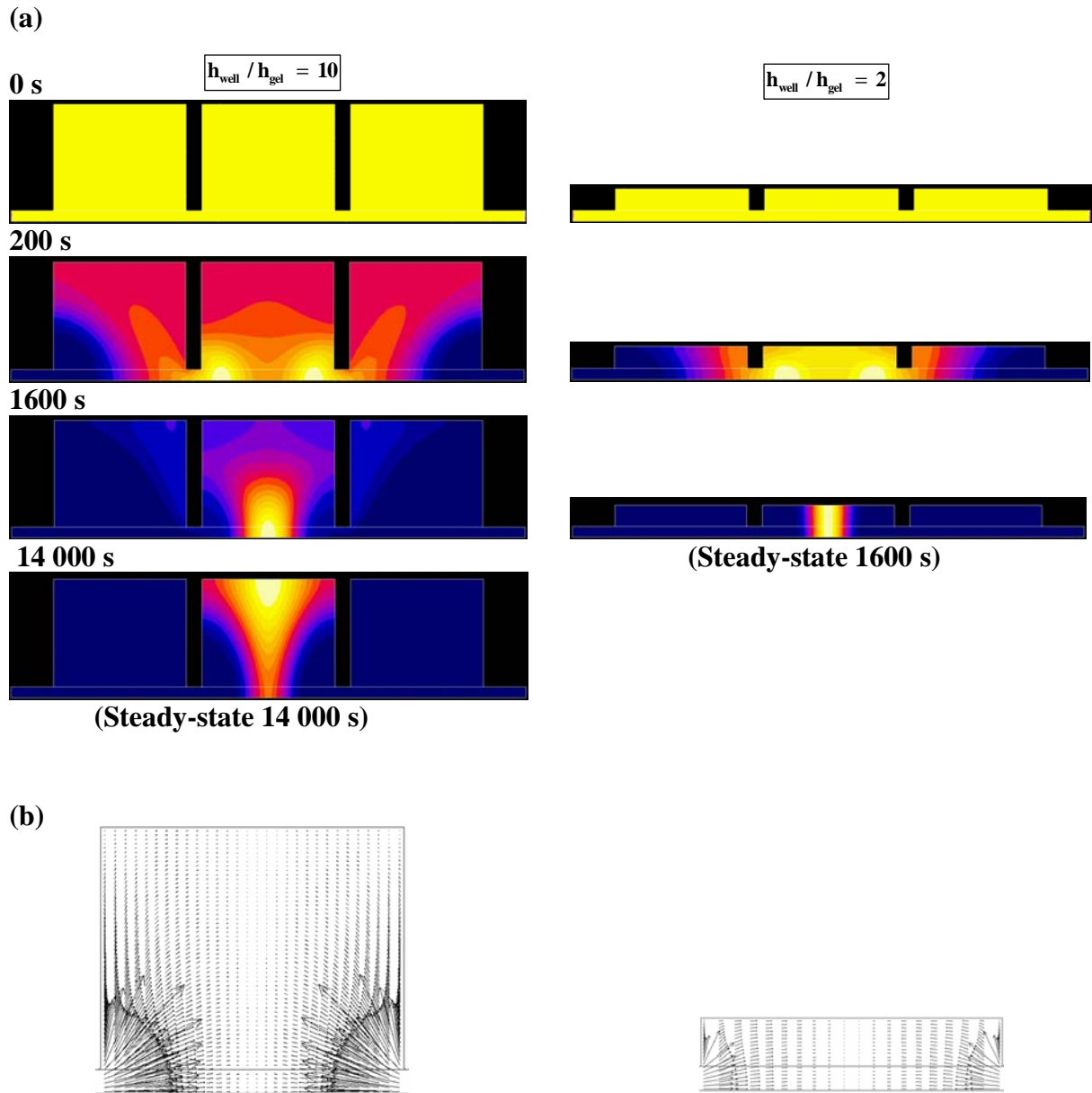


Figure 7: Effect of the well height: (a) concentration isovalues of angiotensin II ($pI = 7.25$) at different times for two height ratios $h_{\text{well}}/h_{\text{gel}}=10$ and 2. IEF conditions: constant applied voltage of $100 \text{ V}\cdot\text{cm}^{-1}$ and pH gradient of $0.5 \text{ pH}\cdot\text{cm}^{-1}$, (b) distribution of the current lines in the wells under the same conditions.

The two focusing steps can be correlated with the distribution of migration velocities, shown in Figure 7b for both height ratios. In a high well, the migration velocity has a non-negligible vertical component, which is the driving force for the vertical focusing, whereas in the low well, the current lines are all parallel to the gel (except at the corners). The vertical

focusing is quasi nonexistent. Thus, it takes approximately 10 times longer to reach the steady state in high wells than it does in low wells (14000 s for a height ratio of 10 vs. 1600 s for a height ratio of 2). In the high well, once the species reaches the top of the well, the solution horizontal focusing gives broader shape, due to the lower local values of the migration (i.e., electric field) compared to the diffusion.

However, the final to initial quantity ratio recovered in solution is higher for the high wells, as shown in Figure 8. The recovery percentage is an interesting parameter, which is defined as the ratio of the quantity of focused species in the central well to the initial quantity (i.e., in all the wells and the gel) and noted $n_{\text{well}}/n_{\text{tot}}$. It illustrates that although the steady state is reached faster for low wells than for high wells, the recovery is still better for high wells. For height ratios of: $h_{\text{well}}/h_{\text{gel}}=10, 4, \text{ and } 1$ recovery of 96%, 82% and 50% were obtained, respectively. These values of recovery could be theoretically predicted by geometrical considerations, as shown in Figure 8, where the values theoretically expected for the recovery are 91%, 80% and 50% respectively for height ratios of 10, 4, and 1. The 2-D effect of the vertical focusing is amplifying the recovery for high wells (5% more than the predicted recovery for height ratio of 10). This enhancement in the recovery observed for high wells can be explained by the higher proportion of current lines penetrating the well compared to the ones in the gel (Figure 7b).

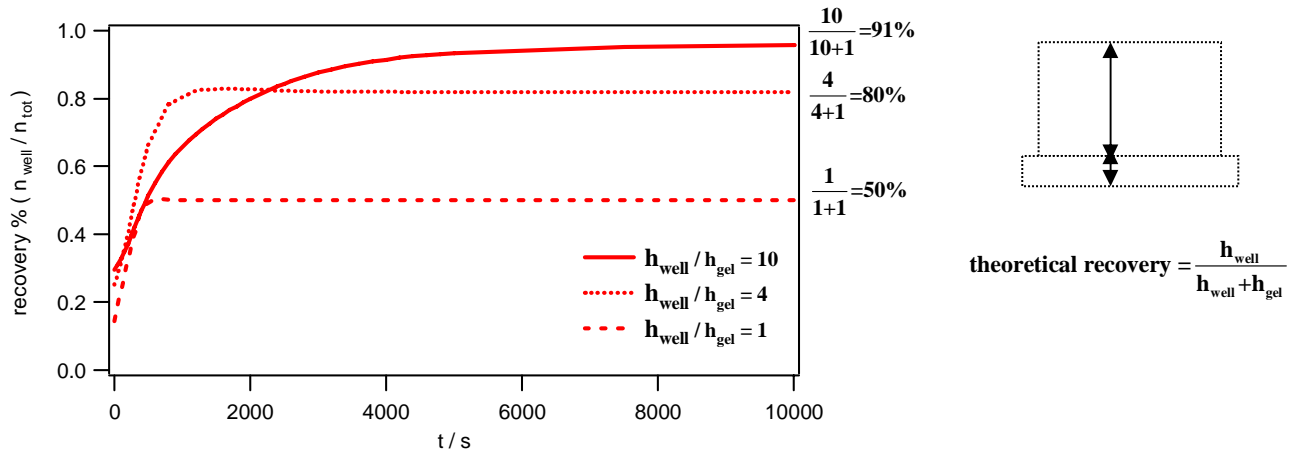


Figure 8: Recovery percentage in the focusing well solution versus time for different height ratios $h_{\text{well}}/h_{\text{gel}}$

3.5 Effect of the well shape on the recovery and focusing time

The effect of the well shape was also studied. In particular, three shapes were considered, as illustrated in Figure 9, and compared to determine which shape should be optimal for the IEF. Shape S0 is the straight well used for the simulations presented above. S1 is the well with narrow top and S2 is the well with narrow bottom. The concentration factor, defined as the ratio of final concentration to initial concentration in the focusing well solution, is displayed in Figure 9a for different shapes. The concentration factor is slightly higher for the shapes S1 and S2, compared with S0 (straight well), which indicates that the recovery should be only slightly higher for these shapes, if the initial concentration is the same in all cases. But most striking is the difference in focusing time. For narrow-top and straight wells, the focusing is almost 2 times faster than for narrow-bottom wells (12000 and 14000 s versus 22000 s, respectively).

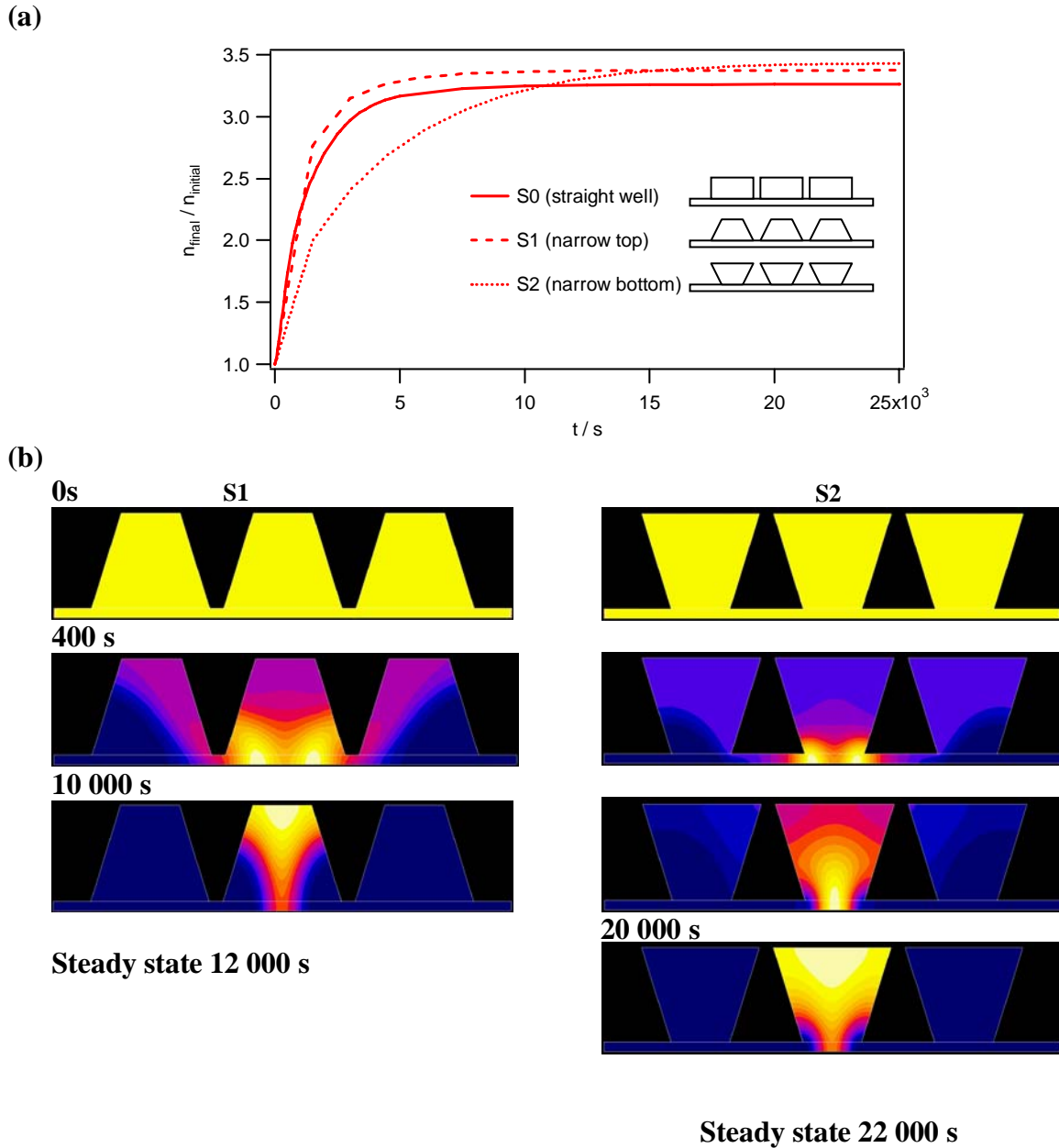


Figure 9: (a) Final to initial peptide concentration ratio in the focusing well (mean value), for three different well shapes, (b) peptide concentration isovalues for narrow–top and narrow–bottom wells at different time steps. Same IEF conditions as in Figure 7.

The difference in focusing times could be explained by the presence of “dead zones” in S2 (see Figure 9b). These are the zones in the top corners of the well, where the electric current lines are quasi nonexistent. Consequently, the migration in these zones is not efficient and only diffusion takes place. In S1, where these zones are reduced because of the narrow

top, the steady state is reached faster than in S2. Moreover, in S2, the current lines have to go through a longer way to enter the basis of wells (see Figure 9b), thus adding to the time needed to reach steady state. However, in terms of practicability, the straight wells or wide-top wells should be better to introduce or retrieve the sample.

3.6 IEF of peptides in a seven-well device

Three peptides (leucine enkephalin, angiotensin II and angiotensin III) were used to visualize the focusing in an OFFGEL device with seven wells. IEF conditions were as close as possible to the experimental conditions. A constant voltage was applied between anode and cathode (mean value of $100 \text{ V}\cdot\text{cm}^{-1}$); a pH gradient of $0.8 \text{ pH}\cdot\text{cm}^{-1}$ was taken (for comparison, a 3-10 pH gradient on a 13 cm strip for OFFGEL IEF gives a pH gradient of $0.54 \text{ pH}\cdot\text{cm}^{-1}$). Figure 10 displays the concentration isovalues for each peptide at different time steps.

Here as well, the two phases of horizontal and vertical focusing are observed, especially clearly for the “flat peptide”. At 100 s, that peptide is still migrating toward the well corresponding to its pI , whereas the other two peptides, which are steeper, have already reached their focusing well. For comparison, the ratio of focusing time for the flat peptide over the one for steep peptide ($t_{\text{flat}}/t_{\text{steep}}$) is 3.33 for 2-D geometry, while it was equal to 8.89 for 1-D geometry. This shows clearly the 2-D effect, which tends to reduce the discrepancy between a flat and a steep peptide in terms of focusing time. This could be explained by the vertical focusing step, during which the steep peptide is “losing its advance” on the “flat peptide”. Not much difference was observed between the focusing times of the last two peptides, and their charge slope at pI was very close (0.64 for angiotensin II and 0.49 for angiotensin III). Even though the distance to migrate is longer for angiotensin III than for angiotensin II, only the charge slope at pI is to be considered, and for this case, it does not induce a big difference in focusing time.

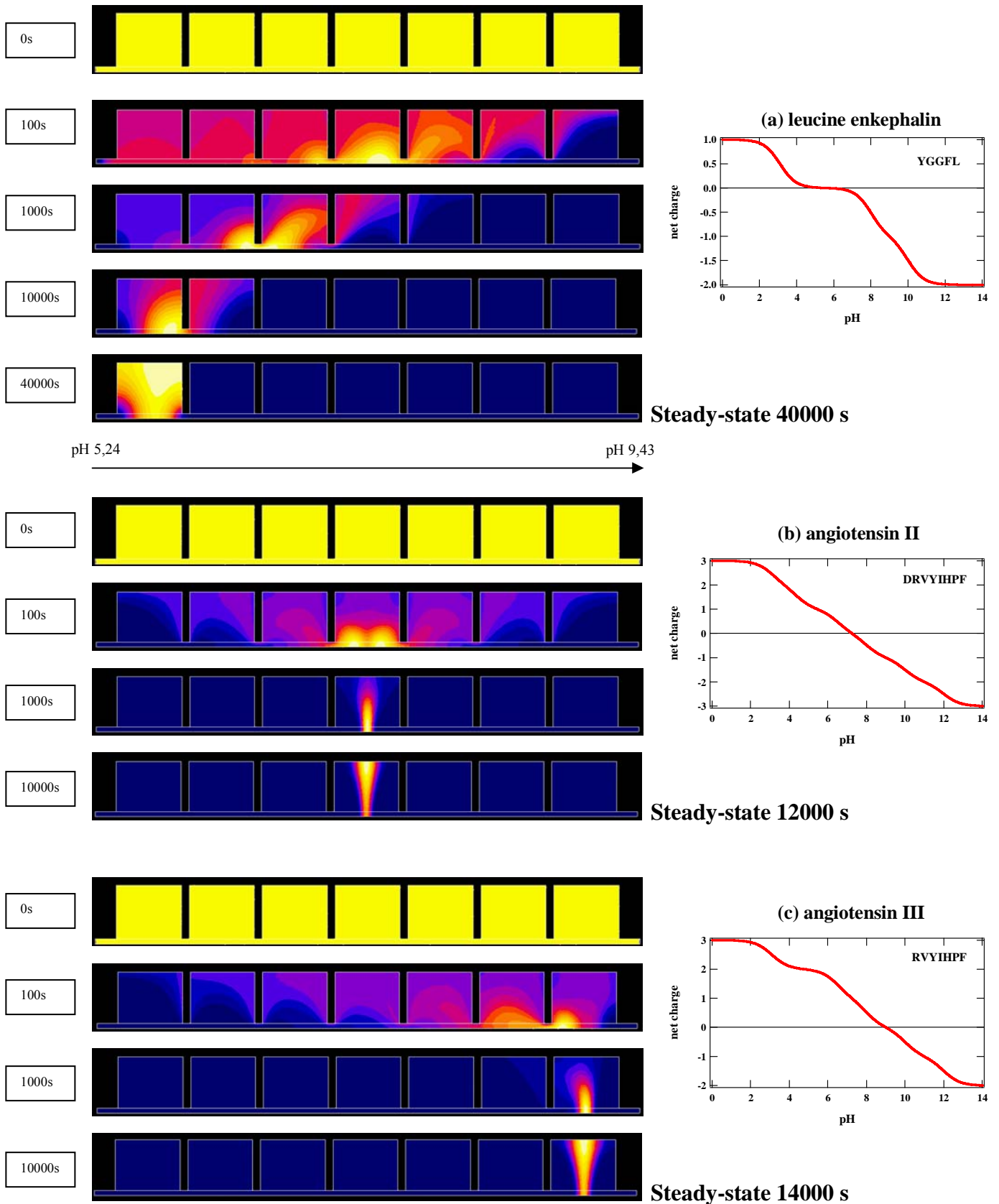


Figure 10: Peptide concentration isovalues in a seven-compartment OFFGEL device. IEF conditions: all initial concentration 1mM, pH gradient = 0.8 pH unit·cm⁻¹, voltage = 100 V·cm⁻¹

4. Concluding remarks

A preliminary *in silico* tryptic digestion of the proteomes from three different organisms was performed, to give an overview of the distribution of peptide charge slopes at pI . The influence of this charge slope at pI was then investigated. The main result is that this slope not only acts on the focused peak shape, but also constitutes the limiting factor in the focusing kinetics, the charge far from pI having no influence. By modeling the peak width as a function of the charge gradient at pI , we demonstrate that 90% of peptides should be correctly focused in at most two wells, considering the geometry used. This interestingly confirms recent experimental results and strongly suggests the high-resolution power of OFFGEL and its relevance in shotgun proteomic strategies. Concerning the use of peptides pI as a filtering/validating tool in the identification of peptides and proteins, not only the pI value, but also the slope of the titration curve at pI , is important when setting the limits of exclusion based on the pI of peptides. Other geometrical parameters were also investigated (well height and shape). For higher wells, the recovery of peptides is much more important than for lower wells, although it takes longer to recover the maximal quantity of peptides. As for the shape of the wells, straight or narrow-top wells are optimal for faster focusing.

Appendix

Appendix 2 is the table of pK_a values used for the calculations. Appendix 3 gives details about parameters of the simulation (Peclet number, mesh size).

5. References

1. Rabilloud, T.; Luche, S.; Chevallet, M., Gel electrophoresis techniques in proteomic analysis. *Biofutur* **2002**, 11-19.
2. Gorg, A.; Weiss, W.; Dunn, M. J., Current two-dimensional electrophoresis technology for proteomics. *Proteomics* **2004**, 4, (12), 3665-3685.
3. Rabilloud, T., Two-dimensional gel electrophoresis in proteomics: Old, old fashioned, but it still climbs up the mountains. *Proteomics* **2002**, 2, (1), 3-10.
4. Domon, B.; Aebersold, R., Review - Mass spectrometry and protein analysis. *Science* **2006**, 312, (5771), 212-217.
5. Righetti, P. G.; Castagna, A.; Antonioli, P.; Boschetti, E., Prefractionation techniques in proteome analysis: The mining tools of the third millennium. *Electrophoresis* **2005**, 26, (2), 297-319.
6. Righetti, P. G.; Castagna, A.; Herbert, B.; Reymond, F.; Rossier, J. S., Prefractionation techniques in proteome analysis. *Proteomics* **2003**, 3, (8), 1397-1407.
7. Hoffmann, P.; Ji, H.; Moritz, R. L.; Connolly, L. M.; Frecklington, D. F.; Layton, M. J.; Eddes, J. S.; Simpson, R. J., Continuous free-flow electrophoresis separation of cytosolic proteins from the human colon carcinoma cell line LIM 1215: A non two-dimensional gel electrophoresis-based proteome analysis strategy. *Proteomics* **2001**, 1, (7), 807-818.
8. Zischka, H.; Weber, G.; Weber, P. J. A.; Posch, A.; Braun, R. J.; Buhringer, D.; Schneider, U.; Nissum, M.; Meitinger, T.; Ueffing, M.; Eckerskorn, C., Improved proteome analysis of *Saccharomyces cerevistae* mitochondria by free-flow electrophoresis. *Proteomics* **2003**, 3, (6), 906-916.
9. Moritz, R. L.; Ji, H.; Schutz, F.; Connolly, L. M.; Kapp, E. A.; Speed, T. P.; Simpson, R. J., A proteome strategy for fractionating proteins and peptides using continuous free-flow electrophoresis coupled off-line to reversed-phase high-performance liquid chromatography. *Analytical Chemistry* **2004**, 76, (16), 4811-4824.
10. Weber, G.; Islinger, M.; Weber, P.; Eckerskorn, C.; Volkl, A., Efficient separation and analysis of peroxisomal membrane proteins using free-flow isoelectric focusing. *Electrophoresis* **2004**, 25, (12), 1735-1747.
11. Moritz, R. L.; Simpson, R. J., Liquid-based free-flow electrophoresis - Reversed-phase HPLC: A proteomic tool. *Nature Methods* **2005**, 2, (11), 863-873.
12. Moritz, R. L.; Skandarajah, A. R.; Ji, H.; Simpson, R. J., Proteomic analysis of colorectal cancer: Prefractionation strategies using two-dimensional free-flow electrophoresis. *Comparative and Functional Genomics* **2005**, 6, (4), 236-243.
13. Righetti, P. G.; Wensch, E.; Faupel, M., Preparative Protein-Purification in a Multi-Compartment Electrolyzer with Immobiline Membranes. *Journal of Chromatography* **1989**, 475, 293-309.
14. Herbert, B.; Righetti, P. G., A turning point in proteome analysis: Sample prefractionation via multicompartment electrolyzers with isoelectric membranes. *Electrophoresis* **2000**, 21, (17), 3639-3648.
15. Pedersen, S. K.; Harry, J. L.; Sebastian, L.; Baker, J.; Traini, M. D.; McCarthy, J. T.; Manoharan, A.; Wilkins, M. R.; Gooley, A. A.; Righetti, P. G.; Packer, N. H.; Williams, K. L.; Herbert, B. R., Unseen proteome: Mining below the tip of the iceberg to find low abundance and membrane proteins. *Journal of Proteome Research* **2003**, 2, (3), 303-311.
16. Wall, D. B.; Kachman, M. T.; Gong, S. Y.; Hinderer, R.; Parus, S.; Misek, D. E.; Hanash, S. M.; Lubman, D. M., Isoelectric focusing nonporous RP HPLC: A two-dimensional liquid-phase separation method for mapping of cellular proteins with identification using MALDI-TOF mass spectrometry. *Analytical Chemistry* **2000**, 72, (6), 1099-1111.

17. Ros, A.; Faupel, M.; Mees, H.; van Oostrum, J.; Ferrigno, R.; Reymond, F.; Michel, P.; Rossier, J. S.; Girault, H. H., Protein purification by Off-Gel electrophoresis. *Proteomics* **2002**, 2, (2), 151-156.
18. Michel, P. E.; Reymond, F.; Arnaud, I. L.; Josserand, J.; Girault, H. H.; Rossier, J. S., Protein fractionation in a multicompartiment device using Off-Gel (TM) isoelectric focusing. *Electrophoresis* **2003**, 24, (1-2), 3-11.
19. Essader, A. S.; Cargile, B. J.; Bundy, J. L.; Stephenson, J. L., A comparison of immobilized pH gradient isoelectric focusing and strong-cation-exchange chromatography as a first dimension in shotgun proteomics. *Proteomics* **2005**, 5, (1), 24-34.
20. Cargile, B. J.; Talley, D. L.; Stephenson, J. L., Immobilized pH gradients as a first dimension in shotgun proteomics and analysis of the accuracy of pI predictability of peptides. *Electrophoresis* **2004**, 25, (6), 936-945.
21. Cargile, B. J.; Bundy, J. L.; Freeman, T. W.; Stephenson, J. L., Gel based isoelectric focusing of peptides and the utility of isoelectric point in protein identification. *Journal of Proteome Research* **2004**, 3, (1), 112-119.
22. Cargile, B. J.; Stephenson, J. L., An alternative to tandem mass spectrometry: Isoelectric point and accurate mass for the identification of peptides. *Analytical Chemistry* **2004**, 76, (2), 267-275.
23. Krijgsveld, J.; Gauci, S.; Dormeyer, W.; Heck, A. J. R., In-gel isoelectric focusing of peptides as a tool for improved protein identification. *Journal of Proteome Research* **2006**, 5, (7), 1721-1730.
24. Xie, H.; Rhodus, N. L.; Griffin, R. J.; Carlis, J. V.; Griffin, T. J., A catalogue of human saliva proteins identified by free flow electrophoresis-based peptide separation and tandem mass spectrometry. *Molecular and Cellular Proteomics* **2005**, 4, (11), 1826-1830.
25. Xie, H.; Bandhakavi, S.; Griffin, T. J., Evaluating preparative isoelectric focusing of complex peptide mixtures for tandem mass spectrometry-based proteomics: A case study in profiling chromatin-enriched subcellular fractions in *Saccharomyces cerevisiae*. *Analytical Chemistry* **2005**, 77, (10), 3198-3207.
26. Xie, H. W.; Bandhakavi, S.; Griffin, T. J., Evaluating preparative isoelectric focusing of complex peptide mixtures for tandem mass spectrometry-based proteomics: A case study in profiling chromatin-enriched subcellular fractions in *Saccharomyces cerevisiae*. *Analytical Chemistry* **2005**, 77, (10), 3198-3207.
27. Tan, A. M.; Pashkova, A.; Zang, L.; Foret, F.; Karger, B. L., A miniaturized multichamber solution isoelectric focusing device for separation of protein digests. *Electrophoresis* **2002**, 23, (20), 3599-3607.
28. Baczek, T., Fractionation of peptides and identification of proteins from *Saccharomyces cerevisiae* in proteomics with the use of reversed-phase capillary liquid chromatography and pI-based approach. *Journal of Pharmaceutical and Biomedical Analysis* **2004**, 35, (4), 895-904.
29. Baczek, T., Fractionation of peptides in proteomics with the use of pI-based approach and ZipTip pipette tips. *Journal of Pharmaceutical and Biomedical Analysis* **2004**, 34, (5), 851-860.
30. Heller, M.; Michel, P. E.; Morier, P.; Crettaz, D.; Wenz, C.; Tissot, J. D.; Reymond, F.; Rossier, J. S., Two-stage Off-Gel (TM) isoelectric focusing: Protein followed by peptide fractionation and application to proteome analysis of human plasma. *Electrophoresis* **2005**, 26, (6), 1174-1188.
31. Heller, M.; Ye, M. L.; Michel, P. E.; Morier, P.; Stalder, D.; Junger, M. A.; Aebersold, R.; Reymond, F. R.; Rossier, J. S., Added value for tandem mass spectrometry shotgun proteomics data validation through isoelectric focusing of peptides. *Journal of Proteome Research* **2005**, 4, (6), 2273-2282.

32. Hörth, P.; Miller, C. A.; Preckel, T.; Wenz, C., Efficient fractionation and improved protein identification by peptide OFFGEL electrophoresis. *Molecular & Cellular Proteomics* **2006**, *5*, 1968-1974.
33. Michel, P. E.; Crettaz, D.; Morier, P.; Heller, M.; Gallot, D.; Tissot, J. D.; Reymond, F.; Rossier, J. S., Proteome analysis of human plasma and amniotic fluid by Off-Gel (TM) isoelectric focusing followed by nano-LC-MS/MS. *Electrophoresis* **2006**, *27*, (5-6), 1169-1181.
34. Burgess, J. A.; Lescuyer, P.; Hainard, A.; Burkhard, P. R.; Turck, N.; Michel, P.; Rossier, J. S.; Reymond, F.; Hochstrasser, D. F.; Sanchez, J. C., Identification of brain cell death associated proteins in human post-mortem cerebrospinal fluid. *Journal of Proteome Research* **2006**, *5*, (7), 1674-1681.
35. Arnaud, I. L.; Jossierand, J.; Rossier, J. S.; Girault, H. H., Finite element simulation of Off-Gel (TM) buffering. *Electrophoresis* **2002**, *23*, (19), 3253-3261.
36. Thormann, W.; Mosher, R. A.; Bier, M., Experimental and Theoretical Dynamics of Isoelectric-Focusing - Elucidation of a General Separation Mechanism. *Journal of Chromatography* **1986**, *351*, (1), 17-29.
37. Mosher, R. A.; Thormann, W.; Bier, M., Experimental and Theoretical Dynamics of Isoelectric-Focusing .2. Elucidation of the Impact of the Electrode Assembly. *Journal of Chromatography* **1988**, *436*, (2), 191-204.
38. Mosher, R. A.; Dewey, D.; Thormann, W.; Saville, D. A.; Bier, M., Computer-Simulation and Experimental Validation of the Electrophoretic Behavior of Proteins. *Analytical Chemistry* **1989**, *61*, (4), 362-366.
39. Mosher, R. A.; Thormann, W., Experimental and Theoretical Dynamics of Isoelectric-Focusing .4. Cathodic, Anodic and Symmetrical Drifts of the Ph Gradient. *Electrophoresis* **1990**, *11*, (9), 717-723.
40. Mosher, R. A.; Thormann, W., High-resolution computer simulation of the dynamics of isoelectric focusing using carrier ampholytes: The post-separation stabilizing phase revisited. *Electrophoresis* **2002**, *23*, (12), 1803-1814.
41. Thormann, W.; Huang, T. M.; Pawliszyn, J.; Mosher, R. A., High-resolution computer simulation of the dynamics of isoelectric focusing of proteins. *Electrophoresis* **2004**, *25*, (2), 324-337.
42. Thormann, W.; Mosher, R. A., High-resolution computer simulation of the dynamics of isoelectric focusing using carrier ampholytes: Focusing with concurrent electrophoretic mobilization is an isotachophoretic process. *Electrophoresis* **2006**, *27*, (5-6), 968-983.
43. Mosher, R. A.; Bier, M.; Righetti, P. G., Computer-Simulation of Immobilized Ph Gradients at Acidic and Alkaline Extremes - a Quest for Extended Ph Intervals. *Electrophoresis* **1986**, *7*, (2), 59-66.
44. Tonani, C.; Faupel, M.; Righetti, P. G., Isoelectric Membrane Simulator - a Computational Approach for Isoelectric Immobilized Membranes. *Electrophoresis* **1991**, *12*, (9), 631-636.
45. Tonani, C.; Righetti, P. G., Immobilized Ph Gradients (Ipg) Simulator - an Additional Step in Ph Gradient Engineering .1. Linear Ph Gradients. *Electrophoresis* **1991**, *12*, (12), 1011-1021.
46. Di Maio, I., Off-Gel (TM) electrophoresis: characterisation of a novel isoelectric focusing fractionation method. *Thesis N° 3064, EPFL* **2004**.
47. Weiller, G. F.; Caraux, G.; Sylvester, N., The modal distribution of protein isoelectric points reflects amino acid properties rather than sequence evolution. *Proteomics* **2004**, *4*, (4), 943-949.
48. *CRC Handbook of Chemistry and Physics*. 87th ed.; CRC Press: 2006-2007.

49. Bjellqvist, B.; Hughes, G. J.; Pasquali, C.; Paquet, N.; Ravier, F.; Sanchez, J. C.; Frutiger, S.; Hochstrasser, D., The focusing positions of polypeptides in immobilized pH gradients can be predicted from their amino acid sequences. *Electrophoresis* **1993**, 14, (10), 1023-1031.
50. Halligan, B. D.; Ruotti, V.; Jin, W.; Laffoon, S.; Twigger, S. N.; Dratz, E. A., ProMoST (Protein Modification Screening Tool): A web-based tool for mapping protein modifications on two-dimensional gels. *Nucleic Acids Research* **2004**, 32, (WEB SERVER ISS.).
51. Arnaud, I. L.; Josserand, J.; Jensen, H.; Lion, N.; Roussel, C.; Girault, H. H., Salt removal during Off-Gel (TM) electrophoresis of protein samples. *Electrophoresis* **2005**, 26, (9), 1650-1658.
52. Lam, H. T.; Pereira, C. M.; Roussel, C.; Carrupt, P. A.; Girault, H. H., Immobilized pH gradient gel cell to study the pH dependence of drug lipophilicity. *Analytical Chemistry* **2006**, 78, (5), 1503-1508.

CHAPTER IV: *Design and Characterization of a homemade OFFGEL device*

1. Introduction.....	118
2. Chemicals and instrumental	121
2.1 Chemicals and biologicals.....	121
2.2 OFFGEL (OG-) IEF in the homemade device	122
2.3 Capillary electrophoresis (CE)	123
2.4 Tryptic digestion.....	123
2.5 LC-MS.....	123
2.6 Protein extraction from E. coli	124
2.7 2-D PAGE	124
3. Results and discussion.....	125
3.1 Description of the OFFGEL homemade device	125
3.2 Voltage and current monitoring.....	127
3.3 pH characterization.....	130
3.4 Loading capacity for proteins.....	134
3.5 OG-IEF of peptides	138
3.6 OG-IEF of proteins under denaturing conditions	142
4. Concluding remarks	145
5. References.....	146

1. Introduction

Face to the high complexity and large dynamic range of proteomics samples, efficient and reproducible separation has become an essential step in the strategies to analyze such samples. In a typical proteomics experiment, a sample of interest is separated either at the protein level or at the peptide level after enzymatic digestion of the proteins, followed by protein identification by mass spectrometry (MS).

Isoelectric focusing (IEF) is a high-resolution electrophoretic technique used to separate and concentrate amphoteric biomolecules at their isoelectric point (pI) in a pH gradient and under the application of an electric field. In comparison with other electrophoretic separation techniques, isoelectric focusing (IEF) offers the highest resolution, due to the inherent nature of the focusing process: it is a dynamic process resulting from the constant equilibrium between diffusion and migration. IEF thus combines separation and concentration, a useful feature for preparative or semi-preparative purposes.

In the context of the evolution of gel-based separations towards gel-free strategies, many techniques have recently been introduced to allow the fractionation of proteins and peptides in solution, such as continuous Free Flow Electrophoresis (FFE),¹ Rotofor,² multicompartiment electrolyzers (MCE)^{3, 4} and Off-gel electrophoresis (OGE)⁵ (more details on these techniques are given in chapter I). Initially, these techniques were designed for preparative purposes and protein purification. Most of them handle volumes in the range of preparative (MCE, Rotofor, FFE). Off-gel requires volumes in the order of semi-preparative to analytical range. Later, the preparative techniques evolve into “mini” or “micro” formats, designed for analytical purposes. The initial preparative MCE (commercialized as IsoPrime™ by GE Healthcare, 30 mL)³ evolved into an analytical system (commercialized as Zoom™ by Invitrogen, 500–700 μ L per chamber).^{6, 7} Early versions of the FFE² (commercialized by Tecan, now BD) have evolved to miniaturized devices as well, going down to volumes of 0.2

μL required for the analysis on chip.⁸ The Rotofor (commercialized by Bio-Rad) evolved to a semi-preparative system (1 mL per fraction).⁹ However, these techniques are today still widely used for preparative purposes.¹⁰

OFFGEL IEF was first described by Ros et al. (2002),⁵ as a free-flow technique to purify proteins according to pI and to isolate the protein fraction of interest, in a one-chamber device. The technique was later adapted to a more versatile multicompartiment format, in order to recover fractions of well-defined pI values at the end of the separation, and submit them to further analysis or detection.¹¹ The particular advantages of multicompartiment OFFGEL IEF are: (i) the low volumes used (100–300 μL per compartment), positioning it as a semi-preparative device, useful for prefractionation purposes, but also for analytical uses, and (ii) the direct recovery of liquid fractions, making it fit elegantly into the usual LC-MS workflow. Recirculation OFFGEL was also described to concentrate the same pI fraction of proteins by circulating the same fraction repeatedly through a one-chamber channel.¹² This was demonstrated to be useful for enrichment of proteins.

In the present chapter, we report the characterization of a device for OFFGEL IEF, built in-house, based on the geometrical considerations and numerical calculations of chapter III. The dimensions of the device were chosen in such a way to obtain optimal resolution for the separation of proteins and peptides as well as practical recovery/retrieval of the liquid fractions. A setup was designed to monitor the evolution of the current and potential during IEF, useful to assess the end of the separation. The device was then characterized in terms of reproducibility, loading capacity, performance and resolution of the separation. The reproducibility of the pH in the OFFGEL multiple chambers was first tested. This aspect is of utmost importance, for the accuracy of the determination of pI especially if the pI is to be used as information for validation of peptides experimentally found in a given compartment. The loading capacity was then determined for a mixture of model proteins, to set a working

range for the homemade device. OFFGEL IEF of peptides was then performed to demonstrate the high resolution of the device and evaluate the sharpness of the separation, for shotgun proteomics analysis. Finally, the separation of *Escherichia coli* protein extract was carried out, under denaturing conditions, to show the applicability of the present OFFGEL device for proteome prefractionation of a complex biological mixture.

2. Chemicals and instrumental

2.1 Chemicals and biologicals

OFFGEL: Immobiline Drystrips, linear pH range 3–10 of 13 cm in length (for protein and peptide fractionation) and 4–7 of 13 and 7 cm in length (for *Escherichia coli* protein extract fractionation, and 2-D mini-gels, respectively) were purchased from GE Healthcare (Otelfingen, Switzerland), as well as IPG buffers pH 3–10 and pH 4–7 (carrier ampholytes mixtures). **Proteins:** seven proteins were analyzed. Bovine serum albumin (BSA), myoglobin, α -lactalbumin, β -lactoglobulin B, and trypsin inhibitor were purchased from Sigma (Buchs, Switzerland). Amyloglucosidase (*Aspergillus Niger*) and cytochrome C were from Fluka (Buchs, Switzerland). **Digestion and LC-MS:** Ammonium hydrogenocarbonate (> 98%), 1,4-dithio-DL-threitol (DTT, > 99.5%) were from Fluka (Buchs, Switzerland). Porcine trypsin sequencing grade was from Promega (Madison, WI, USA). Formic acid and acetonitrile (> 99.5%, Fluka, Buchs, Switzerland) were used without further purification. ***Escherichia coli* sample:** urea, thiourea, 3-[3-cholamidopropyl dimethylammonio]-1-propansulfonate (CHAPS), and the *Escherichia coli* lyophilized cells were all from Sigma (Buchs, Switzerland). **SDS and 2D:** sodium dodecyl sulphate (SDS), Trizma base, bromophenol blue, ammonium persulfate (APS), N,N,N',N'-tetramethylethylenediamine (TEMED), iodoacetamide, the visible stain Brilliant Blue G (for colloidal Coomassie blue preparation), and the mixture of acrylamide and bisacrylamide were all from Sigma (Buchs, Switzerland). Deionized water (18.5 M Ω ·cm) was prepared using a Milli-Q system from Millipore (Bedford, MA, USA).

2.2 OFFGEL (OG-) IEF in the homemade device

OFFGEL electrophoresis (OGE) separations were performed with a prototype apparatus described below, composed of a linear row of twenty adjacent but independent wells, opened in both extremities. In this way, the wells can be placed over the IPG gel and the introduction/uptake of the sample in contact with the IPG gel can be made directly over the gel. The multicompartment device was placed on top of a 13 cm reswelled Immobiline Drystrip exhibiting a linear pH gradient (ranging from 3–10 or 4–7). A platinum electrode was placed in each compartment (lowest and highest pH).

OG-IEF was performed with a high voltage power supply Spellman CZE 1000R (Spellman High Voltage Electronics Corp., NY, USA), controlled by a computer using software written in LabView (National Instrument, Austin, TX, USA).

The separations were performed by dispensing 50 μ L protein or peptide solution in each well (the total volume loaded in all wells is thus 1 mL) and the potential was fixed during 1 h at 500 V, then 1 h at 1000 V, and finally 3-5 h at 5000 V. The current limit was set at 200 μ A per strip, to avoid too much Joule heating. At the end of the separation, the volume of each well was collected, vacuum dried or not, and submitted to further analysis.

For the OGE of proteins, pH ranges 3–10 and 4–7 on 13 cm have been used (loading estimation and *E. coli* proteins fractionation, respectively). The fractions were then analyzed directly by CE or 2-D PAGE without any particular treatment. For the OGE of peptides, pH range 3–10 on 13 cm has been used. The fractions were then vacuum-dried and then further analyzed by LC-MS.

2.3 Capillary electrophoresis (CE)

CE experiments were performed using a P/ACE MDQ system (Beckman Coulter, Munich, Germany) equipped with a photodiode-array detector, an autosampler and a power supply able to deliver up to 30 kV. Data were handled by the Beckmann software and then extracted and treated using IGOR software (Wavemetrics, Portland). Fused silica capillaries were obtained from BGB Analytik AG (Böckten, Switzerland). The capillaries were presenting 50 and 375 μm internal and external diameters respectively, and 21 and 31 cm effective and total length respectively. Samples were injected by hydrodynamic injections (30 mbar, 5 s). The anode was set at the injection end of the capillary. The new bare fused silica capillary was activated as follows: 10 min 1M NaOH rinse, 10 min 0.1M NaOH rinse, then 10 min water rinse. Between different separation in the same background electrolyte, a water and buffer rinse were successively performed.

2.4 Tryptic digestion

1 mg of BSA was dissolved in 1 mL ammonium hydrogenocarbonate solution (50 mM, pH 8), and 1.23 mg DTT (8 mM) and 10 μg trypsin (protein ratio of 1:100 w/w) were added. The digestion was run at 37 °C for 4h. The solution was then divided in two aliquots of 500 μL and stored at -20 °C, until used for the experiments.

2.5 LC-MS

The capillary HPLC system was an LC Packings (Dionex) Ultimate™ Plus, with a PepMap C18, 3 μm , 0.3 \times 150 mm capillary column and a pre-column. Sample volume injected was 1 μL (injection loop). The mobile phase consisted of solvents A (water/ACN 98:2 (v/v) with 0.1% (v/v) formic acid) and B (water/ACN 20:80 (v/v) with 0.085% (v/v) formic acid). The column was developed with a biphasic gradient from 2–50% of solvent B in 40 min, followed

by an increase from 50–100% of B in 10 min. The column was regenerated with 3 column volumes of B followed by 3 volumes of A. Chromatography was run at a flow rate of 4 $\mu\text{L}/\text{min}$. MS analysis was conducted on a LCQ Duo ion trap from Thermo Finnigan (San Jose, CA, USA). All experiments were done in full scan mode (m/z 150–2000) without averaging, and the heated capillary was kept at 200°C.

2.6 Protein extraction from *E. coli*

The starting material was an *E. coli* suspension (*E. coli* lyophilized cells from strain B-ATCC 11303, Sigma) stored at -20°C . The procedure was as follows: 250 mg *E. coli* were diluted in 5 mL of Rabilloud buffer composed of 7 M urea, 2 M thiourea, 4% (w/v) CHAPS and 1% (w/v) DTT. The cell suspension was then disrupted on ice with an ultrasonic probe during 3 min, to ensure cell lysis and protein extraction. After centrifugation at 40,000 g for 10 min, the supernatant was diluted (1:1) in Rabilloud buffer. Protein concentration was estimated by the Bradford protein assay test (according to Bio-Rad protocol) to be approximately 8 mg/mL.

2.7 2-D PAGE

For the analysis of the fractions recovered from OGE IEF fractionation of an *E. coli* protein extract, mini 2-D PAGE analysis was performed. For the first dimension, 7 cm IPG strips of pH range 4-7 were rehydrated overnight with 150 μL of protein solution (60 μL of the fractions recovered after OFFGEL IEF, adjusted to 150 μL with 2-D sample buffer). IEF was carried out with an initial voltage gradient from 200 up to 3500 V during 1h30, followed by constant voltage for 1h30, as recommended in the manual from Amersham Biosciences.¹³ For the second dimension, the IPG strips were equilibrated and then laid on a vertical 12% polyacrylamide SDS gel plate. The electrophoretic run was performed at 80 V initially and by setting a current limit of 30 mA for fifteen minutes. Then the voltage was gradually increased with the same current limit, in approx. 2 h to 150 V, until bromophenol blue reached the gel

bottom. Gels were then immediately stained by Coomassie blue according to the protocol from Bio-Rad. The 2-D gels were scanned with Kodak Scientific Imaging Systems (Eastman Kodak Company, New Haven, CT, USA). The first dimension was run with the Multiphor flatbed system (Amersham Biosciences) and the power supply EPS 3501 XL. The second dimension was run with the Mini-Protean II electrophoresis cell and power supply (Bio-Rad).

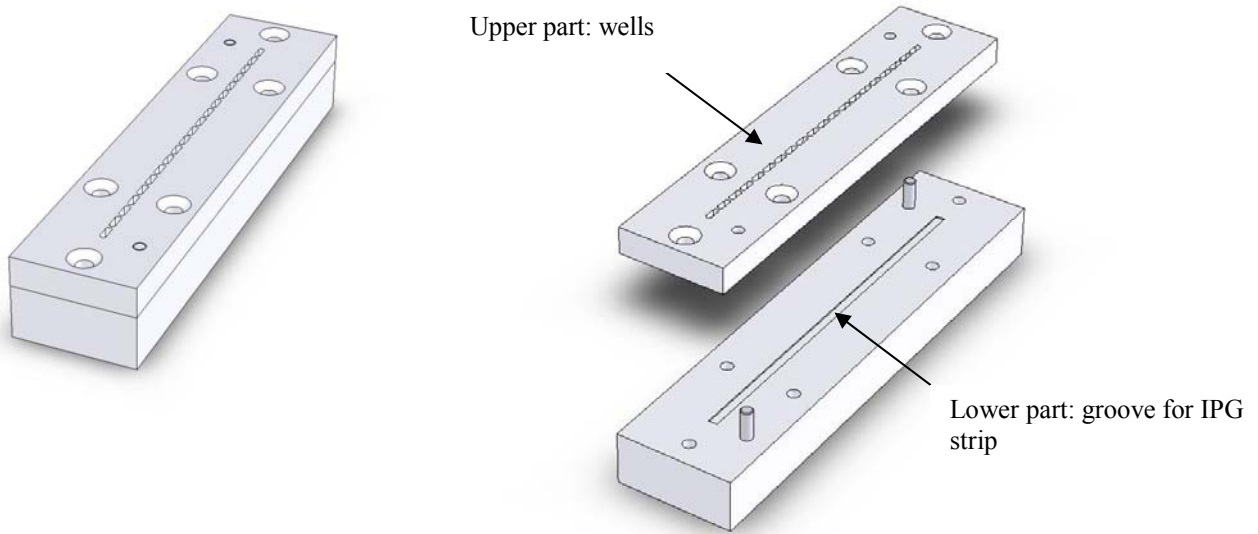
3. Results and discussion

3.1 Description of the OFFGEL homemade device

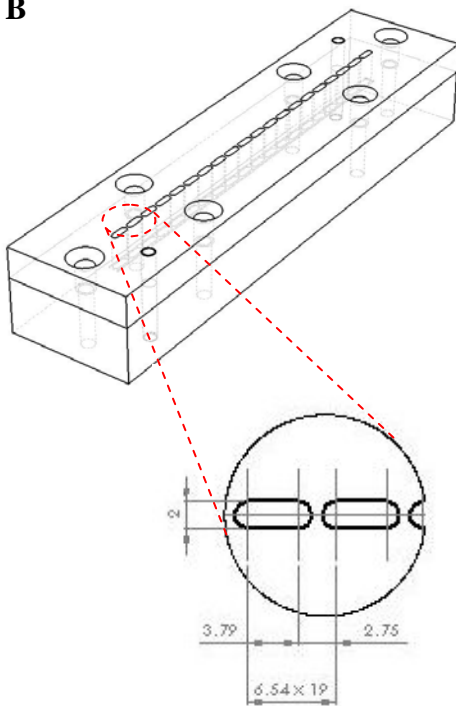
Figure 1 shows some drawings of the in-house cell designed for OFFGEL electrophoresis, the dimensions are consistent with our previous simulation results and with former prototype devices for OGE.¹¹

Basically, the present device is constituted of two polyoxymethylene (POM) blocks. The upper part, in which multiple chambers were machined, having the following size: 6 mm length, 2 mm width and 1 mm height, each well capable of containing 100 μ L at most. The lower part, in which a groove was designed to hold an IPG strip, fits directly under the multicompartments (Figure 1A). The cell allows the collection of 20 fractions, but this number is variable, depending on the resolution expected, one can design in such a way to work with longer strips and/or with narrower pH gradients. Indeed, the resolution of the separation depends on the pH gradient and on the length of the IPG gel as well as on the size of the compartments and on the number of wells under which the gel is placed. *pI* resolutions between 0.05 and 0.3 units have been reported in other prototype devices.¹¹

A



B



C

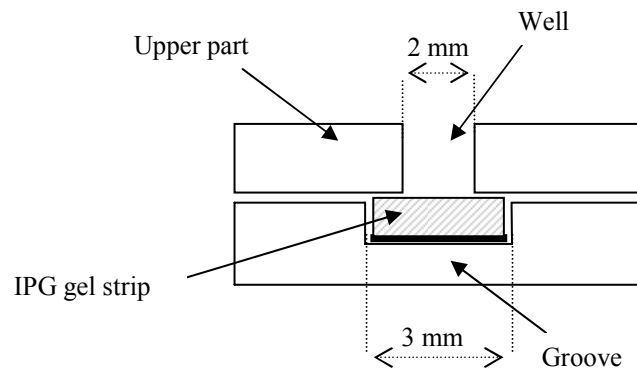


Figure 1: Drawing of the homemade OFFGEL device. Panel (A) shows the device, constituted of two parts, the upper part in which the wells were carved, and the lower part, where the groove for the IPG gel strip lies. Panel (B) shows the dimensions of two adjacent chambers. Panel (C) shows a transversal view of the IPG strip placed in the groove, under the chamber, and the sealing made by the gel between the different chambers.

Figure 1B shows the detailed dimensions of the wells, as well as the distance between wells. Typically, if a 13 cm long IPG strip with pH gradient 3–10 is placed under the wells; one well covers 0.31 pH unit, the interspace between wells corresponding to 0.04 pH unit.

Figure 1C is a transversal cut of a compartment, showing the IPG gel strip placed in the groove, with the gel side in contact with the chambers. The gel assures the sealing of the different compartments during OGE, thus the migration of species takes place in the gel only, and liquid fractions are recovered from the chambers at the end.

3.2 Voltage and current monitoring

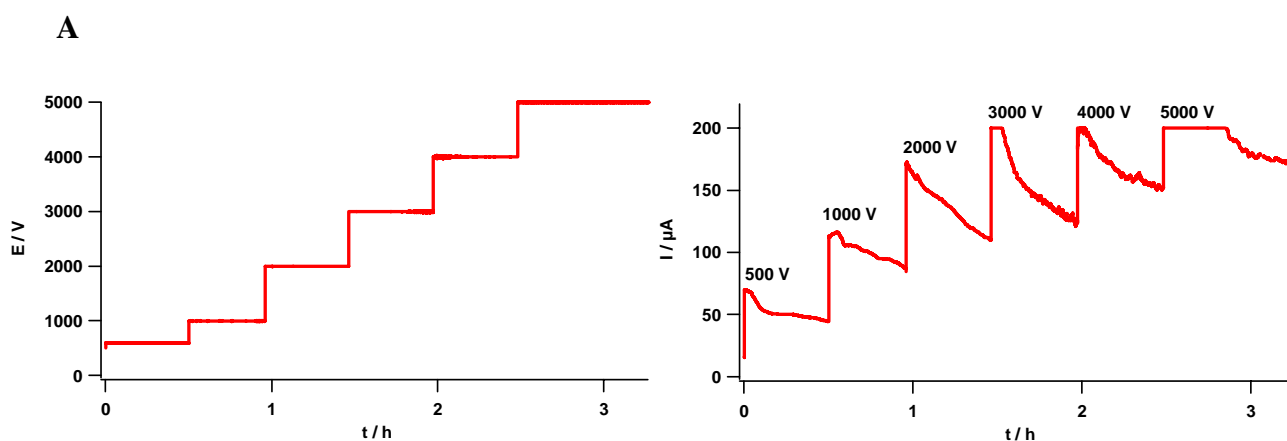
The usual online detection methods for analytical IEF instruments are optical or conductivity detection.¹⁴⁻¹⁶ However, today's commercial preparative instruments seldom have online optical or conductivity detection, thus requiring other methods to monitor the IEF process, such as offline analysis of fractions.¹⁷ In-gel IEF is usually a long process, and as there is no clear way to determine the end of an IEF separation, and operators usually let long time for the run, with the justification that the longer the separation, the better the resolution.¹⁸ Determining the end of IEF has become crucial, to avoid long and useless time of focusing. Monitoring the current during IEF could be a useful way to detect the end of IEF, because the evolution of the current is linked to the migration of species.¹⁹

Monitoring the current and the voltage is also important to understand the resulting resolution, thus allowing the optimization of the focusing parameters to improve that resolution. Moreover, the evolution of current during IEF can give indications on the kinetics of the separation. Thus monitoring of the current during IEF is interesting in terms of practical run but as well for optimization and understanding of the process.

A LabView program was written, which, in interaction with a Spellman High Voltage source, allows doing two things:

- 1) Apply a given voltage program, and at the same time set a limit to the current (hundreds of microamperes)
- 2) Monitor the effective voltage applied and the resulting current.

Figure 2 shows the voltage and current monitored for two IEF runs. The first run (Figure 2A) was a test run, where a mixture of three proteins was submitted to different increasing steps of voltage from 500 V to 5000 V, every half an hour, and the response in current was measured. The current limit was set at 200 μA . For the first three steps (500, 1000 and 2000 V), it can be observed that the higher the voltage, the higher the current drop. For the next steps, the current response reached the limit; the current drop could not be estimated. After 3.5 hours, the IEF was not finished, the current continued to drop, meaning that the steady-state was not reached yet.



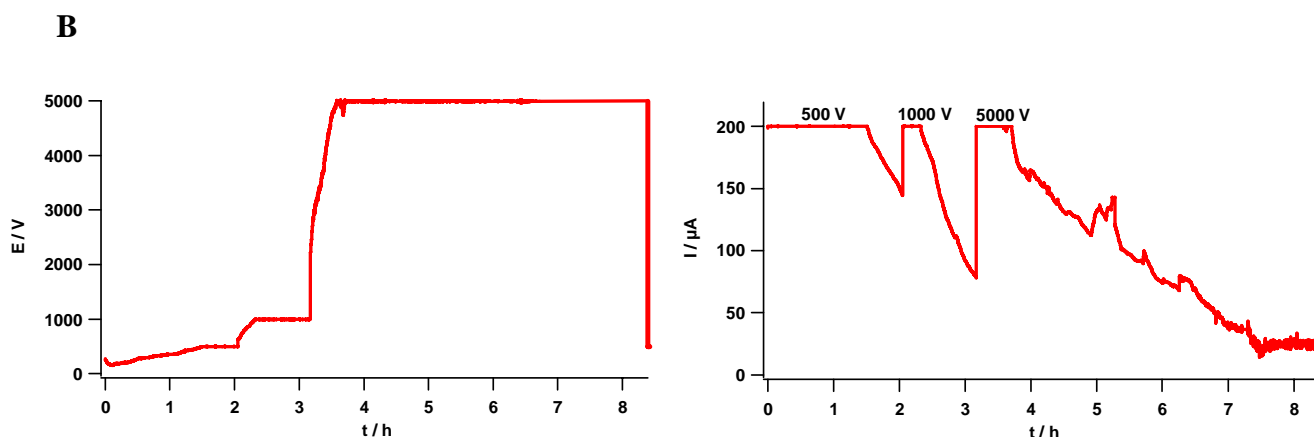


Figure 2: Evolution of the voltage and current vs. time. Panel (A) shows the voltage and current during a test OGE fractionation of a mixture of three proteins at 0.1 mg/mL. The potential was increased in multiple steps from 500 V to 5000 V. Panel (B) shows the voltage and current during the OGE fractionation of an *E. coli* protein extract, with a total initial load of 400 μg . The voltage program was 500 V for 2 h, 1000 V for 1 h, and 5000 V for 4 h. The current was in both cases limited to 200 μA per IPG strip.

The second run (Figure 2B) shows the voltage and current during the IEF separation of *E. coli* protein extract. The first voltage step (500 V) already results in a limit current. At the beginning of the run, it is thus crucial to limit the current, to avoid Joule heating. The sample loaded is usually not desalted and for biological samples, it usually contains detergents, salts which help solubilize the proteins. After 7.5h of focusing, the current is stabilizing around 30 μA , and around 5 μA if dropping the voltage to the initial value of 500 V. This residual current (approx. 2.5% of the current limit) can be explained by the equilibrium between diffusion and migration and reminds that IEF is a dynamic equilibrium method.

An interesting point is that the integration of the current curve against time gives information on the electric charge of the system ($I = dq/dt$). Thus, the surface under the curve represents the charge contained in the system, and shows that even at equilibrium, the system has a residual charge, mainly due to the reactions at the electrodes and the splitting of water in the neutral region.

3.3 pH characterization

The characterization of the pH gradient established during OGE IEF is important, in terms of pH and reproducibility, because the precision of the pH of each IEF fraction is crucial, due to the increasing use of the *pI* as a validation tool.^{18, 20, 21} To do so, 3-10 IPG strips of 13 cm were used with the 20 fractions OGE device. In OGE, the pH gradient is established by the IPG and more precisely, by the Immobilines present in the polymerized gel. But the separation media usually contains a small amount of CAs that are used to increase protein or peptide solubility at pH close to their *pI*,²² as well as help stabilize the pH gradient, because proteins and peptides are ampholyte species, therefore, according to their concentration, they could act on the buffering capacity of the gel.

In order to evaluate the reproducibility of the pH gradient and whether the CA concentration has an influence on the established pH, we considered two CA concentrations (0.5% and 2%) and, for each CA concentration, OGE fractionation of a mixture of three proteins (myoglobin, beta-lactoglobulin and alpha-lactalbumin) were repeated three times. The concentration of the three proteins was kept constant (0.1 mg/mL per protein) in all the experiments. The obtained pH profiles are shown on Figure 3.

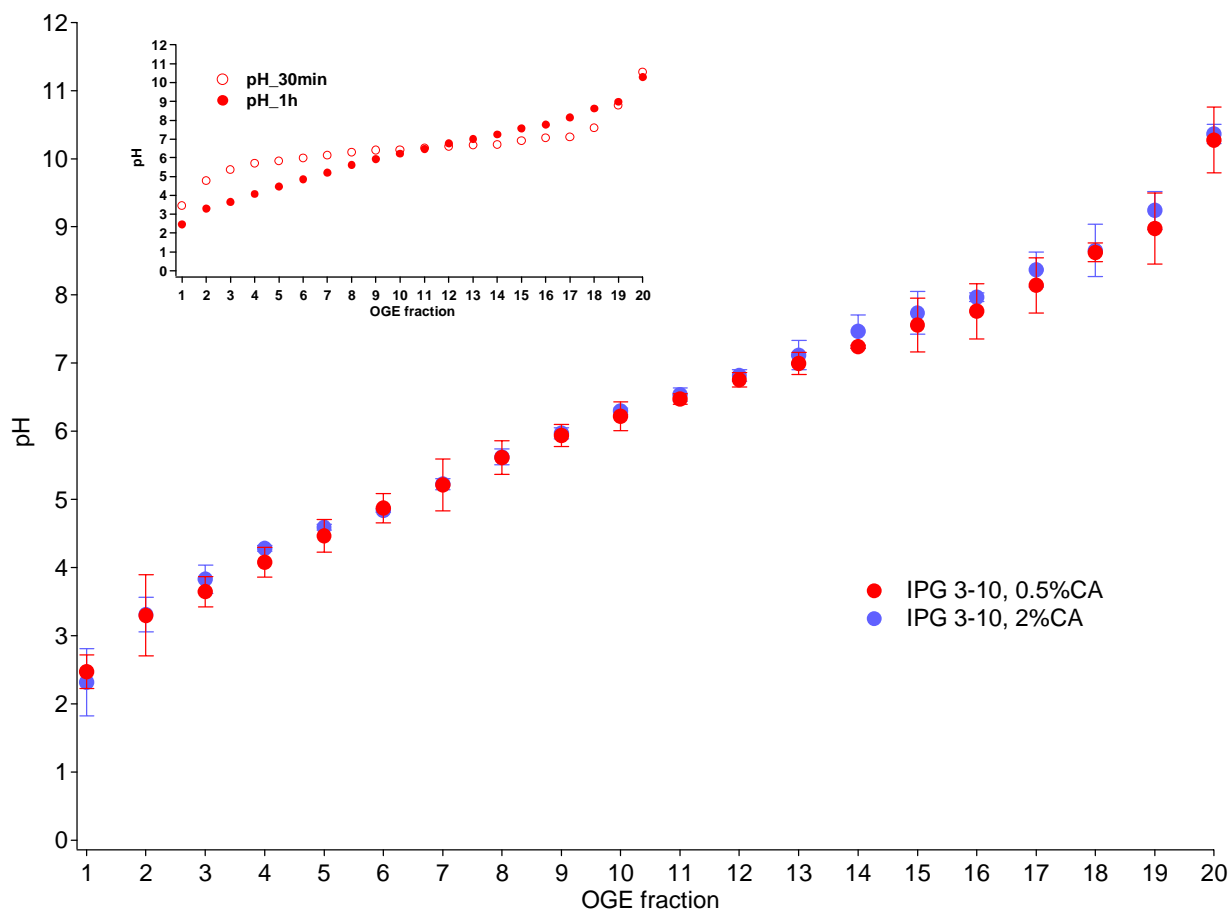


Figure 3: pH gradient stability and reproducibility during OGE IEF. The influence of the concentration of carrier ampholytes on the pH gradient has been evaluated for two CA concentrations (0.5% and 2%). Inset is the development of the pH gradient after 30 min (empty circles) and 1 h (full circles) at 500 V.

It first appears that the pH gradient is already well developed after 1 h at 500 V, confirming the assumptions previously formulated in the numerical calculations (chapter III), that the establishment of the pH gradient is faster than the focusing process itself. The reproducibility of the pH is very good, given that the fractions pH show a relative standard deviation (RSD) comprised between 0.2% and 9% ($n = 3$). The majority (80%) of the fractions also present a RSD below 3%, leading to a maximal theoretical error of 0.3 pH unit. Consequently, OGE IEF can not only be considered a useful fractionation technique, but also

a relevant characterization tool, justifying the further use of the peptide pI as a validating tool for peptide and protein identification.

It can also be seen that the CA concentration does not play significantly on the fraction pH, thus a CA concentration of 0.5% will be used in further experiments.

The fractions collected after OGE of the mixture of three proteins have been analyzed by capillary electrophoresis, in HEPES buffer, ionic strength 100 mM and pH 8.9. At that pH the proteins should be negatively charged and thus no adsorption on the capillary wall should be observed. The corresponding CE chromatograms are shown in Figure 4. Panel A shows the case where α -lactalbumin is found in the same well as β -lactoglobulin, in the fraction pH 5.40, and panel B shows that for another OGE run, the two proteins are found in two adjacent wells, with pH 5.12 for lactalbumin and pH 5.53 for lactoglobulin. This illustrates quite well how the position of the gel, and thus the position of the pI under the well, is important. However, this does not influence the reproducibility of the experiment, because in both cases, the proteins are found in the fraction having the pH corresponding to their pI .

In addition, it is relevant to note that the resolution of the separation is not necessarily due to the sharpness of the separation in itself, but can also be due to the location of the pI relative to the recovery wells. Thus, if sometimes a protein/peptide is found in two wells, it might be that their pI location on the gel is exactly under the interspace between two wells. This would be relevant in the case of peptide validation based on pI for example.

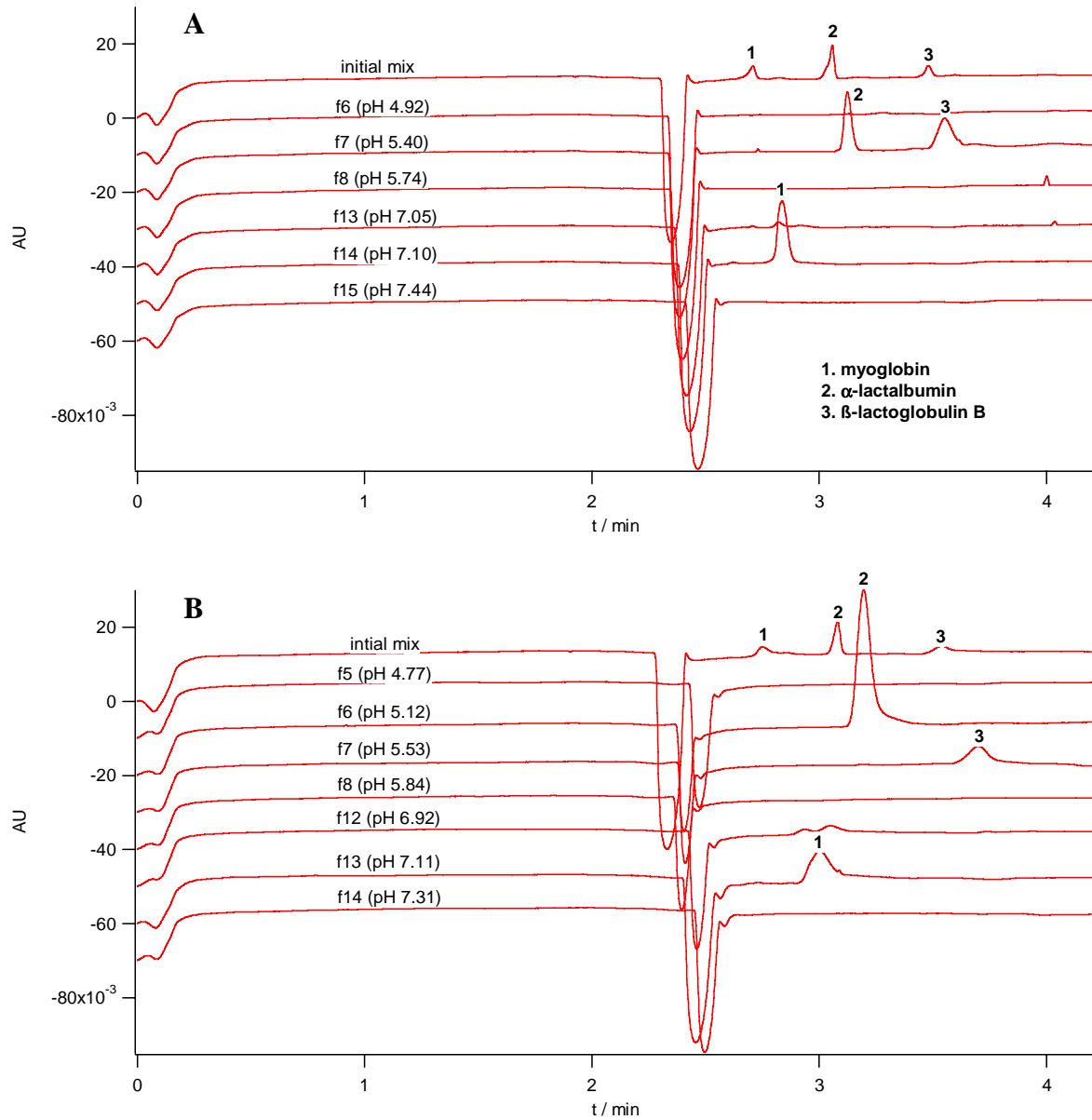


Figure 4: CE chromatograms of OGE fractions of three proteins. Separations were performed in 120 mM HEPES buffer, pH 8.9. Fused silica capillary; total/effective length 31/21 cm, ID 50 μ m; voltage 12 kV; hydrodynamic injection 30 mbar, 5 s; UV absorbance at 214 nm. Panels A and B represent the chromatograms for two different series of OGE fractions.

3.4 Loading capacity for proteins

Practically, the loading capacity is the mass of sample/analyte that can be applied on the device and effectively separated with a correct resolution. For gel media IEF, maximum protein loads were experimentally estimated to be 1–10 mg/component/cm of gel.²³ Equations for the mass load of a protein zone in density gradient IEF have shown that the capacity rises with the square of the resolving power.²³ Thus, high resolving power should allow high loading capacity, explaining why much work has been done using narrow pH range IEF, where the resolution is higher.²⁴ In proteomics, loading capacity is especially crucial when searching for low abundance proteins, because the initial protein load then needs to be higher to isolate and detect these low abundance proteins. It is thus important to know how much amount can be separated under given conditions of voltage and time.

To roughly estimate the loading capacity of the OGE device using a 3-10 pH range, a set of seven proteins was separated. A first fractionation was performed with equimolar concentration of the proteins (0.4 mg/mL each protein, resulting in a total protein load of 2.8 mg), during 6 hours under the following voltage conditions (1 h at 500 V, then 1 h at 1000 V, and finally 4 h at 5000 V). The 20 fractions were collected and analyzed by CE with phosphate buffer pH 7.35. A second experiment was performed by doubling the concentration of the proteins (0.8 mg/mL for each protein except for myoglobin, the concentration was 1 mg/mL, resulting in a total protein load of 5.8 mg). The fractions were analyzed by CE in the same buffer. The results are shown on Figure 5.

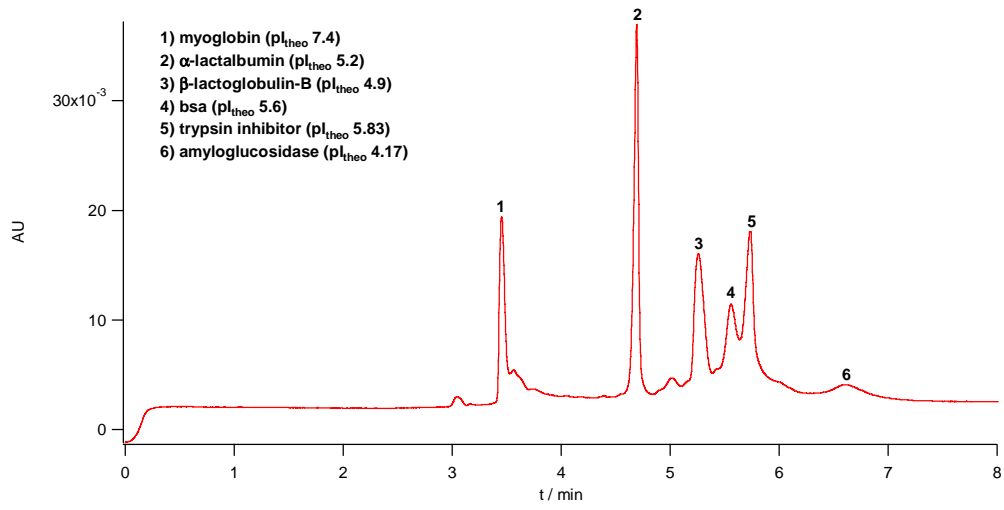
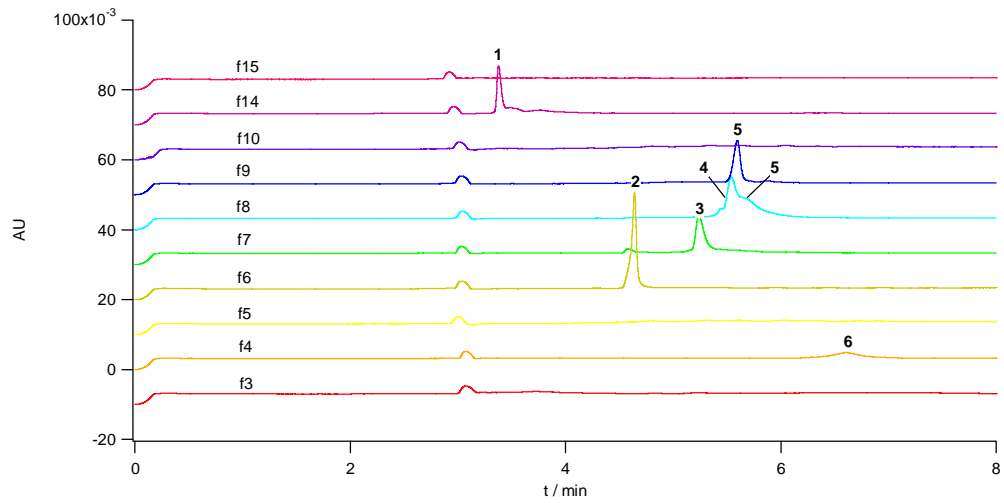
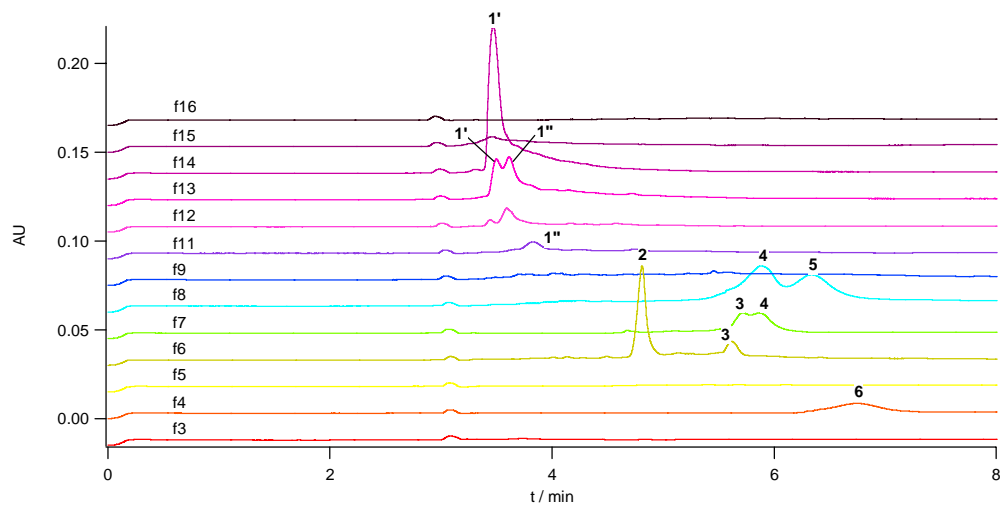
A**B****C**

Figure 5: CE chromatograms of the fractions recovered after OGE IEF of a mixture of proteins. Separations were performed in 100 mM phosphate buffer, pH 7.54. Fused silica capillary; total/effective length 31/21 cm, ID 50 μm ; voltage 15 kV; hydrodynamic injection 30 mbar, 5 s; UV absorbance at 214 nm. Panel A is the initial protein mixture before OGE fractionation. Panel B shows the fractions recovered from OGE IEF with initial protein load of 0.4 mg/mL for each protein. Panel C shows the fractions recovered from OGE IEF with initial protein load of 0.8 – 1 mg/mL for each protein.

Figure 5A shows the initial mixture analyzed by CE, before OGE IEF, to check the purity and migration time of the proteins. The phosphate buffer was used for CE, and not the HEPES buffer, because the resolution is better concerning some proteins (β -lactoglobulin B, bovine serum albumin and trypsin inhibitor). Cytochrom C was added as colored indicator, to allow a visual monitoring of the IEF. It was added at the same concentration as the other proteins in both experiments.

Figure 5B shows a good separation for all the proteins at low concentration. Each protein is recovered in one well, except for the trypsin inhibitor, which appears already in the adjacent fraction. An amount of almost 3 mg of total proteins was loaded, and allows a correct separation in 6 h.

Figure 5C shows that the CE chromatograms of the fractions recovered from the OGE fractionation of a more concentrated mixture. The fractionation was performed in exactly the same time, however it does not allow to focus each protein in one well. The BSA appears in two wells, as well as the β -lactoglobulin B. Myoglobin appears in five wells, due to the higher concentration loaded initially. But it is quite interesting to note that two peaks were observed for myoglobin (1' and 1''), peaks that are most likely due to its isoforms. Horse myoglobin is known to have a major isoform at pI 7.4 and a minor isoform at pI 6.9, which have been separated by gel electrophoresis.²⁵ The two peaks observed in fraction N°13 probably correspond to these isoforms, as one peak is mainly present in fractions N°12 and 13

(measured pI values 6.7 and 7.0 respectively) and the other mainly isolated in fractions N°13 and 14 (measured pI values 7.0 and 7.24 respectively). Apparently, the two isoforms of myoglobin could be separated by OGE. Each isoform appears in three wells.

As a conclusion, loading of 0.8 mg for each protein (6 mg total protein load) stills allows a correct separation, with each protein recovered in two wells and three for myoglobin. It is however relevant to note that the loading capacity depends on the actual number of compounds and their solubility at the pI . For complex biological mixtures, the concentrations of the different proteins constituting the mixture are not equimolar, a large dynamic range is observed. Proteins with a large concentration have higher risk to be recovered in several wells, and low abundant proteins in one well.

The upper limit for the loading capacity can be understood in terms of change in the local electric field. The high concentration of a species near its pI should provoke a change in the local conductivity, resulting in a change of the apparent electric field seen by the species, thus affecting their migration. Thus, the high concentration should result in an apparent lower migration term compared to the diffusion. The species cannot focus anymore, resulting in a broad unfocused peak, explaining why one protein can be found in several wells.

In some cases also, the recovery of proteins may be problematic due to the precipitation of proteins due to high concentration of globally neutral species near pI . The ampholytes mixture is used to improve solubilization near the isoelectric point. But a way to load more on the OGE device would be to allow a continuous extraction of the proteins into another phase. This would allow the focusing of higher concentrations loaded. Another way would be to design a free-flow OFFGEL device, to allow continuous feed of sample and continuous outlet of the fractions. A recirculation of the fractions would also concentrate the amount of proteins at each step of the recirculation. This approach is currently under development in the lab.

3.5 OG-IEF of peptides

To test the high resolving power of the device, as demonstrated by numerical simulations (chapter III), we here perform OFFGEL IEF of peptides derived from tryptic digestion of proteins.

One aliquot of BSA tryptic digest was diluted to 1 mL, in water containing 1% DTT and the total volume (corresponding to 500 μg initial protein load) was then loaded on the OGE cell, with a 13 cm IPG strip with pH range 3–10, to be separated into 20 fractions by in-solution IEF. After OGE, liquid fractions were withdrawn, and a supplementary step to enhance the protein yield was performed. For this purpose, 100 μL of a water/methanol/formic acid (49:50:1 by volume) was added per well and incubated for 60 min without voltage. Corresponding peptide fractions were pooled and lyophilized by vacuum centrifugation prior to LC-MS analysis. Peptide fractions were reconstituted in 25 μL of 2% acetonitrile with 0.01% formic acid, and 1 μL was injected on the chromatographic column. The summarized workflow is shown on Figure 6.

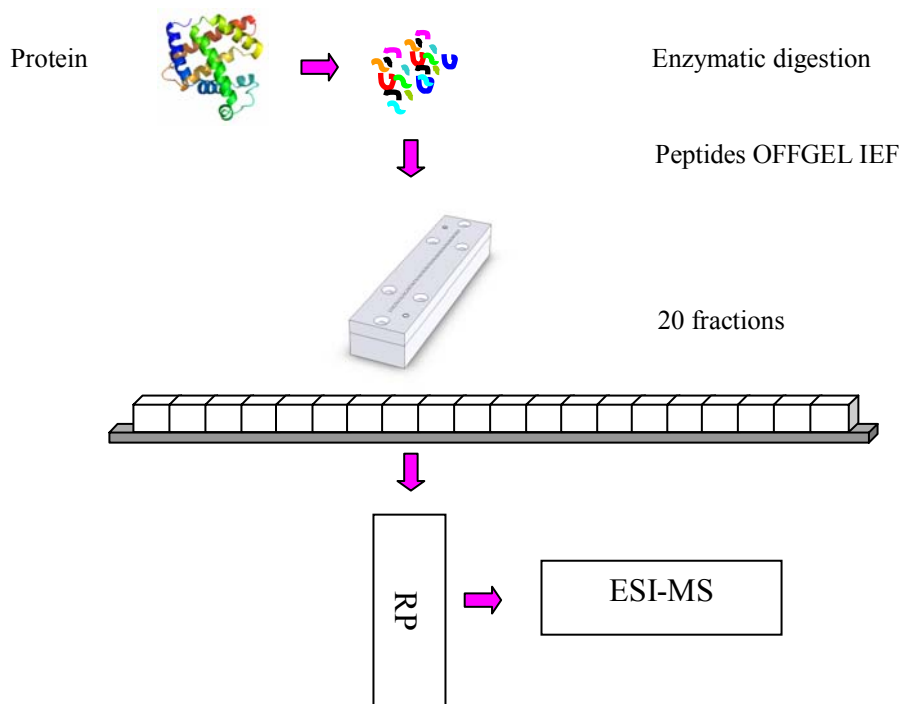


Figure 6: Workflow for the OGE fractionation of peptides and further analysis by LC-ESI-MS.

The resulting chromatograms are shown on Figure 7, the pH values indicated for the fractions are calculated based on the sequence of peptides identified in that fraction and using an in-house software (chapter III) taking into account the amino acids pKa values from Bjellqvist et al.²⁶ Table 1 gives the peptides identified in fraction 9 associated with their LC retention times.

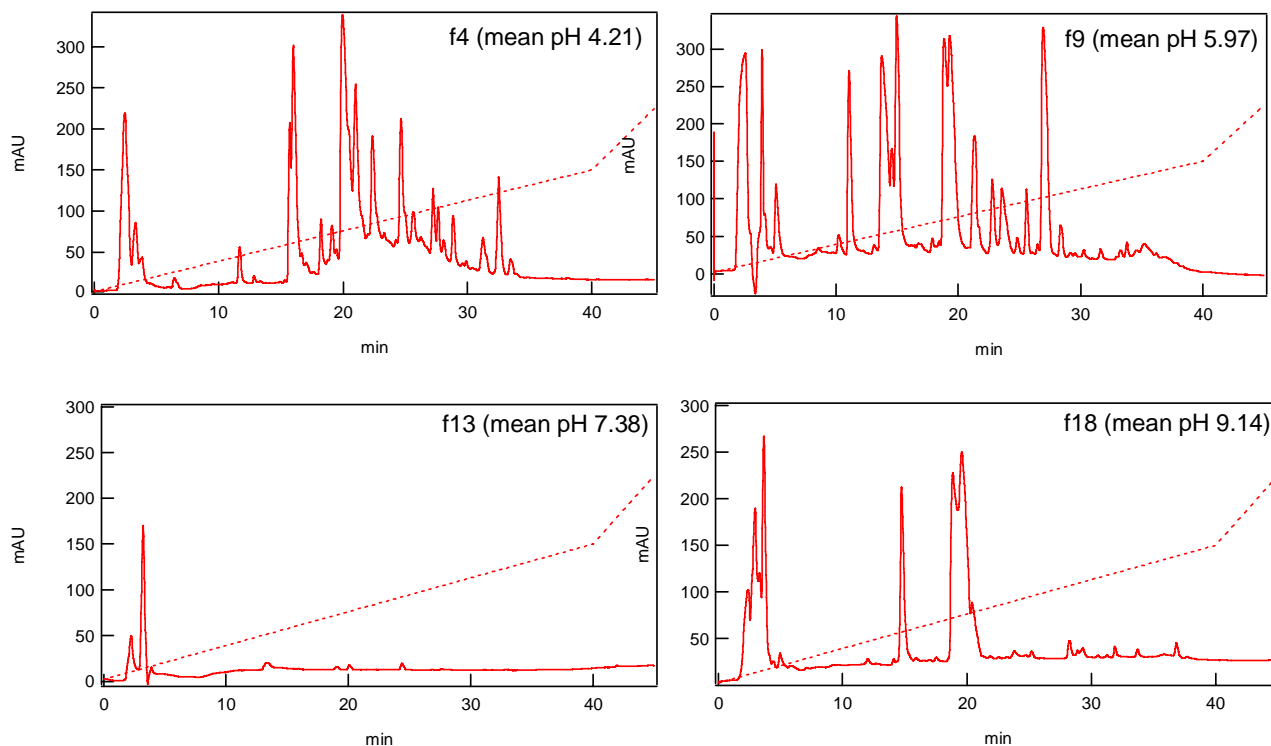


Figure 7: LC chromatograms at 214 nm of OGE fractions after IEF of peptides from protein digest. Elution gradient of the LC run is shown in dashed lines.

Table 1: Identified peptides in OGE fraction 9 (mean pH calculated 5.83).

RT (min)	Sequence	Monoisotopic mass (Da)	pI (calculated with pK values from ²⁶)
3.98	FPKAEFVEVTK	1294.7	6.14279
5.28	NYQEAK	752.2	6.00076
6.42	FGER	508.2	6.00235
15.17	FKDLGEEHFK	1249.5	5.44534
16	LVTDLTK	789.3	5.83572
20.15	YLYEIAR	927.4	6.00076
22.66	LVVSTQTALA	1002.3	5.56992
24.15	SLHTLFGDELCK	1362.5	5.31998
24.97	QTALVELLK	1014.5	6.00156
27.01	LGEYGFQNALIVR	1479.7	6.00156

The chromatograms indicate that the distribution of peptides separated by OGE IEF is rather heterogeneous. This is in agreement with the *in silico* tryptic digestion of BSA and distribution of peptides as shown in Figure 8.

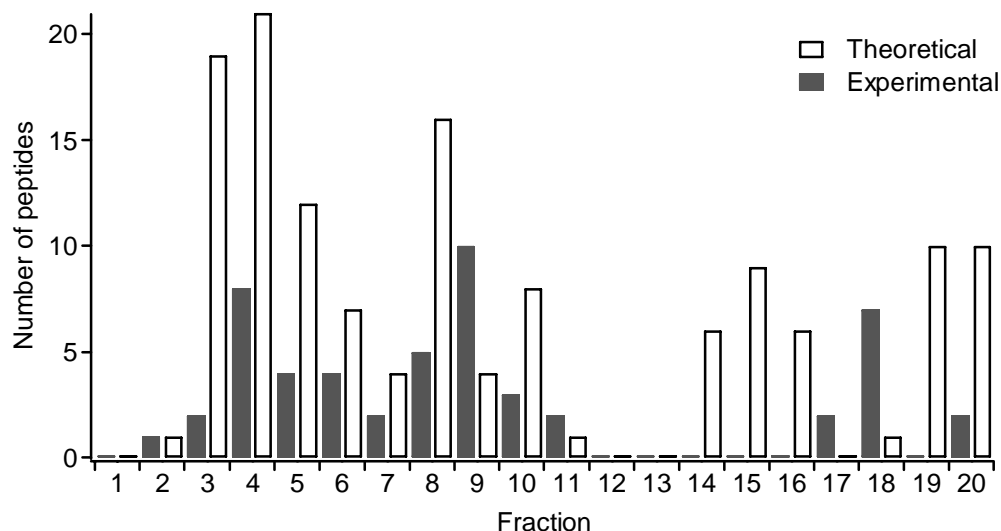


Figure 8: Peptide distribution from experimental results and theoretical predictions.

One way to evaluate the quality of the fractionation is to look at the number of fractions in which each distinct peptide was found. As shown on Figure 9A, 81.8 % of the identified peptides are found in one fraction and the rest in two fractions. No peptide was found in more than two wells, which demonstrates the high resolution of the OFFGEL peptide separation. These results are well in line with the simulation results. The final results are summarized in Figure 9B, showing the distribution of peptides that are unique to a given fraction.

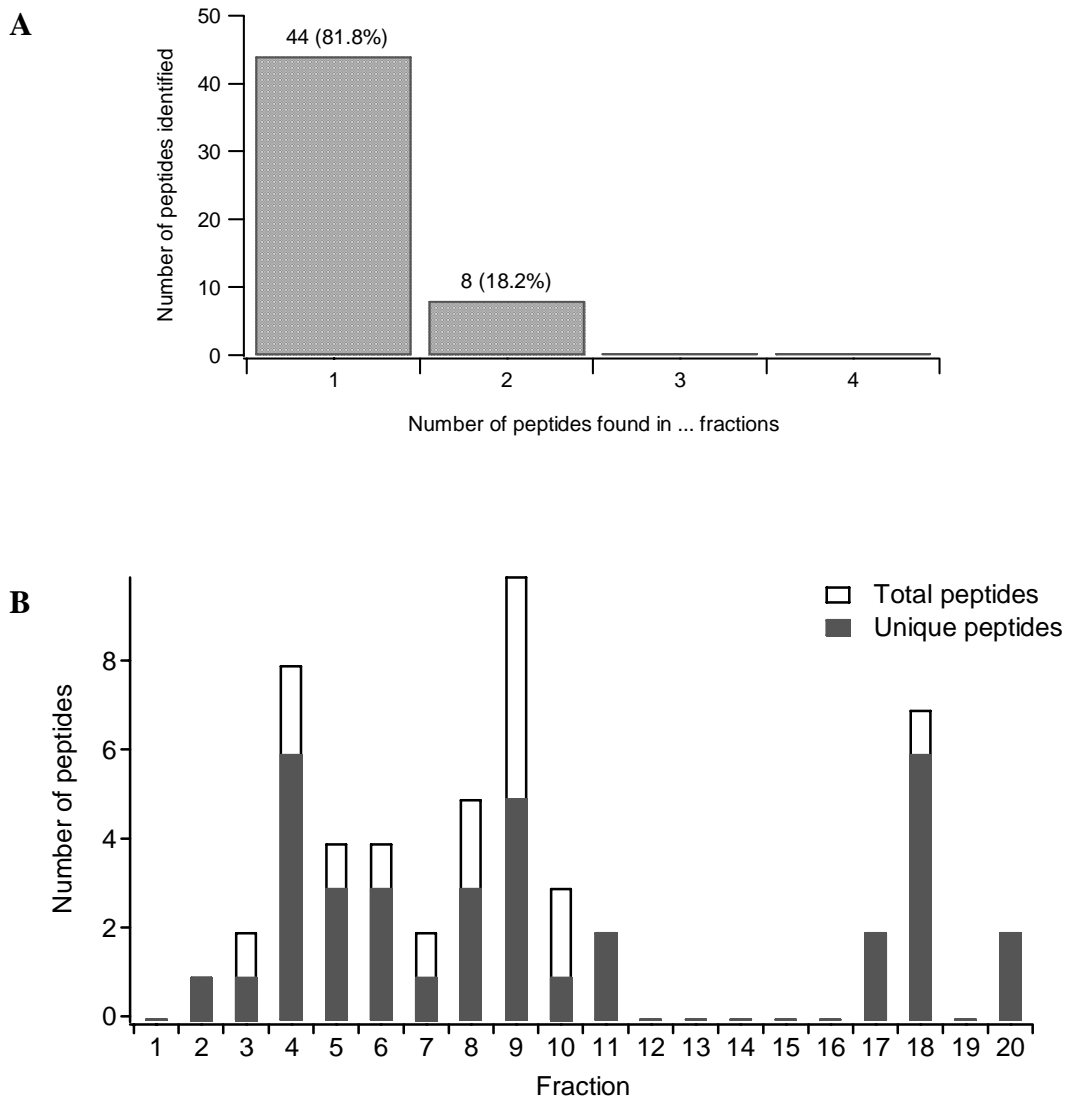


Figure 9: (A) Number of peptides found in a given number of fractions. (B) Total number of peptides identified in each fraction, the dark shaded area indicates the peptides unique to each fraction.

The explanation for peptides focusing in more than one well can probably be found in studying the titration curve of the concerned peptides. For example, peptide LVVSTQTALA was found in fractions 9 and 10. Figure 10 (left) shows the titration curve for that peptide. The curve displays a particularly flat slope near the pI , this probably accounting for the lower resolution of the focusing. In addition, the titration curve of all the peptides found in two wells show a flat slope near the pI , except for two peptides, displaying a steep slope at pI

(Figure 10, right). The steep slope should give a sharp resolution. The only reason accounting for the presence in two wells could be the position of the pI , probably situated in the interspace between two wells, as already mentioned above.

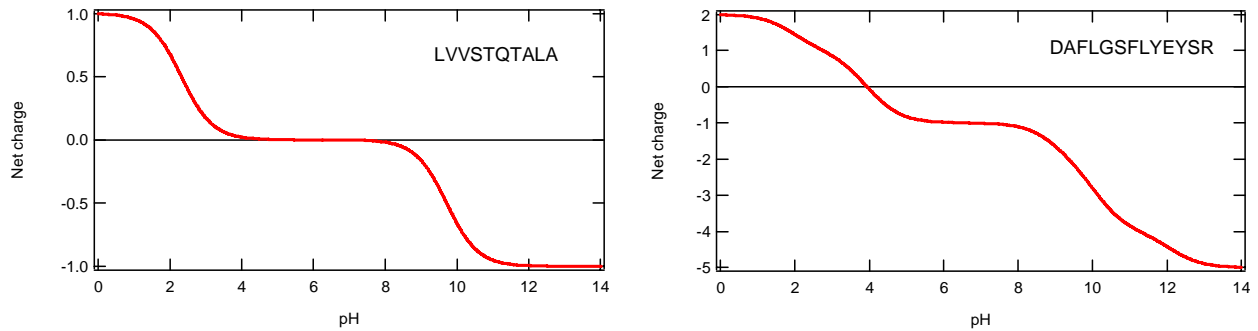


Figure 10: Titration curves of peptides found in two wells.

The prediction of pI values allows validating the peptides identified. Indeed, from the peptides identified in a fraction, an average fraction pI value can be calculated as well as the standard deviation. These values allow setting a tolerance window and eliminating peptides deviating too far from the average value, thus considering these peptides as false positive. But this point will be further discussed in detail in the next chapter, concerning enhanced protein identification by peptide mass fingerprinting.

3.6 OG-IEF of proteins under denaturing conditions

To demonstrate that the present OFFGEL device could perform good separation on a more complex biological mixture and that the denaturing conditions (presence of urea, thiourea and detergent such as CHAPS) do not affect the separation, the fractionation of *E. coli* protein extract was performed. For that, 400 μg of an *E. coli* protein extract was solubilized in the Rabilloud buffer and loaded on the OGE cell with a pH gradient 4-7, and IEF was performed

with the following voltages: 1 h at 500 V, then 1 h at 1000 V, and finally 5 h at 5000 V. The current limit was set at 200 μ A.

A 1-D IEF was first performed on an IPG strip, to check the *pI* range of unfractionated *E. coli* proteins (Figure 11), and shows that all proteins are comprised in the range of *pI* 4–7. Thus the OGE fractionation as well as the 2-D maps will further be carried out within that range, to allow a better resolution (narrower range of *pH*).

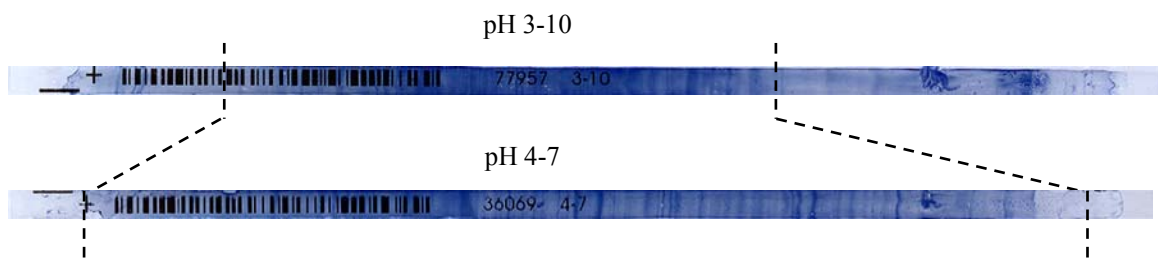


Figure 11: 1-D IEF to check the *pI* range of *E. coli* proteins

Figure 12 displays the results of the fractionation experiments for *E. coli*. Panel A shows a 2-D map of a control, unfractionated protein extract of *E. coli* (total protein load 400 μ g). 2-D maps of various fractions are displayed in Figure 12 panels B and C. These maps are related to fractions N° 3 (*pH* 4.32 upper left), and 4 (*pH* 4.47 bottom left), as well as N°10 (*pH* 5.42, upper right) and 11 (*pH* 5.58, bottom right). It can be appreciated that, even though the sample was quite complex before fractionation, narrow *pI* cuts were obtained and no spot overlap was observed between the adjacent fractions, showing the good separation and resolution of the device. It can be concluded that the presence of urea and detergents do not affect the separation process.

4. Concluding remarks

The results reported in this chapter demonstrate that the in-house designed device for OFFGEL IEF allows a powerful and versatile approach to sample fractionation. With the high reproducibility of the pH gradient, a relatively high loading capacity for proteins, a sharp focusing for the peptides generated from tryptic digestion of proteins, and a minimal overlap/good resolution observed for complex biological mixture, this device is suitable for the separation of peptides and proteins. The monitoring of the current evolution during IEF allowed the determination of the steady-state of the focusing. The resolution was estimated to be approx. 0.3 pH unit and the two isoforms of myoglobin could be separated and recovered in solution in a concentrated form, without the need for further extraction steps. In the perspective of a more complete approach, each OGE fraction of protein can further be amenable to proteolytic digestion, and the resulting peptides could be applied to a second round of OGE fractionation on the same device, to perform a two-stage separation strategy, in the perspective of bottom up approaches in proteomics.

As a summary, there is clear evidence that OFFGEL IEF is a powerful, high resolution, versatile technology to achieve prefractionation and separation of biological samples, and that the present device built in-house allows correct fractionation of proteins/peptides in approx. 5 to 8 hours, depending on the complexity of the sample and the resolution desired. Another interesting application of OFFGEL IEF combined with chemical tagging for the enhanced identification of proteins by their peptides is further presented in the next chapter.

5. References

1. Hannig, K., New Aspects in Preparative and Analytical Continuous Free-Flow Cell Electrophoresis. *Electrophoresis* **1982**, 3, (5), 235-243.
2. Bier, M., Recycling isoelectric focusing and isotachopheresis. *Electrophoresis* **1998**, 19, (7), 1057-1063.
3. Righetti, P. G.; Wenisch, E.; Faupel, M., Preparative Protein-Purification in a Multi-Compartment Electrolyzer with Immobiline Membranes. *Journal of Chromatography* **1989**, 475, 293-309.
4. Righetti, P. G.; Wenisch, E.; Jungbauer, A.; Katinger, H.; Faupel, M., Preparative Purification of Human Monoclonal-Antibody Isoforms in a Multicompartment Electrolyzer with Immobiline Membranes. *Journal of Chromatography* **1990**, 500, 681-696.
5. Ros, A.; Faupel, M.; Mees, H.; van Oostrum, J.; Ferrigno, R.; Reymond, F.; Michel, P.; Rossier, J. S.; Girault, H. H., Protein purification by Off-Gel electrophoresis. *Proteomics* **2002**, 2, (2), 151-156.
6. Zuo, X.; Speicher, D. W., A method for global analysis of complex proteomes using sample prefractionation by solution isoelectrofocusing prior to two-dimensional electrophoresis. *Analytical Biochemistry* **2000**, 284, (2), 266-278.
7. Tang, H. Y.; Speicher, D. W., Complex proteome prefractionation using microscale solution isoelectrofocusing. *Expert Review of Proteomics* **2005**, 2, (3), 295-306.
8. Xu, Y.; Zhang, C. X.; Janasek, D.; Manz, A., Sub-second isoelectric focusing in free flow using a microfluidic device. *Lab on a Chip* **2003**, 3, (4), 224-227.
9. Davidsson, P.; Nilsson, C. L., Peptide mapping of proteins in cerebrospinal fluid utilizing a rapid preparative two-dimensional electrophoretic procedure and matrix-assisted laser desorption/ionization mass spectrometry. *Biochimica Et Biophysica Acta-General Subjects* **1999**, 1473, (2-3), 391-399.
10. Brobey, R. K. B.; Soong, L., Establishing a liquid-phase IEF in combination with 2-DE for the analysis of Leishmania proteins. *Proteomics* **2007**, 7, (1), 116-120.
11. Michel, P. E.; Reymond, F.; Arnaud, I. L.; Josserand, J.; Girault, H. H.; Rossier, J. S., Protein fractionation in a multicompartment device using Off-Gel (TM) isoelectric focusing. *Electrophoresis* **2003**, 24, (1-2), 3-11.
12. Di Maio, I., Off-Gel (TM) electrophoresis: characterisation of a novel isoelectric focusing fractionation method. *Thesis N° 3064* **2004**, EPFL.
13. www.amershambiosciences.com, 2-D Electrophoresis using immobilized pH gradients. Principles and Methods. In *Online manual*.
14. Pritchett, T. J., Capillary isoelectric focusing of proteins. *Electrophoresis* **1996**, 17, (7), 1195-1201.
15. Wang, T. S.; Hartwick, R. A., Whole Column Absorbency Detection in Capillary Isoelectric-Focusing. *Analytical Chemistry* **1992**, 64, (15), 1745-1747.
16. Fang, X. H.; Tragas, C.; Wu, J. Q.; Mao, Q. L.; Pawliszyn, J., Recent developments in capillary isoelectric focusing with whole-column imaging detection. *Electrophoresis* **1998**, 19, (13), 2290-2295.
17. Bottenus, D.; Ivory, C. F., On-line optical fiber detection in a preparative free-flow electrofocusing apparatus. *Biotechnology Progress* **2006**, 22, (3), 842-846.

18. Krijgsveld, J.; Gauci, S.; Dormeyer, W.; Heck, A. J. R., In-gel isoelectric focusing of peptides as a tool for improved protein identification. *Journal of Proteome Research* **2006**, *5*, (7), 1721-1730.
19. Stoyanov, A. V.; Das, C.; Fredrickson, C. K.; Fan, Z. H., Conductivity properties of carrier ampholyte pH gradients in isoelectric focusing. *Electrophoresis* **2005**, *26*, (2), 473-479.
20. Cargile, B. J., Gel based isoelectric focusing of peptides and the utility of isoelectric point in protein identification. *Journal of Proteome Research* **2004**, *3*, (1), 112-119.
21. Cargile, B. J., Immobilized pH gradients as a first dimension in shotgun proteomics and analysis of the accuracy of pI predictability of peptides. *Electrophoresis* **2004**, *25*, (6), 936-945.
22. Zhu, M. D.; Rodriguez, R.; Wehr, T., Optimizing Separation Parameters in Capillary Isoelectric-Focusing. *Journal of Chromatography* **1991**, *559*, (1-2), 479-488.
23. Righetti, P. G., *Isoelectric Focusing: Theory, Methodology and Applications*. Elsevier Biomedical Press: Amsterdam, 1983; Vol. 11.
24. Zuo, X.; Speicher, D. W., Comprehensive analysis of complex proteomes using microscale solution isoelectrofocusing prior to narrow pH range two-dimensional electrophoresis. *Proteomics* **2002**, *2*, (1), 58-68.
25. Tulp, A.; Verwoerd, D.; Benham, A.; Jalink, K.; Sier, C.; Neefjes, J., High performance density gradient electrophoresis of subcellular organelles, protein complexes and proteins. *Electrophoresis* **1998**, *19*, (7), 1171-1178.
26. Bjellqvist, B.; Hughes, G. J.; Pasquali, C.; Paquet, N.; Ravier, F.; Sanchez, J. C.; Frutiger, S.; Hochstrasser, D., The focusing positions of polypeptides in immobilized pH gradients can be predicted from their amino acid sequences. *Electrophoresis* **1993**, *14*, (10), 1023-1031.

**CHAPTER V: OFFGEL IEF combined with cysteine
chemical tagging for improved protein identification**

1. Introduction	150
2. Experimental	154
2.1 Chemicals	154
2.2 Tryptic digestion.....	154
2.3 OFFGEL IEF of peptides (OG-IEF).....	155
2.4 Chemical tagging reaction.....	155
2.5 MALDI-TOF	155
2.6 LC-ESI-MS	156
2.7 Database search parameters.....	156
3. Results and discussion.....	157
3.1 pI as validation information to eliminate false positive identifications.....	157
3.2 Counting cysteines for enhanced protein identification by PMF.....	162
4. Concluding remarks	172
5. References.....	173

1. Introduction

“Shotgun” proteomics or “bottom up” approaches involve proteolytic cleavage of mixtures of proteins, resulting in a very large number of peptides to be analyzed (up to tens of thousands for “shotgun” approaches). Separation steps are usually required, followed by mass spectrometry (MS) detection, either by electrospray ionization (ESI-MS) or matrix assisted laser desorption ionization (MALDI-MS). Identification of proteins is achieved by searching for the best match between the experimentally determined masses and those calculated by theoretical cleavage of each of the proteins in the sequence database.¹⁻⁵

However, complete protein sequence coverage is rarely achieved, giving low level of confidence in protein identification, sometimes also leading to ambiguous identifications. This occurs for example when the protein mixture is highly complex, or when only very small amounts of the proteins are isolated, or when peptides are lost due to inefficient ionization. In such cases, it is advantageous to use supplementary information, to constrain the database search by limiting the number of candidate proteins and increase the confidence of protein identification.⁶⁻⁸ Peptide sequencing by online MS/MS is one way to gain that discriminating information. Such additional information improves the level of confidence of the identification, but generally requires a more complex and time-consuming analysis than in the case of simple peptide mapping,⁹ not taking into account that a non-negligible amount of these automatically generated data often result in false-positive identifications.

Indeed, false-positive peptide sequence matches in shotgun proteomics, resulting from searching large-scale MS/MS data against protein sequence databases, are a challenge in high-throughput global protein profiling studies.¹⁰ The use of physicochemical properties such as accurate mass, reverse-phase μ -LC retention time, peptide isoelectric point (pI) has been shown to provide more accurate results and increase the confidence of peptide/protein identifications. Several groups have demonstrated that highly accurate mass information of

peptides can provide more confident sequence database search results.¹¹⁻¹⁵ Smith et al. have reported the use of reverse phase μ -LC elution time as a constraint in peptide sequence matches demonstrating the ability to partially predict the elution times of peptides from reverse-phase columns, and the use of this information in the peptide identification process.¹⁶⁻¹⁸ The use of accurate mass and time tag approach (AMT) was also reported, combining μ -LC retention time and accurate mass to identify peptides, and was successfully applied to profiling of human plasma proteome, eliminating the need for tandem MS analyses.^{19, 20} Recently, Cargile et al., as well as other groups, have reported on the use of peptide *pI* information, obtained by peptide separations using immobilized pH gradient (IPG) gels,²¹⁻²⁴ free-flow electrophoresis (FFE)²⁵⁻²⁷ or other devices,²⁸⁻³⁰ to assist in the identification of peptides. These studies have demonstrated the utility of peptide *pI* information in reducing the false-positive matches and significantly increasing the confidence of peptide identifications.

Another way to obtain additional information on peptide sequence, apart from performing MS/MS fragmentation, is chemically labeling amino acids of interest in the peptides. Chemical tagging reactions have played a major role in MS-based proteomics, especially in protein identification. The main application fields of chemical tagging include enrichment of subclasses of peptides by affinity tags, and *in vitro* stable isotope labeling for quantification.³¹ Chemical modifications can be of two types. “Global” approaches target common functional groups, *i.e.* amino groups at the N-terminus of a peptide or protein, and on lysine side-chains, or carboxylic acids at C-terminus and on aspartic and glutamic acid residues. This type of labeling would ensure the highest possible coverage, since every peptide will theoretically carry the tag. More targeted approaches are directed towards specific amino acids such as cysteine and tryptophan, particularly in the context of affinity tagging. Post-translational modifications (PTMs) such as phosphorylation and glycosylation

can also be targeted. An overview of the usual targets of chemical tagging is given in Figure 1.

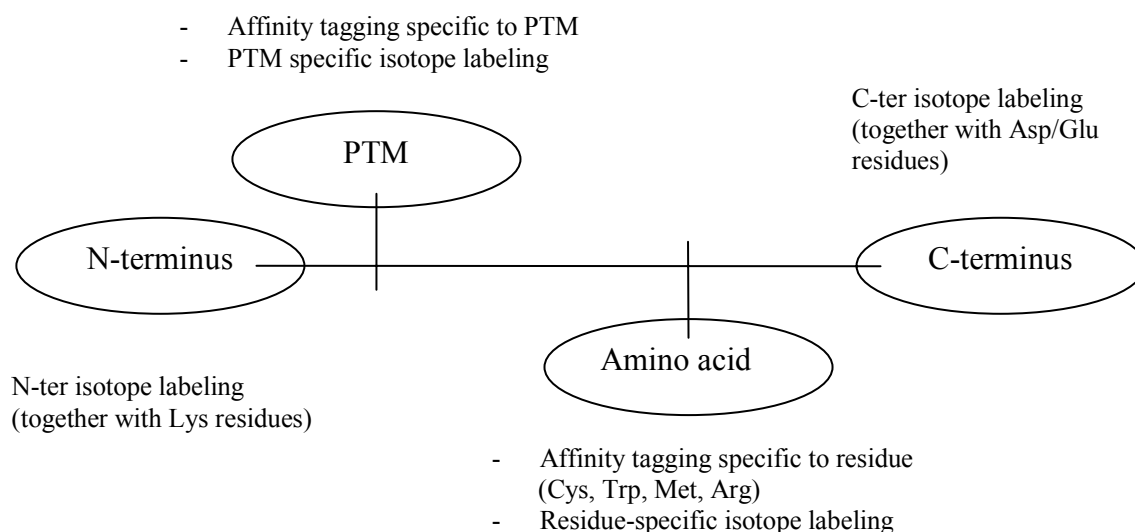


Figure 1: Overview of tagging reactions in peptides or proteins.

Of interest here is the labeling of cysteine residues in peptides. It was observed that cysteine residues are present in 89.3% of all proteins in human cells.³² Thus, cysteine is the most frequently probed amino acid for peptide enrichment and relative quantification purposes. Namely, the isotope-coded affinity tag (ICAT) reagents have been used to label the cysteine residues for quantification purposes.^{33, 34} Combined fractional diagonal chromatography (COFRADIC) has been used for the isolation of cysteinyl peptides.³⁵⁻³⁷ Concerning protein identification, the modification of cysteine residues by alkylation was shown to be a very useful tool for peptide mapping and database interrogation.^{38, 39} Any chemical labelling that gives the knowledge of the presence or absence of cysteine residues in peptides highly constrains the number of candidate proteins during the identification step.

In particular, the adducts formed by cysteinyl peptides with benzoquinone have been thoroughly characterized by Mason and Liebler, using ESI-MS.⁴⁰ The principle of the 1,4-Michael addition of benzoquinone on the cysteine residue was recently used in our laboratory,

to electrochemically label cysteinyl peptides during ESI-MS. This study showed that counting the cysteines in peptides gives additional information that results in dramatic increase in the level of confidence of protein identification by peptide mass fingerprinting (PMF).⁴¹

In this chapter, we present a methodology combining OFFGEL isoelectric focusing of peptides and chemical labeling by benzoquinone of cysteine residues in peptides as an effective means to improve the identification of proteins by peptide mass fingerprinting (PMF). In the first part, we emphasize the use of *pI* as validation/filtering tool for the peptides identified and its usefulness for the elimination of false-positive identifications, thus ensuring more accurate protein identification. In a second part, we describe the implementation of a simple workflow that includes OFFGEL fractionation to obtain the useful *pI* information, and the chemical labeling/counting of cysteines residues in peptides, giving additional information on the sequence of peptides, thus increasing the level of confidence in identification of proteins. The proof of concept of the methodology is demonstrated on a protein digest, and with some adjustments, the workflow could easily be applied to more complex digests.

2. Experimental

2.1 Chemicals

Bovine serum albumin (BSA) was purchased from Sigma-Aldrich (Dübendorf, Switzerland). Ammonium hydrogenocarbonate (> 98%), 1,4-dithio-DL-threitol (DTT, > 99.5%), 1,4-benzoquinone were from Fluka (Buchs, Switzerland). Porcine trypsin was from Promega (Madison, WI, USA). Formic acid and acetonitrile (> 99.5%, Fluka, Buchs, Switzerland), trifluoroacetic acid (TFA, 99%, Riedel de Haen, Darmstadt, Germany) were used without further purification. Synthetic peptides AIKCTKF, $M = 810.02 \text{ g}\cdot\text{mol}^{-1}$, ALRCTCS, $M = 752.90 \text{ g}\cdot\text{mol}^{-1}$, and ACKCTCM, $M = 758.98 \text{ g}\cdot\text{mol}^{-1}$ (> 70%) were prepared by Catherine Servis at the Institut de Biochimie (Faculté de Médecine, Epalinges, Switzerland). Deionized water ($18.5 \text{ M}\Omega\cdot\text{cm}$) was prepared using a Milli-Q system from Millipore (Bedford, MA, USA). Immobiline Drystrips, linear pH range 3–10 of 13 cm in length were purchased from GE Healthcare (Otelfingen, Switzerland), as well as IPG buffer pH 3–10 (carrier ampholytes mixtures). 2,5-dihydroxybenzoic acid (DHB, > 98%) for MALDI matrix was from Sigma.

2.2 Tryptic digestion

1 mg of BSA was dissolved in 1 mL ammonium hydrogenocarbonate solution (50 mM, pH 8), and 1.23 mg DTT (8 mM) and 10 μg trypsin (trypsin to protein ratio of 1:100 w/w) were added. The digestion was run at 37 °C for 4h. 10 % of formic acid was added to lower the pH of the medium and stop the digestion. The solution was then divided in two aliquots of 500 μL and stored at $-20 \text{ }^\circ\text{C}$, until used for the experiments.

2.3 OFFGEL IEF of peptides (OG-IEF)

OFFGEL IEF of peptides was performed with the apparatus and setup described in chapter IV. The multicompartiment device was placed on top of a 13 cm reswelled Immobiline Drystrip exhibiting a linear pH gradient over the range of pH 3–10. A platinum electrode was placed in each of the two extreme compartments (anode and cathode). The separation was performed by dispensing 50 μL of peptide solution in each well (total of 1 mL) and the potential was fixed during 1 h at 500 V, then 1 h at 1000 V, and finally 4 h at 5000 V. The current limit was set at 200 μA . After OG-IEF, liquid fractions were collected, and a supplementary step to enhance the protein yield was performed. For this purpose, 100 μL of a water/methanol/formic acid (49:50:1 by volume) was added per well and incubated for 60 min without voltage. Corresponding peptide fractions were pooled and lyophilized by vacuum centrifugation prior to further analysis.

2.4 Chemical tagging reaction

The collected vacuum-dried fractions of peptides were reconstituted in 25 μL of 0.1% TFA water. 5 μL of each fraction was modified by addition of 30% (v/v) of BQ reagent at 100 mM in acetonitrile. No incubation time was necessary for the reaction. The tagged mixture was immediately spotted on the MALDI plate, according to the procedure described below.

2.5 MALDI-TOF

Analysis was performed on a MALDI–TOF mass spectrometer (Shimadzu Biotech/Kratos). The sample was spotted on stainless Nickel plate with 1 μL of freshly prepared matrix solution. 2,5-dihydroxybenzoic acid (DHB) was used as matrix. Signals from 100 to 200 laser shots were summed per mass spectrum. Peptide masses were acquired over a range of m/z 500 to 5000.

2.6 LC-ESI-MS

The capillary HPLC system was an LC Packings (Dionex) Ultimate™ Plus, with a PepMap C18, 3 μm , 0.3 \times 150 mm capillary column and a pre-column. Sample volume injected was 1 μL (injection loop). The mobile phase consisted of solvents A (water/ACN 98:2 (v/v) with 0.1% (v/v) formic acid) and B (water/ACN 20:80 (v/v) with 0.085% (v/v) formic acid). The column was developed with a biphasic gradient from 2–50% of solvent B in 40 min, followed by an increase from 50–100% of B in 10 min. The column was regenerated with 3 column volumes of B followed by 3 volumes of A. Chromatography was run at a flow rate of 4 $\mu\text{L}/\text{min}$. MS analysis was conducted on an LCQ Duo ion trap from Finnigan (San Jose, CA, USA). All experiments were done in full scan mode (m/z 150–2000) without averaging, and the heated capillary was kept at 200°C.

2.7 Database search parameters

Searches were performed against Swiss-Prot database using MASCOT database search software.⁴² The following parameters were used for the search: oxidation of methionine, taxonomy Chordata, 1 missed tryptic cleavage was allowed. Charge states of +1, +2 and +3 were used for the results from ESI-Ion trap, and single charge state was used for the results from MALDI-TOF. The mass tolerance for peptide masses was set to 0.3 Da, respectively 0.15 Da, when ESI-Ion trap, respectively MALDI-TOF, was used.

3. Results and discussion

3.1 *pI* as validation information to eliminate false positive identifications

In this section, in order to show that the isoelectric point allows the validation of peptides identified and to describe the procedure used for the elimination of false positive peptides, the results from experiments of chapter IV are used (section IV.3 – OFFGEL of peptides). BSA was digested and the resulting peptides separated by OFFGEL fractionation into 20 liquid fractions. Each fraction was further analyzed by LC-ESI-MS. The entire list of peptides detected was submitted to Mascot peptide mass fingerprinting,⁴² for a search in the Swiss-Prot database. The search engine then identified the protein based on the peptides mass and indicates the score obtained (oppositely related to the probability that the protein match occurs at random) and the sequence coverage, as well as the list of peptides identified.

An in-house program was used to calculate theoretical *pI* values according to computing algorithms with the *pKa* values set from Bjellqvist *et al.*⁴³ The experimental *pI* value of each fraction of peptides was calculated by averaging the *pI* values of the peptides in a fraction, knowing their sequence. For wells where there are no or not enough peptides identified to calculate a mean *pI* value, the theoretical mean *pH* value was taken, and a rather large but reasonable *pI* tolerance window of ± 0.675 was taken (which corresponds to the *pH* difference between two wells, from one end of the first well to the other end of the second well).

The prediction of *pI* values allows validating the peptides identified. Indeed, from the peptides identified in a fraction, an average fraction *pH* value can be calculated as well as the standard deviation (Stdev). These values allow setting a tolerance window and eliminating peptides deviating too far from the average value, thus considering these peptides as false-

positive. In the present case, pI filtering was performed using one to two pI Stdev boundaries, as shown in Table 1. Narrow ranges are defined as the pH window set with ± 1 Stdev, middle ranges are defined with a window of ± 1.5 Stdev, and wide ranges are defined with a window of ± 2 Stdev.

Table 1: Experimentally measured and theoretically calculated pI values in each of the 20 OG fractions.

Fractions	pI_{exp}^a	pI_{calc}^b	Stdev	narrow range ^c (1 σ)	middle range ^d (1.5 σ)	wide range ^e (2 σ)	Npep (eliminated after 1 σ / 1.5 σ / 2 σ)
1	2.47	3.15	-	-	-	-	0
2	3.30	4.07	-	-	-	-	1
3	3.65	4.24	0.12	4.12 – 4.36	4,06 – 4,43	3,99 – 4,49	2
4	4.08	5.43	2.33	3.09 – 7.76	1,93 – 8,93	0,76 – 10,09	8 (1/1/1)
5	4.46	5.37	1.90	3.47 – 7.27	2,52 – 8,22	1,57 – 9,17	4 (1/1/0)
6	4.87	4.49	0.09	4.41 – 4.58	4,37 – 4,63	4,32 – 4,67	4
7	5.21	4.60	0.1	4.50 – 4.70	4,45 – 4,75	4,40 – 4,79	2
8	5.61	6.44	2.01	4.43 – 8.44	3,43 – 9,45	2,43 – 10,45	5 (1/1/0)
9	5.94	5.83	0.28	5.55 – 6.11	5,41 – 6,26	5,27 – 6,39	10
10	6.22	6.68	1.33	5.35 – 8.02	4,69 – 8,69	4,02 – 9,35	3 (1/0/0)
11	6.47	6.46	0.41	6.05 – 6.87	5,84 – 7,07	5,63 – 7,28	2
12	6.76	7.03	-	-	-	-	0
13	7.00	7.38	-	-	-	-	0
14	7.24	7.73	-	-	-	-	0
15	7.56	8.08	-	-	-	-	0
16	7.76	8.43	-	-	-	-	0
17	8.14	8.48	0.37	8.11 – 8.86	7,93 – 9,04	7,74 – 9,23	2
18	8.63	8.32	2.16	6.16 – 10.48	5,07 – 11,56	3,99 – 12,65	7 (3/1/0)
19	8.98	9.49	-	-	-	-	0
20	10.27	9.87	0.18	9.71 – 10.05	9,61 – 10,14	9,52 – 10,23	2

^a Measured pH value in each OG well. ^b Calculated by averaging pI values of all peptides found in the fraction. ^c pH interval calculated from the mean pI of identified peptides in each OG fraction ± 1 Stdev. ^d pH interval calculated from the mean pI of identified peptides in each OG fraction ± 1.5 Stdev. ^e pH interval calculated from the mean pI of identified peptides in each OG fraction ± 2 Stdev.

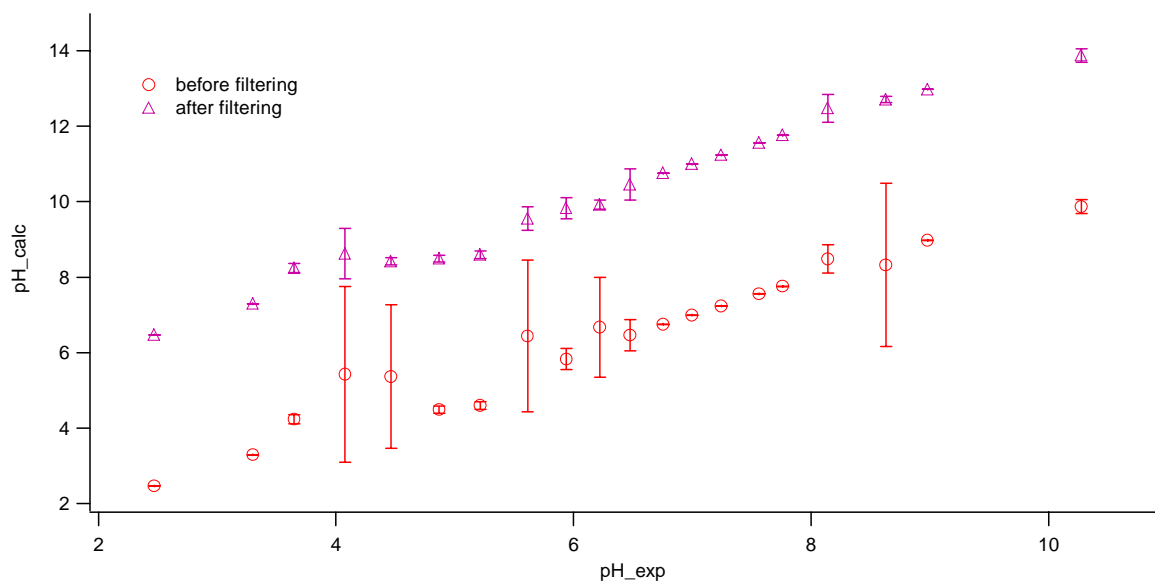


Figure 2: mean pI values (with standard deviations) calculated from averaging peptides pI in the fractions versus pI values experimentally measured. The mean pI values have been calculated before (circles) and after (triangles) pI filtering using a narrow tolerance window. For reasons of display, the two curves are offset by 4 pH units.

Figure 2 is the plot of calculated pI values versus measured pI values. It clearly illustrates that, before filtering (circles), some fractions show abnormally high values of standard deviation, namely the fractions 4, 5, 8, 10 and 18. For these fractions, narrow, middle and wide ranges of pI were used to filter out the potential false positive identifications.

Table 2 shows in details the peptides identified in fraction 4, with the corresponding retention times. The mean value for the fraction pH was calculated to be 5.43 with a standard deviation of 2.33. The relatively high value of standard deviation for this fraction indicates the possible presence of false positive. Indeed, in that fraction, a peptide was discarded, considering any tolerance window (± 1 Stdev or ± 2 Stdev). The pH calculated after elimination of the false peptide is 4.43, and the standard deviation 0.66. The standard deviation is lowered when discarding the suspicious peptides, as shown in Table 3 and in Figure 2 (triangles).

Table 2: Peptides identified in OG fraction 4 (pH calculated 5.43). Existence of a false-positive: pH calculated 4.63 after discarding the false peptide

RT (min)	Sequence	Molecular weight (Da)	pI_theo ^a
17,87	YICDNQDTISSK	1386,4	4,21
21,99	DDPHACYSTVFDK	1497,5	4,65
22,76	ADEKK	590,8	6,07
22,76	EYEATLEECCA	1388,3	4,33
24,14	SLGKVGTR	817,3	11,00
24,14	YNGVFQECCQAEDK	1633,3	4,14
30,64	DAFLGSFLYEYSR	1567,5	4,67
34,32	TVMENFVAFVDK	1399,4	4,37

^apI calculated with pK_a set from Bjellqvist *et al.*⁴³

Table 3: Experimentally measured and theoretically calculated pI values before and after filtering, in the “suspicious” OG fractions.

Fractions	pI_exp	pI_calc	Stdev	pI_calc after filtering with 1σ	Stdev	Npеп (eliminated after 1σ)
4	4.08	5.43	2.33	4.63	0.66	8 (1)
5	4.46	5.37	1.90	4.42	0.09	4 (1)
8	5.61	6.44	2.01	5.55	0.31	5 (1)
10	6.22	6.68	1.33	5.92	0.12	3 (1)
18	8.63	8.32	2.16	8.71	0.08	7 (3)

With narrow range (± 1 Stdev), a total of 7 peptides could be eliminated as false positive identifications considering all the fractions. With wide range (± 2 Stdev), only one peptide was eliminated, and with middle range (± 1.5 Stdev), 4 peptides were eliminated. A ± 1 pI Stdev filter results in better data quality than the ± 2 pI Stdev filter, but there are most probably higher risks of losing true positive identifications with a too narrow filter, this should be confirmed by further MS/MS data on the “uncertain” peptides.

In this way, when considering a tolerance window of ± 1 Stdev, a total of seven peptides were eliminated, over a number of 44 peptides matched, representing 16% of matched peptides. After pI validation/filtering, Mascot PMF of the peptide masses from LC-MS allowed the identification of BSA with a score of 139 (versus 147 before pI validation)

with sequence coverage of 54% (versus 56% before pI validation). The level of confidence decreases due to the lower sequence coverage. However, the identification is more correct due to the elimination of deviating false positive peptides. As a summary, Figure 3 shows the distribution of peptides before and after pI filtering, compared to the predicted distribution.

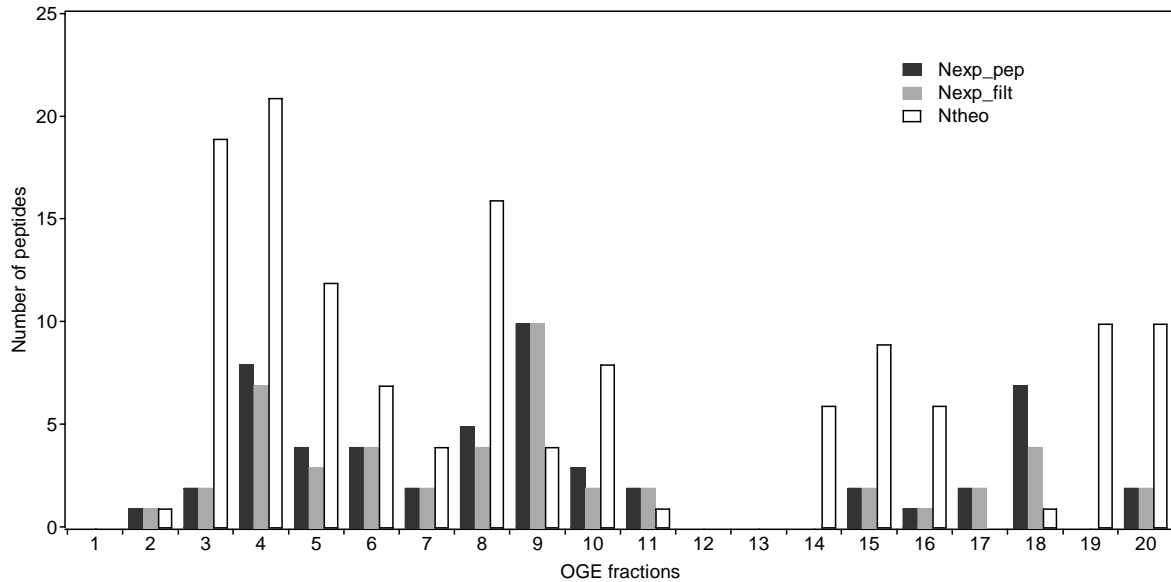


Figure 3: Peptide distribution from experimental results and theoretical predictions.

This study shows that the pI is a powerful tool allowing more correct identifications. The algorithm for pI prediction is quite useful in this task. The number of peptides eliminated depends on the tolerance window set for the validation. These considerations reflect the need to accept a certain error tolerance in order not to discard true positives. However, by applying more than one acceptance criteria, it becomes less likely that falsely identified peptides would pass all the filters and the choice of larger tolerance windows can be accepted.

3.2 Counting cysteines for enhanced protein identification by PMF

Workflow combining OFFGEL IEF and chemical tagging

In this section, to simultaneously use the information on the isoelectric point for data validation/filtering and the composition in cysteines of peptides to increase the confidence of identifications, a simple workflow, as described in Figure 4, was used.

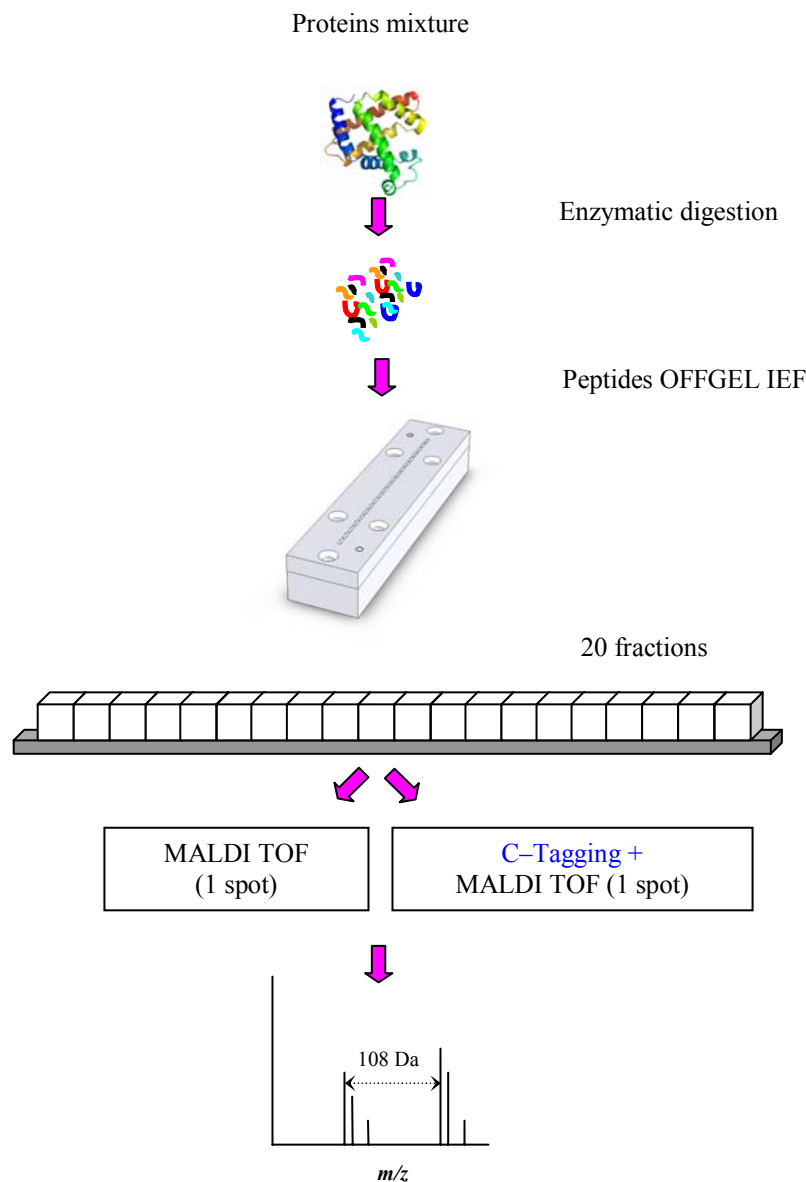


Figure 4: Workflow combining OFFGEL IEF with chemical tagging of cysteines in peptides.

First, proteins are digested with trypsin, according to the protocol, and the resulting peptides are then separated by OFFGEL IEF, giving twenty liquid fractions. Finally, each of

the fractions is divided in two volumes, one is directly submitted to MALDI-TOF analysis, and the other is tagged, by addition of the benzoquinone reagent, and then also submitted to MALDI-TOF analysis. Thus, on the MALDI plate, each fraction corresponds to two spots, one without tagging and one with tagging. A differential analysis later allows determining which peptides contain cysteine residues, and the number of these residues. This workflow is fast for simple protein mixtures, but as the complexity of the mixture increases, an intermediate step of LC separation just before the MALDI-TOF would be necessary.

Chemical tagging of cysteine residues by benzoquinone in synthetic peptides

The choice of the tagging reagent is based on previous results concerning the tagging of cysteines by benzoquinone reagents.⁴⁴ The addition of benzoquinone onto the cysteine residue proceeds through a 1,4-Michael addition (Figure 5) and the benzoquinone-peptide adducts have been thoroughly characterized by Mason and Liebler.⁴⁰ The study of several benzoquinone derivatives showed that 1,4-benzoquinone, one of the most stable benzoquinone, guarantees quantitative reactivity and 100% selectivity for cysteine residues in acidic medium. Other reagents either reacted incompletely or not selectively with groups other than thiols.⁴⁴

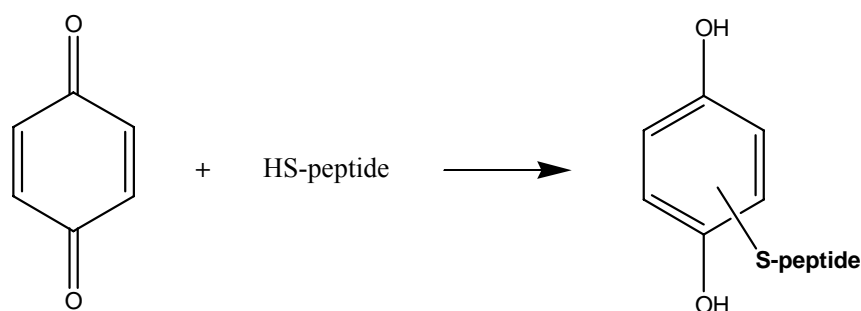


Figure 5: Reaction of 1,4-benzoquinone with peptide cysteinyl thiols to form S-cysteinyloxybenzoquinol adducts.

To test the applicability of the tagging reaction on tryptic peptides, 1,4-benzoquinone was first tested on synthetic peptides containing one, two and three cysteines. The reagent was added to the peptide dissolved in the digestion medium, and two spots were deposited on the MALDI plate, one for the untagged peptide and the other for the tagged peptide. The results for the peptides containing one cysteine (AIKCTKF, $M = 810.02 \text{ g}\cdot\text{mol}^{-1}$) and three cysteine residues (ACKCTCM, $M = 758.98 \text{ g}\cdot\text{mol}^{-1}$) are shown on Figure 6, illustrating that up to three cysteines can be tagged and detected in MALDI MS.

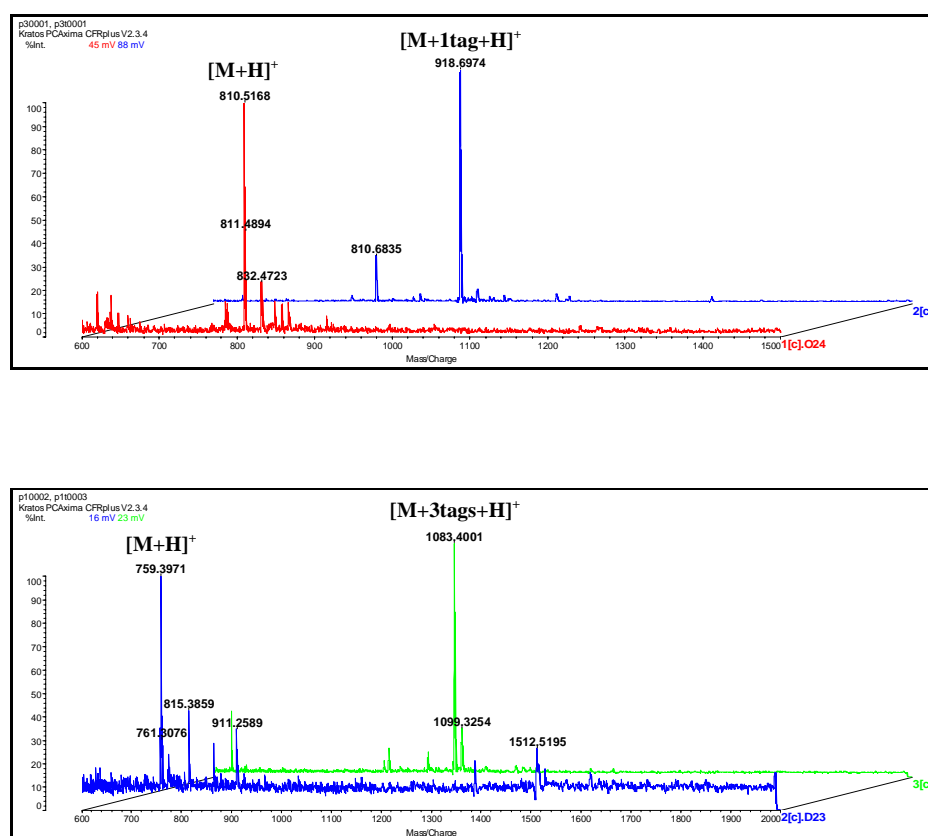


Figure 6: MALDI mass spectra of peptide AIKCTKF (panel A) and peptide ACKCTCM (panel B) with their respective adducts formed by the addition of 1,4-benzoquinone. The mass spectra of the tagged peptides and the peptide before tagging are displayed on the same spectrum, but shifted, for presentation reasons.

Application to enhanced peptide mass fingerprinting of a protein digest

To show that the chemical tagging can be applied to tryptic peptides and the additional information can be used to increase the level of confidence in peptide mass fingerprinting, a tryptic digestion of BSA was performed and fractionated by OFFGEL IEF, according to the workflow in Figure 6, then tagged and analyzed by MALDI MS.

Figure 7 shows a MALDI spectrum of the unfractionated tryptic digest of BSA. Due to the differences of ionization efficiency, not all the peptides can be observed in one spectrum. The unfractionated tryptic digest allowed identification of the BSA but with low sequence coverage only (20%). The sequence coverage is thus not high enough to assure a high level of confidence in the identification. A preliminary separation step, such as OFFGEL IEF, would allow decreasing the differences of ionization efficiency.

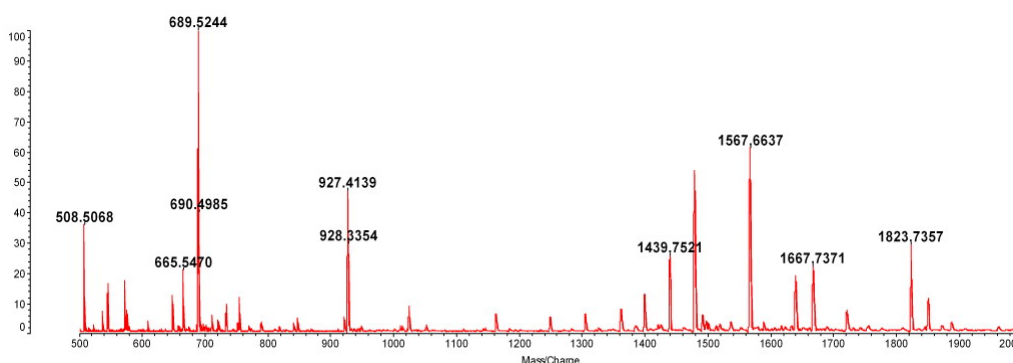


Figure 7: MALDI mass spectrum of the tryptic digest of BSA before OFFGEL fractionation.

Figure 8 displays the MALDI spectra before and after tagging, for OFFGEL fractions 3 and 5. It illustrates the tagging efficiency even in complex mixture (mixture of digestion) containing salts and carrier ampholytes. The low concentration of carrier ampholytes (0.5%) obviously does not disturb the chemical tagging process, as well as the MALDI detection, proving that MALDI is appropriate and has a higher tolerance according to contaminants than ESI-MS for example. The reactivity and quantity of benzoquinone are enough to tag multiple cysteinyl peptides in one fraction, and up to two cysteines in one peptide, as observed in fraction 3. The tagging of other residues than cysteines was not observed.

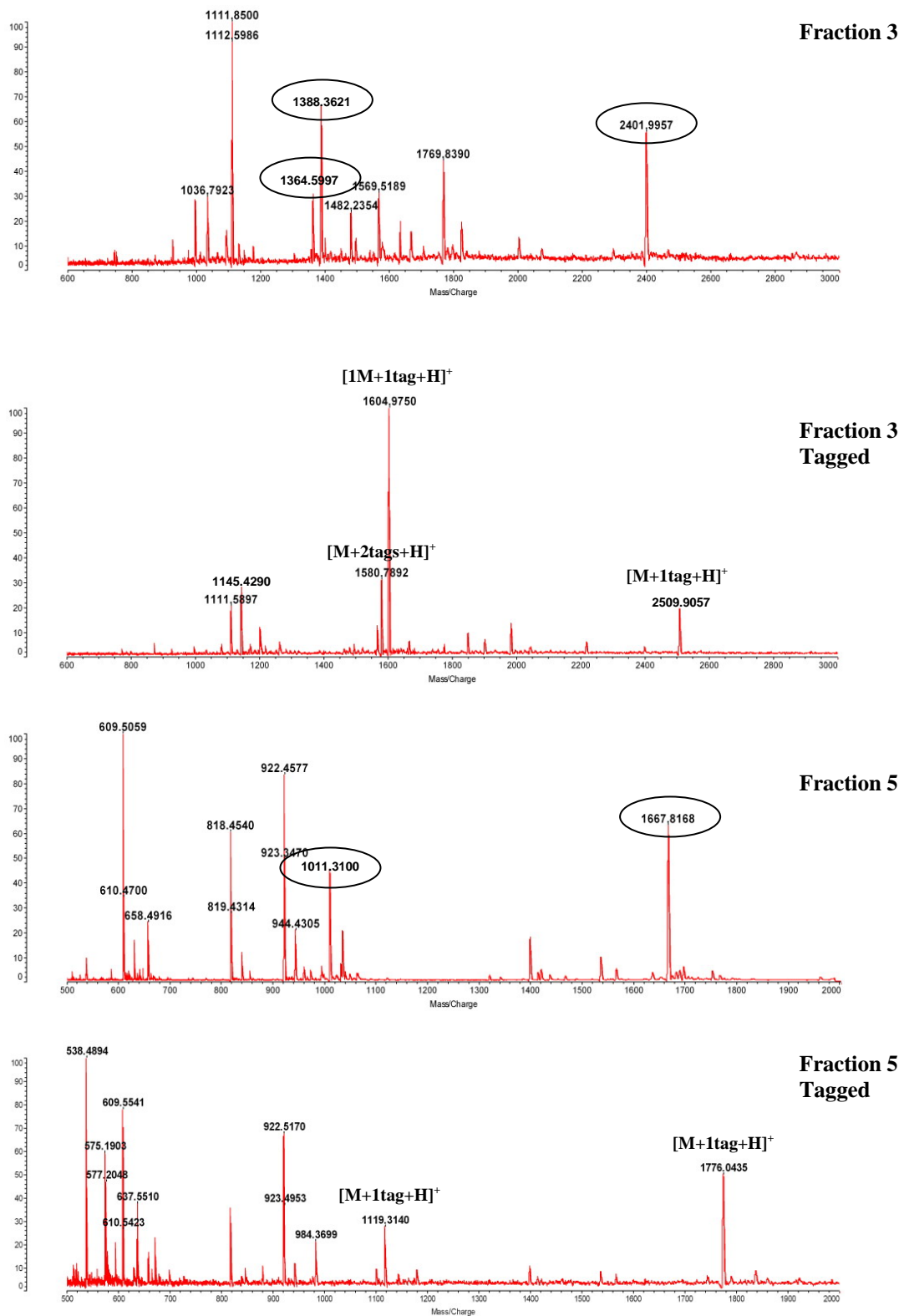


Figure 8: MALDI mass spectra of OFFGEL fractions, before and after tagging of cysteines by the addition of 1,4-benzoquinone. Circled masses are cysteinyl peptides, which are shifted after the tagging. The number of tags is indicated in brackets on the tagged mass spectra.

Figure 9 shows a diagonal representation of the tagging of cysteines, representing the masses observed after cysteine tagging versus the masses before tagging. Peptides containing one or more cysteine residues are not located on the main diagonal, but on parallel lines shifted of 108 Da vertically, and corresponding to one cysteine (1C line), two cysteines (2C line), etc. This diagonal representation offers a rapid overview: all the peptides that are not on the diagonal are tagged, thus contain cysteine residues.

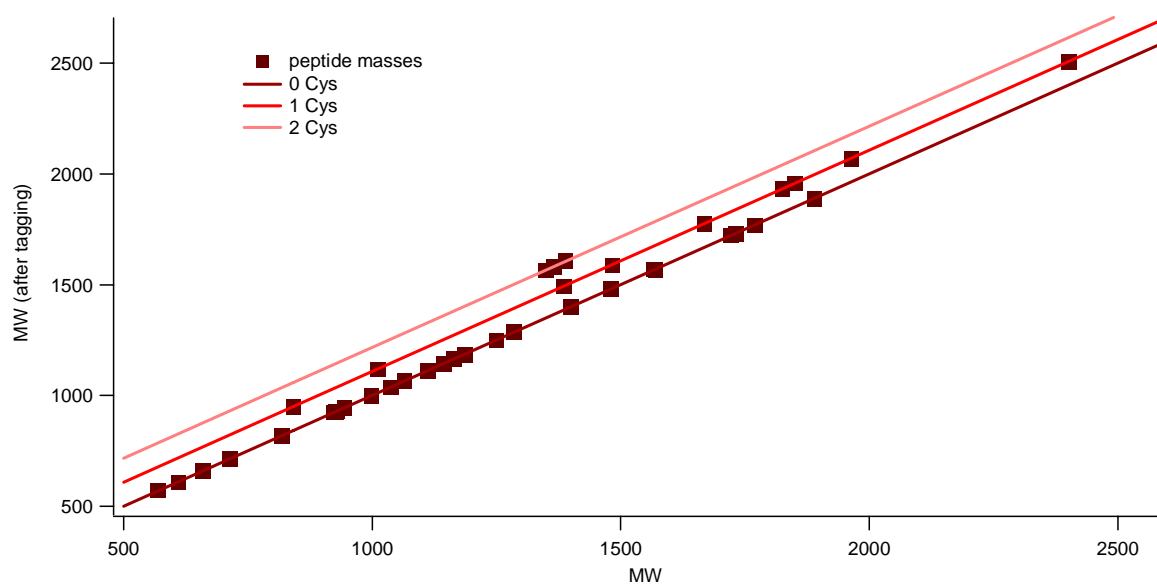


Figure 9: Diagram showing peptide masses observed after cysteine tagging vs. peptide masses observed before tagging. Peptides containing one or more cysteine residues are not on the diagonal, but on parallel lines shifted of 108 Da vertically and corresponding to one cysteine (1C line) and two cysteines (2C line). This type of diagram offers a rapid overview of the presence of cysteine-containing peptides.

The validation and filtering of peptides based on predicted pI values is done in the same way as described in the previous section (3.1). Unfortunately (or fortunately!), even with a narrow pI tolerance window of ± 1 Stdev, only one peptide was eliminated, which was identified in fraction 3. Obviously, the data generated from MALDI are less numerous than the data from LC-MS on such a simple digest, the risk of identifying a false positive here is thus reduced. In addition, the mass accuracies are different (higher mass accuracy for

MALDI-TOF), which may explain the low error level. The elimination of false positive would be more obvious and relevant on a more complex mixture, generating more true and false peptides. However, the aim was rather to show a proof of concept for the workflow allowing the use of additional information: the *pI* as validation tool and the determination of the number of cysteines for higher confidence in identification.

So, the entire list of peptides was submitted to Mascot sequence query for a search in the Swiss-Prot database. Without specifying the information on the cysteine content, BSA was identified with a score of 166 (157 after *pI* filtering) and sequence coverage of 32% (31% after *pI* filtering). These scores are slightly higher than in the case of LC-ESI-MS (cf. section 3.1), probably due to the fact that in LC-ESI-MS, there are more contaminants, even though more peptides are recovered, and it was observed that the presence of contaminants can decrease the score significantly. When the information on the cysteine content gathered by the tagging of peptides was added, the score increased to 247 (237 if *pI* filtering). This is illustrated on Figure 10. When only the 12 tagged peptides were entered with their cysteine content, the score was 217 with 19% coverage (9 peptides found), proving that the cysteine information is a powerful data, enhancing the level of confidence in the identification. This also shows that chemical tagging of peptides, coupled to OFFGEL IEF, would allow the selection and isolation of cysteinyl peptides, which is of high interest in bioanalytics.

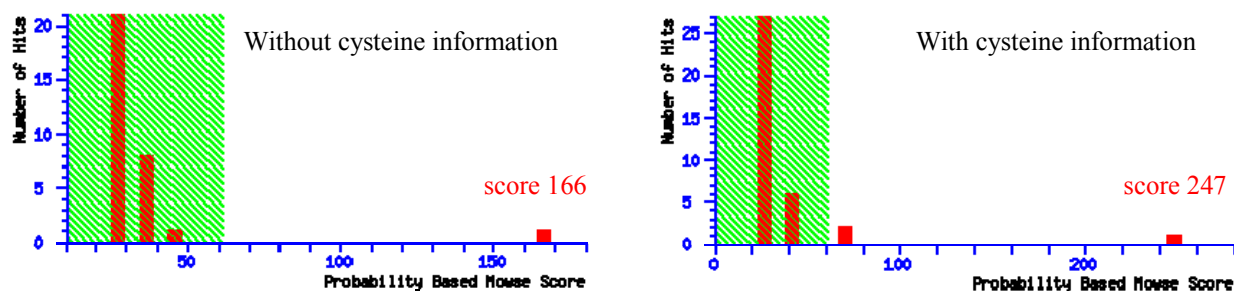


Figure 10: Identification scores without and with cysteine information obtained by chemical tagging for BSA using Mascot search engine.

The analysis of cysteinyl peptides by chemical tagging and MALDI-MS was done as further development of previous work performed in the lab on electrochemical tagging of cysteines, and in the perspective of using the new matrix for MALDI-MS recently developed in the lab. The new type of matrix for MALDI-MS analysis is constituted of a TiO_2 gel and was demonstrated to allow an efficient ionization and labeling of cysteinyl peptides by photo-oxidation of hydroquinone probes.⁴⁵ Figure 11 illustrates the photo-reactive matrix and the principle of on-plate tagging of cysteines. Further work in that direction would be to include that matrix in the workflow presented in this chapter. Especially when an additional step of LC would be necessary for more complex samples, a spotter can directly deposit the OFFGEL fractions separated by LC, on the TiO_2 MALDI matrix already containing hydroquinone, thus allowing an online and automated workflow, with minimal sample consumption.

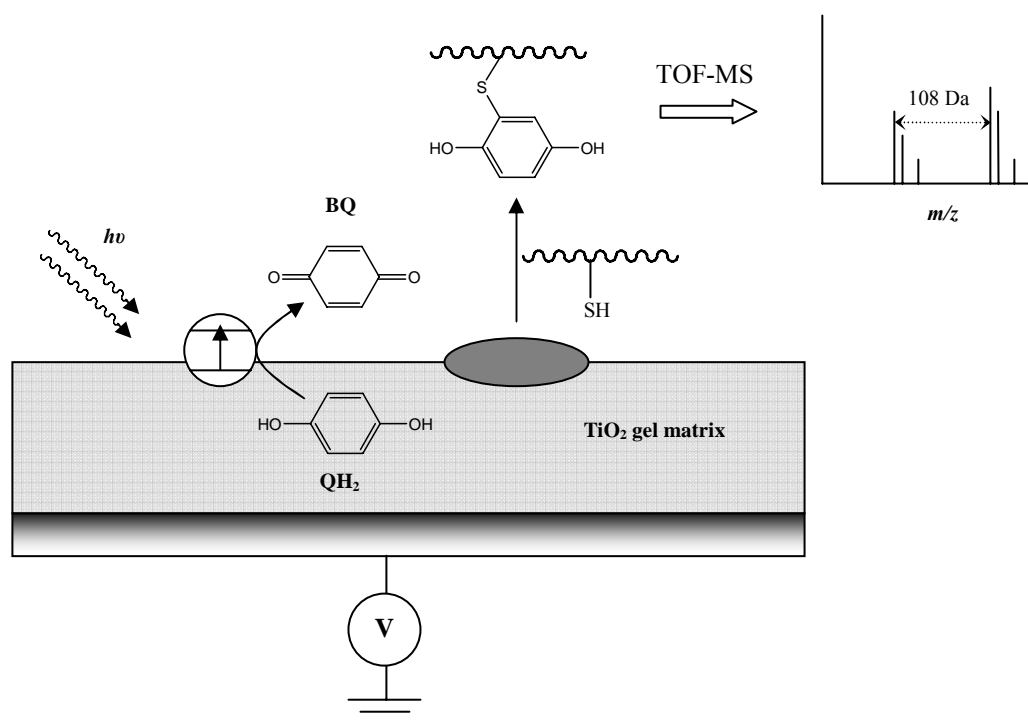


Figure 11: Schematic representation of a photo-reactive MALDI plate. The incorporation of TiO_2 nanoparticles in MALDI matrices allows photo-electrochemical redox reactions of molecules in a sample, namely the oxidation of hydroquinone to benzoquinone. The latter then reacts with the cysteine residues selectively.

In parallel, another possible workflow is being explored, that includes ESI-MS and microspray emitters for online (electro-) chemical tagging of cysteines, as has been shown previously.⁴⁴ By performing OFFGEL IEF of peptides, then coupling LC to a chip-MS and performing chemical tagging (Figure 12), there is the possibility to analyze complex samples and get the information on the pI as well as the number of cysteine residues.

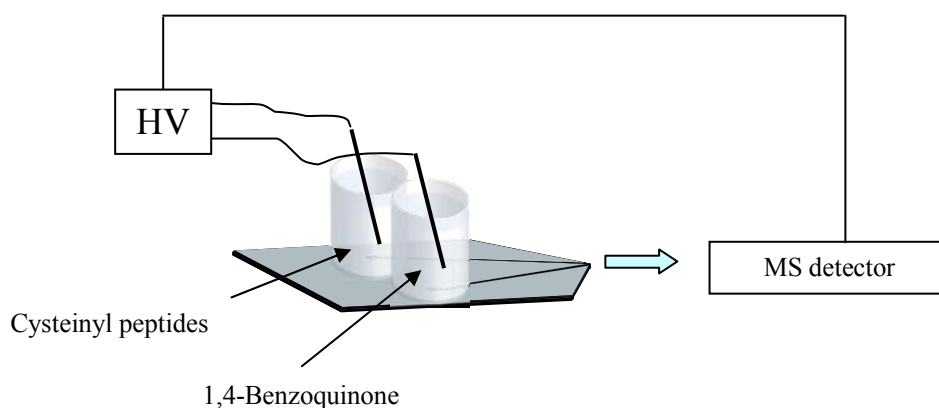


Figure 12: Schematic representation of a dual channel microsprayer allowing the chemical tagging of cysteine residue in a peptide.

The challenge of this workflow would be the multiply charged peaks inherent to electrospray ionization: as the complexity of the sample increases, the complexity of the tagging spectra will increase as well, which is not the case for MALDI spectra (singly charged peaks). A summary of both approaches is given in Figure 13.

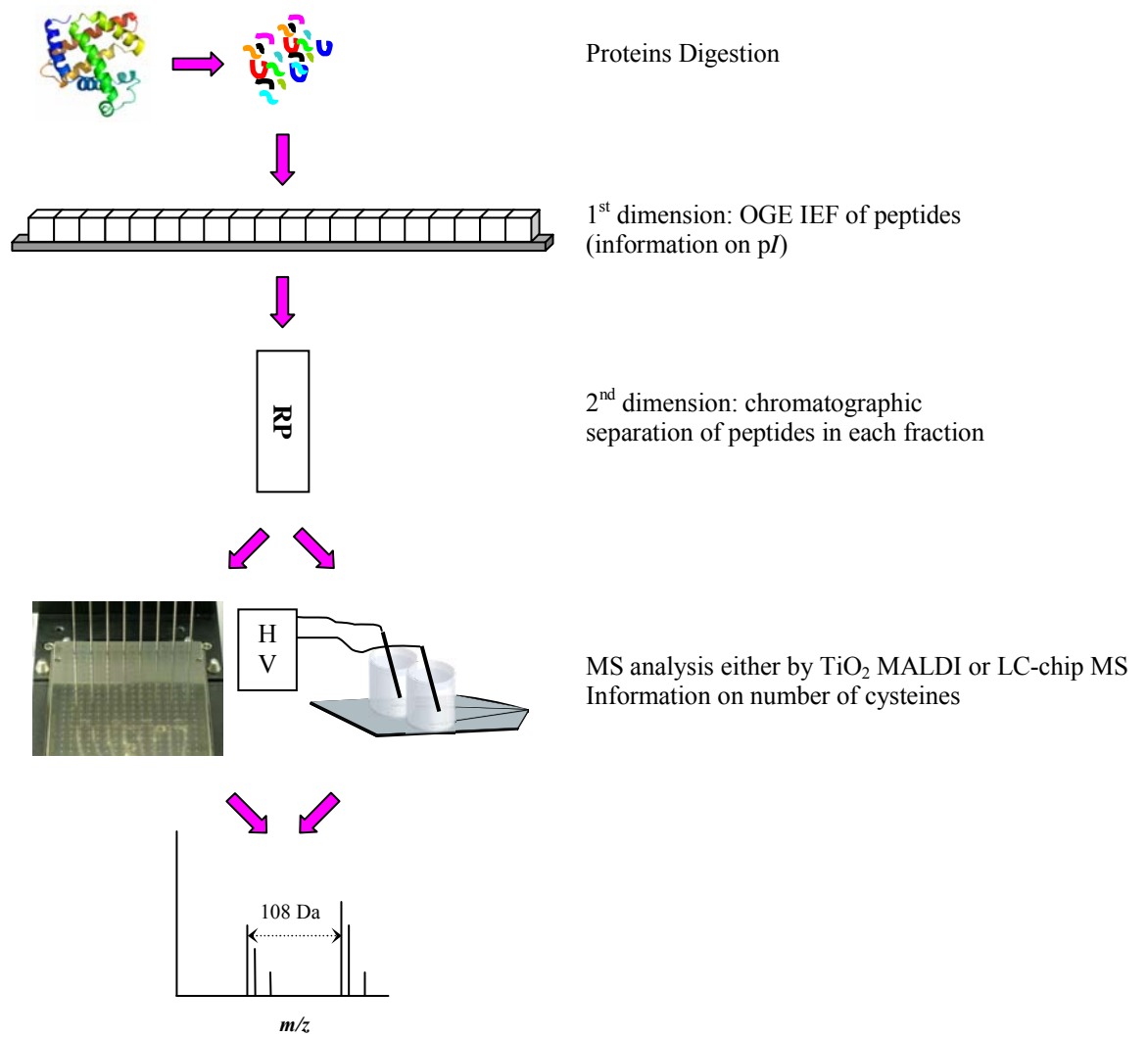


Figure 13: Workflow for a two dimensional strategy to analyze complex protein mixtures.

4. Concluding remarks

In the present chapter, the use of OFFGEL IEF to validate peptides identified by mass spectrometry and eliminate false positive identifications was first shown. The elimination of false-positive identifications leads to a decrease in the score, but allows more accurate identifications. This study demonstrates that the *pI* is a potentially very powerful tool adding significance to the identification process. The number of peptides eliminated depends on the tolerance window set for the validation. The question of the definition of the *pI* tolerance window is crucial, in order not to eliminate true-positive during filtering. However, by applying more than one acceptance criteria, it becomes less likely that falsely identified peptides would pass all the filters and the choice of larger tolerance windows can be accepted.

The approach was then adapted in order to combine the use of OFFGEL IEF and chemical tagging of cysteine residues. This labeling step gives the information on the number of cysteine residues, which can be used in the database interrogation, and was shown to enhance the level of confidence in protein identification (increase of the score). The chemical labeling is a fast and selective step. The advantage of MALDI analysis is also that only small amounts of sample are needed. With the development of TiO₂ matrices mentioned earlier, as well as the use of a MALDI spotter, allowing the direct online deposition and tagging, high-throughput analyses could be envisaged. This study opens wide perspectives for the analysis of more complex biological mixtures, though more complex mixtures need to be studied to strongly validate this approach.

5. References

1. Henzel, W. J.; Billeci, T. M.; Stults, J. T.; Wong, S. C.; Grimley, C.; Watanabe, C., Identifying Proteins from 2-Dimensional Gels by Molecular Mass Searching of Peptide-Fragments in Protein-Sequence Databases. *Proceedings of the National Academy of Sciences of the United States of America* **1993**, 90, (11), 5011-5015.
2. Mann, M.; Hojrup, P.; Roepstorff, P., Use of Mass-Spectrometric Molecular-Weight Information to Identify Proteins in Sequence Databases. *Biological Mass Spectrometry* **1993**, 22, (6), 338-345.
3. Pappin, D. J. C.; Hojrup, P.; Bleasby, A. J., Rapid Identification of Proteins by Peptide-Mass Fingerprinting. *Current Biology* **1993**, 3, (6), 327-332.
4. Yates, J. R.; Speicher, S.; Griffin, P. R.; Hunkapiller, T., Peptide Mass Maps - a Highly Informative Approach to Protein Identification. *Analytical Biochemistry* **1993**, 214, (2), 397-408.
5. James, P.; Quadroni, M.; Carafoli, E.; Gonnet, G., Protein Identification by Mass Profile Fingerprinting. *Biochemical and Biophysical Research Communications* **1993**, 195, (1), 58-64.
6. Patterson, S. D., From Electrophoretically Separated Protein to Identification - Strategies for Sequence and Mass Analysis. *Analytical Biochemistry* **1994**, 221, (1), 1-15.
7. Patterson, S. D.; Aebersold, R., Mass-Spectrometric Approaches for the Identification of Gel-Separated Proteins. *Electrophoresis* **1995**, 16, (10), 1791-1814.
8. Yates, J. R., Mass spectrometry and the age of the proteome. *Journal of Mass Spectrometry* **1998**, 33, (1), 1-19.
9. Wolters, D. A.; Washburn, M. P.; Yates, J. R., An automated multidimensional protein identification technology for shotgun proteomics. *Analytical Chemistry* **2001**, 73, (23), 5683-5690.
10. Qian, W. J.; Jacobs, J. M.; Liu, T.; Camp, D. G.; Smith, R. D., Advances and challenges in liquid chromatography-mass spectrometry-based proteomics profiling for clinical applications. *Molecular & Cellular Proteomics* **2006**, 5, (10), 1727-1744.
11. Conrads, T. P.; Anderson, G. A.; Veenstra, T. D.; Pasa-Tolic, L.; Smith, R. D., Utility of accurate mass tags for proteome-wide protein identification. *Analytical Chemistry* **2000**, 72, (14), 3349-3354.
12. Smith, R. D.; Pasa-Tolic, L.; Lipton, M. S.; Jensen, P. K.; Anderson, G. A.; Shen, Y. F.; Conrads, T. P.; Udseth, H. R.; Harkewicz, R.; Belov, M. E.; Masselon, C.; Veenstra, T. D., Rapid quantitative measurements of proteomes by Fourier transform ion cyclotron resonance mass spectrometry. *Electrophoresis* **2001**, 22, (9), 1652-1668.
13. Smith, R. D.; Anderson, G. A.; Lipton, M. S.; Pasa-Tolic, L.; Shen, Y. F.; Conrads, T. P.; Veenstra, T. D.; Udseth, H. R., An accurate mass tag strategy for quantitative and high-throughput proteome measurements. *Proteomics* **2002**, 2, (5), 513-523.
14. Lipton, M. S.; Pasa-Tolic, L.; Anderson, G. A.; Anderson, D. J.; Auberry, D. L.; Battista, K. R.; Daly, M. J.; Fredrickson, J.; Hixson, K. K.; Kostandarthes, H.; Masselon, C.; Markillie, L. M.; Moore, R. J.; Romine, M. F.; Shen, Y. F.; Stritmatter, E.; Tolic, N.; Udseth, H. R.; Venkateswaran, A.; Wong, L. K.; Zhao, R.; Smith, R. D., Global analysis of the *Deinococcus radiodurans* proteome by using accurate mass tags. *Proceedings of the National Academy of Sciences of the United States of America* **2002**, 99, (17), 11049-11054.

15. Olsen, J. V.; Mann, M., Improved peptide identification in proteomics by two consecutive stages of mass spectrometric fragmentation. *Proceedings of the National Academy of Sciences of the United States of America* **2004**, 101, (37), 13417-13422.
16. Petritis, K.; Kangas, L. J.; Ferguson, P. L.; Anderson, G. A.; Pasa-Tolic, L.; Lipton, M. S.; Auberry, K. J.; Strittmatter, E. F.; Shen, Y. F.; Zhao, R.; Smith, R. D., Use of artificial neural networks for the accurate prediction of peptide liquid chromatography elution times in proteome analyses. *Analytical Chemistry* **2003**, 75, (5), 1039-1048.
17. Palmblad, M.; Ramstrom, M.; Markides, K. E.; Hakansson, P.; Bergquist, J., Prediction of chromatographic retention and protein identification in liquid chromatography/mass spectrometry. *Analytical Chemistry* **2002**, 74, (22), 5826-5830.
18. Shen, Y. F.; Zhao, R.; Belov, M. E.; Conrads, T. P.; Anderson, G. A.; Tang, K. Q.; Pasa-Tolic, L.; Veenstra, T. D.; Lipton, M. S.; Udseth, H. R.; Smith, R. D., Packed capillary reversed-phase liquid chromatography with high-performance electrospray ionization Fourier transform ion cyclotron resonance mass spectrometry for proteomics. *Analytical Chemistry* **2001**, 73, (8), 1766-1775.
19. Qian, W. J.; Monroe, M. E.; Liu, T.; Jacobs, J. M.; Anderson, G. A.; Shen, Y. F.; Moore, R. J.; Anderson, D. J.; Zhang, R.; Calvano, S. E.; Lowry, S. F.; Xiao, W. Z.; Moldawer, L. L.; Davis, R. W.; Tompkins, R. G.; Camp, D. G.; Smith, R. D.; Injury, I. H. R.; , Quantitative proteome analysis of human plasma following in vivo lipopolysaccharide administration using O-16/O-18 labeling and the accurate mass and time tag approach. *Molecular & Cellular Proteomics* **2005**, 4, (5), 700-709.
20. Zimmer, J. S. D.; Monroe, M. E.; Qian, W. J.; Smith, R. D., Advances in proteomics data analysis and display using an accurate mass and time tag approach. *Mass Spectrometry Reviews* **2006**, 25, (3), 450-482.
21. Cargile, B. J., Potential for false positive identifications from large databases through tandem mass spectrometry. *Journal of Proteome Research* **2004**, 3, (5), 1082-1085.
22. Cargile, B. J., Immobilized pH gradients as a first dimension in shotgun proteomics and analysis of the accuracy of pI predictability of peptides. *Electrophoresis* **2004**, 25, (6), 936-945.
23. Cargile, B. J., Gel based isoelectric focusing of peptides and the utility of isoelectric point in protein identification. *Journal of Proteome Research* **2004**, 3, (1), 112-119.
24. Krijgsveld, J.; Gauci, S.; Dormeyer, W.; Heck, A. J. R., In-gel isoelectric focusing of peptides as a tool for improved protein identification. *Journal of Proteome Research* **2006**, 5, (7), 1721-1730.
25. Xie, H. W.; Bandhakavi, S.; Griffin, T. J., Evaluating preparative isoelectric focusing of complex peptide mixtures for tandem mass spectrometry-based proteomics: A case study in profiling chromatin-enriched subcellular fractions in *Saccharomyces cerevisiae*. *Analytical Chemistry* **2005**, 77, (10), 3198-3207.
26. Xie, H. W.; Rhodus, N. L.; Griffin, R. J.; Carlis, J. V.; Griffin, T. J., A catalogue of human saliva proteins identified by free flow electrophoresis-based peptide separation and tandem mass spectrometry. *Molecular & Cellular Proteomics* **2005**, 4, (11), 1826-1830.
27. Xie, H. W.; Griffin, T. J., Trade-off between high sensitivity and increased potential for false positive peptide sequence matches using a two-dimensional linear ion trap for tandem mass spectrometry-based proteomics. *Journal of Proteome Research* **2006**, 5, (4), 1003-1009.
28. An, Y. M.; Fu, Z. M.; Gutierrez, P.; Fenselau, C., Solution isoelectric focusing for peptide analysis: Comparative investigation of an insoluble nuclear protein fraction. *Journal of Proteome Research* **2005**, 4, (6), 2126-2132.

29. Heller, M., Added value for tandem mass spectrometry shotgun proteomics data validation through isoelectric focusing of peptides. *Journal of Proteome Research* **2005**, *4*, (6), 2273-2282.
30. Horth, P.; Miller, C. A.; Preckel, T.; Wenz, C., Efficient fractionation and improved protein identification by peptide OFFGEL electrophoresis. *Molecular & Cellular Proteomics* **2006**, *5*, (10), 1968-1974.
31. Leitner, A.; Lindner, W., Chemistry meets proteomics: The use of chemical tagging reactions for MS-based proteomics. *Proteomics* **2006**, *6*, (20), 5418-5434.
32. Regnier, F. E.; Riggs, L.; Zhang, R. J.; Xiong, L.; Liu, P. R.; Chakraborty, A.; Seeley, E.; Sioma, C.; Thompson, R. A., Comparative proteomics based on stable isotope labeling and affinity selection. *Journal of Mass Spectrometry* **2002**, *37*, (2), 133-145.
33. Gygi, S. P.; Rist, B.; Gerber, S. A.; Turecek, F.; Gelb, M. H.; Aebersold, R., Quantitative analysis of complex protein mixtures using isotope-coded affinity tags. *Nature Biotechnology* **1999**, *17*, (10), 994-999.
34. Schmidt, F.; Donahoe, S.; Hagens, K.; Mattow, J.; Schaible, U. E.; Kaufmann, S. H. E.; Aebersold, R.; Jungblut, P. R., Complementary analysis of the Mycobacterium tuberculosis proteome by two-dimensional electrophoresis and isotope-coded affinity tag technology. *Molecular & Cellular Proteomics* **2004**, *3*, (1), 24-42.
35. Gevaert, K.; Ghesquiere, B.; Staes, A.; Martens, L.; Van Damme, J.; Thomas, G. R.; Vandekerckhove, J., Reversible labeling of cysteine-containing peptides allows their specific chromatographic isolation for non-gel proteome studies. *Proteomics* **2004**, *4*, (4), 897-908.
36. Gevaert, K.; Vandekerckhove, J., COFRADIC™: the Hubble telescope of proteomics. *Drug Discovery Today: TARGETS* **2004**, *3*, S12-S22.
37. Gevaert, K.; Van Damme, P.; Martens, L.; Vandekerckhove, J., Diagonal reverse-phase chromatography applications in peptide-centric proteomics: Ahead of catalogue-omics? *Analytical Biochemistry* **2005**, *345*, (1), 18-29.
38. Sechi, S.; Chait, B. T., Modification of cysteine residues by alkylation. A tool in peptide mapping and protein identification. *Analytical Chemistry* **1998**, *70*, (24), 5150-5158.
39. Fenyo, D.; Qin, J.; Chait, B. T., Protein identification using mass spectrometric information. *Electrophoresis* **1998**, *19*, (6), 998-1005.
40. Mason, D. E.; Liebler, D. C., Characterization of benzoquinone-peptide adducts by electrospray mass spectrometry. *Chemical Research in Toxicology* **2000**, *13*, (10), 976-982.
41. Dayon, L.; Roussel, C.; Prudent, M.; Lion, N.; Girault, H. H., On-line counting of cysteine residues in peptides during electrospray ionization by electrogenerated tags and their application to protein identification. *Electrophoresis* **2005**, *26*, (1), 238-247.
42. http://www.matrixscience.com/search_form_select.html, accessed June 2007.
43. Bjellqvist, B.; Hughes, G. J.; Pasquali, C.; Paquet, N.; Ravier, F.; Sanchez, J. C.; Frutiger, S.; Hochstrasser, D., The Focusing Positions of Polypeptides in Immobilized Ph Gradients Can Be Predicted from Their Amino-Acid-Sequences. *Electrophoresis* **1993**, *14*, (10), 1023-1031.
44. Dayon, L., Thiol-targeted microspray mass spectrometry of peptides and proteins through on-line ec-tagging. *Thesis N°3525* **2006**, EPFL.
45. New United Kingdom Patent Application Number 0700475.7.

**CHAPTER VI: Gel-free Isoelectric Focusing in a Membrane-sealed
Multicompartment Cell for Proteome Prefractionation***

1. Introduction.....	178
2. Materials and methods.....	181
2.1 Chemicals and biologicals.....	181
2.2 Sample prefractionation by IEF in the static chamber.....	182
2.3 SDS-PAGE.....	182
2.4 2-D PAGE analysis.....	183
3. Results.....	183
3.1 Description of the instrument.....	183
3.2 Performance of the instrument.....	185
3.3 Biological results.....	186
4. Discussion.....	191
5. References.....	193

* based on H.-T. Lam, P. Antonioli, P. G. Righetti, A. Citterio, H. H. Girault, *Electrophoresis* 2007, 28, 1860-1866

1. Introduction

In this third millennium, characterized by an exasperate march towards miniaturization at all costs (just to have a glimpse at the field, one could consult a number of special issues of Electrophoresis devoted to this topic, e.g., *Electrophoresis* 2000, 21, pp. 1-254; *ibid.* 2001, 22, pp. 185-370 and pp. 3843-4031; *ibid.* 2002, 23, pp. 3459-3645, *ibid.* 2003, 24, 3521-3833), scientists have forgotten (or perhaps they have never known) that isoelectric focusing (IEF, still one of the leading techniques in today's Separation Science horizon) was born as a preparative technique in large size columns (accommodating either 110 or 440 mL sample volumes) filled with a density gradient, supporting the pH gradient, for preventing electro-decantation phenomena (i.e., sedimentation of the denser, focused protein zones that would occur in free liquid).¹⁻³ An entire experiment, including column set up, focusing, elution, and the analysis of hundreds of fractions, required a minimum of one week of hard labor. Notwithstanding the intensive labor involved, the trend towards large-scale preparative fractionation devices continued over the years. Thus, in 1975, Rilbe and Petterson described two additional types of columns, this time extremely short and thick, one with a column volume of 440 mL, the other accommodating 110 mL of sample volume. In such columns, more than 1 g of sperm whale myoglobin could be fractionated, the main band containing as much as 800 mg protein, an appreciable amount to be carried by a density gradient.⁴ Abandoning vertical density gradient columns, Rilbe's group started developing multicompartiment electrolyzers still based on the IEF fractionation principle. The first of such electrolyzers was built with 20-chambers and could be filled with up to 1000 mL of sample, with a load capacity of several grams of protein per day (separations were over in a 24-hour period).⁴ As a last evolutionary step, a mammoth-size apparatus was described,⁵ containing 46 separation compartments, accommodating a total volume of 7.6 L and encompassing a length

of 1 m. Fourteen grams of whey proteins could be completely separated into its main components (i.e. serum albumin, α -lactalbumin and β -lactoglobulin).

With the advent of immobilized pH gradients (IPG),⁶ preparative separations still were implemented on a rather large scale. The first preparative attempts contemplated focusing in progressively thicker IPG gels (5-mm-thick), first in standard 5%T, 4%C matrices,^{7, 8} and then in progressively diluted polyacrylamide matrices, down to as low as 2.8%T, cast in horizontal troughs filled with 125 mL total gel volume.³ Upon realizing the severe drawbacks of preparative runs in gel matrices, Righetti's group reverted to the idea of multicompartiment electrolyzers (MCE), exploiting the fine Immobiline chemistry. Such devices exploited the unique idea of isoelectric, buffering, zwitterionic membranes, able to confine groups of proteins, according to their pI values, into any compartment delimited by two membranes of precise pI value.³ Also these electrolyzers (6 sample collection chambers, plus two electrode reservoirs) were meant for processing large sample volumes and sizable proteins amounts, since they were connected to external reservoirs from which a continuous sample feed was guaranteed via recycling.

In recent years, however, due to the development of high sensitivity protein analysis techniques, including mass spectrometers (MS) able to handle minute (of the order of picomole) sample levels, the trend has been towards miniaturization even in preparative instrumentation. Additionally, due to the extreme complexity of any proteome,⁹ prefractionation by any means (chromatographic and electrophoretic) has now become a common trend.¹⁰ Aware of this new trend, the MCE with isoelectric membranes was miniaturized, so as to adapt it to proteome prefractionation with minute sample amounts.¹¹ The new instrument was shown to perform quite well in collecting proteome sub-fractions of very precise pI intervals, void of contamination from adjacent pI species.^{3, 12, 13} An interesting variant of this approach is OFFGEL IEF in multi-compartment devices.¹⁴⁻¹⁶ If a series of

chambers (up to 20), containing the proteome sample to be sub-fractionated, are placed directly on top of an IPG gel, in any desired pH interval, which is subjected to a voltage gradient, the sample proteins will move along the IPG migration path till reaching their pI value and thus collecting, at null surface charge, into the cup standing directly over the IPG gel segment titrating such species to their respective pI value. Just like the original MCE with isoelectric membranes, OFFGEL IEF permits collection of proteins in solution, a most desirable feature when proteins have to be further analyzed for ascertaining their identity. This instrument too was shown to perform quite well for fractionation not only of proteins, but also of their tryptic digests.¹⁷⁻¹⁹

Notwithstanding the advantages of proteome prefractionation in IPG-based separation processes (high precision in pH gradient engineering, very high resolution, retrieval of sample uncontaminated by carrier ampholytes), separations in conventional IEF in soluble amphoteric buffers have also been adopted recently, especially in the Rotofor system (and in the mini-Rotofor version).²⁰ The Rotofor is assembled from 20 sample chambers, separated by liquid-permeable nylon screens, except at the extremities, where cation- and anion-exchange membranes are placed against the anodic and cathodic compartments, respectively, so as to prevent diffusion within the sample chambers of noxious electrodic products. At the end of the preparative run, the twenty focused fractions are collected simultaneously by piercing a septum at the chambers' bottom via twenty needles connected to a vacuum source. The narrow-pI range fractions can then be used for generating conventional 2-D maps. In recent times, this methodology has taken another, unexpected turn: the Rotofor is used directly as the first dimension of a peculiar 2-D methodology, in which each fraction is further analyzed by hydrophobic interaction chromatography, using non-porous reversed-phase HPLC.²¹ Each peak collected from the HPLC column is then digested with trypsin, subjected to matrix assisted laser desorption ionization–time of flight (MALDI-TOF) MS analysis and MS-Fit

database searching. More recently, Xiao et al.²² have reported an unexpected application of the Rotofor, not just for fractionation of intact proteins in presence of carrier ampholytes, but for fractionation of peptide digests of an entire proteome (in this case, human serum) in an ampholyte-free environment. The peptides themselves would act as CA-buffers and create a pH gradient via an “autofocusing” process (with a caveat, though: the pH gradient will be quite poor, since only a few peptides have good buffering power and conductivity in the pH 5-8 range).

Due to the fact that the Rotofor is still a complex machine to operate and even in its mini-version it handles sizeable amounts of liquids in each chamber (at least 0.5 mL), we report here a static apparatus (in that no rotational stabilization is adopted), for proteome prefractionation, accommodating minute sample volumes (100 μ L per chamber) based on a novel design in the chamber construction and in the fraction collection at the end of the IEF run.

2. Materials and methods

2.1 Chemicals and biologicals

Urea, sodium dodecyl sulphate, thiourea, 3-[3-cholamidopropyl dimethylammonio]-1-propansulfonate (CHAPS), Tris, acetic acid, sodium hydroxide, Ampholines pH 3-10, the visible stain Brilliant Blue G (for colloidal Coomassie blue preparation) and the *Escherichia coli* lyophilized cells were all from Sigma-Aldrich, St Louis, Mo. Tributylphosphine (TBP), and acrylamide solution were purchased from Fluka (Buchs, Switzerland). IPG strips pH 3-10 linear range, Laemmli sample buffer and whatman paper were provided by Bio-Rad (Hercules, CA). Pharmalytes pH 2.5-5.0 and 5.0-8.0 were purchased from GE-Healthcare

(Chalfont St. Giles, UK). The human cancer cells U2Os were a kind gift from Dr. S. C. Righetti, Istituto Nazionale dei Tumori, Milan.

2.2 Sample prefractionation by IEF in the static chamber

The human cancer cells U2Os, as well as the *E. coli* lysates, were directly solubilized in “2-D sample buffer” (7 M urea, 2 M thiourea, 3% CHAPS, 5 mM TBP and 10 mM acrylamide) and allowed to be alkylated at room temperature for 60 minutes. To stop the alkylation reaction, 10 mM DTT was added to the solution, followed by 2.5% Ampholine pH interval 3-10 (for the U2Os lysate) or 3% Pharmalyte pH interval 2.5-8.0 (for *E. coli* proteins, obtained by mixing 1.5% Pharmalyte 2.5-5.0 and 1.5% Pharmalyte 5.0-8.0).

The 8-chamber device was loaded with 960 μL of cell lysate (120 μL per trough), whereas the anodic and cathodic chambers were filled with whatman paper soaked with 250 μL of 50 mM free acetic acid (pH 3.0) at the anode and 50 mM free sodium hydroxide (pH 12.0) at the cathode, respectively. The two electrolytes were dissolved in the same solution as the one used for protein solubilisation. The total amount of sample loaded was 1 mg. Focusing was continued for up to 3 hrs by setting a limiting power of 1 W, which allowed for a ramp voltage going from 300 V to 1000 V at room temperature. At the end of the run, the 8 fractions were collected and analyzed by SDS-PAGE and by 2-D mapping.

2.3 SDS-PAGE

Mono-dimensional SDS-PAGE of the samples collected from the present fractionation instrument was performed using 10-well, 1-mm-thick, 13% polyacrylamide glycine gel plates. Fifteen μL of each fraction were mixed with Laemmli sample buffer 2X and boiled for 5 minutes, after that thirty μL of the 8 mixtures were loaded per lane and electrophoretic migration performed at 130 volts until bromophenol blue, added as a running marker, reached

the gel bottom. Staining and de-staining were performed with Colloidal Coomassie Blue and a 7% acetic acid water solution, respectively.

2.4 2-D PAGE analysis

Seven-cm long IPG strips (Bio-Rad) pH 3-10 were rehydrated with 150 μ L of protein solution (60 μ L of the content of each chamber as per section 2.2, diluted to 150 μ L with 2-D sample buffer), for 4 hrs. Isoelectric focusing (IEF) was carried out with an initial voltage gradient from 100 up to 1000 V, followed by 1000 volts constant for 5 hours. The voltage was then increased again rapidly up to 5000 volts in 30 min, and kept at such a value until reaching 30 kVh. For the second dimension the IPG strips were laid on a 10-20% acrylamide gradient SDS-PAGE. The electrophoretic run was performed by setting a current of 5 mA / gel for 1h, followed by 10 mA / gel for 1h and 20 mA / gel until the dye front reached the bottom of the gel. Gels were then immediately stained in colloidal Coomassie Blue. Destaining was performed in 7% acetic acid until the background became completely transparent. The 2-DE gels were scanned with a Versa-Doc Imaging System (Model 3000, Bio-Rad, Hercules CA).

3. Results

3.1 Description of the instrument

Figure 1 gives drawings of the cell block (A and B) and a photograph (top view, C) of the assembled instrument. Basically, the instrument consists of 3 main acetal-polyoxymethylene (POM) blocks assembled onto an 8 x 9 cm base. In the fixed block (part A) 8 sample wells are machined, having the following size: 7 mm width, 3 mm depth and 10 mm height, each accommodating 100 to 120 μ L sample volume. At the two extremities, anodic and cathodic compartments are carved into the block, having the same width and height as the sample

chambers, but with a depth of 6 mm, thus accepting up to 250 μL of electrodic solutions. The wells are visible in Figure 1B, in which the mobile block (part B) has been removed.

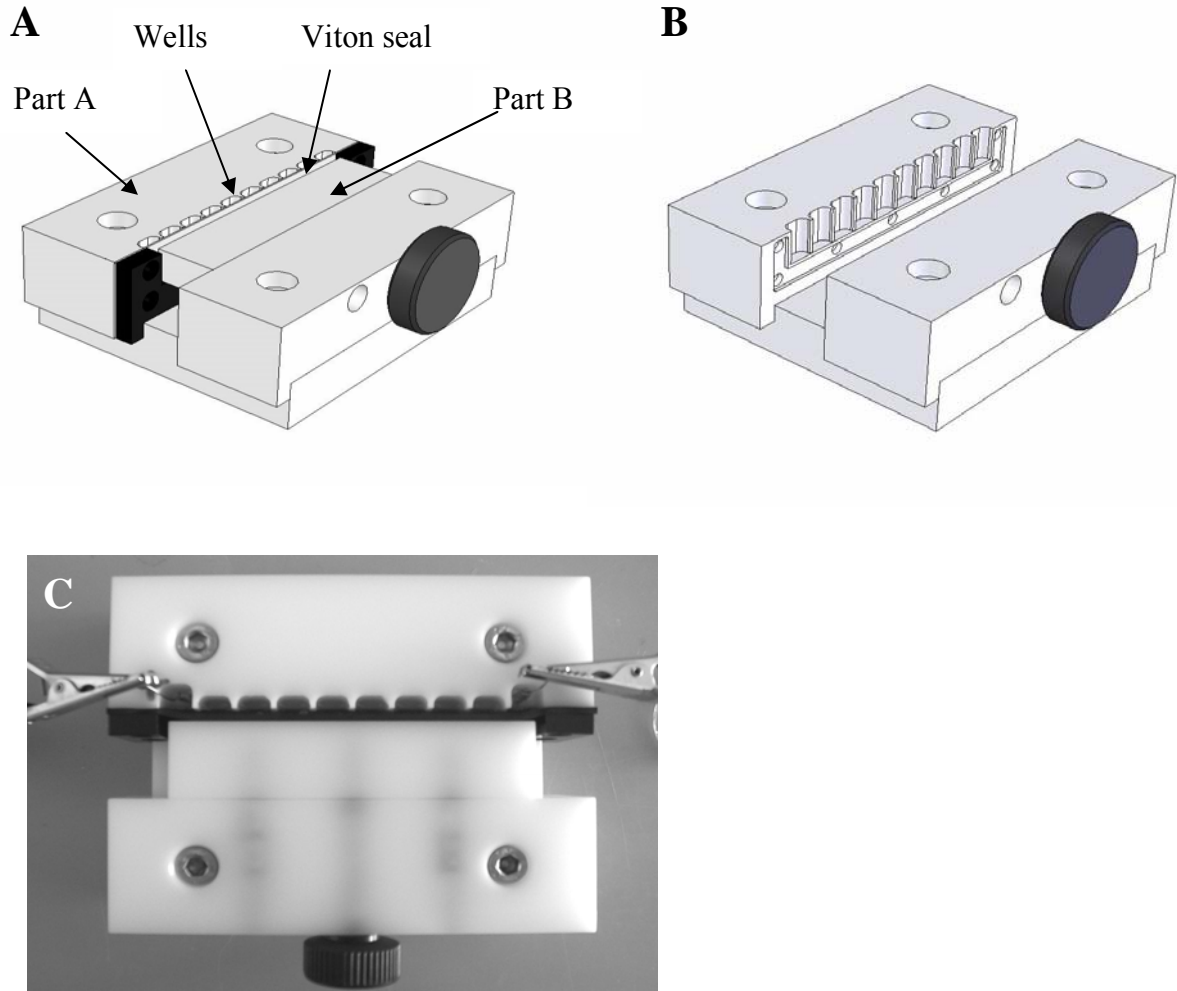


Figure 1: Drawing of the miniaturized gel-free IEF instrument for proteome prefractionation (A and B) and photograph of the actual apparatus in operation (C). Automatic fractionation is achieved, at the end of the focusing, by pressing the movable block B against the rubber wall (Viton seal). Panel B shows the profile of the 10 chambers in absence of the movable block B.

The novel idea in this construction is how the content of the various chambers is isolated from the neighbouring ones at the end of the IEF run. This is obtained by acting on the mobile block (part B), that acts onto a rubber wall (Viton seal). During IEF operation, the rubber wall is withdrawn by approximately one millimeter, so that the liquid overflows from

the diaphragms separating the various chambers, thus ensuring liquid continuity and current flow. At the end of the IEF run, by turning the black knob, the mobile block B is pressed against the rubber wall, thus automatically sealing all the chambers. The content of each chamber is then withdrawn with a syringe or directly with an 8-tip pipette.

3.2 Performance of the instrument

Figure 2 gives the evolution of current *vs.* time, for two different applied voltages. It can be seen that, in both cases, focusing is obtained in *ca.* 20 min, not surprisingly, considering that the electrode distance is only 7 cm. Figure 3 gives the formation of pH gradient as a function of focusing time. It can be appreciated that the pH gradient is already formed after a 15 min run and is maintained (and fully developed) after 45 min of focusing. When running the multichamber device in presence of proteins, focusing is continued for up to 3 hrs, so as to ensure reaching a steady-state for all proteins present in the sample. When measuring the conductivity profile of the liquid in the 8 chambers, one obtains a U-shaped function, with a minimum at approx. pH 6-7, as is well-known in IEF (not shown).²³

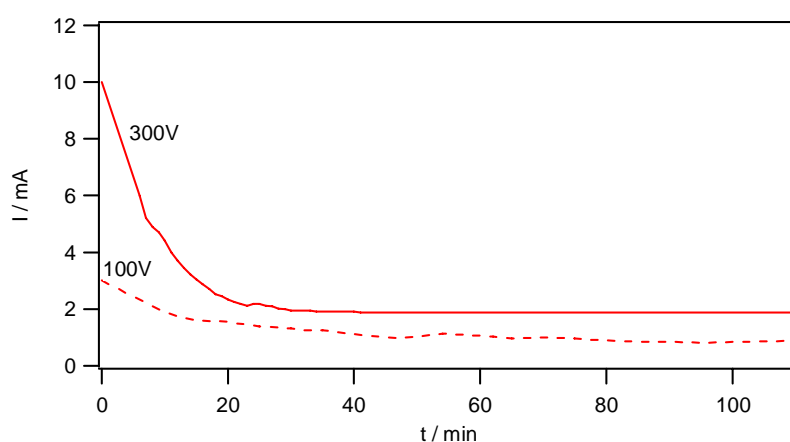


Figure 2: Evolution of current (I) vs. time for two different voltages applied (300 V, continuous tracing and 100 V, dotted line)

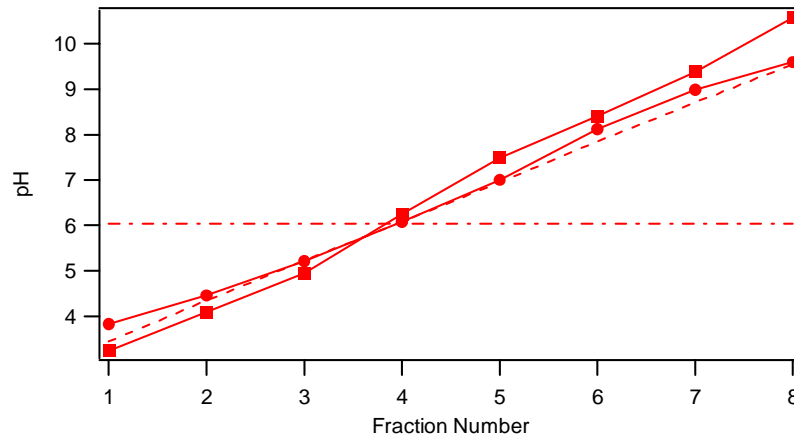


Figure 3: Time course of pH gradient formation. The horizontal line represents the pH prior to focusing. The slanted and broken line indicates the theoretical pH predicted for 3-10 ampholytes in an 8-chambers device. The circles and squares represent the pH measured after 15 min and 45 min of focusing, respectively.

3.3 Biological results

In order to assess the performance in proteome prefractionation of this novel instrument, we have selected a total cell lysate of the human cancer cells U2Os and the water-soluble protein fraction of *E. coli*. Figure 4 to Figure 6 display the results of these experiments. Panel A of Figure 4 shows a 2-D map of a control, unfractionated total human cancer cell lysate, run in an IPG pH 3-10 in the first dimension. Panel B shows the mono-dimensional SDS-PAGE profiling of the contents of each chamber after fractionation on a 3-10 pH gradient (below the fraction Nos. the pH value of each eluted fraction is reported). It can be appreciated that the SDS patterns are specific for each isoelectric fraction. In order to see how precise the pI cuts are, 2-D maps of some eluted fractions are displayed in Figure 5. These maps are related to fractions No. 1 (pH 4.33, upper), No. 3 (pH 5.76, upper middle) and No. 6 (pH 8.84, bottom panel). It can be appreciated that they display quite narrow pI cuts, with essentially no spot overlaps among the different fractions.

In order to prove that steady-state conditions had been reached, the experiment was repeated with an *E. coli* total cell lysate, that was run for 1 and 3 hrs on a 2.5-8.0 pH interval. It can be appreciated (Figure 6 A through C) that the two 2-D profiles obtained from the same fractions after 1-hour or 3-hour fractionation are quite similar, indicating that even the shorter focusing times are adequate for ensuring proper separations.

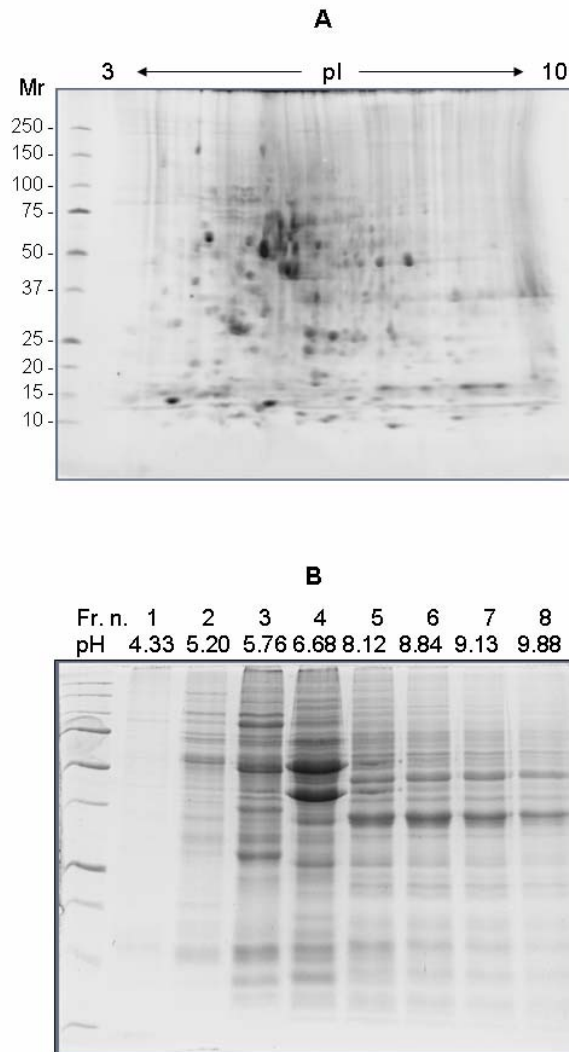


Figure 4: Analysis of a total cell lysate of human cancer cells U2Os. Upper panel: control 2-D map of the cell lysate in an IPG pH 3-10 interval. Lower panel: mono-dimensional SDS-PAGE of the content of each chamber after focusing in the mini-device using 3% Ampholine pH interval 3-10. Below the fraction No the pH of each fraction is reported.

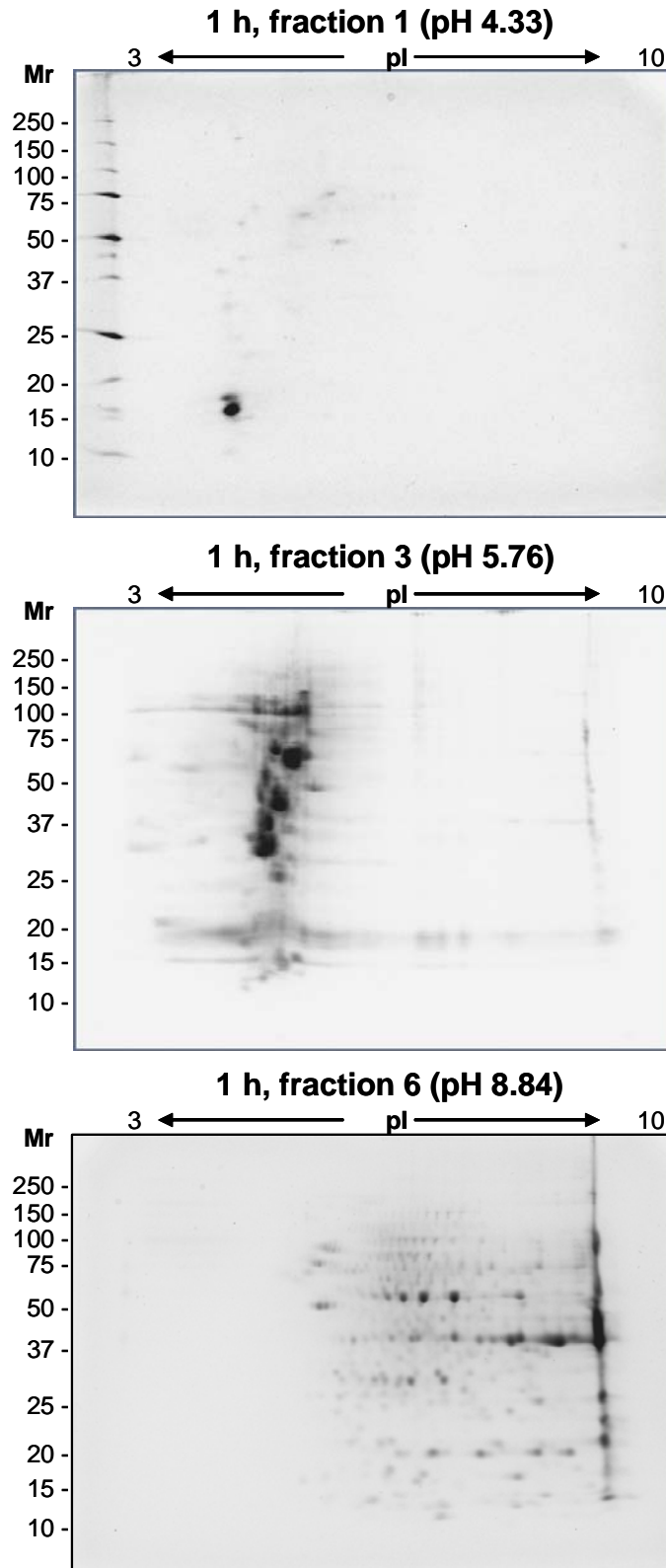


Figure 5: Two-dimensional maps of the content of chambers 1 (upper), 3 (intermediate) and 6 (bottom) panels, after fractionating the total cell lysate in the device of Fig. 1 for 1 hour on a 3-10 pH interval (2.5% Ampholine). No spot overlap is experienced in the various chambers.

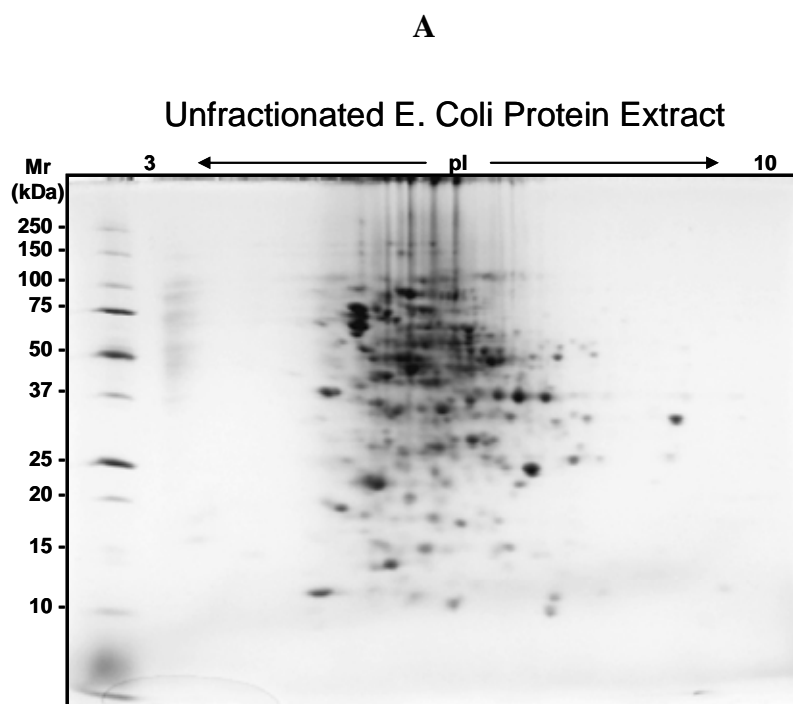
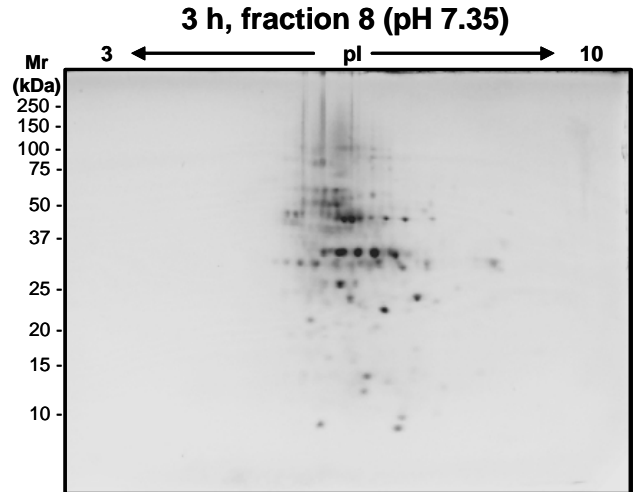
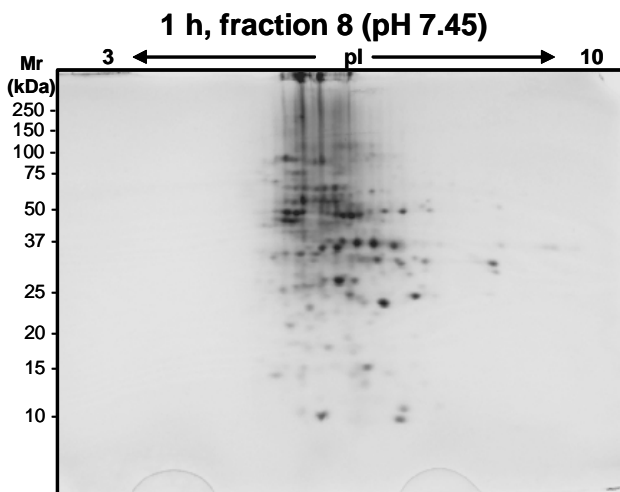
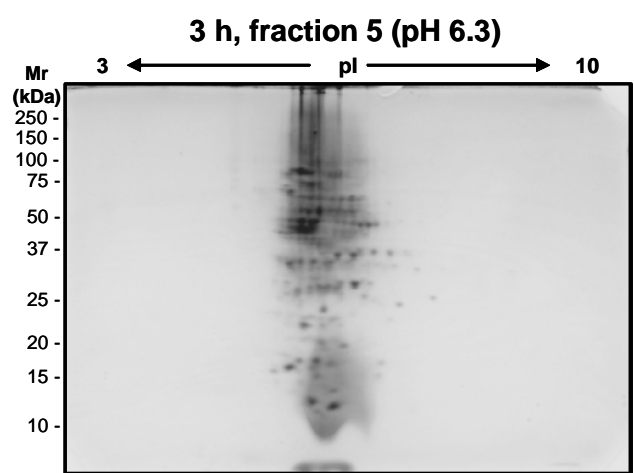
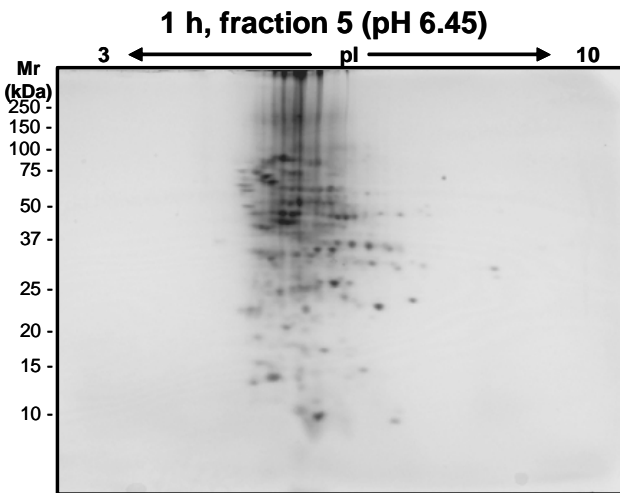
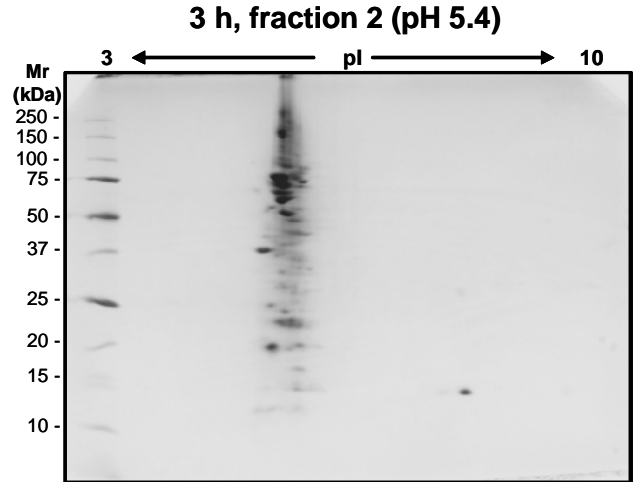
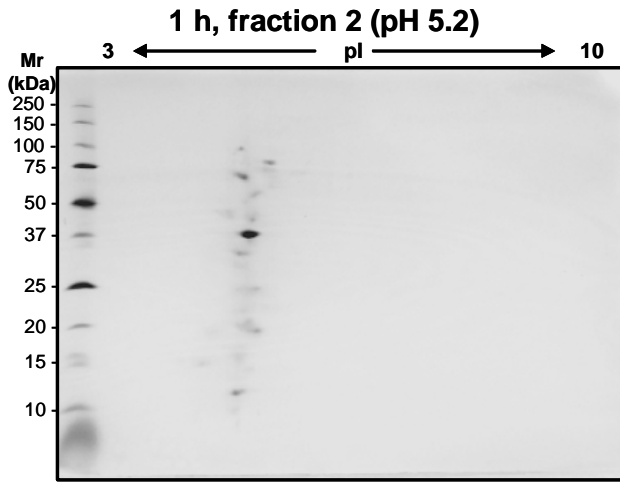


Figure 6: Time course of a fractionation of a total E coli lysate in the present instrument on a 2.5-8.0 pH gradient (3% Pharmalyte 2.5-8.0). Panel A: 2-D map of a control, unfractionated lysate. Panel B: 2-D maps of the content of 3 chambers (2, 5 and 8) after 1 hour of focusing. Panel C: 2-D maps of the content of 3 chambers (2, 5 and 8) after 3 hours of focusing.

B

C



4. Discussion

As stated in the introduction, although prefractionation exploiting the IPG methodology has been preferred up to the present, more and more reports have appeared in the last few years dealing with prefractionation via conventional IEF in soluble carrier ampholyte (CA) buffers. Although we have reported only a few, selected applications based on the Rotofor, other instruments exist for performing this task, such as continuous flow (CF) IEF devices, as epitomized by the Octopus,²⁴ allowing the collection of as many as 96 fractions. For instance, Hoffman et al.²⁵ have proposed CF-IEF as the first dimension of a 2-D map, the eluted fractions being directly analysed by orthogonal SDS-PAGE. In turn, individual bands in the second SDS dimension were eluted and analysed by ESI-IT-MS. By this approach, they could identify a number of cytosolic proteins of a human colon carcinoma cell line. One advantage of CF-IEF (and of course of all focusing techniques in a gel-free environment) is immediately evident from their data: large proteins (e.g. vinculin, Mr 116.6 kDa) could be well recovered and easily identified; on the contrary, recovery of large Mr species has always been problematic in IPG gels. In addition to that, it is also known that IPG matrices tend to adsorb irreversibly hydrophobic and membrane proteins, rendering thus problematic their recovery and identification.

All these phenomena do not occur when IEF is performed in a plain liquid phase, which probably accounts for the popularity of the Rotofor instrument. Our mini-device greatly simplifies the approach to gel-free IEF: it is compact, it allows for very small sample volumes (as little as 100 μ L), for very simple fraction recovery and it disposes of the rotational stabilization implemented in the Rotofor. In fact, in our system, we do not experience any electro-decantation of proteins at (or in proximity of) their pI value, possibly because, since most proteome fractionation and analysis protocols call for a strongly denaturing mixture of

urea and thiourea, the density of such solutions would prevent protein sedimentation in a free-liquid phase.

Another way of performing prefractionation for proteome analysis is the well-known “Radola technique”,²⁶ already described in the early seventies, consisting in focusing in a horizontal trough filled with Sephadex beads. This method has been recently re-introduced by Goerg et al..²⁷ However, this last approach again exploits a gel phase, which means scooping up segments of the Sephadex bed between anode and cathode and eluting the isoelectric fractions for further analysis.

Perhaps one of the major drawbacks of IEF in CA buffers is that the fractionation of alkaline proteins is not quite so good. This is not due to the short focusing times of 1 h (see Figure 5 and Figure 6 B), since experiments run for longer times (see Figure 6 C) still show poor focusing in the alkaline region. In fact, while in the acidic region longer prefractionation times seem to produce slightly better pI cuts, as it can be appreciated in fraction 2 (Figure 6C), which presents a slightly better resolution and a considerable protein enrichment with respect to the same fraction displayed in Figure 6B, such an amelioration cannot be observed in the alkaline interval (see fraction 8, Figure 6B and 6C, bottom panels). This could possibly be due to the onset of electroosmotic flow, an ever present hazard in all IEF experiments in presence of soluble CA buffers. Righetti’s group recently found out what is the major problem: essentially all commercial brands of CAs, in the alkaline region, contain a majority of “poor” species, *i.e.* of carrier ampholytes displaying rather large (pI-pK) values, thus unable to focus and properly buffer along the pH gradient²⁸. Thus, an improvement on the synthesis of alkaline CA buffers is sorely needed.

5. References

1. Svensson, H., Isoelectric Fractionation, Analysis, and Characterization of Ampholytes in Natural Ph Gradients .3. Description of Apparatus for Electrolysis in Columns Stabilized by Density Gradients and Direct Determination of Isoelectric Points. *Archives of Biochemistry and Biophysics* **1962**, Suppl. 1, 132-&.
2. Vesterbe.O; Wadstrom, T.; Vesterbe.K; Svensson, H.; Malmgren, B., Studies on Extracellular Proteins from Staphylococcus Aureus .I. Separation and Characterization of Enzymes and Toxins by Isoelectric Focusing. *Biochimica Et Biophysica Acta* **1967**, 133, (3), 435-&.
3. Righetti, P. G., Isoelectric Focusing: Theory, Methodology and Applications *Isoelectric Focusing: Theory, Methodology and Applications, Elsevier, Amsterdam* **1983**, 88-129.
4. Rilbe, H.; Forcheimer, A.; Pettersson, S.; Johnsson, M., in: *Progress in Isoelectric Focusing and Isotachopheresis, Righetti P.G. (Ed), Elsevier, Amsterdam* **1975**, 51-63.
5. Jonsson, M.; Rilbe, H., Large-scale fractionation of proteins by isoelectric focusing in a multi-compartment electrolysis apparatus. *Electrophoresis* **1980**, 1, 3-14.
6. Bjellqvist, B.; Ek, K.; Righetti, P. G.; Gianazza, E.; Gorg, A.; Westermeier, R.; Postel, W., Isoelectric-Focusing in Immobilized Ph Gradients - Principle, Methodology and Some Applications. *Journal of Biochemical and Biophysical Methods* **1982**, 6, (4), 317-339.
7. Ek, K.; Bjellqvist, B.; Righetti, P. G., Preparative Isoelectric-Focusing in Immobilized Ph Gradients .1. General-Principles and Methodology. *Journal of Biochemical and Biophysical Methods* **1983**, 8, (2), 135-155.
8. Gelfi, C.; Righetti, P. G., Preparative Isoelectric-Focusing in Immobilized Ph Gradients .2. A Case-Report. *Journal of Biochemical and Biophysical Methods* **1983**, 8, (2), 157-172.
9. Anderson, N. L.; Anderson, N. G., The human plasma proteome - History, character, and diagnostic prospects. *Molecular & Cellular Proteomics* **2002**, 1, (11), 845-867.
10. Hamdan, M.; Righetti, P. G., Proteomics today: . *Proteomics today: Protein Assessment and Biomarkers Using Mass Spectrometry, 2-D Electrophoresis and Microarray Technology, Wiley-VCH, Hoboken* **2005**, 373-390.
11. Herbert, B.; Righetti, P. G., A turning point in proteome analysis: Sample prefractionation via multicompartment electrolyzers with isoelectric membranes. *Electrophoresis* **2000**, 21, (17), 3639-3648.
12. Pedersen, S. K.; Harry, J. L.; Sebastian, L.; Baker, J.; Traini, M. D.; McCarthy, J. T.; Manoharan, A.; Wilkins, M. R.; Gooley, A. A.; Righetti, P. G.; Packer, N. H.; Williams, K. L.; Herbert, B. R., Unseen proteome: Mining below the tip of the iceberg to find low abundance and membrane proteins. *Journal of Proteome Research* **2003**, 2, (3), 303-311.
13. Herbert, B.; Pedersen, S. K.; Harry, J. L.; Sebastian, L., *Pharma. Genomics* **2003**, 3, 22-36.
14. Ros, A.; Faupel, M.; Mees, H.; van Oostrum, J.; Ferrigno, R.; Reymond, F.; Michel, P.; Rossier, J. S.; Girault, H. H., Protein purification by Off-Gel electrophoresis. *Proteomics* **2002**, 2, (2), 151-156.
15. Arnaud, I. L.; Josserand, J.; Rossier, J. S.; Girault, H. H., Finite element simulation of Off-Gel (TM) buffering. *Electrophoresis* **2002**, 23, (19), 3253-3261.
16. Michel, P. E.; Reymond, F.; Arnaud, I. L.; Josserand, J.; Girault, H. H.; Rossier, J. S., Protein fractionation in a multicompartment device using Off-Gel (TM) isoelectric focusing. *Electrophoresis* **2003**, 24, (1-2), 3-11.

17. Heller, M.; Ye, M. L.; Michel, P. E.; Morier, P.; Stalder, D.; Junger, M. A.; Aebersold, R.; Reymond, F. R.; Rossier, J. S., Added value for tandem mass spectrometry shotgun proteomics data validation through isoelectric focusing of peptides. *Journal of Proteome Research* **2005**, 4, (6), 2273-2282.
18. Heller, M.; Michel, P. E.; Morier, P.; Crettaz, D.; Wenz, C.; Tissot, J. D.; Reymond, F.; Rossier, J. S., Two-stage Off-Gel (TM) isoelectric focusing: Protein followed by peptide fractionation and application to proteome analysis of human plasma. *Electrophoresis* **2005**, 26, (6), 1174-1188.
19. Michel, P. E.; Crettaz, D.; Morier, P.; Heller, M.; Gallot, D.; Tissot, J. D.; Reymond, F.; Rossier, J. S., Proteome analysis of human plasma and amniotic fluid by Off-Gel (TM) isoelectric focusing followed by nano-LC-MS/MS. *Electrophoresis* **2006**, 27, (5-6), 1169-1181.
20. Bier, M., Recycling isoelectric focusing and isotachopheresis. *Electrophoresis* **1998**, 19, (7), 1057-1063.
21. Zhu, K.; Yan, F.; O'Neil, K. A.; Hamler, R.; Lin, L.; Barder, T. J.; Lubman, D. M., Proteomic Analysis Using 2-D Liquid Separations of Intact Proteins From Whole-Cell Lysates. *Current Protocols in Protein Science* **2003**, 23, 23.3.1-23.3.28.
22. Xiao, Z.; Conrads, T. P.; Lucas, D. A.; Janini, G. M.; Schaefer, C. F.; Buetow, K. H.; Issaq, H. J.; Veenstra, T. D., Direct ampholyte-free liquid-phase isoelectric peptide focusing: Application to the human serum proteome. *Electrophoresis* **2004**, 25, (1), 128-133.
23. Haglund, H., Isoelectric Focusing. *Isoelectric Focusing*, Arbuthnott, J.P., Beeley, J.A. (Eds.), Butterworths, London **1975**, 3-22.
24. Kuhn, R.; Wagner, H., Application of Free-Flow Electrophoresis to the Preparative Purification of Basic-Proteins from an Escherichia-Coli Cell Extract. *Journal of Chromatography* **1989**, 481, 343-351.
25. Hoffmann, P.; Ji, H.; Moritz, R. L.; Connolly, L. M.; Frecklington, D. F.; Layton, M. J.; Eddes, J. S.; Simpson, R. J., Continuous free-flow electrophoresis separation of cytosolic proteins from the human colon carcinoma cell line LIM 1215: A non two-dimensional gel electrophoresis-based proteome analysis strategy. *Proteomics* **2001**, 1, (7), 807-818.
26. Radola, B. J., Analytical and Preparative Isoelectric Focusing in Gel-Stabilized Layers. *Annals of the New York Academy of Sciences* **1973**, 209, (Jun15), 127-143.
27. Gorg, A.; Boguth, G.; Kopf, A.; Reil, G.; Parlar, H.; Weiss, W., Sample prefractionation with Sephadex isoelectric focusing prior to narrow pH range two-dimensional gels. *Proteomics* **2002**, 2, (12), 1652-1657.
28. Sebastiano, R.; Simo, C.; Mendieta, M. E.; Antonioli, P.; Citterio, A.; Cifuentes, A.; Peltre, G.; Righetti, P. G., Mass distribution and focusing properties of carrier ampholytes for isoelectric focusing: I. Novel and unexpected results. *Electrophoresis* **2006**, 27, (20), 3919-3934.

**CHAPTER VII: Immobilized pH Gradient gel cell to study the pH
dependence of drug lipophilicity***

1. Introduction.....	196
2. Electrochemistry at the ITIES	199
2.1 Thermodynamics of ion transfer at ITIES	199
2.2 Electrochemistry to measure drug lipophilicity.....	201
2.3 Facilitated ion transfer.....	202
2.4 Differential Pulse Voltammetry.....	203
3. Experimental	204
3.1 Chemicals	204
3.2 Setup and electrochemical measurements	205
3.3 Methodology: use of an internal reference ion	207
4. Results and discussion.....	209
4.1 Experimental validation of the electrochemical cell based on transfer of simple permanent ions	209
4.2 Ionic partition diagram of ionizable compounds.....	211
5. Conclusions.....	217
6. References.....	219

* based on H.-T. Lam, C. M. Pereira, C. Roussel, P.-A. Carrupt, H. H. Girault, Analytical Chemistry 2006, 78, 1503-1508.

1. Introduction

Recently, the electrochemical study of the transfer of ionic species across the interface between two immiscible electrolyte solutions (ITIES) has gained great significance due to its wide applicability in different fields such as ion-selective electrodes for application to amperometric sensors, solvent extraction, drug lipophilicity and its consequences on drug delivery.¹⁻⁴ Unlike numerous traditional chromatographic and potentiometric systems developed to study the distribution of ionic species and giving an indirect access to partition coefficients, voltammetry at the ITIES allowed us to evaluate the standard partition coefficient of both the neutral and the ionized forms.^{5, 6} The four-electrode system initially introduced by Samec et al.⁷ was later used intensively by Reymond et al.² to study the transfer of many ionizable drugs at the interface between water and 1,2-dichloroethane (W/DCE), and the introduction of ionic partition diagrams revealed a most interesting aspect for the study of drug lipophilicity.⁸ Indeed, a partition diagram of a specific drug between two immiscible liquids is a representation of the conditions corresponding to the predominance of different forms of the compound (basic, neutral, acid) as a function of the Galvani potential difference and the pH of the aqueous phase. This representation has been revealed to be a useful tool to mimic the passage of a drug through a biological membrane and help understand the action of that drug.

However, the initial systems used to study the distribution of ionic species between two immiscible solutions used large ITIES, requiring quite large volumes of each phase². Thus, when only limited amount of species is available, micro-ITIES are more suitable, such as liquid/liquid (L/L) interfaces supported at the tip of micropipets^{9, 10} or systems using a droplet of organic phase or aqueous phase.^{11, 12} For example, Gobry et al.¹³ reported experiments with an aqueous droplet supported at an Ag/AgCl disk electrode covered with an organic solution. More recently, Ulmeanu et al.¹⁴ have studied the profiling of ionized drugs

using a four-electrode system and small volumes of phase in a 96-well plate, to study transfer reactions at a water/2-nitrophenyl octyl ether (NPOE) interface, allowing us to trace ionic partition diagrams of lipophilic compounds. Zhang et al.¹⁵ recently reported the study of ionizable drugs transfer across the water/DCE interface with a three-electrode system, using limited amount of drugs.

Until now, many studies on partition coefficients have been achieved at a water/DCE interface and biological interpretations based on cyclic voltammetry measurements have only been made for these systems.^{8, 16, 17} However, the high volatility and the toxicity of DCE limit its use and call for its replacement by a more appropriate organic solvent. Given its absence of known toxicity and interesting physicochemical properties (low solubility in water, low vapor pressure), NPOE has recently been introduced as an alternative for DCE in electrochemistry^{18, 19} and medicinal chemistry.^{5, 20} In addition, solvatochromic analysis have shown NPOE to be a good candidate to replace DCE in measurements of lipophilicity.^{20, 21} Furthermore, it has been shown that for a series of small ions the Gibbs energy of ion transfer from water to DCE directly correlates with the Gibbs energy of ion transfer from water to NPOE,^{18, 22} suggesting that the standard partition coefficient in NPOE offers a convenient alternative to the one in DCE.

In the present chapter, we describe a two-electrode setup to study the transfer of ionizable compounds at a micro interface water/NPOE where a commercial immobilized pH gradient (IPG) gel is originally taken as the aqueous phase, with the aim of tracing the ionic partition diagrams for two lipophilic compounds. IPG gels, offering linear pH gradients, have long been commercialized with the aim to serve proteomics studies and, more precisely, to be used in fractionation methods, such as isoelectric focusing and 2D gel electrophoresis.^{23, 24} Recently, the use of IPG gel was reported for the size-selective separation of gold nanoparticles by IEF.²⁵ Besides, the influence of the presence of a gel in the water phase on

the transfer of ionic compounds across a large water/DCE interface was investigated by Fantini et al.,²⁶ and the experimental characteristics of the drug transfer were shown to be in good agreement with a nongelled water/DCE interface. In addition, it was pointed out that a gel/liquid interface has a better mechanical stability than a liquid/liquid interface. With the use of an IPG gel in the present setup, there is no need to prepare several aqueous solutions at different pH to scan the overall pH domain to obtain the ionic partition diagram of a specific drug. Using this method, after few improvements, a high-throughput system to measure the partition diagram of a specific drug in one experiment could be obtained. With the proposed system using a micro interface, the *IR* drop effect is not too high, when compared to other large ITIES, thus allowing the use of only two electrodes, adding to the simplicity of the setup. Another important issue is the use of small amounts of sample (5 μL at most) due to the size of the interface and experimental setup.

The method is validated using simple tetraalkylammonium ions (TBA^+ , TEA^+ , TMA^+) which were already fully investigated by many authors, and can therefore be used as calibration for this new method. The present setup is then used to trace the ionic partition diagram of two lipophilic compounds: pyridine and 2,4-dinitrophenol. The values of standard transfer potential, Gibbs energy of transfer, and partition coefficients are deduced from electrochemical studies performed with differential pulse voltammetry. Additionally, in the case of lipophilic acids and bases, not only the $\log(P)$ of the ionized species can be determined from the ionic partition diagram, but also the $\log(P)$ of the neutral species can be determined from the observed shift in $\text{p}K_{\text{a}}$.

2. Electrochemistry at the ITIES

2.1 Thermodynamics of ion transfer at ITIES

When two immiscible electrolyte phases α and β are in contact with each other, the partition of the salts between the two phases occurs due to the difference in their energy of solvation. This generates an interfacial region where the electrical field strength differs from zero, so that a Galvani potential difference is established across the interface between the two phases:

$$\Delta_{\beta}^{\alpha}\phi = \phi^{\alpha} - \phi^{\beta} \quad (7.1)$$

where ϕ is the inner potential of the respective phase.

By expressing the electrochemical potential into a chemical and an electrical potential:

$$\tilde{\mu}_i^{\alpha} = (\mu_i^{0,\alpha} + RT \ln a_i^{\alpha}) + z_i F \phi^{\alpha} \quad (7.2)$$

where $\mu_i^{0,\alpha}$ is the standard chemical potential of phase α , a_i^{α} the activity of the ion i in the phase α , R and T the gas constant and the temperature respectively, z_i the charge of the ion, and F the Faraday constant. At thermodynamic equilibrium, the electrochemical potentials of a species i in two adjacent phases are equal:

$$\tilde{\mu}_i^{\beta} = \tilde{\mu}_i^{\alpha} \quad (7.3)$$

The standard Gibbs energy of transfer being defined as:

$$\Delta G_{tr,i}^{0,\alpha \rightarrow \beta} = \mu_i^{0,\beta} - \mu_i^{0,\alpha} \quad (7.4)$$

the Galvani potential difference defined in (7.1) can thus be written as:

$$\Delta_{\beta}^{\alpha}\phi = \frac{\Delta G_{tr,i}^{0,\alpha \rightarrow \beta}}{z_i F} + \frac{RT}{z_i F} \ln \left(\frac{a_i^{\beta}}{a_i^{\alpha}} \right) \quad (7.5)$$

The standard potential of transfer for i is defined as:

$$\Delta_{\beta}^{\alpha}\phi^0 = \frac{\Delta G_{tr,i}^{0,\alpha \rightarrow \beta}}{z_i F} \quad (7.6)$$

The Galvani potential difference in (7.5) becomes:

$$\Delta_{\beta}^{\alpha}\phi = \Delta_{\beta}^{\alpha}\phi^0 + \frac{RT}{z_i F} \ln \left(\frac{a_i^{\beta}}{a_i^{\alpha}} \right) \quad (7.7)$$

This equation is called the Nernst equation for ion transfer and is analogous to the classical Nernst equation for redox reactions. Equation (7.7) can be rewritten in terms of concentrations, replacing the standard potential of transfer by the formal potential of transfer, $\Delta_{\beta}^{\alpha}\phi^{0'}$, which includes the activity coefficients γ_i , and gives Equation (7.9):

$$\Delta_{\beta}^{\alpha}\phi^{0'} = \Delta_{\beta}^{\alpha}\phi^0 + \frac{RT}{z_i F} \ln \left(\frac{\gamma_i^{\beta}}{\gamma_i^{\alpha}} \right) \quad (7.8)$$

$$\Delta_{\beta}^{\alpha}\phi = \Delta_{\beta}^{\alpha}\phi^{0'} + \frac{RT}{z_i F} \ln \left(\frac{c_i^{\beta}}{c_i^{\alpha}} \right) \quad (7.9)$$

This relation shows that the Galvani potential is fixed by the ratio of concentrations in both phases. If a salt is dissolved in two immiscible phases in contact, the distribution of salt induces a polarization of the interface. The resulting Galvani potential is defined by writing the Nernst equation for the cation and anion at the interface:

$$\Delta_{\beta}^{\alpha}\phi = \Delta_{\beta}^{\alpha}\phi_{+}^0 + \frac{RT}{F} \ln \left(\frac{a_{+}^{\beta}}{a_{+}^{\alpha}} \right) = \Delta_{\beta}^{\alpha}\phi_{-}^0 - \frac{RT}{F} \ln \left(\frac{a_{-}^{\beta}}{a_{-}^{\alpha}} \right) \quad (7.10)$$

In the case of diluted solutions of similar volumes, this equation simplifies to:

$$\Delta_{\beta}^{\alpha}\phi = \frac{1}{2} (\Delta_{\beta}^{\alpha}\phi_{+}^0 + \Delta_{\beta}^{\alpha}\phi_{-}^0) \quad (7.11)$$

This demonstrates that when salts are partitioned between two adjacent phases, the interface becomes polarized at a fixed potential defined by the standard transfer potentials of the different ionic species. Because this potential is fixed, the interface is said to be non-polarizable: it is not possible to polarize the interface without modifying the chemical composition of the two phases.

In the case of a hydrophilic salt dissolved in the water phase and a hydrophobic salt dissolved in the organic phase, such that the concentration of the hydrophilic salt in the organic phase is negligible compared to that of the hydrophobic one, and conversely, the concentration of the hydrophobic salt in water is negligible compared to that of the hydrophilic one, the interface is said to be ideally polarizable: it is possible to apply an external potential without modifying the chemical composition of the adjacent phases, the Galvani potential difference can be controlled by an external source of potential, until a certain limit. Electrochemistry at ITIES is usually working in the limits of the polarization window, such that it is possible to polarize the interface up to a point where the applied Galvani potential difference reaches the transfer potential of an electrolyte ion. The electrolyte cation and anion define the potential window.

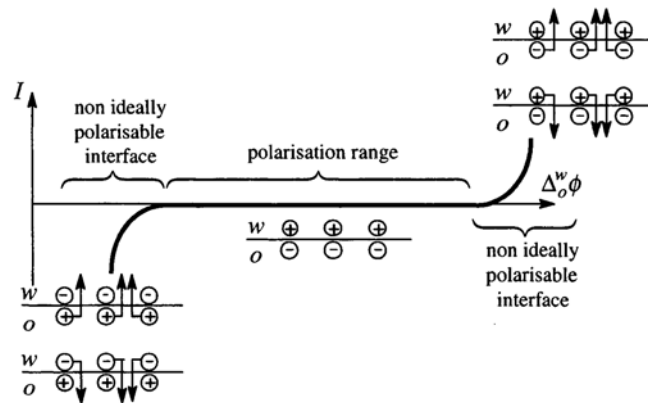


Figure 1: scheme of the interfacial processes within the polarization range

2.2 Electrochemistry to measure drug lipophilicity

For an ionized species, the partition coefficient depends on the potential and can be deduced from (7.7):

$$\log P_i = \log \left(\frac{a_i^\beta}{a_i^\alpha} \right) = \frac{z_i F}{RT \ln 10} (\Delta_\beta^\alpha \phi - \Delta_\beta^\alpha \phi^0) = \frac{z_i F}{RT \ln 10} \Delta_\beta^\alpha \phi - \frac{\Delta G_{tr,i}^{0,\alpha \rightarrow \beta}}{RT \ln 10} \quad (7.12)$$

which reduces into:

$$\log P_i = \frac{z_i F}{RT \ln 10} \Delta_\beta^\alpha \phi + \log P_i^0 \quad (7.13)$$

where $\log P_i^0$ is the standard partition coefficient, which is related to the standard transfer potential of the ionized species. $\log P_i^0$ represents the proportion of ions present in each phase if the interface is not polarized.

2.3 Facilitated ion transfer

The facilitating effect of ionophores on the ion transfer process has been widely studied since the pioneering work of Koryta.²⁷ Assisted ion transfer consists in decreasing the Gibbs energy of transfer by combining the complexation of ions and transfer of species. A decrease in the $\Delta G_{tr,i}^{0,\alpha \rightarrow \beta}$ means a decrease in the transfer potential, therefore, the presence of the ionophore translates in a shift of the potential wave of the cation transfer towards more positive potentials. This shift is crucial, because it allows observing transfers that were theoretically outside the polarization range.

Depending on its nature, the ionophore (or ligand to refer to the complexation reaction) can be dissolved in the organic or aqueous phase. Four types of mechanisms are then observed and were described by Girault et al.²⁸ and are represented in Figure 2.

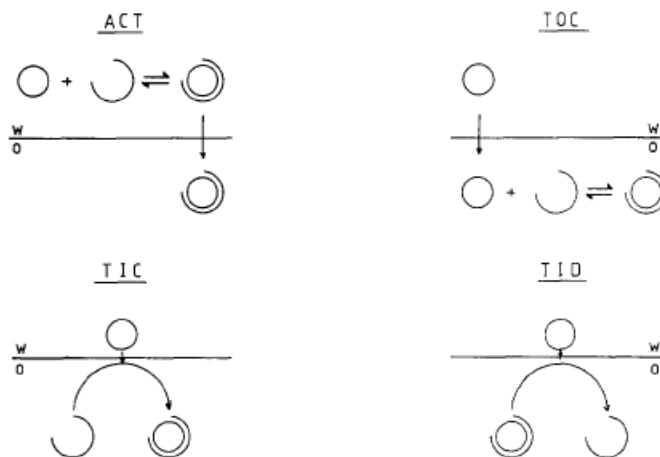


Figure 2: schematic mechanisms of assisted ion transfer, reprinted from ²⁸. ACT: aqueous complexation followed by transfer, TOC: transfer followed by organic complexation, TIC: transfer by interfacial complexation, TID: transfer by interfacial dissociation.

2.4 Differential Pulse Voltammetry

Cyclic voltammetry is the most used technique for measures at the ITIES. However, differential pulse techniques are more sensitive and differential pulse voltammetry is used for electrochemical measurements in this chapter.

The differential pulse technique is known as a very powerful technique for trace determination. Like all pulsed techniques, it is based on the differences of decay of the capacitive and faradaic current. The capacitive current decays exponentially and the faradaic current decays as $1/(\text{sqrt of time})$. The rate of decay of the capacitive current is thus much faster, and it is negligible at the end of the potential step, therefore only the faradaic current is measured. The important parameters are the following: the **pulse amplitude** (height of the potential pulse, constant or not depending on the technique), the **pulse width** (duration), the **sample period** (time at the end of the pulse during which the current is measured), and the **pulse period**, as illustrated in Figure 3.

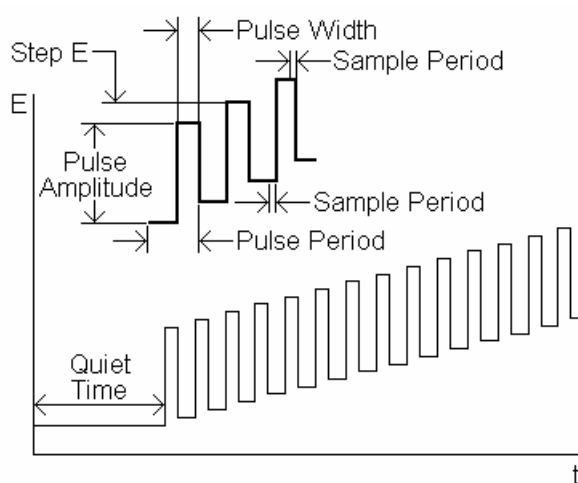


Figure 3: potential wave form for differential pulse voltammetry, taken from²⁹

The potential wave form consists of small pulses (of constant amplitude) superimposed upon a staircase wave form. The current is sampled twice in each pulse period (once before the pulse, and at the end of the pulse), and the difference between these two current values is measured and plotted versus the applied potential. A voltammetric wave is thus obtained in a peak shape, with the height being proportional to the analyte concentration and with the peak potential corresponding to the half wave potential of the reaction.

The discrimination against the capacitive current that is inherent in the pulse techniques leads to lower detection limits (when compared to linear sweep techniques), which makes these techniques suitable for quantitative analysis.

3. Experimental

3.1 Chemicals

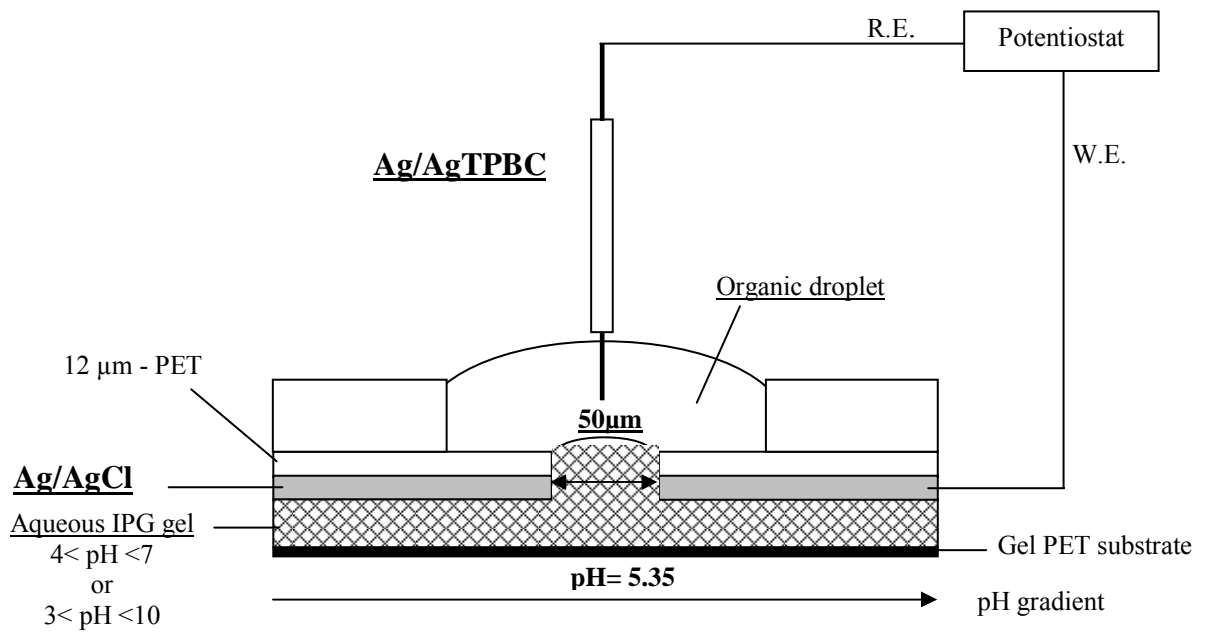
IPG gels (Immobiline DryPlates, linear pH range 4.0-7.0, 11-cm length and Immobiline Drystrips, linear pH range 3.0-10.0, 18-cm length) were purchased from Amersham Biosciences. These IPG gels are received in a dried format and reswelled in aqueous solutions before use. In the gel, the pH gradient is built by acrylamide derivatives, called Immobilines which are covalently fixed in the polyacrylamide gel.³⁰ The general chemical formula of Immobilines is $\text{CH}_2=\text{CH}-\text{CO}-\text{NH}-\text{R}$, where R is either a carboxylic acid or an amino group. Lithium chloride (LiCl > 99% purity), tetramethylammonium chloride (TMACl), tetraethylammonium chloride (TEACl), tetrabutylammonium chloride (TBACl), NPOE, pyridine (PY) and 2,4-dinitrophenol (DNP) were purchased from Fluka and used as received. All aqueous solutions were prepared with deionized water from MilliQ System (Millipore) with 18.2 M Ω .cm resistivity. The organic supporting electrolyte was prepared by metathesis of equimolar quantities of bis-(triphenylphosphoranylidene) ammonium chloride (BTPPACl)

and potassium tetrakis(4-chlorophenyl)borate (KTPBCl) providing a BTPPATPBCl precipitate which was filtered and recrystallized twice from acetone before use. BTPPATPBCl is very lipophilic and therefore gives a wide potential window.

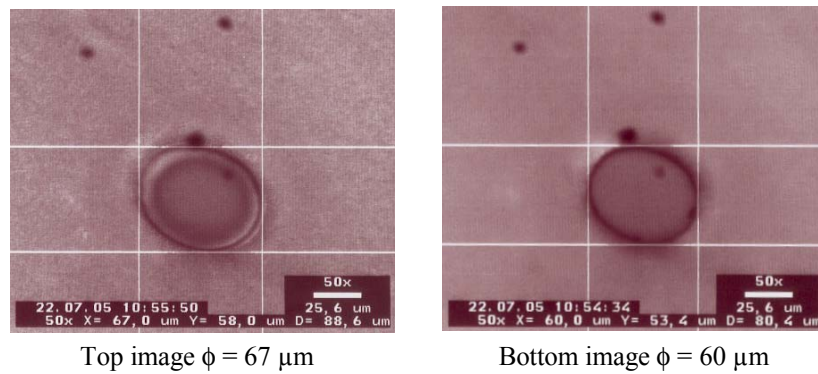
3.2 Setup and electrochemical measurements

A two-electrode cell with an Ag/AgCl working electrode in contact with the aqueous gel and a Ag/AgTPBCl reference electrode in the organic phase were used. A piece of IPG gel of a given pH range was reswelled in a 100 mM LiCl aqueous solution. A 12- μm -thick polyethylene terephthalate (PET) film was coated with a layer of Ag/AgCl (Ercon) screenprinting and the resulting PET/Ag/AgCl electrode was dried for 2 h at 60 °C. In the PET/Ag/AgCl film, micro-holes of $\sim 50 \mu\text{m}$ were drilled by photoablation (UV excimer laser, wavelength 193 nm, energy 200 mJ). The drilled PET/Ag/AgCl film electrode was then placed on the reswelled piece of gel with the silver/silver chloride side in contact with the gel, Ag/AgCl thus acting as the working electrode for the aqueous gel. A droplet of organic phase was then used to cover the micro-hole and thus producing a micro-ITIES. A silver wire coated with silver tetrakis(4-chlorophenyl)borate (Ag/AgTPBCl), obtained by electrolysis of an Ag wire in a KTPBCl solution, was immersed in NPOE acting as the reference electrode for the organic phase. The corresponding setup and the image of the film under the optical microscope are presented in Figure 4.

(a)



(b)



(c)

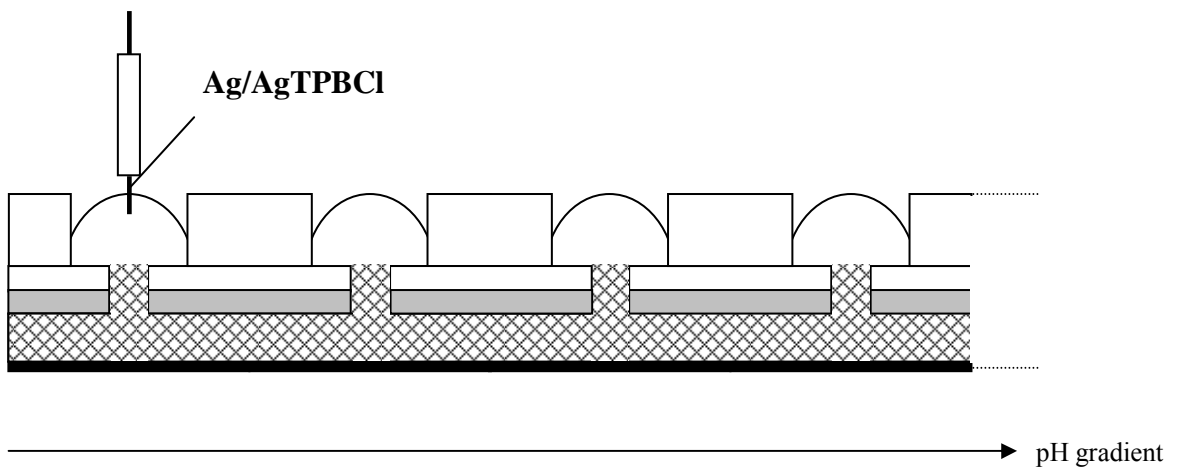


Figure 4: (a) Schematic presentation of the setup for the ITIES measurement at a single micro-hole at pH = 5.35, (b) a micro-hole shape obtained after laser photoablation, seen under optical microscope, (c) complete setup for lipophilicity measurements.

The advantage of the IPG gel in such a setup is that it offers a linear pH gradient, which allows scanning overall the pH domain in one experiment and thus could lead to a high-throughput setup (Figure 4c) to measure partition coefficients. The linearity of the pH gradient has already been verified,³¹ and the geometric position of the micro-hole on the IPG gel strip thus determines, by linearity, the pH of the point where electrochemical measurements take place.

Electrochemical measurements were performed on an Autolab PGSTAT 12 with GPES version 4.9, Eco Chemie B.V. (Netherlands). Differential pulse voltammetry (DPV) was used as electrochemical technique because for some of the drugs, traditional cyclic voltammograms display the peak close to the limit of the potential window, and therefore, it is not an easy task to monitor the displacement of peak potential with pH. The use of a differential pulse technique allows a better sensitivity, allowing the use of lower amounts of drugs for analysis. The presence of a peak instead of a wave also improves the discrimination of the transfer process from that of the base electrolytes. Furthermore, DPV also displays the experimental curves in a way that can be easily subtracted from the baseline, with a further increase in the discrimination against the base electrolytes.

Differential pulse voltammograms were registered after a 30-s equilibration at -500 mV, followed by a scan from -400 mV to $+500$ mV, with a modulation time of 60 ms, an interval time of 400 ms, a step potential of 2 mV, and a modulation amplitude of 50 mV.

3.3 Methodology: use of an internal reference ion

The applied potential difference, E , is theoretically defined as the potential applied between the two reference electrodes and is related to the Galvani potential difference $\Delta_0^w \phi$ across the water/NPOE interface by:

$$E = \Delta_o^w \phi + \Delta E_{\text{ref}} \quad (7.14)$$

where ΔE_{ref} depends on the reference electrodes, so that E refers only to the electrochemical cell used.

To calibrate the transfer potential, it is necessary to define a potential scale. The “TATB” assumption is most commonly used to define the standard Gibbs energy of transfer of an ion through an ITIES.³² Briefly, it states that the cation and anion of tetraphenylarsonium tetraphenylborate (TPAsTPB) have equal standard Gibbs energy of transfer for any pair of solvents, assuming that the solvation energies for both the cation and the anion are equal. On this basis, a scale for standard Gibbs energies of ion transfer and therefore for the standard transfer potential or the formal transfer potential can be obtained. For instance, the formal transfer potential of tetrabutylammonium (TBA^+) at a water/NPOE interface can be estimated as -241.5 mV .²² In the following experiments, TBA^+ and tetramethylammonium (TMA^+) will be used as internal reference ions to transpose the potentials measured to the potential scale on the basis of the “TATB” assumption, by the following relationship

$$E_i^{\text{peak}} - \Delta_o^w \phi_i^{0'} = E_{\text{TBA}^+ \text{ or TMA}^+}^{\text{peak}} - \Delta_o^w \phi_{\text{TBA}^+ \text{ or TMA}^+}^{0'} \quad (7.15)$$

where E_i^{peak} is the peak potential measured by DPV for the transfer of compound i , and $\Delta_o^w \phi_i^{0'}$ is the formal standard transfer potential of compound i .

4. Results and discussion

4.1 Experimental validation of the electrochemical cell based on transfer of simple permanent ions

The following cell I is used to study the transfer of tetrabutylammonium (TBA^+), tetraethylammonium (TEA^+), and TMA⁺ across the aqueous gel/NPOE interface.

Cell I

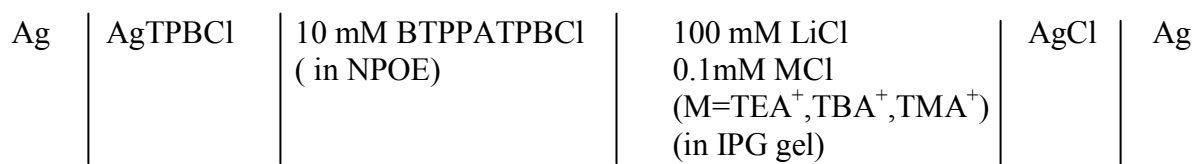


Figure 5 dotted line shows the baseline measured by DPV when LiCl is in the aqueous gel (pH = 4.8), defining the potential window of this electrochemical system. When the pH of the IPG gel is changed, there is no marked effect on the potential window for the differential pulse voltammograms (results not shown). This is also an indication that the acid–base buffer used in the IPG strip manufacturing does not introduce any transferable species into the electrochemical system. The positive side of the voltammogram (water versus organic phase) is limited by the transfer of Li^+ ($\Delta_{\circ}^{\text{w}}\phi_{\text{Li}^+}^{0'} = +576 \text{ mV}^{33}$) and the negative side by the transfer of Cl^- ($\Delta_{\circ}^{\text{w}}\phi_{\text{Cl}^-}^{0'} = -470 \text{ mV}^{34}$). The range of potential window observed is $\sim 700 \text{ mV}$ and is similar to that obtained with a four-electrode setup or other three-electrode setups.

The solid line in Figure 5 shows the resulting DPV when all three ions were dissolved in the aqueous gel and their transfer across the gel/NPOE interface takes place. A higher potential is needed to transfer TEA^+ from the aqueous to the organic phase than to transfer TBA^+ . TBA^+ is thus a less hydrophilic ion than TEA^+ , which is less hydrophilic than TMA^+ .

Based on the “TATB” assumption (see Methodology: use of an internal reference ion), the standard transfer potentials of TEA^+ and TMA^+ can be determined, if taking TBA^+ as internal reference. The value of the standard transfer potential of TBA^+ was determined by Samec et al.²² to be -241.5 mV. The relative transfer potentials measured by DPV for TBA^+ , TEA^+ and TMA^+ are $E_{\text{TBA}^+}^{\text{peak}} = -157$ mV, $E_{\text{TEA}^+}^{\text{peak}} = 109$ mV, and $E_{\text{TMA}^+}^{\text{peak}} = 230$ mV, respectively. The standard transfer potentials of TEA^+ and TMA^+ can be calculated by Equation (7.15) as 24.5 mV and 145.5 mV, respectively, values that are quite close to the values reported in the literature (see Table 1).

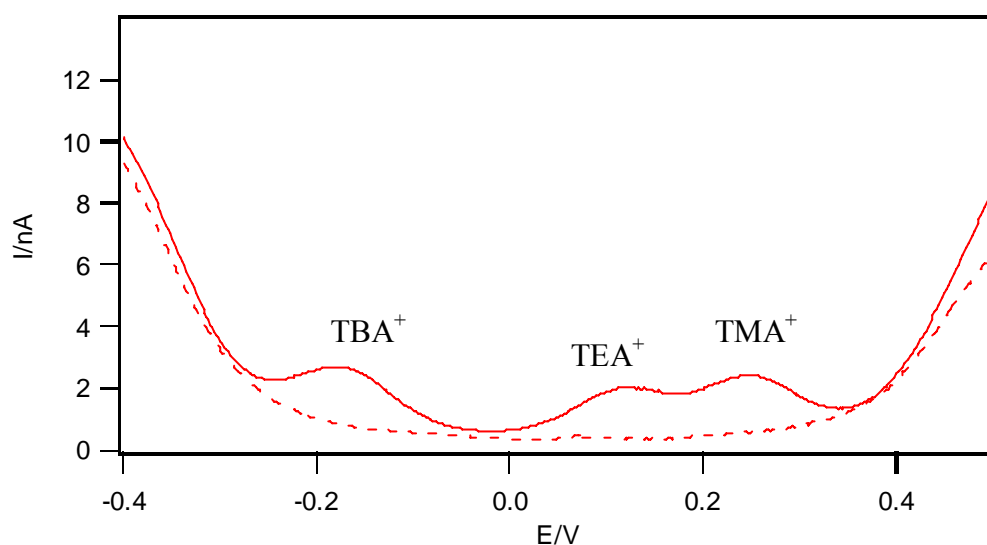


Figure 5: Transfer of TBA^+ , TEA^+ , TMA^+ (solid line) and potential window (dotted line) seen by differential pulse voltammetry (modulation amplitude 50 mV, modulation time 60 ms, interval time 400 ms, step potential 2 mV).

Table 1: Thermodynamic data obtained for the transfer of simple ions at the NPOE/water interface.

	TBA ⁺	TEA ⁺	TMA ⁺
$\Delta_o^w \phi^{0'}$ / mV ^(a)	--	24.5	145.5
$\Delta G_{tr}^{0,w \rightarrow o}$ / kJ.mol ⁻¹ ^(a)	--	2.4	14.0
$\Delta_o^w \phi^{0'}$ / mV ^(b)	-241.5	27	111
$\Delta G_{tr}^{0,w \rightarrow o}$ / kJ.mol ⁻¹ ^(b)	-23.3	2.6	10.7
$\Delta_o^w \phi^{0'}$ / mV ^(c)	--	26	140
$\Delta G_{tr}^{0,w \rightarrow o}$ / kJ.mol ⁻¹ ^(c)	--	2.5	13.5

(a) according to this work , (b) according to Samec et al.²² , (c) according to Wilke et al.¹⁸

The results show that the present two-electrode electrochemical cell is validated and can be used, in an easy and fast way, to measure the standard transfer potential for simple permanent ions. It also indicates that for simple and permanent ions, the hydration in the aqueous gel medium is similar to that in free aqueous solution, and that for these ions, the interface between aqueous gel and NPOE behaves like a water/NPOE interface.

4.2 Ionic partition diagram of ionizable compounds

Ionic partition diagrams were first developed by Reymond et al.⁸ as a representation of the predominance area of the various species of an ionizable compound as a function of the Galvani potential difference and the pH and taking into account the thermodynamic equilibrium governing the distribution of various acid/base forms of molecules involved. Two adjacent areas of predominance are separated by equiconcentration boundary lines. These diagrams have shown to be a useful tool to predict and interpret the transfer mechanisms of ionizable drugs at the ITIES and their concept is similar to the potential–pH diagrams of metals (Pourbaix diagrams). Initial studies were dedicated to drawing ionic partition diagrams for hydrophilic ionizable compounds, but more recent studies by Gobry et al.¹³ have extended this partition diagram model to lipophilic species. For lipophilic molecules, the concentration

of the neutral form in the aqueous phase is negligible compared to that in the organic phase, and ionic partition diagrams displaying the neutral species in water as was the case for hydrophilic diagrams, are less relevant in the case of lipophilic molecules. The new model for lipophilic compounds takes into account the neutral species in the organic phase when deriving the equations defining the boundary lines.

As shown previously,¹³ for a lipophilic monobase B partitioned between two immiscible phases, the ionic partition diagram is determined by three boundary lines (equiconcentration convention):

$$\text{Line 1: } \Delta_o^w \phi = \Delta_o^w \phi_{\text{BH}^+}^{0'} \quad (7.16)$$

$$\text{Line 2: } \text{pH} = \text{p}K_a - \log P_B^0 \quad (7.17)$$

$$\text{Line 3: } \Delta_o^w \phi = \Delta_o^w \phi_{\text{BH}^+}^{0'} + \frac{2.3RT}{F}(\log P_B^0 - \text{p}K_a) + \frac{2.3RT}{F} \text{pH} \quad (7.18)$$

For a lipophilic monoacid AH partition between two immiscible phases, the ionic partition diagram is determined by the following boundary lines (equiconcentration convention)¹³:

$$\text{Line 1: } \Delta_o^w \phi = \Delta_o^w \phi_{\text{A}^-}^{0'} \quad (7.19)$$

$$\text{Line 2: } \text{pH} = \text{p}K_a + \log P_B^0 \quad (7.20)$$

$$\text{Line 3: } \Delta_o^w \phi = \Delta_o^w \phi_{\text{A}^-}^{0'} - \frac{2.3RT}{F}(\log P_{\text{AH}}^0 + \text{p}K_a) + \frac{2.3RT}{F} \text{pH} \quad (7.21)$$

As an illustration of the methodology using the two electrode gel cell described above, a monobase, pyridine, and a monoacid, 2,4-dinitrophenol, were investigated by DPV. Cell II is used to study the transfer of the two drugs across the IPG gel/NPOE interface at different pH values, to evaluate their standard transfer potentials and partition coefficients and draw their ionic partition diagrams.

Cell II

Ag	AgTPBCl	10 mM BTTPPATPBCl (in NPOE) 0.6 mM PY or 1.13 mM DNP	100 mM LiCl 1 mM MCl (in IPG gel)	AgCl	Ag
----	---------	--	---	------	----

and $M^+ = TBA^+$ for PY and TMA^+ for DNP.

In each case, small amounts of drugs were added to the organic phase, the volume of the droplet of organic phase needed was 3 μ L. TBA^+ was added to the gel phase to work as internal reference when pyridine was studied and TMA^+ when 2,4-dinitrophenol was studied.

Figure 6 shows the evolution of the voltammograms obtained by DPV for pyridine at different pH. For pH values below the pK_a , the standard transfer potential remains independent of the pH (within experimental error) and represents the transfer of protonated pyridine (PyH^+). The peak current decreases as the pH approaches the pK_a , following the decrease in the concentration of PyH^+ . When the pH is higher than the pK_a , the half-wave transfer potential observed shifts toward higher values as can be observed in Figure 6. The peak current is the result of the transfer of a proton facilitated by the neutral pyridine present in the organic phase, and which behaves as an ionophore for the proton. The transfer is limited by the proton concentration, which explains the shift of potential toward higher values (in theory the potential shifts by $2.3RT/zF$ mV per pH unit. Here, one proton is transferred, thus the slope is 59 mV/pH unit). In this case, the mechanism can be described as a transfer by interfacial complexation (TIC).³⁵ In addition, Figure 6 shows that it becomes more difficult to monitor the transfer peak at higher pH, as it is shifting toward the limit of the potential window. This case proves the relevance of using DPV as the electrochemical technique, as it allows subtracting the baseline from the voltammogram measured, thus allowing a better peak discrimination against the base electrolytes.

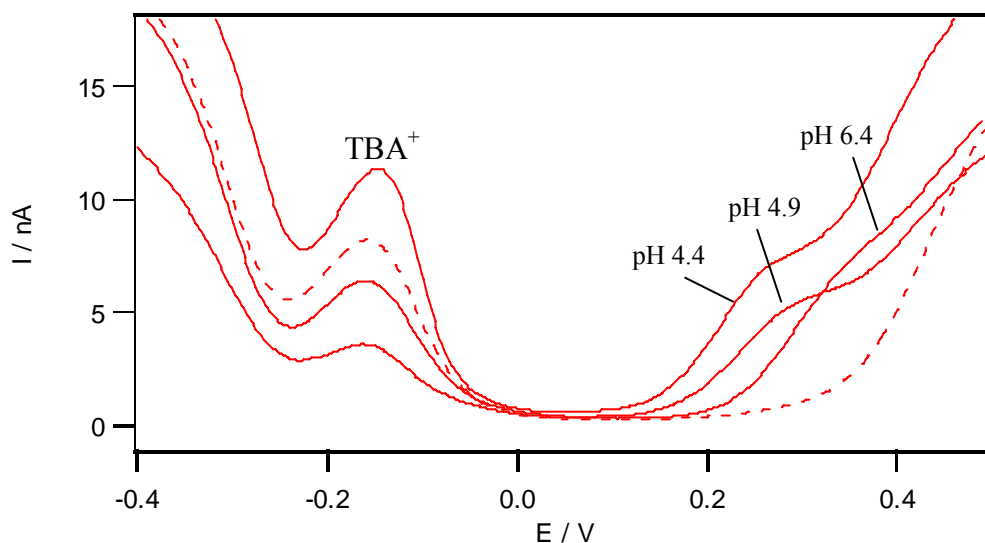


Figure 6: Differential pulse voltammograms representing the transfer for pyridine at the IPG gel/NPOE interface at pH 4.4, 4.9 and 6.4 (solid lines). All the voltammograms are referenced against TBA^+ which was added to the gel phase in the electrochemical cell. The dotted line is the baseline measured in presence of TBA^+ only. (DPV parameters: modulation amplitude 50 mV, modulation time 60 ms, interval time 400 ms, step potential 2 mV).

As shown in Figure 7, the experimental results obtained using DPV at different aqueous pHs can be used to draw the ionic partition diagrams for pyridine (Figure 7a) and for 2,4-dinitrophenol (Figure 7b). For 2,4-dinitrophenol, the processes describing the transfer are similar to the ones described above. For pH values below the $\text{p}K_a$, 2,4-dinitrophenol is in its neutral form (DnpH). Present in the organic phase, it behaves as an ionophore for proton, the assisted proton transfer is thus described as a transfer by interfacial dissociation (TID)³⁵, the potential shifts by 59 mV/pH unit. For pH values higher than the $\text{p}K_a$, the transfer of the deprotonated drug (Dnp^-) is observed and the transfer potential remains independent of the pH.

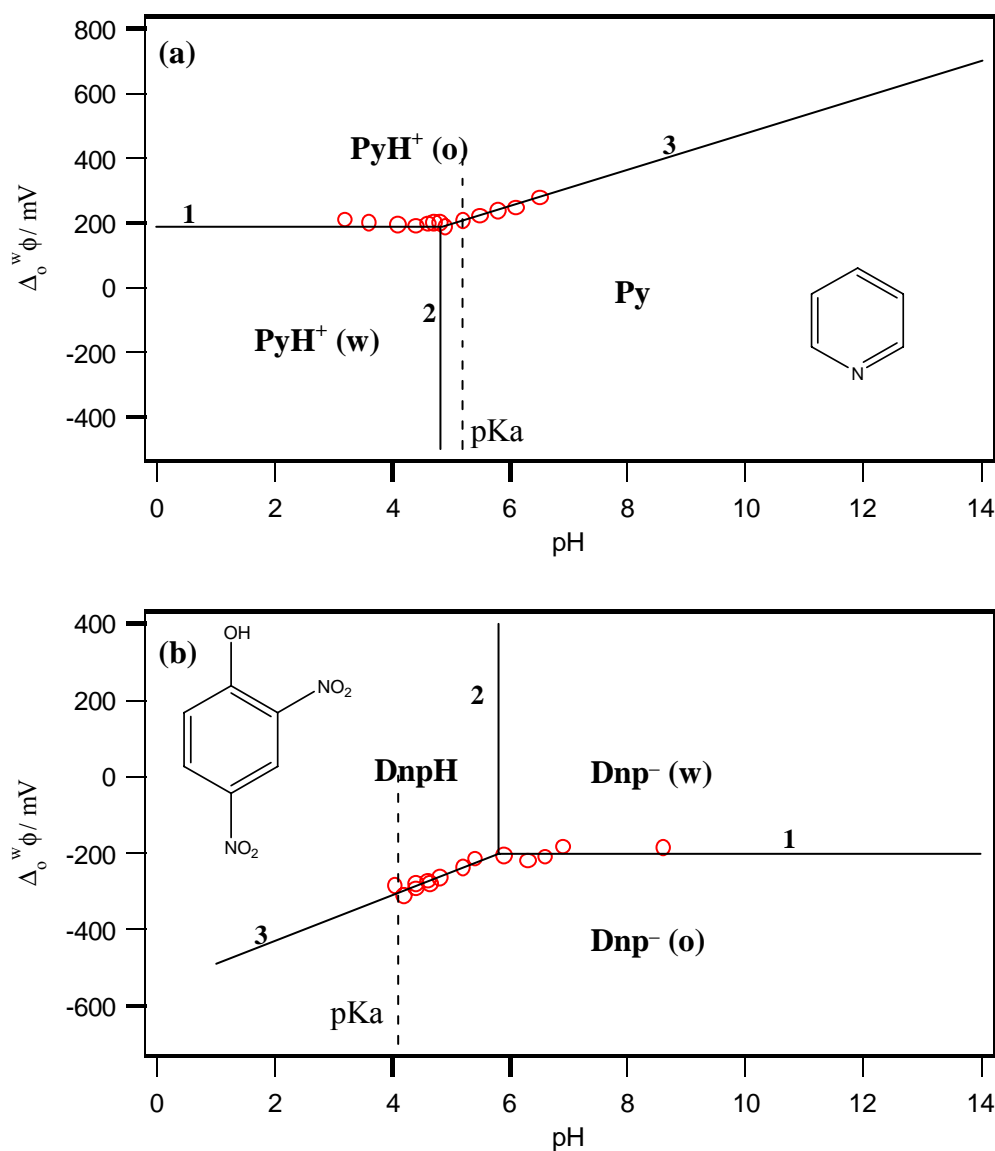


Figure 7: Ionic partition diagrams of (a) pyridine PY (0.6 mM) and (b) 2,4-dinitrophenol DNP (1.13 mM) at the IPG gel/NPOE interface. The dotted lines show the aqueous pK_a value of each compound under study. Equations for lines 1, 2 and 3 are displayed in the text.

For the monobase pyridine, the diagram in Figure 7a shows that, for pH values below the pK_a , the transfer potential measured for the protonated drug remains constant. We can thus obtain the values of the standard transfer potential, the Gibbs energy of transfer, and the

standard partition coefficient of the ionized forms from the DPV and Equations (7.22) and (7.23).

$$\Delta_o^w \phi^{0'} = \frac{\Delta G_{tr}^{0,w \rightarrow o}}{zF} \quad (7.22)$$

$$\log P^0 = -\frac{\Delta G_{tr}^{0,w \rightarrow o}}{2.3RT} \quad (7.23)$$

For the monoacid 2,4-dinitrophenol (Figure 7b) the values of the standard Gibbs energy of transfer and standard partition coefficient of the ionized form can be obtained for pH values higher than the pK_a and from the DPV and Equations (7.22) and (7.23) as well. The thermodynamic data obtained for the two drugs are summarized in Table 2 and are comparable to literature values.

Both diagrams shown in Figure 7 illustrate the shift in pK_a for the vertical line (dotted lines), as predicted for lipophilic compounds. The effective pK_a measured give access to the partition coefficient of the neutral species. For 2,4-dinitrophenol, knowing the aqueous acidic constant ($pK_a = 4.10$), and measuring an effective pK_a of 5.8, the above theory predicts a value of 1.7 for $\log P_{AH}$ of the neutral compound, which is quite close to values measured by Ulmeanu et al.¹⁴ who used cyclic voltammetry and potentiometry. For pyridine, the $\log P_B$ of the neutral compound is estimated to be 0.3, which is comparable to the value measured by Liu et al.⁵ who used potentiometry and the shake flask method. As summarized in Table 2, standard transfer potential values and standard partition coefficients for neutral as well as ionized species can be easily and rapidly deduced from our voltammetric measurements. One problem encountered when performing the measurements was that the reswelled gel would dry faster under higher temperatures, thus disturbing the reproducibility of the measurements and slightly shifting the potential window compared to the baseline. Thus, measurements had to be done in a short time, to avoid the gel drying too much. The conception of a new and

closed setup, where water is constantly provided to reswell the gel would be a solution to this problem.

Table 2: Thermodynamic data obtained for the transfer of ionizable compounds at the NPOE/water interface.

	Pyridine	2,4-dinitrophenol
pK_a	5.16 ^(a)	4.1 ^(b)
$\Delta_o^w \phi^{0'}$ / mV (in NPOE)	190 ^(*)	-200 ^(*)
$\Delta G_{tr}^{0,w \rightarrow \text{NPOE}}$ / kJ.mol ⁻¹	18.3 ^(*)	-18.4 ^(*)
$\log P_{\text{NPOE}}^0$ (ionised)	-3.2 ^(*)	-3.4 ^(*) -2.23 ^(b)
$\log P_{\text{NPOE}}$ (neutral)	0.3 ^(*) 0.26 ^(c)	1.7 ^(*) 2.0 ^(b)

(a) according to Reymond et al.², (b) according to Ulmeanu et al.¹⁴, (c) according to Liu et al.⁵, (*) according to this work

5. Conclusions

The electrochemical behavior of two ionizable drugs has been investigated with a two-electrode gel cell. This setup offers a fast and easy way to measure standard transfer potential for simple permanent ions as well as for ionizable drug compounds, as preparation of the electrochemical cell is simple, there is no need to adjust the pH of aqueous phase as it is determined by a commercial IPG gel. In addition, results obtained with this two-electrode setup are comparable to those obtained with classical L/L systems and it is relevant to notice that only small amounts of organic phase, hence of drugs, were needed. The values of the standard transfer potential, the Gibbs energy of transfer, and the partition coefficients for the ionized and neutral forms of these drugs are evaluated by differential pulse voltammetry. This technique has proven to be superior to cyclic voltammetry for monitoring ion transfer, especially when the peak is close to the limit of the potential window, as is often the case for extreme pH values. The experimental results are presented in the form of ionic partition diagrams that allow predicting which form of an ionizable solute will transfer across the L/L

interface under given conditions of potential and pH. From the pH–potential diagram, it is possible to evaluate the $\log(P)$ of the neutral species from the shift of pK_a observed. Studies on drug transfer mechanisms are of great significance for the understanding of L/L interfaces and drug disposition.

This initial study was done with the perspective to integrate an on-line extraction of proteins and peptides during the OFFGEL electrophoresis of proteins or peptides, to allow a continuous loading of the sample while avoiding protein precipitation or aggregation. Once the micro-electrochemical system validated for ionizable compounds, the next step would be to investigate the transfer of proteins and peptides across the liquid-liquid interface.

6. References

1. Reymond, F.; Fermin, D.; Lee, H. J.; Girault, H. H., Electrochemistry at liquid/liquid interfaces: methodology and potential applications. *Electrochimica Acta* **2000**, *45*, (15-16), 2647-2662.
2. Reymond, F.; Chopineaux-Courtois, V.; Steyaert, G.; Bouchard, G.; Carrupt, P. A.; Testa, B.; Girault, H. H., Ionic partition diagrams of ionisable drugs: pH-lipophilicity profiles, transfer mechanisms and charge effects on solvation. *Journal of Electroanalytical Chemistry* **1999**, *462*, (2), 235-250.
3. Qian, Q. S.; Wilson, G. S.; Bowman-James, K.; Girault, H. H., MicroITIES detection of nitrate by facilitated ion transfer. *Analytical Chemistry* **2001**, *73*, (3), 497-503.
4. Beni, V.; Ghita, M.; Arrigan, D. W. M., Cyclic and pulse voltammetry study of dopamine at the interface between two immiscible electrolyte solutions. *Biosensors and Bioelectronics* **2005**, *20*, 2097-2103.
5. Liu, X.; Bouchard, G.; Girault, H. H.; Testa, B.; Carrupt, P. A., Partition Coefficients of Ionizable Compounds in o-Nitrophenyl Octyl Ether/Water Measured by the Potentiometric Method. *Analytical chemistry* **2003**, *75*, 7036.
6. Bouchard, G.; Galland, A.; Carrupt, P. A.; Gulaboski, R.; Mirceski, V.; Scholz, F.; Girault, H. H., Standard partition coefficients of anionic drugs in the n-octanol/water system determined by voltammetry at three-phase electrodes. *Physical Chemistry Chemical Physics* **2003**, *5*, (17), 3748-3751.
7. Samec, Z.; Marecek, V.; Koryta, J.; Khalil, M. W., Investigation of Ion Transfer across Interface between 2 Immiscible Electrolyte-Solutions by Cyclic Voltammetry. *Journal of Electroanalytical Chemistry* **1977**, *83*, (2), 393-397.
8. Reymond, F.; Steyaert, G.; Carrupt, P. A.; Testa, B.; Girault, H., Ionic partition diagrams: A Potential pH representation. *Journal of the American Chemical Society* **1996**, *118*, (47), 11951-11957.
9. Stewart, A. A.; Taylor, G.; Girault, H. H.; Mcaleer, J., Voltammetry at Microities Supported at the Tip of a Micropipette .1. Linear Sweep Voltammetry. *Journal of Electroanalytical Chemistry* **1990**, *296*, (2), 491-515.
10. Stewart, A. A.; Shao, Y.; Pereira, C. M.; Girault, H. H., Micropipette as a Tool for the Determination of the Ionic Species Limiting the Potential Window at Liquid Liquid Interfaces. *Journal of Electroanalytical Chemistry* **1991**, *305*, (1), 135-139.
11. Nakatani, K.; Sudo, M.; Kitamura, N., A Study on Liquid-Liquid Distribution Based on Single Picoliter Droplets and in Situ Electrochemical Measurements. *Analytical chemistry* **2000**, *72*, 339-342.
12. Ulmeanu, S.; Lee, H. J.; Fermin, D. J.; Girault, H. H.; Shao, Y. H., Voltammetry at a liquid-liquid interface supported on a metallic electrode. *Electrochemistry Communications* **2001**, *3*, (5), 219-223.
13. Gobry, V.; Ulmeanu, S.; Reymond, F.; Bouchard, G.; Carrupt, P. A.; Testa, B.; Girault, H. H., Generalization of ionic partition diagrams to lipophilic compounds and to biphasic systems with variable phase volume ratios. *Journal of the American Chemical Society* **2001**, *123*, (43), 10684-10690.
14. Ulmeanu, S. M.; Jensen, H.; Bouchard, G.; Carrupt, P. A.; Girault, H. H., Water-oil partition profiling of ionized drug molecules using cyclic voltammetry and a 96-well microfilter plate system. *Pharmaceutical Research* **2003**, *20*, (8), 1317-1322.
15. Zhang, M. Q.; Sun, P.; Chen, Y.; Li, F.; Gao, Z.; Shao, Y. H., Studies of effect of phase volume ratio on transfer of ionizable species across the water/1,2-dichloroethane interface by a three-electrode setup. *Analytical Chemistry* **2003**, *75*, (16), 4341-4345.

16. Smith, D. A.; van de Waterbeemd, H., Pharmacokinetics and metabolism in early drug discovery. *Current Opinion in Chemical Biology* **1999**, 3, (4), 373-378.
17. Reymond, F.; Carrupt, P. A.; Testa, B.; Girault, H. H., Charge and delocalisation effects on the lipophilicity of protonable drugs. *Chemistry-a European Journal* **1999**, 5, (1), 39-47.
18. Wilke, S.; Zerihun, T., Standard Gibbs energy of ion transfer across the water vertical bar 2-nitrophenyl octyl ether surface. *Journal of Electroanalytical Chemistry* **2001**, 515, 52-60.
19. Samec, Z.; Langmaier, J.; Trojanek, A.; Samcova, E.; Malek, J., Transfer of protonated anesthetics across the water o-nitrophenyl octyl ether interface: Effect of the ion structure on the transfer kinetics and pharmacological activity. *Analytical Sciences* **1998**, 14, (1), 35-41.
20. Liu, X.; Bouchard, G.; Müller, N.; Galland, A.; Girault, H. H.; Testa, B.; Carrupt, P. A., Solvatochromic analysis of partition coefficients in the o-Nitrophenyl Octyl Ether. *Helvetica Chimica Acta* **2003**, 86, 3533.
21. Gulaboski, R.; Galland, A.; Bouchard, G.; Caban, K.; Kretschmer, A.; Carrupt, P. A.; Stojek, Z.; Girault, H. H.; Scholz, F., A comparison of the solvation properties of 2-nitrophenyloctyl ether, nitrobenzene, and n-octanol as assessed by ion transfer experiments. *Journal of Physical Chemistry B* **2004**, 108, (14), 4565-4572.
22. Samec, Z.; Langmaier, J.; Trojanek, A., Polarization phenomena at the water/o-nitrophenyl octyl ether interface .1. Evaluation of the standard Gibbs energies of ion transfer from the solubility and voltammetric measurements. *Journal of Electroanalytical Chemistry* **1996**, 409, (1-2), 1-7.
23. Gorg, A.; Obermaier, C.; Boguth, G.; Harder, A.; Scheibe, B.; Wildgruber, R.; Weiss, W., The current state of two-dimensional electrophoresis with immobilized pH gradients. *Electrophoresis* **2000**, 21, (6), 1037-1053.
24. Michel, P. E.; Reymond, F.; Arnaud, I. L.; Josserand, J.; Girault, H. H.; Rossier, J. S., Protein fractionation in a multicompartiment device using Off-Gel (TM) isoelectric focusing. *Electrophoresis* **2003**, 24, (1-2), 3-11.
25. Arnaud, I.; Abid, J. P.; Roussel, C.; Girault, H. H., Size-selective separation of gold nanoparticles using isoelectric focusing electrophoresis (IEF). *Chemical Communications* **2005**, 6, (6), 787-788.
26. Fantini, S.; Clohessy, J.; Gorgy, K.; Fusalba, F.; Johans, C.; Kontturi, K.; Cunnane, V. J., Influence of the presence of a gel in the water phase on the electrochemical transfer of ionic forms of beta-blockers across a large water vertical bar 1,2-dichloroethane interface. *European Journal of Pharmaceutical Sciences* **2003**, 18, (3-4), 251-257.
27. Koryta, J., Electrochemical Polarization Phenomena at the Interface of 2 Immiscible Electrolyte-Solutions. *Electrochimica Acta* **1979**, 24, (3), 293-300.
28. Shao, Y.; Osborne, M. D.; Girault, H. H., Assisted Ion Transfer at Micro-Ities Supported at the Tip of Micropipettes. *Journal of Electroanalytical Chemistry* **1991**, 318, (1-2), 101-109.
29. <http://www.epsilon-web.net/EC/manual/Techniques/Pulse/pulse.html>.
30. Bjellqvist, B.; Ek, K.; Righetti, P. G.; Gianazza, E.; Gorg, A.; Westermeier, R.; Postel, W., Isoelectric-Focusing in Immobilized Ph Gradients - Principle, Methodology and Some Applications. *Journal of Biochemical and Biophysical Methods* **1982**, 6, (4), 317-339.
31. DiMaio, I., Characterisation of a novel isoelectric focusing fractionation method. *PhD thesis 3064* **2004**, 51.
32. Parker, A. J., Protic-Dipolar Aprotic Solvent Effects on Rates of Bimolecular Reactions. *Chemical Reviews* **1969**, 69, (1), 1-&.

33. Shao, Y. H.; Weber, S. G., Direct observation of chloride transfer across the water/organic interface and the transfer of long-chain dicarboxylates. *Journal of Physical Chemistry* **1996**, 100, (35), 14714-14720.
34. Shao, Y.; Stewart, A. A.; Girault, H. H., Determination of the Half-Wave Potential of the Species Limiting the Potential Window - Measurement of Gibbs Transfer Energies at the Water 1,2-Dichloroethane Interface. *Journal of the Chemical Society-Faraday Transactions* **1991**, 87, (16), 2593-2597.
35. Shao, Y.; Osborne, M. D.; Girault, H. H., Assisted ion transfer at micro-ITIES supported at the tip of micropipettes. *Journal of Electroanalytical Chemistry* **1991**, 318, 101-109.

CHAPTER VIII: *Conclusions and perspectives*

In the present work, two systems have been designed for isoelectric focusing of proteins and peptides. The main objectives were to design, characterize and validate these devices for the prefractionation of biological samples.

The first device is a multicompartment unit for OFFGEL IEF, using commercial immobilized pH gradient gel strips, with the advantage of allowing the direct recovery in solution of fractionated sample. This feature is of high relevance, considering that the focusing step is used only as a prefractionation step, and that further analyses require liquid fractions, namely liquid chromatography or mass spectrometry. The design of this device was inspired from computer simulation results.

The numerical calculations modeled the isoelectric focusing of peptides in an OFFGEL device. The evolution of the peak width and focusing time was studied as a function of charge gradient at pI . The trends observed allowed predicting the peak width for focused peptides from three proteomes. This allowed drawing a conclusion on the well width in the multicompartment device, in order to obtain high resolution separation of peptides: it was shown that wells of 6-7 mm width should lead to the recovery of peptides in two wells at most. In addition to the design of a separation unit, the simulations allowed a better understanding of the kinetics, by visualizing the two processes underlying OFFGEL IEF: the separation of peptides in the gel, and the diffusion into the solution.

The homemade OFFGEL separation cell was then tested in terms of pH reproducibility, loading capacity for proteins, resolution of the separation of peptides and separation of *E. coli* protein extract. The pH measured in the liquid fractions showed a good reproducibility, thus also demonstrating an efficient buffering of the solution, propitious for high resolution IEF. A loading of ~6 mg of proteins was estimated to be the limit of loading for this device; decrease in resolution and separation quality should be expected when

applying a higher quantity of sample. This value of loading is dependent on the quality of the sample, the voltage program and the duration of voltage program. The fractionation of peptides with this device was then validated and showed a good resolution, with only few peptides being recovered in two fractions. The application of this device for the prefractionation of a more complex sample was finally validated.

One direction also explored in this thesis was the integration of OFFGEL IEF in a proteomics workflow. The device was used to separate peptides generated from protein digest. Each fraction was then subjected to chemical tagging. The information obtained from the OFFGEL IEF (pI) and from the chemical tagging (number of cysteines) could be combined to enhance protein identification by peptide mass fingerprinting. Results show that the pI is a powerful tool for eliminating false positive identifications, and that OFFGEL IEF is thus of high relevance as a first dimension separation. This study also pointed out the need for high resolution IEF of peptides, as well as more sophisticated pI calculation algorithms, in order to use the pI information to validate/filter peptide identifications. The chemical labeling was shown to enhance identification scores. The development of new TiO_2 matrices for MALDI-MS analysis and chemical labeling opens new possibilities for peptide analysis. More experiments on more complex mixtures would show the high-throughput of the method proposed.

The other technical development concerns the design of a completely gel-free membrane-sealed device for prefractionation of biological mixture. The original aspect of the device is the possibility of double configuration all-in-one device: one configuration for the focusing (the membrane allows liquid flowing), and one for the collection of fractions at the end of focusing (the membrane seals the compartments, making each of them independent from one another). Focusing in this unit necessitates the use of carrier ampholytes to form and maintain the pH gradient. The device was characterized in terms of pH formation and

stability. The establishment of the pH gradient is fast (15 min), and is a good indication to estimate the separation time needed. The separation of human cancer cells and *E. coli* protein extract validates the use of this gel-free device for prefractionation of proteomes. The separation is fast (one hour ensures already a good separation) compared to the long time required with the OFFGEL device (6 hours at least). However, the quality of the separation is probably not comparable: this device is predicted to be more suited for prefractionation of proteins than for high resolution fractionation of peptides, though this needs to be confirmed. However, both devices require small sample volumes (~1 mL), are compact and easy of use.

The last part of this work was devoted to the design of an electrochemical cell for the study of the transfer of ionizable molecules across the interface between two immiscible phases: an aqueous phase (IPG gel reswelled in water) and an organic phase (NPOE). The three-electrode cell was validated for the transfer of pyridine and 1,4-dinitrophenol. A future work would be to use this cell for the transfer of peptides or proteins, with the ultimate goal to perform online extraction of proteins/peptides during IEF, to increase sample loading and allow continuous separation.

One interesting perspective concerning the use of OFFGEL IEF is the isolation and detection of post-translational modifications (PTMs), namely phosphorylated peptides and acetylated peptides. Indeed, the use of *pI* for the validation/filtering of peptides has shown to be a powerful tool to provide with more accurate identifications. However, this physicochemical property has not yet been exploited to its full potential. Some groups have already investigated on the fact that a PTM induces *pI* shifts, which can be used to isolate a subpopulation of peptides by IEF, namely phosphopeptides. But this approach could be used for any chemical modification of the peptide.

In the example of phosphopeptides, the phosphorylation (covalent attachment of negatively charged phosphate groups mainly on the neutral hydroxyl groups of serines,

threonines and tyrosines) inherently decreases the pI of a peptide compared to the non-phosphorylated peptide, but there is no clear cut off between phosphorylated (PP)-peptides and non-phosphorylated (non-PP)-peptides, because of the variable numbers of acidic residues D and E in a peptide, which mask this difference. To induce a higher pI difference, the methylation reaction is used. Indeed, it transforms the acid residues in a peptide (glutamic acid, aspartic acid and C-terminus) into methyl esters. The pI difference between methylated PP-peptides ($pI < 7.4$) and methylated non-PP-peptides ($pI > 9$) can then be used to isolate phosphorylated peptides from others by high resolution IEF.

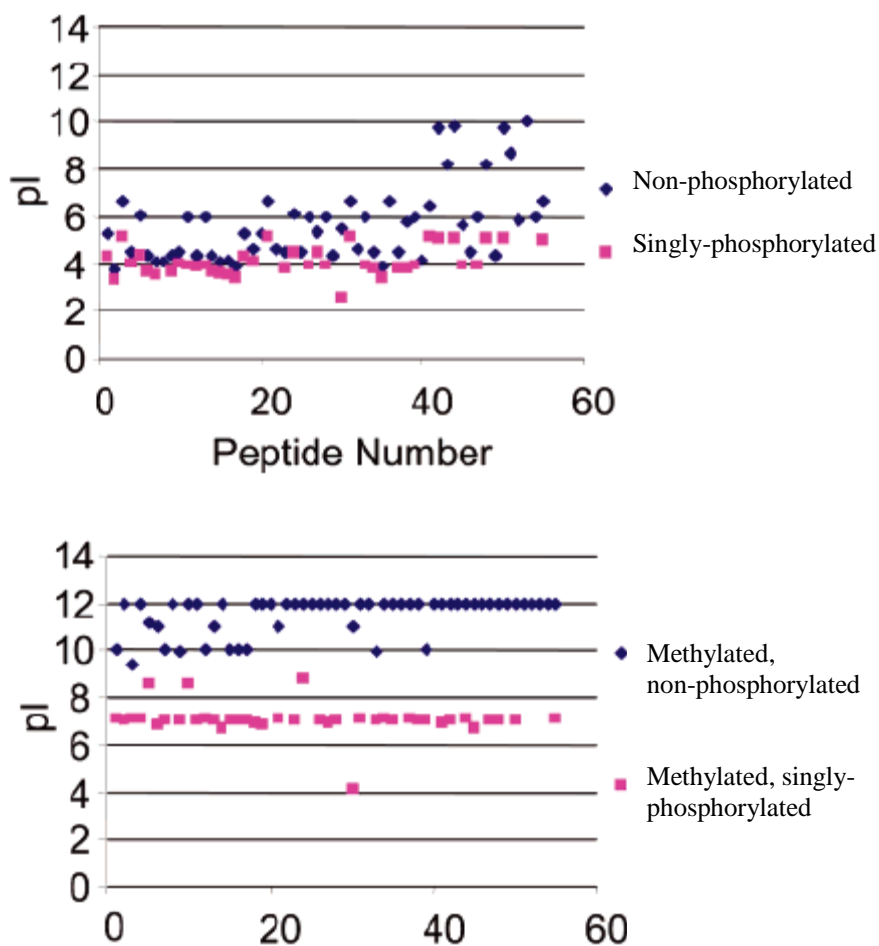


Figure 1: Calculated pI values for BSA tryptic peptides, from Xu et al. (Journal of Proteome Research 2007, 6, 1153-1157).

Appendix I: Buffer capacity of ampholytes

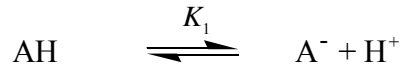
The buffer capacity β is defined as the amount of acid or base necessary to change the pH by one unit. If a concentration of base c_B is added, β is written as:

$$\beta = \frac{dc_B}{d(\text{pH})} \quad (\text{I.1})$$

The higher the buffer capacity of an ampholyte, the better its buffering power (meaning the change in pH is not so much affected by the addition of acid or base).

Monovalent ampholytes

If we consider a monovalent ampholyte:



The dissociation constant can be written as follows:

$$K_1 = \frac{c_{\text{A}^-} c_{\text{H}^+}}{c_{\text{AH}}} \quad (\text{I.2})$$

Noting the total concentration of the ampholyte, $c_{\text{tot}} = c_{\text{AH}} + c_{\text{A}^-}$, and combining with the dissociation constant, we can derive:

$$c_{\text{A}^-} = K_1 c_{\text{tot}} / (c_{\text{H}^+} + K_1) \quad (\text{I.3})$$

$$c_{\text{AH}} = c_{\text{H}^+} c_{\text{tot}} / (c_{\text{H}^+} + K_1) \quad (\text{I.4})$$

The charge balance of the monoacid, to which a certain amount of base (for example NaOH) is added, follows as:

$$c_{\text{H}^+} + c_{\text{Na}^+} = c_{\text{A}^-} + c_{\text{OH}^-} \quad (\text{I.5})$$

For pH between 4 and 10, the dissociation of water is negligible, with respect to the concentration of the monoacid. Equation (I.5) is thus simplified as:

$$c_B = c_{Na^+} = c_{A^-} \quad (I.6)$$

As written in equation (I.3), the concentration of base is thus:

$$c_B = \frac{K_1 c_{tot}}{c_{H^+} + K_1} \quad (I.7)$$

Thus the buffering capacity can be calculated by deriving the previous equation:

$$\beta = \frac{dc_B}{d(\text{pH})} = \ln 10 \frac{K_1 c_{tot} c_{H^+}}{(c_{H^+} + K_1)^2} \quad (I.8)$$

The maximal buffer capacity is given by the condition $\frac{d\beta}{d(\text{pH})} = 0$, which gives only one

solution: $c_{H^+} = K_1$

The maximal buffer capacity for a monovalent ampholyte is thus:

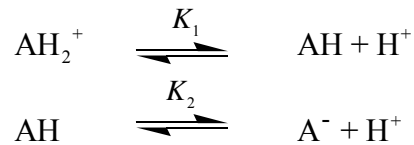
$$\beta_{\text{mono}} = \frac{\ln 10 c_{tot}}{4} \quad (I.9)$$

And the maximal molar buffer capacity is:

$$B_{\text{mono}} = \frac{\ln 10}{4} \quad (I.10)$$

Bivalent ampholytes

If we consider a biprotic ampholyte:



The two dissociation constants associated to these reactions can be written as follows:

$$K_1 = \frac{c_{AH} c_{H^+}}{c_{AH_2^+}} \quad (I.11)$$

$$K_2 = \frac{c_{A^-} c_{H^+}}{c_{AH}} \quad (I.12)$$

From the dissociation constants, we can derive:

$$c_{AH_2^+} = c_{H^+} c_{AH} / K_1 \quad (I.13)$$

$$c_{A^-} = K_2 c_{AH} / c_{H^+} \quad (I.14)$$

The total concentration c_{tot} of the ampholyte is noted:

$$c_{tot} = c_{AH_2^+} + c_{AH} + c_{A^-} \quad (I.15)$$

By adding the two equations together with c_{AH} to obtain the total concentration, the concentration of the three species can be deduced:

$$c_{AH_2^+} = c_{H^+}^2 c_{tot} / (c_{H^+}^2 + c_{H^+} K_1 + K_1 K_2) \quad (I.16)$$

$$c_{AH} = c_{H^+} K_1 c_{tot} / (c_{H^+}^2 + c_{H^+} K_1 + K_1 K_2) \quad (I.17)$$

$$c_{A^-} = K_1 K_2 c_{tot} / (c_{H^+}^2 + c_{H^+} K_1 + K_1 K_2) \quad (I.18)$$

The charge balance for the ampholyte solution to which a certain amount of base c_B is added, can be written as (if neglecting water dissociation):

$$c_B + c_{AH_2^+} = c_{A^-} \quad (I.19)$$

Combining Equation (I.16) and Equation (I.18), the base concentration can be expressed as:

$$c_B = \frac{c_{tot} (K_1 K_2 - c_{H^+}^2)}{c_{H^+}^2 + c_{H^+} K_1 + K_1 K_2} \quad (I.20)$$

Differentiation of c_B leads to β :

$$\beta = \frac{dc_B}{d(pH)} = \frac{\ln 10 c_{tot} K_1 c_{H^+} (K_1 K_2 + 4c_{H^+} K_2 + c_{H^+}^2)}{(c_{H^+}^2 + c_{H^+} K_1 + K_1 K_2)^2} \quad (I.21)$$

At the isoelectric point, we obtain the following expression for the molar buffer capacity:

$$B_i = \frac{\ln 10}{1 + \sqrt{K_1 / 4K_2}} \quad (I.22)$$

The molar buffer capacity for a monovalent ampholyte was shown to be $B_{mono} = \ln 10 / 4$.

Division of Equation (I.22) by Equation (I.10) gives the **relative molar buffer capacity** at the

isoelectric point, i.e. the capacity in units of the maximum molar buffer capacity of a monovalent ampholyte:

$$B_{i,\text{rel}} = \frac{4}{1 + \sqrt{K_1 / 4K_2}} \quad (\text{I.23})$$

This ratio must be smaller than 2, because the bivalent ampholyte cannot be a better buffering ampholyte than the monovalent ampholyte. This leads to the conditions:

$$K_1 \geq 4K_2 \quad \text{and} \quad \Delta pK \geq \log 4 \approx 0.6 \quad (\text{I.24})$$

where pK_1 and pK_2 are the dissociation constants of the acid and basic groups, respectively.

The buffer capacity of carrier ampholytes at and near their isoelectric point is important, because they should exhibit a buffer action stronger than that of the proteins and therefore dictate the pH gradient.

Appendix II: Table of pKa

Table 1: pKa values of amino acids, C-terminus and N-terminus used in the calculations of peptide isoelectric points, taken from¹

Amino acid	C-ter	Side chain	N-ter
Ala	2.33	NA	9.71
Arg	2.03	9.00	12.10
Asn	2.16	NA	8.73
Asp	1.95	9.66	3.71
Cys	1.91	10.28	8.14
Gln	2.18	NA	9.00
Glu	2.16	4.15	9.58
Gly	2.34	NA	9.58
His	1.70	6.04	9.09
Ile	2.26	NA	9.60
Leu	2.32	NA	9.58
Lys	2.15	10.67	9.16
Met	2.16	NA	9.08
Phe	2.18	NA	9.09
Pro	1.95	NA	10.47
Ser	2.13	NA	9.05
Thr	2.20	NA	8.96
Trp	2.38	NA	9.34
Tyr	2.24	10.10	9.04
Val	2.27	NA	9.52

1. *CRC Handbook of Chemistry and Physics*. 87th ed.; CRC Press: 2006-2007.

Appendix III: Numerical parameters

Numerical mesh size and Peclet number

A linear algorithm was used with a time step of 20 s (0.09 % error compared to 0.1 s time step). The mesh size ranges from 200 to 300 μm (0.22 % to 0.77 % error respectively, compared to 50 μm), it has been reduced to 10 μm at the corners of the wells to take into account the edge effects (i.e. the over intensity of the flux at the corners). The migration

Peclet number, defined as the ratio of the migration rate to the diffusion rate ($Pe_m = \frac{v_m}{D/\delta}$), ranges from 80 to 120. This value is at the limit of the acceptable range defined previously⁵³.

If the Peclet parameter is for example too high, it means that, on a characteristic length, the migration term is too high compared to the diffusion term (which is for example the case for highly charged species far from the pI). An increasing value of the Peclet above the typical value of 100 leads progressively to inaccuracy, and later to instability of the calculations.

Curriculum Vitae

Name: Hoang-Trang LAM

Nationality: French

Date of birth: 27/03/1980

EDUCATION

2003 – 2007 **Ecole Polytechnique Fédérale de Lausanne (EPFL), Switzerland** – PhD candidate in Laboratoire d'Electrochimie Physique et Analytique

2000 – 2003 **Ecole Européenne de Chimie, Polymères et Matériaux (ECPM), Strasbourg, France** – Engineering Degree in Chemistry, specialization Analytical Chemistry

1998 – 2000 Lycée Kléber, Strasbourg, France – Baccalauréat scientifique – Classes Préparatoires aux grandes écoles

LANGUAGES

French and Vietnamese: native

English: very good level (Cambridge First Certificate Grade B, TOEIC score 980/990)

German: good (6 months working in German-speaking part of Switzerland and in Germany)

Japanese: basic knowledge (2 years)

Spanish: basic knowledge (1 year)

PROFESSIONAL EXPERIENCE

2003 – 2007 **EPFL** – Teaching assistant for the course “Analytical separation methods” and lab assistant for analytical chemistry

2003 (6 months) **Laboratoire de Chimie Physique, ECPM, Strasbourg (France)** – Research project: development and optimization of a membrane reactor for oxidative deshydrogenation of propane

2002 (3 months) **Bosch GmbH, Stuttgart (Germany)** – Engineering internship: determination of the alteration of diesel fuel blended with biodiesel and evaluation of the influence of particle filter additives

2001 (2 months) **Streuli Pharma AG, Uznach (Switzerland)** – Technician internship: quantification of drug compounds by high performance liquid chromatography

INTERESTS

Swimming – Dancing (rock'n'roll and salsa) – Musicals and Irish dance shows – English and French novels

FIRST-AUTHOR PUBLICATIONS

An IPG gel cell to study the pH-dependence of drug lipophilicity, Lam H.-T., Pereira C. M., Roussel C., Carrupt P. A., Girault H. H., *Analytical Chemistry* 2006, 78, 1503-1508.

Modeling the isoelectric focusing of peptides in an OFFGEL multicompartement cell, Lam H.-T., Josserand J., Lion N., Girault H. H., *Journal of proteome research* 2007, 6, 1666-1766.

Gel-free isoelectric focusing in a membrane-sealed multi-compartment cell for proteome pre-fractionation, Lam H.-T., Antonioli P., Righetti P. G., Citterio A., Girault H. H., *Electrophoresis* 2007, 28, 1860-1866.

POSTER PRESENTATIONS

2006 Congress of the Swiss Chemical Society, Zürich, Switzerland, October 2006: Immobilized pH Gradient to study the pH dependence of drug lipophilicity

2005 Research Day EPFL Lausanne, Switzerland November 2005: OFFGEL and FLOW FREE IEF of peptides

1er symposium chimie analytique et bio-analytique, Montpellier, France, September 2005: Simulation of OFFGEL IEF of peptides